



UNIVERSITY
OF COLOGNE

EXTREMES IN WIND AND PHOTOVOLTAIC POWER
PRODUCTION IN EUROPE ANALYSED USING SYNOPTIC
WEATHER PATTERNS

INAUGURAL-DISSERTATION
ZUR
ERLANGUNG DES DOKTORGRADES
DER MATHEMATISCH-NATURWISSENSCHAFTLICHEN FAKULTÄT
DER UNIVERSITÄT ZU KÖLN

VORGELEGT VON
LINH TRAN THUY HO
AUS DAKLAK, VIETNAM
KÖLN, 2023

BERICHTERSTATTER:

PROF DR. STEPHANIE FIEDLER

PROF DR. ROEL NEGGERS

TAG DER MÜNDLICHEN PRÜFUNG:

30 OCTOBER 2023

ABSTRACT

As Europe increases its share of photovoltaic (PV) and wind power to achieve the climate-neutral targets by 2050, its electricity system also increasingly depends on weather conditions. Extreme events in PV and wind power production can undermine the electricity system's stability when their total production deviates significantly from the anticipated values. Identifying what weather conditions are associated with extremes in PV and wind power production across Europe, and how they might change in the future compared to the present-day installation, would provide valuable insights for the energy sector.

This thesis addresses these issues through comprehensive analyses of PV plus wind power production variability in Europe using synoptic weather patterns. To that end, the Renewable Energy Model (REM) was developed to simulate PV and wind power production with high-resolution reanalysis data from COSMO-REA6 for the period 1995–2017. The installed capacity data were derived from the CLIMIX dataset projected for 2050 and scaled for 2019 to compare changes in weather dependency between present-day and future installations. The anomalies in PV and wind power production from REM were analysed using a synoptic weather pattern classification of 29 patterns with the advantage of capturing day-to-day and regional variability in meteorological conditions across Europe. This thesis explores the topic in two studies.

The first study examines the climatological variations in the total production of PV plus wind power across Europe associated with 29 weather patterns over the period 1995–2017. The study also assesses the sensitivity of these associations with different event durations, regions, and installations. The results show that the influence of wind power variability is pronounced in the present-day installation, while the future installation exhibits increased influence from PV power variability. *Dark doldrum* weather patterns become more problematic, with reduced production in both PV and wind power, particularly in the pattern South-Shifted Westerly (Ws) with a reduction of -12.1% in the total production compared to the climatological mean. Associations of weather patterns with low total production strongly depend on the event duration and installed capacity. In contrast, high total production correlates with dominant westerly wind patterns, irrespective of the event duration or installation. Associa-

tions of weather patterns vary more significantly in southern European regions, attributed to a higher proportion of PV power installations. This study also compiles a catalogue of climatological anomalies in PV and wind power production associated with each weather pattern, showing how these anomalies are distributed spatially across Europe. This could aid the energy sector with a quick estimation of renewable power production anomalies during a given meteorological condition without an extensive energy model.

The second study investigates extreme events in total production in Germany, with a focus on the seasonal differences in their meteorological conditions. The results show that the future installation foresees an increased frequency of extremely low production events in the summer half of the year, notably in May. Stationary weather patterns that last over five days play an important role in 14-day low production events, with distinct characteristics between summer and winter events. Winter events, occurring from October to March, relate to atmospheric blockings (stationary anticyclonic patterns), which are characterised by a very low wind power production and a slightly low PV power production compared to the climatological means, up to -37% and -9% , respectively. In contrast, summer events, occurring from April to September, are associated with stationary cyclonic patterns and characterised by moderately low production in both PV and wind power of up to -19% compared to the climatological means. The direction of the pressure system movement to Germany influences the effectiveness of cross-border transmission lines in the North–South or West–East direction. The study raises concerns regarding prolonged low production events in summer in the future installation, which could pose a combined threat to the electricity system as the demand for cooling increases due to more frequent heatwaves.

CONTENTS

1	INTRODUCTION	1
1.1	Motivation	1
1.2	Aims and hypotheses	4
1.3	Contributions within this thesis	6
2	BACKGROUND KNOWLEDGE	9
2.1	Modelling renewable energy from a meteorological perspective	9
2.1.1	Modelling photovoltaic power	11
2.1.2	Modelling wind power	14
2.2	Impacts of synoptic weather on renewable energy . . .	18
2.2.1	Definition and nomenclature	18
2.2.2	Synoptic weather in renewable energy	22
3	DATA AND METHODS	25
3.1	Data	25
3.1.1	COSMO-REA6	25
3.1.2	CLIMIX model	27
3.1.3	Weather pattern classification	28
3.2	The renewable energy model	30
3.2.1	The PV power simulation	32
3.2.2	The wind power simulation	34
3.2.3	Model evaluation	36
3.3	Model assemble	42
4	STUDIES	49
4.1	A climatology of weather-driven anomalies in European photovoltaic and wind power production	49
4.2	More summertime low-power production extremes in Germany with a larger solar power share	64
4.3	Extremes in energy demand sector - the dena study . .	77
5	DISCUSSION AND CONCLUSION	81
5.1	Summary	82
5.1.1	Study I - A climatology of weather-driven anomalies in European photovoltaic and wind power production	82
5.1.2	Study II - More summertime low-power production extremes in Germany with a larger solar power share	84
5.2	Methodological limitations and uncertainties	85
5.3	Significance and Outlook	87

I	SUPPLEMENTARY OF STUDY I	89
II	SUPPLEMENTARY OF STUDY II	109
	BIBLIOGRAPHY	139

LIST OF FIGURES

Figure 1.1	Distribution of different sources in electricity generated by renewable sources in the EU-27 in 2020	3
Figure 1.2	Net electricity generation from various energy sources in Germany for the week 33 rd in 2016	4
Figure 2.1	Three most common types of PV panels	13
Figure 2.2	PV power potential and country-aggregated capacity factors in Europe	15
Figure 2.3	Components of a typical wind turbine with a horizontal axis	16
Figure 2.4	Wind power potential and country-aggregated capacity factors in Europe	19
Figure 2.5	Varied scales of atmospheric phenomenon in size and life span	20
Figure 3.1	Domain of COSMO-REA6	26
Figure 3.2	The domain used to define weather patterns	30
Figure 3.3	Domains of CDS and REM data	37
Figure 3.4	Offset in time coordinates of PV power data	38
Figure 3.5	Density distribution of REM, CDS, and Renewables Ninja data	41
Figure 3.6	Diurnal and seasonal cycles in PV power capacity factors between REM and CDS data	44
Figure 3.7	Diurnal and seasonal cycles in PV power capacity factors between REM and Renewables Ninja data	45
Figure 3.8	Diurnal and seasonal cycles in wind power on-shore capacity factors between REM and CDS data	46
Figure 3.9	Diurnal and seasonal cycles in wind power on-shore capacity factors between REM and Renewables Ninja data	47
Figure 4.1	Mean potential capacity factor of PV and wind power in DJF	78
Figure 4.2	Anomalies of wind speed and irradiance during Jan 1997 and Dec 2007 events	79

LIST OF TABLES

Table 1	Technical specifications of the three most common types of PV panels	13
Table 2	Factors determining the spatial distribution of renewable installations	28
Table 3	Names of 29 weather patterns	31
Table 4	Average potential capacity factors for four selected countries	39

Erklärung zur Dissertation
gemäß der Promotionsordnung vom 12. März 2020

Diese Erklärung muss in der Dissertation enthalten sein.
(This version must be included in the doctoral thesis)

„Hiermit versichere ich an Eides statt, dass ich die vorliegende Dissertation selbstständig und ohne die Benutzung anderer als der angegebenen Hilfsmittel und Literatur angefertigt habe. Alle Stellen, die wörtlich oder sinngemäß aus veröffentlichten und nicht veröffentlichten Werken dem Wortlaut oder dem Sinn nach entnommen wurden, sind als solche kenntlich gemacht. Ich versichere an Eides statt, dass diese Dissertation noch keiner anderen Fakultät oder Universität zur Prüfung vorgelegen hat; dass sie - abgesehen von unten angegebenen Teilpublikationen und eingebundenen Artikeln und Manuskripten - noch nicht veröffentlicht worden ist sowie, dass ich eine Veröffentlichung der Dissertation vor Abschluss der Promotion nicht ohne Genehmigung des Promotionsausschusses vornehmen werde. Die Bestimmungen dieser Ordnung sind mir bekannt. Darüber hinaus erkläre ich hiermit, dass ich die Ordnung zur Sicherung guter wissenschaftlicher Praxis und zum Umgang mit wissenschaftlichem Fehlverhalten der Universität zu Köln gelesen und sie bei der Durchführung der Dissertation zugrundeliegenden Arbeiten und der schriftlich verfassten Dissertation beachtet habe und verpflichte mich hiermit, die dort genannten Vorgaben bei allen wissenschaftlichen Tätigkeiten zu beachten und umzusetzen. Ich versichere, dass die eingereichte elektronische Fassung der eingereichten Druckfassung vollständig entspricht.“

Teilpublikationen:

Ho-Tran, L. and Fiedler, S., 2024. A climatology of weather-driven anomalies in European photovoltaic and wind power production. *Communications Earth & Environment*, 5(1), p.63.
Ho-Tran, L. and Fiedler, S., 2024. More summertime low-power production extremes in Germany with a larger solar power share. *Solar Energy*, 283, p.112979.

Datum, Name und Unterschrift

10.08.2023, Linh Tran Thuy Ho

INTRODUCTION

1.1 MOTIVATION

To mitigate climate change, Europe has set its targets to reduce 55% of its greenhouse gas emissions by 2030 and to become climate-neutral by 2050 (European Commission, 2021; The European Commission, 2020). To achieve these targets, a key strategy involves a substantial increase in energy generation from renewable sources, particularly solar and wind power. As of 2020, Europe produced 18.8% of its energy from combined solar and wind power (Eurostat, 2022) (Fig. 1.1). There have been large investments on wind and solar power in Europe, which led to increases in their installed capacities, improvement in efficiency, and reduction in costs (IRENA, 2021). However, as the share of solar and wind power in the energy mix grows, the energy system becomes more dependent on weather conditions, posing challenges to ensure a stable energy supply across Europe.

The challenge arises from the flexibility requirements of the energy system. Currently, nuclear and coal-fueled power plants serve as the base load, providing a consistent power supply to meet the fundamental demands of the energy system. Fluctuations in demand are then met by additional coal-fueled plants and renewable sources like wind and solar power. While fluctuations in demand exhibit some regular patterns, such as diurnal or weekly cycles, there is significant uncertainty regarding the level of demand at any given time, influenced by factors like heating, cooling, or television programme. Therefore, energy sources must be flexible to accommodate these fluctuations and maintain the grid frequency within the allowed deviation ($50 \text{ Hz} \pm 10 \text{ mHz}$)¹. However, this flexibility is challenged by non-dispatchable² energy sources, such as wind and solar power, as their production cannot be directly controlled.

An example of the electricity supply fluctuation in Germany is shown in Fig. 1.2. It illustrates how the electricity demand ("load" in the figure) in Germany was met by various energy sources in the 33th week of 2016. During this period, wind power production was notably low, while PV power generated the average amount for summer during the first five days. However, on August 15, 2016, around sunrise and

¹ https://www.mainsfrequency.com/frequ_info_en.php

² Energy sources that can not be controlled how much they will produce

sunset (6:00 and 18:00), the electricity demand exceeded the energy produced from national sources. This residual (not-met) demand was met through electricity imports from outside Germany.

New challenges arise in extreme situations where low renewable energy production cannot meet high demand, or when excessive energy production leads to curtailment³ and economic loss⁴. Extreme events, such as prolonged periods of low irradiance and/or wind speed, or sudden wind speed increases (ramp), pose growing concerns for energy system operators (Gallego-Castillo et al., 2015; Reindl et al., 2017). Although several measures exist to address electricity supply fluctuations, including transmission through electricity grids, energy storage solutions, and demand response⁵, these measures might prove insufficient in markets with a significant share of renewable energy when fossil fuel phases out (Armaroli and Balzani, 2011; Huber et al., 2014).

Resolving these challenges requires understanding the variability of combined wind and solar power production under different meteorological conditions for distribution networks at a continental scale and for future energy installations. Knowledge in synoptic weather conditions can be useful in understanding the combined variability of wind and solar power production (Brayshaw et al., 2011; Engeland et al., 2017; Wiel et al., 2019a). Extreme events in both energy sources simultaneously can place substantial stress on the energy operating system (Drücke et al., 2020; Huber et al., 2014; Wiel et al., 2019b). One way to cope with the variability of energy sources is to exploit the balancing effect, i.e., a negative correlation in energy production between two or more regions (Frank et al., 2018; Henckes et al., 2020). Grid-connected regions can complement each other by trading surplus energy to regions with energy shortages.

At a scale of 1000 km, synoptic weather conditions influence wind and solar power production across Europe simultaneously. Monitoring synoptic weather conditions provides valuable insights into the spatial and temporal variability of key meteorological variables impacting wind and solar power, such as irradiance and wind speed. For instance, if a high pressure system is established over the North Sea extending to the Iberian Peninsula, the decrease in wind power production offshore in the North Sea may be balanced by the higher power production from PV power in Iberia via inter-country electricity transmission (Frank et al., 2020b). Additionally, synoptic weather varies at sub-seasonal time scale which provides the opportunity for

³ Curtailment is a deliberate reduction of energy production below the potential to match the energy demand.

⁴ <https://www.next-kraftwerke.com/knowledge/curtailment-electricity>

⁵ Measures to regulate the electricity demand to match the supply.

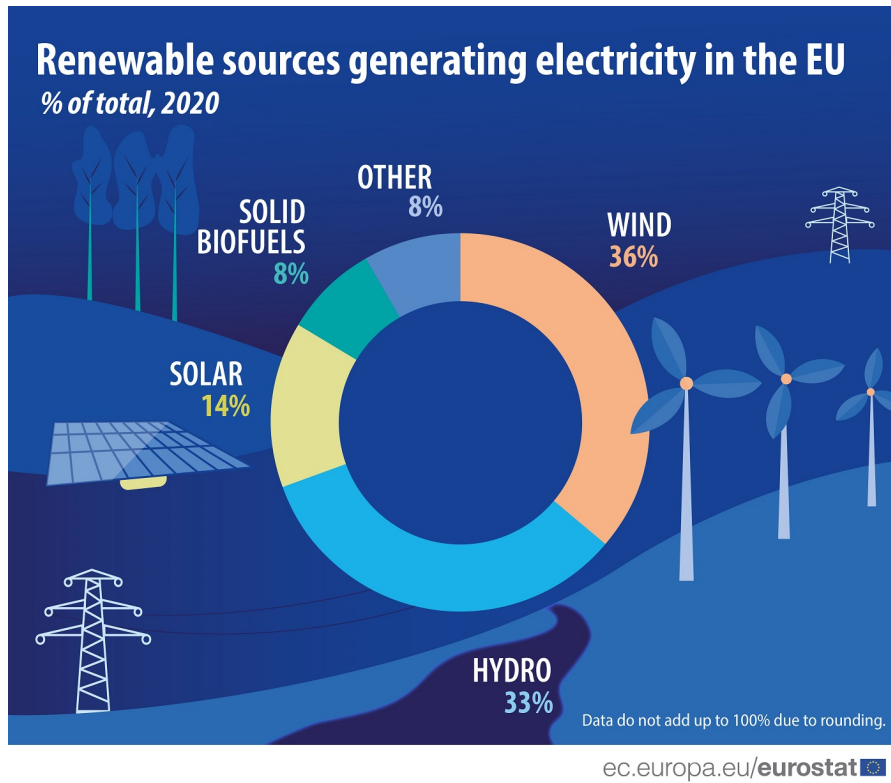
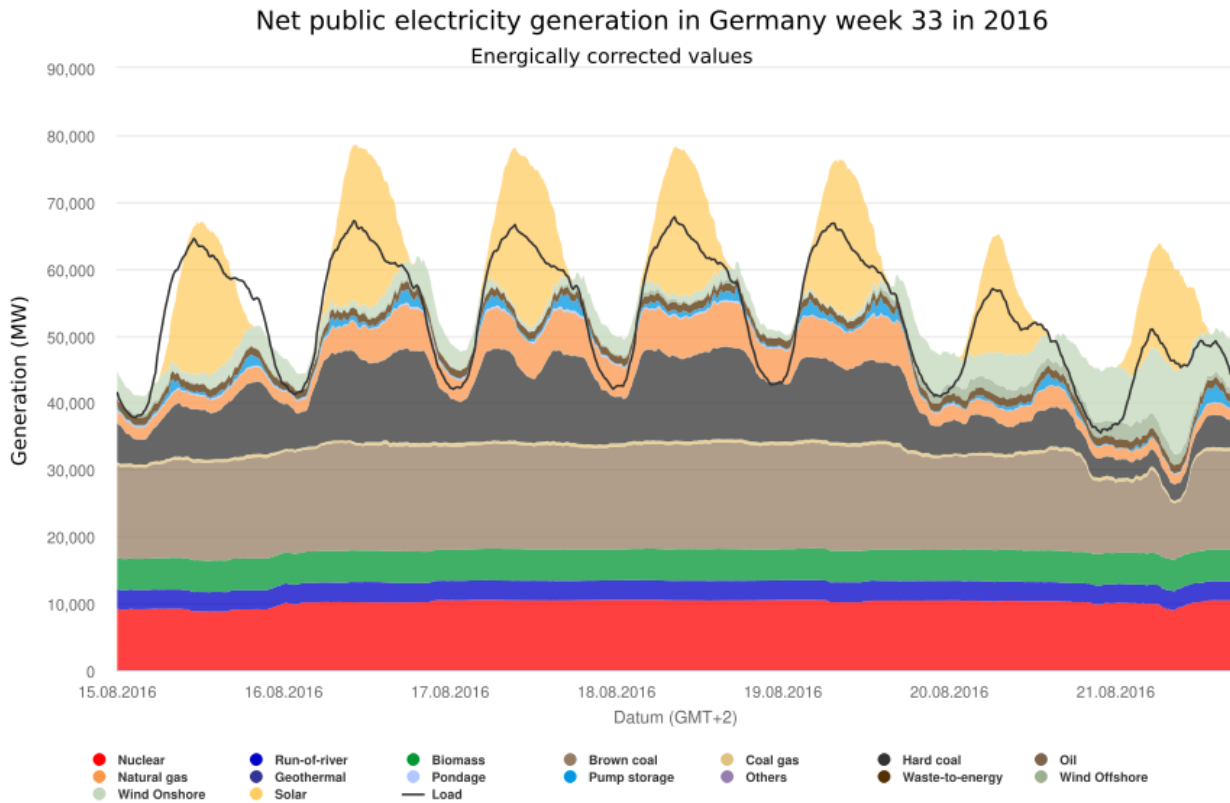


Figure 1.1: Distribution of different sources in electricity generated by renewable sources, which in turn account for 37.5% of gross total electricity consumption in the EU-27 in 2020, from Eurostat (2022).

longer range forecasting (Büeler et al., 2021). Better understanding on how these synoptic weather conditions influence wind and solar power in Europe can guide better planning and operation of energy systems with a high share of renewable energy in Europe.

The motivation of this thesis is to explore possible methods to apply the knowledge on the synoptic weather in the renewable energy sector in Europe. The main approach involves investigating the association between the weather pattern classification data with anomalies in renewable energy production, simulated using reanalysis data. Weather pattern classifications offer the advantage of capturing day-to-day variability, enabling forecasts a few days ahead (Huang et al., 2020). Several catalogues of weather pattern classification are available and routinely maintained, such as from the German Weather Service (James, 2007) and the UK MetOffice (Neal et al., 2016), providing readily available resources for this analysis. By establishing connections between specific weather patterns and anomalous wind and solar power production, we can utilize the weather pattern catalogue to anticipate variations in renewable energy output without resorting to complex energy system modeling. Reanalysis data, such



Energy-Charts.info; Datenquelle: ENTSO-E, AGEE-Stat, Destatis, Fraunhofer ISE, AG Energiebilanzen; Letztes Update: 12.01.2023, 20:50 MEZ

Figure 1.2: Net electricity generation from various energy sources in Germany for the week 33rd in 2016, from www.energy-charts.info.

as the regional COSMO-REA6 dataset used in this project, offer consistent coverage across Europe with a high horizontal resolution of 6 km, thus has the benefit of capturing smaller-scale spatial (Bollmeyer et al., 2015). It provides appropriate meteorological variables for simulating wind and solar power production (Frank et al., 2020b; Henckes et al., 2018). The combination of the synoptic weather and reanalysis data is proven to be beneficial for renewable energy applications (Frank et al., 2020b; Grams et al., 2017; Wiel et al., 2019a,b).

1.2 AIMS AND HYPOTHESES

This thesis aims to investigate the association between synoptic weather conditions and extremely high and low power production from wind and solar energy, focusing on photovoltaic (PV) technology. The primary objective is to determine whether certain synoptic weather patterns are more likely to lead to extremely anomalous power production in the total production of wind and PV power in Europe.

In detail, this thesis explores the relationship between weather patterns and extreme events in power production from various perspectives, including positive and negative anomalies in power production, considering different event durations, installed capacities, and seasonal variations. Previous studies have mainly focused on the low production aspect (Drücke et al., 2020; Wiel et al., 2019b), using present-day installations (Drücke et al., 2020; Grams et al., 2017), and have indicated that extreme events in renewable energy occur in winter (Drücke et al., 2020; Grams et al., 2017; Wiel et al., 2019b).

However, there are more aspects of extreme events in renewable energy that need better understanding. Prolonged low power production strains the electricity system, necessitating additional non-renewable sources like coal-fueled power plants, which are being phased out due to climate change concerns. On the other hand, events with high power production can help reduce dependence on non-renewable sources and replenish battery storage, but an excess of power production during low demand periods may require curtailment. Moreover, weather patterns linked to low power production in PV and wind power during summer can significantly differ from those in winter in terms of flow characteristics, meteorological development, and their impact on wind and PV power individually. Considering the future scenario of climate change, electricity demand for cooling during summers is expected to rise in Europe, making it crucial to understand the seasonal variations in extreme events.

As renewable energy installations increase in the future, these challenges will escalate. The proportion between PV and wind power in Europe may also change, influencing their combined production under varying weather conditions. To address these aspects, this thesis performs analyses and comparisons between present-day and projected future installed capacities (simulated for 2019 and 2050), with ratios of PV to wind power installation of 0.7:1 and 2:1, respectively.

This thesis utilises the benefits of the high-resolution regional reanalysis dataset COSMO-REA6 (Frank et al., 2018; Henckes et al., 2018) and the ability to represent the day-to-day variability of meteorological conditions in weather pattern classification (Huang et al., 2020; James, 2007). The research objectives are as follows:

1. Provide a comprehensive analysis of the variability of PV and wind power and their total production in Europe associated with synoptic weather patterns.
2. Investigate the dependency of the total production-weather pattern relationship on temporal scales (ranging from hourly to 14 days), spatial scales (Europe and selected regions/countries),

and installed capacity (for both present-day and future scenarios).

3. Identify specific weather patterns associated with extreme events in renewable energy that require monitoring in the European and German energy systems.
4. Study the seasonal differences in extreme events in renewable energy during winter and summer in Germany.

1.3 CONTRIBUTIONS WITHIN THIS THESIS

To that end, the Renewable Energy Model (REM) was developed to simulate PV and wind power production in Europe using the re-analysis dataset COSMO-REA6 with a high horizontal resolution of 6 km (Bollmeyer et al., 2015). The installed capacity data from the CLIMIX model (Jerez et al., 2015a) was used to simulate the capacity for present-day (2019) and future (2050) scenarios at the same resolution. The output consists of hourly power production of PV and wind power for Europe during the period 1995–2017. The output is then paired with a weather pattern classification of 29 patterns (James, 2007) to gain insights into the associations between weather patterns and the variability in PV, wind power, and their total production. The model is described in detail in Chapter 3.2.

The thesis includes two studies to address the research objectives:

Study I - A climatology of weather-driven anomalies in European photovoltaic and wind power production

The research objectives (1–3) are addressed in the first study (Section 4.1). It examines the climatology of weather patterns associated with anomalies in PV and wind power production, with the following research questions:

1. Which weather patterns are associated with extremely anomalous power production in PV plus wind power in Europe?
2. Are there any common characteristics in weather patterns associated with extreme events in power production with different event durations and seasons?
3. How are the anomalies of power production distributed spatially during these weather patterns?
4. How sensitive are the results to the installations with different ratios of PV to wind power installed capacities?

Study II - More summertime low-power production extremes in Germany with a larger solar power share

The research objectives (3–4) are addressed in the second study (Section 4.2). It examines extreme events in total production (PV plus wind power), with a focus on prolonged low production events that last for 14 days. The study addresses the following research questions:

1. Do seasonal differences in extreme events in renewable energy change between the present-day and future installations?
2. Are there different characteristics in weather patterns involved in extreme events between winter and summer?
3. Are there any differences in meteorological conditions when prolonged low power production events progress between winter and summer events?

The thesis follows this structure:

- Chapter 2 provides background knowledge from existing literature, covering topics such as PV and wind power production modeling and synoptic weather patterns.
- Chapter 3 details the simulation of PV and wind power production data and evaluations of the simulation output.
- Results of the analyses using this data are presented in Chapter 4: *Study I* offers a comprehensive overview of weather pattern impacts on PV and wind power production anomalies in Europe, while *Study II* compares extreme events in power production between winter and summer in Germany.
- Chapter 5 summarizes key findings and their significance and provides an outlook on future research directions to advance knowledge in this area.

BACKGROUND KNOWLEDGE

To understand the influence of synoptic weather on the renewable energy system, it is important to understand each component. The following provides an overview of current knowledge regarding (1) modelling wind and photovoltaic (PV) power using meteorological information, and (2) synoptic weather conditions and their impact on the renewable energy system in Europe.

2.1 MODELLING RENEWABLE ENERGY FROM A METEOROLOGICAL PERSPECTIVE

Modelling energy system can have various approaches and methods, depending on the model's purpose and its spatial and temporal coverage (Jebaraj and Iniyan, 2006; Laha and Chakraborty, 2017). Addressing the challenges posed by climate change requires an increasing share of renewable energy to achieve climate-neutral targets (European Commission, 2018). Among renewable sources, PV and wind power are non-dispatchable¹ and strongly depend on weather conditions. Given the currently limited energy storage capacities, understanding the variability of these energy sources from a meteorology perspective is crucial.

Modelling PV and wind power can be categorised into four main groups, depending on their purpose and target user:

1. Energy planning models (also known as energy system models) offer various scenarios with diverse factors. They are often used for optimisation purposes involving cost consideration or spatial allocations (Pfenninger et al., 2014; Sasse and Trutnevyte, 2019; Schlachtberger et al., 2018). These models predominantly serve to inform policy decisions, e.g., the energy model from the ISE Fraunhofer institute². PV and wind power are included in these models to address energy security and climate change policies. Important information to include are total

¹ If an energy source is non-dispatchable, the operators cannot control how much it will produce to meet the fluctuation in demand. Examples include wind and solar power. Small batteries can be used to regulate the variability in a short period of time.

² <https://www.ise.fraunhofer.de/en/business-areas/power-electronics-grids-and-smart-systems/energy-system-analysis/energy-system-models-at-fraunhofer-ise.html>

energy source capacities within the country and their standard yield power production (Sasse and Trutnevyte, 2019).

2. Supply-demand models (or electricity market modelling) serve more specific objectives, such as optimising investments or improving transmission system operations (Connolly et al., 2010). In these models, PV and wind power modelling are included as components of the functioning energy system (Ventosa et al., 2005). While similar to planning models in group (1), these models include more technical specifications. Meteorological data used in this context may involve a "typical meteorological year", e.g., one year of solar irradiance data with diurnal and seasonal cycles is fed into a detailed grid peak load model with a PV power component (Kumary et al., 2014). Extreme weather situations can also be integrated to assess the stress load on the energy system (EWI (2021)).
3. Models designed for operational purposes are gaining significance, especially with the increasing integration of distributed intermittent power sources like rooftop PV and small wind turbines. These models include specific features such as various installed capacity and limited battery storage. They aim to predict intra-day or now-casting PV and wind power using meteorological variables such as wind speed or irradiance. Meteorological data from satellites and observational stations can be incorporated typically with artificial intelligence tools (Perveen et al., 2019). Efforts are also underway to extend predictability ranges to weeks or months ahead, as shown in works by Bloomfield et al. (2021), Graham et al. (2022), and the S2S4E project³.
4. Models developed for research purposes from a meteorological standpoint use meteorological data (solar irradiance, wind speed, temperature, etc.) to gain insights into the impacts of weather or climate on the energy system. These models often employ simplified technical specifications involving parameters like the tilt angle of PV panels, hub height of wind turbines, and efficiency rates of energy conversion in PV and wind power simulations (Frank et al., 2018; Jerez et al., 2019; Saint-Drenan et al., 2018; Tobin et al., 2018).

The renewable energy model in this thesis belongs to the fourth category. Following is a summary of some current methods to simulate PV and wind power from a meteorological perspective.

³ Sub-seasonal to Seasonal for Energy (S2S4E) project <https://s2s4e.eu/>

2.1.1 *Modelling photovoltaic power*

Photovoltaics (PV) refer to technologies that convert solar energy into electricity. Another solar panel technology is thermal panels that convert the energy from sunlight into heat. This discussion focuses solely on PV panels. The process of modelling photovoltaic power involves two main steps. First, the amount of solar irradiance, including direct and diffused short-wave radiation that reach the PV panels need to be defined. Second, the conversion of this irradiance energy into useful energy within the PV cells must be calculated.

In terms of nomenclature, solar radiation, measured in J, refers to the energy emitted by the sun. Solar irradiation, measured in J/m^2 , is the energy received on Earth per unit area. Irradiance is the instantaneous rate of irradiation received per unit time, measured in power units such as J/sm^2 or W/m^2 . In terms of PV devices, a solar cell refers to an individual PV device that absorb sunlight and generates electrical charge. A PV module comprises of multiple solar cells connected as a unit to convert electrical charges into alternating current. A PV panel consists of multiple PV modules assembled as an installable unit, while a PV array comprises multiple PV panels connected together.

Accurate irradiance data is crucial as it determines the potential PV power a location can harness (Fig. 2.2). Uncertainties in solar radiation data can magnify uncertainties in the PV model (Urraca et al., 2018b). Various methods exist to obtain solar irradiance data (Kumar et al., 2020), including numerical weather prediction models, satellite images processing, observational networks, and data-driven methods such as deep neural networks (Alzahrani et al., 2017). Combining these methods can aid in irradiance forecasting (Ahmed et al., 2020). The need to forecast solar irradiance intra-day and day-ahead increases with the rise of microgrids⁴ using PV power (Husein and Chung, 2019).

Historical irradiance data can be obtained from reanalysis datasets such as COSMO-REA, ERA5, or MERRA (Bollmeyer et al., 2015; Gelaro et al., 2017; Rohrer et al., 2019) (Fig. 2.2). These datasets offer extensive spatial coverage and long-term availability. Besides, they also provide variables inducing stress on the PV module such as wind gust (Camus et al., 2019). However, these datasets may have known biases due to the representation of cloud and aerosol effects (Urraca et al., 2018a). For example, ERA5 irradiance data have slight positive biases, and COSMO-REA6 irradiance data have negative biases against observational data from most stations in Europe (Urraca et al., 2018a).

⁴ Microgrids are local isolated grids distributed within communities, hence are particularly susceptible to fluctuations in solar irradiance.

Moreover, their temporal resolutions might not capture rapid variations in PV power, making them less suitable for certain applications. For example, a system using 15-minute irradiance data as in COSMO-REA6 can capture up to 22% less PV power compared to a resolution of seconds (Kreuwel et al., 2020).

The actual conversion of irradiance into electricity by a PV panel is influenced by two angles: the tilt angle (relative to the horizontal surface) and the azimuth angle (relative to the north direction). In theory, the tilt angle should be optimised to receive the maximum incoming radiation on the PV panel's surface. However, in practice, the actual tilt angle is reduced from the optimised value to mitigate shadow effects. For instance, PV panels in European countries typically use tilt angles at approximately 70% of the optimized values (Saint-Drenan et al., 2018). As a result, the tilt angle for European domain ranges from 21° to 50° (Frank, 2019). Regarding the azimuth angle, PV panels face south to maximise the amount of received irradiance (Frank, 2019).

When simulating PV power production, three main methods are commonly used: linear or non-linear techniques, and artificial intelligence (Khatib et al., 2012). Linear technique establish a linear correlation between PV power production and variables like irradiance on the PV panel and ambient temperature with parameters defined through empirical methods. Classic non-linear techniques use similar approaches but with polynomial functions, whereas artificial intelligence and fuzzy logic methods can be considered innovative non-linear techniques (Garud et al., 2021; Sen, 2008).

In this discussion, the focus is on the classic non-linear technique which is used in the model in this thesis (see section 3.2.1). Because the parameters are empirically estimated, they are heavily dependent on the technology employed in manufacturing the PV cell. The most common material used for PV cells is silicon. Another less common material is Gallium arsenide (GaAs). Silicon can be integrated into the PV cell in the form of crystalline silicon or a thin film⁵. The efficiency rates of three common types of PV panels, in decreasing order, are monocrystalline (~20%), polycrystalline (~15%), and thin-film (~10%) (Fig. 2.1 and Table 1).⁶ According to the radiative efficiency limit (the Shockley–Queisser limit), the maximum conversion efficiency for a conventional solar cell (with a single p-n junction) is 33.7% (Rühle, 2016). However, in another PV technology utilising concentrated sunlight (concentrated PV cell, or CPV), the efficiency can reach up to 86.8% for multiple-junction cell (De Vos, 1980).

⁵ https://en.wikipedia.org/wiki/Solar_cell

⁶ <https://www.greenmatch.co.uk/blog/2015/09/types-of-solar-panels>

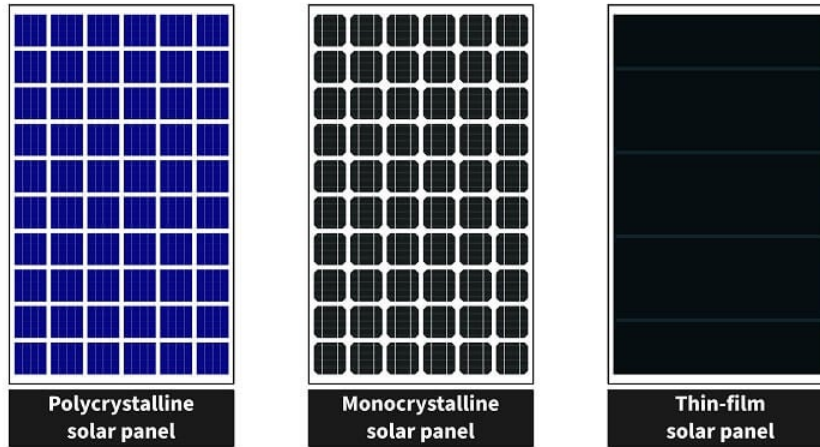


Figure 2.1: Three most common types of PV panels, from theEcoExperts⁷.

Table 1: Technical specifications of the three most common types of PV panels, adapted from Solvoltaics, Solarreviews and theEcoExperts⁸. Note that the price gap between monocrystalline and polycrystalline is narrowing.

	Polycrystalline	Monocrystalline	Thin-film
Efficiency rate	13–16%	15–20%	7–13%
Lifespan	30–40 years	30–50 years	10–20 years
Price	Mid-cost	Expensive	Lower cost
Note	Most popular for residential	Durable	Mostly for large-scale use

Considering that PV panels do not generate power at night, the country-aggregated daily average capacity factor for European countries is around 10–15% (Fig. 2.2b). Various factors influence PV power, including the spectral distribution of irradiance, the reflectivity on the PV panel’s surface, and other environmental factors. The simulation can incorporate these factors to varying degrees of detail depending on the model’s purpose. Most meteorological datasets provide broadband global horizontal irradiance as a standard variable. Using such broadband irradiance data makes PV simulations susceptible to errors as PV production is sensitive to the spectral distribution of solar irradiance (Lindsay et al., 2020). Additionally, the model’s performance can be influenced by the reflectivity on the panel’s surface, which in itself is affected by incoming irradiance and the panel’s temperature (Urraca et al., 2018b). Furthermore, substantial discrepancies

⁸ <https://solvoltaics.com/solar-panel-components/>, <https://www.solarreviews.com/blog/pros-and-cons-of-monocrystalline-vs-polycrystalline-solar-panels>, and <https://www.theecoexperts.co.uk/solar-panels/solar-panels-types>, accessed on 22-03-2023.

in PV power modeling may arise from differences in power-rating conversion, performance indoors and outdoors, and the parameters used to characterise the PV module (Changmai et al., 2022; Friesen et al., 2007; Kenny et al., 2003).

2.1.2 Modelling wind power

Modelling wind power production is comparatively simpler than modelling PV power, mainly because the process of converting wind speed into energy is more straightforward. As the wind moves the turbine blades, its kinetic energy is readily converted into electricity in the generator (Fig. 2.3), akin to how a steam engine turbine operates. Nevertheless, there are also two main steps involved in modelling wind power production: (1) obtaining the wind speed data reaching the turbine blades, and (2) converting the energy from wind speed into electricity.

For the first step, it is necessary to determine the wind speed at the hub height of a wind turbine, typically at 80–150 m¹⁰ above the ground. One common approach is to extrapolate the wind speed at hub height from the wind speed data near the surface, for instance, using 10 m wind speed data from reanalysis dataset. This extrapolation is achieved using either the logarithmic law or the Hellman exponential law (power law) (Emeis and Turk, 2007; Staffell and Pfenniger, 2016). Although the exponential law tends to yield more accurate results (Emeis and Turk, 2007; Gualtieri, 2019), these extrapolation approaches can introduce significant uncertainty, especially due to wind shear effects (Crippa et al., 2021; Frank et al., 2020a; Honrubia et al., 2010). To mitigate this issue, reanalysis data can be employed, which interpolates wind speed from vertical layers with heights similar to the hub height of the turbine. For instance, the simulation in this thesis uses data of wind speed from the vertical layers 36th and 37th (equivalent to 116–178 m above sea level, varying based on the land topography) from the COSMO-REA6 reanalysis dataset (Bollmeyer et al., 2015; DWD, 2022). The wind speed data from COSMO-REA6 has demonstrated to be beneficial in wind power applications (Brune et al., 2021; Frank et al., 2020a; Henckes et al., 2018).

Using reanalysis data, wind speed magnitude is calculated at each grid point based on two horizontal components: eastward and northward vectors (u and v). Wind direction, calculated as $\arctan(v/u)$,

⁹ https://re.jrc.ec.europa.eu/pvg_tools/en/, accessed on 16-03-2023.

¹⁰ Wind turbines have been rapidly increasing in size. As of February 2023, the tallest offshore wind turbine in the world is Vestas' V236-15.0 MW in Denmark, with a hub height of 280 m, a rotor diameter of 236 m and a rated power of 15 MW. For comparison, the biggest wind turbine in 2014 was SeaTitan 10MW with a hub height of 125 m. Source: www.vestas.com/en/products/offshore/V236-15MW

a

Photovoltaic Solar Electricity Potential in European Countries

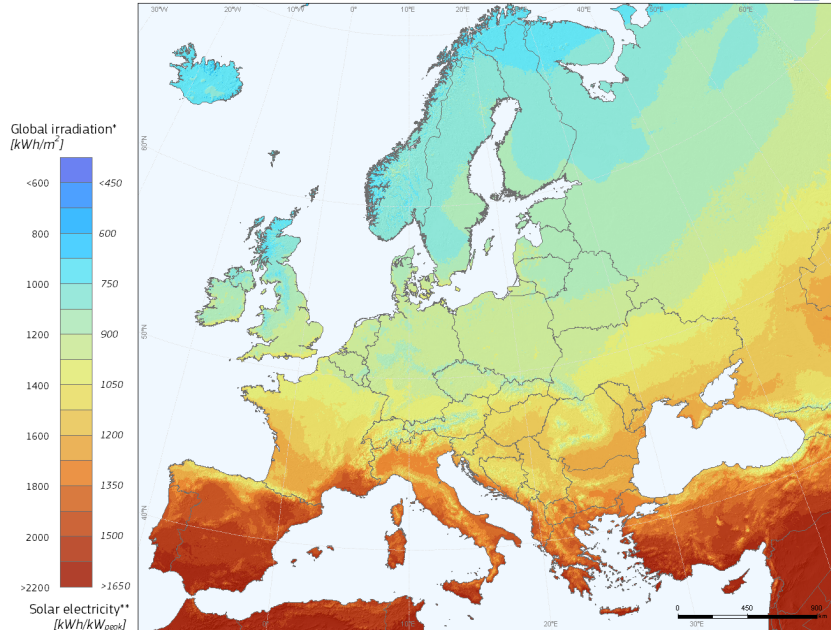
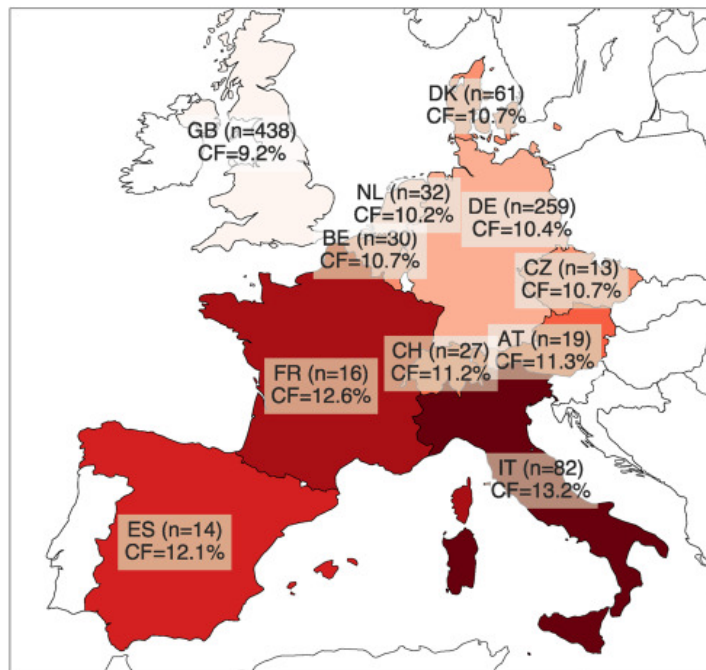
**b**

Figure 2.2: (a) PV power potential in Europe in 2012 defined from global horizontal irradiation [KWh/m²], from Huld et al. (2012) and PVGIS tool⁹; (b) Country-aggregated average capacity factor, n is the number of sites to measure PV power output, from Pfenninger and Staffell (2016).

is typically not considered in wind power calculations as wind turbines are assumed to adjust their nacelle position using anemome-

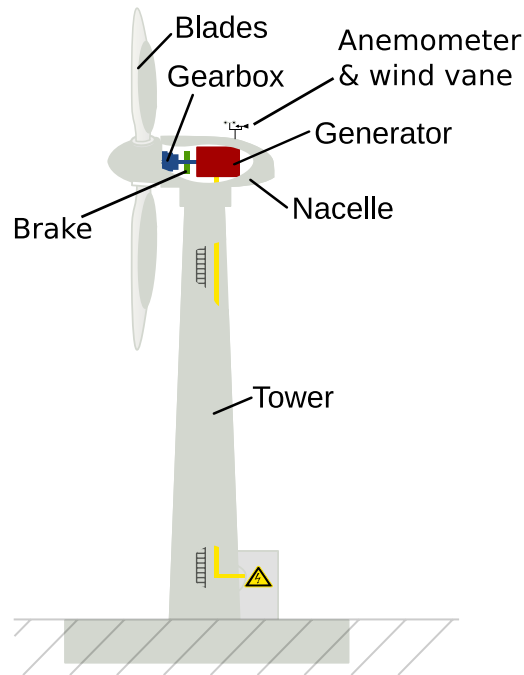


Figure 2.3: Components of a typical wind turbine with a horizontal axis, adapted from Arne Nordmann (norro), Windkraftanlage¹¹.

ters and wind vanes (Fig.2.3). Similar to PV power, wind speed data from reanalysis datasets have relatively low temporal resolution, e.g., hourly in ERA5 or 15 minutes in COSMO-REA6. This resolution has limited ability to adequately capture the impact of very high wind speeds on wind power production, such as wind gusts (Steinheuer and Friederichs, 2019) or nocturnal low level jets (Weide Luiz and Fiedler, 2022). These high wind speed situations can cause ramping rates and curtailments in the power system (Vargas et al., 2014).

The interaction of wind turbines in a cluster can lead to a reduction in wind speed downwind due to the drag from the so-called wake effect (González-Longatt et al., 2012). This effect can induce vertical turbulence (Emeis and Frandsen, 1993) and increase the overturn rate of the atmosphere (Lundquist and Bariteau, 2015). Notably, it impacts the performance of not only the wind turbines downwind in a wind farm but can extend up to 50 km downwind to affect other wind farms, particularly in stable atmospheric conditions, such as those offshore (Akhtar et al., 2021; Lundquist et al., 2019). Furthermore, the wake effect has the potential to alter the long-term local climate (Bodini et al., 2021), demonstrating the importance of including wind

¹¹ <https://commons.wikimedia.org/wiki/File:Windkraftanlage.svg>

farm parameterisations in meso-scale weather modelling (Fischereit et al., 2022).

The produced energy strongly depends on the wind speed condition. Specifically, the power generated by the wind turbine is proportional to the cubic of wind speed at hub height. The most common method to estimate the energy produced by a wind turbine is using the power curve (Equation 2.2). In addition, the air density at hub height also affects the efficiency of converting wind speed into power (ρ_{hub} in equation 2.2). The "heavier" (higher density) the air is, the more power the wind turbine generates, as the resistance is higher when the blade sweeps through the air. Dry air density at a certain altitude is calculated as a function of pressure and air temperature using a molar form of the ideal gas law, as shown in equation 1.

$$\rho_{hub} = \rho_0 \cdot \left(1 - \frac{L h_{hub}}{T}\right)^{\left(\frac{gM}{RT} - 1\right)} \quad (2.1)$$

where

ρ_{hub} is the dry air density [kg/m^3] at the hub height,

ρ_0 is the air density at sea level, $1.2295 \text{ kg}/\text{m}^3$,

L is the temperature lapse rate, $0.0065 \text{ K}/\text{m}$,

h_{hub} is the hub height [m],

T is the absolute temperature [K]

g is the earth-surface gravitational acceleration, $9.807 \text{ m}/\text{s}^2$,

M is the molar mass of dry air, $0.02896 \text{ kg}/\text{mol}$,

R is the ideal gas constant, $8.314 \text{ J}/(\text{mol} \cdot \text{K})$

Wind turbines generally yield higher capacity factors than PV modules, with average values ranging from 20% to 30% for onshore wind power in European countries (Fig. 2.4b). Offshore wind turbines, benefiting from fewer obstacles and higher hub heights, achieve even higher average capacity factors, reaching 40% to 50% in 2019 (International Energy Agency, 2019).

$$P_{out} = \begin{cases} 0 & \text{if } v_{hub} < v_{cut-in} \\ \frac{1}{2} \pi R^2 c_p \rho_{hub} \cdot v_{hub}^3 & \text{if } v_{cut-in} \leq v_{hub} < v_{rated} \\ C_{plant} & \text{if } v_{rated} \leq v_{hub} < v_{cut-out} \\ 0 & \text{if } v_{cut-out} \leq v_{hub} \end{cases} \quad (2.2)$$

where

ρ is the air density at hub height,

v_{hub} is the wind speed at hub height,

$v_{\text{cut-in}}$ and $v_{\text{cut-out}}$ are the cut-in and cut-out wind speeds, defined as the threshold wind speeds for the onset and stop producing power of wind turbine,

v_{rated} is the rated wind speed, at which or above, the wind turbine produces maximum power

The application of the power curve law to calculate power generated from wind speed relies on knowledge of specific wind turbine specifications, such as rotor diameter, hub height, and rated power (installed capacity). However, when simulated data for installed capacity and hub height are derived from models, like the CLIMIX model (Jerez et al., 2015a), discrepancies between the assigned hub height and actual installed capacity may arise. In such cases, it is more appropriate to calculate the capacity factor (a dimensionless value between 0 and 1, representing the ratio between generated power and installed capacity) and then multiply it by the installed capacity to obtain the power production. The capacity factor depends on the wind speed at hub height and the values of rated, cut-in, and cut-out wind speeds, as expressed by Equation 2.3). To obtain data for installed capacity, one can refer to available datasets as demonstrated in Henckes et al. (2020), or model the grid configuration similarly to meteorological data using approaches such as those discussed in Jerez et al. (2015a), Staffell and Pfenninger (2016), and Tobin et al. (2016).

$$CF = \begin{cases} 0 & \text{if } v_{\text{hub}} < v_{\text{cut-in}} \\ \frac{v_{\text{hub}}^3 - v_{\text{cut-in}}^3}{v_{\text{rated}}^3 - v_{\text{cut-in}}^3} & \text{if } v_{\text{cut-in}} \leq v_{\text{hub}} < v_{\text{rated}} \\ 1 & \text{if } v_{\text{rated}} \leq v_{\text{hub}} < v_{\text{cut-out}} \\ 0 & \text{if } v_{\text{cut-out}} \leq v_{\text{hub}} \end{cases} \quad (2.3)$$

2.2 IMPACTS OF SYNOPTIC WEATHER ON RENEWABLE ENERGY

2.2.1 Definition and nomenclature

Synoptic weather refers to meteorological processes that occur on a spatial scale of the order of 1000 km. It represents the lower end of large-scale weather, larger than meso-scale weather but smaller than

¹² <https://globalwindatlas.info/en/>, accessed on 16-03-2023.

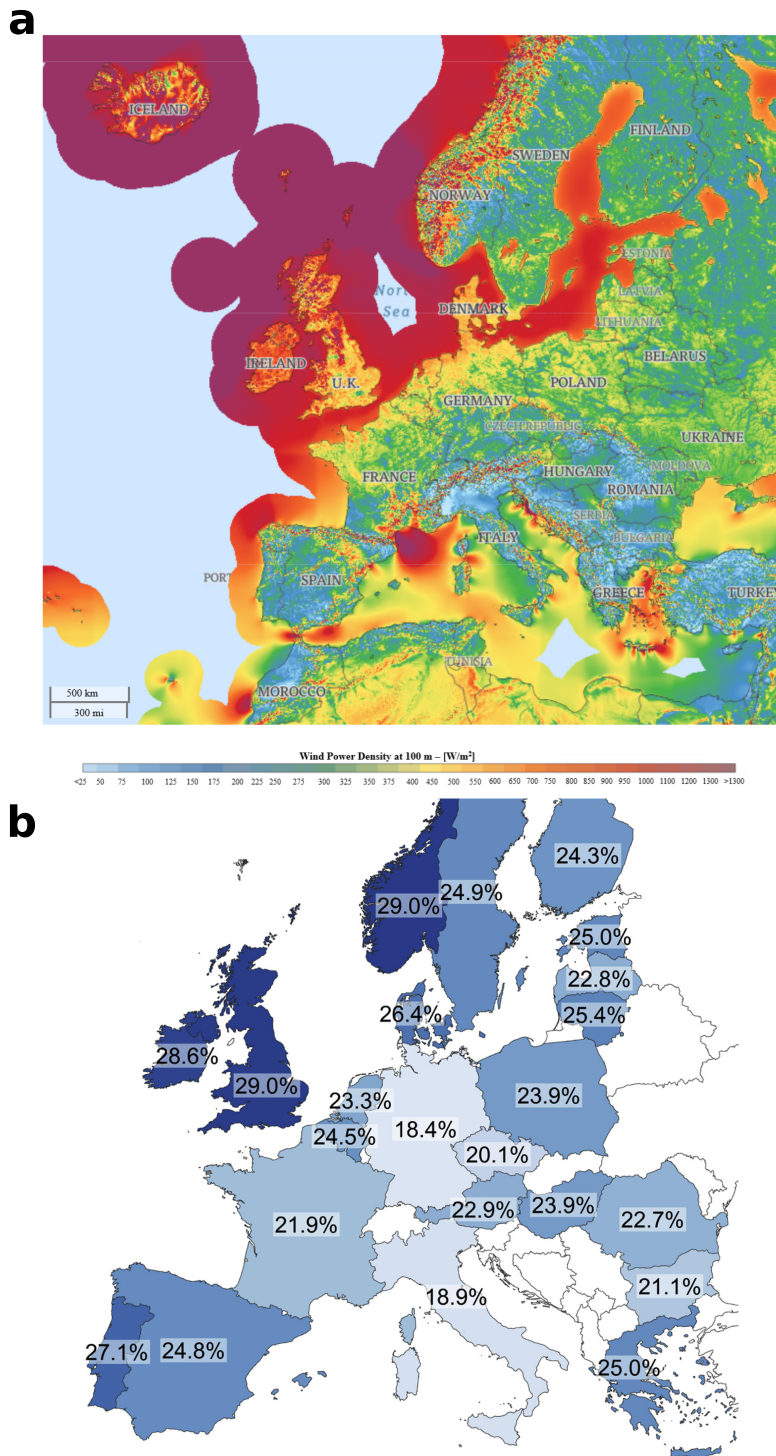


Figure 2.4: (a) Wind power potential in Europe from Ghigo et al. (2020) and the Global wind atlas tool¹²; (b) Country-aggregated average capacity factor of wind power in the period 2005–2014 from Staffell and Pfenninger (2016).

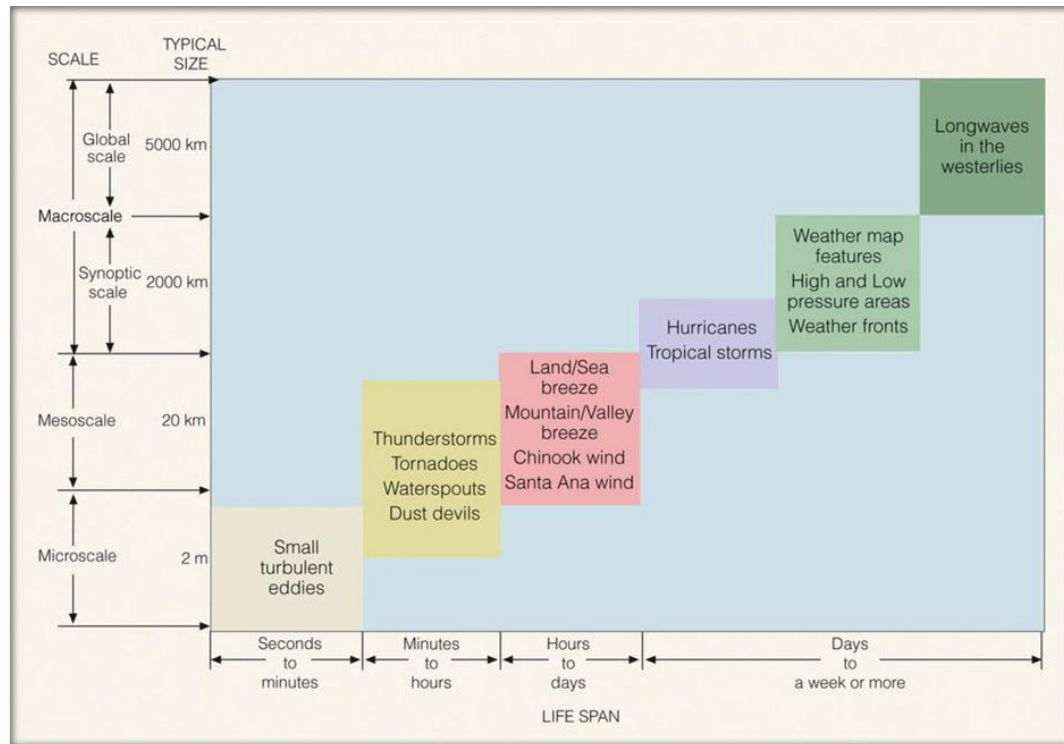


Figure 2.5: Varied scales of atmospheric phenomenon in size and life span, from Ch.9 Ahrens (2015).

planetary scale weather (Fig. 2.5). In mid-latitude regions, certain synoptic atmospheric circulations display recurrent and quasi-stationary characteristics, persisting for several days to a week or more (Grams et al., 2020). Some of these persistent synoptic weather conditions are associated with extreme weather conditions such as cold spells and heat waves (Ferranti et al., 2019; Zschenderlein et al., 2018).

Weather regimes are finite categories into which synoptic weather conditions can be classified due to their recurring and persistent nature. The first mention of synoptic weather regimes is in 1951 with the Atlantic blocking and its impact on European precipitation (Rex, 1951). Over the years, weather regime classification has evolved from subjective methods, like Lamb weather type (Lamb, 1972) or *Grosswetterlage* (Hess and Brezowsky, 1969), to more objective and reproducible approaches, such as in the work from James (2007) and Jones et al. (2014). The most common method of classification is cluster analysis based on empirical orthogonal functions (EOFs) applied to large-scale flow fields, such as anomalies of geopotential height at 500 hPa (GH500) or mean sea level pressure (James, 2007; Michelangeli et al., 1995). The classification of weather regimes involves the attribution of clusters of EOFs to 4-20 weather categories, which are named after the prominent air mass location and the flow direction (anticyclonic

or cyclonic). In many occasions, there are days with weak relation. To avoid transient state changes too frequently, a persistent criterion is applied, typically the regime should last at least 3 to 10 days (Grams et al., 2020). Commonly used weather regimes in Europe include positive/negative NAO (North Atlantic Oscillation), Atlantic Ridge, and European Blocking (Fabiano et al., 2021; Grams et al., 2017; Li et al., 2020).

Weather regimes offer predictability potential through their connections with the stratosphere and teleconnections with phenomena such as ENSO (El Niño–Southern Oscillation). In particular, there is a clear relation between the activity of stratospheric polar vortex and the state of NAO (Beerli and Grams, 2019). Coupling stratosphere–troposphere can increase the skill of numerical weather forecast of four weather regimes by 10–30% in the North-Atlantic basin (Charlton-Perez et al., 2018). This is the foundation of seasonal forecast with medium-range (up to 16 days) (Matsueda and Palmer, 2018) and a few days ahead forecast (Vitart and Robertson, 2018). Additionally, teleconnection such as ENSO and NAO can be used in forecasting weather regime (Beerli and Grams, 2019; Herceg-Bulić et al., 2017; Oehrlein et al., 2019). This predictability has many applications in several sectors such as energy, agriculture, water management, and gas trading (Büeler et al., 2020; Grams et al., 2017; Rex, 1951). In order to increase the benefit of this predictability, the cluster classification needs to be robust in representing the weather regimes and the transition to the next condition.

Increasing the number of clusters in weather regime classifications offers several advantages, including finer spatial and temporal variations, better representation of atmospheric variance (Grams et al., 2020), and shorter-term predictability (Boer, 2003). A classification of synoptic weather with more than 20 categories can capture day-to-day variability in atmospheric conditions and enable applications like predicting temperature-related mortality during cold spells or heatwaves (Huang et al., 2020).

Based on the differentiation from Huang et al. (2020) and Grams et al. (2020), in this thesis, *weather regimes* refers to classifications with 4–7 categories that last a week or more, such as the work from Casou (2008) and Grams et al. (2017). With more categories than *weather regime*, *weather patterns* refers to classifications with 20–30 categories which can capture day-to-day variability in a smaller domain, e.g., the weather pattern classification provided by the German Weather Service (DWD) with 29 patterns (James, 2007), or the classification from the UK MetOffice with 30 patterns (Neal et al., 2016). *Weather type* such as Lamb weather type is similar to weather pattern. But in this thesis, the term *weather pattern* specifically refers to the weather

pattern classification with 29 types from James (2007) that was extensively used in this thesis.

2.2.2 *Synoptic weather in renewable energy*

Synoptic weather conditions have well-known impacts on the surface, including extreme weather events like cold spells and heatwaves (Ferranti et al., 2019). Studies in renewable energy have also highlighted the association between synoptic weather conditions and extreme events in PV and wind power production (Drücke et al., 2020; Grams et al., 2017; Wiel et al., 2019a,b).

Synoptic weather classification offers a valuable tool to comprehend the day-to-day variability in renewable power production. Weather regime classifications are used to define critical weather conditions for wind power temporal variability and wind ramps (Couto et al., 2014; Gibson and Cullen, 2015; Ohba et al., 2016). They are also employed to identify three sub-regions in Europe with distinctive inter-regime behaviour of wind power production: Northern Europe, South-eastern Europe, and Western Mediterranean (Grams et al., 2017). The study also suggests that the surplus wind power potential in the Balkans can potentially complement the wind power deficit in the North Sea.

It is crucial to assess the combined variability of PV and wind power sources as their total production can differ from their individual contributions due to their anti-correlation effect. For instance, amongst European countries, there is less than 10% chance of extremes simultaneously in both PV and wind power (Frank et al., 2020b). Recent efforts have explored the link between synoptic weather condition and anomalies in PV and wind power production in combination, indicating distinctive differences in magnitude of anomalies and spatial distribution in PV and wind power potential associated with four weather regimes based on the NAO index (Wiel et al., 2019a). Atmospheric blocking, characterized by high-pressure systems lasting over 7 days, can lead to prolonged low production events in both PV and wind power (7- and 14-day events) in Western Europe (Wiel et al., 2019b) and in Germany (Drücke et al., 2020). The prolonged period of anomalously high or low temperature (in summer or winter) can also significantly increase the electricity demand (EWI (2021)).

However, classifications of four to seven types of weather regimes are inadequate to comprehensively grasp the variability on timescales shorter than a week (Wiel et al., 2019a). Previous studies have predominantly either focused on low production events (Drücke et al., 2020; Wiel et al., 2019a,b), examined only one type of energy (Grams

et al., 2017), or concentrated only on individual countries (Couto et al., 2014; Drücke et al., 2020). Facilitating electricity transmission across country borders in Europe can alleviate the challenges associated with meeting the variable demand in individual countries with 100% renewable energy systems (Rodriguez et al., 2014). Therefore, to enhance the benefits for energy operation purposes, further research needs to focus on a systematic assessment of the impacts of synoptic weather conditions across Europe with finer temporal and spatial resolution (Maimó-Far et al., 2022).

DATA AND METHODS

The cornerstone of the project is the Renewable Energy Model (REM) of which output are used for further analyses. This model simulates both photovoltaic (PV) and wind power production in Europe at the same spatial and temporal resolution. This method allows to combine these two individual energy types into the total power production, and to further examine its variability based on weather patterns comprehensively. This chapter describes the components used to construct REM and some evaluations on REM's output.

3.1 DATA

In this project, three datasets for the European domain are used. Firstly, the meteorological reanalysis dataset COSMO-REA6 (Bollmeyer et al., 2015) provides essential meteorological variables in PV and wind power simulations. Secondly, the spatial installation of PV and wind power projected for the future scenario (2050) from the climate and energy mix model (CLIMIX) (Jerez et al., 2015a). These two gridded datasets are integrated into the REM, resulting in the output of PV and wind power production (see Section 3.2.1 and 3.2.2). Lastly, the classification of weather patterns by James (2007) (see Section 3.1.3) is then used to investigate the association between synoptic weather patterns and anomalies in renewable power production at the European scale, in various sub-regions and in Germany.

3.1.1 COSMO-REA6

The COSMO-REA6 reanalysis dataset, developed within the Hans-Ertel Center for Weather Research (HErZ) (Bollmeyer et al., 2015), is used extensively in this thesis. It offers a high horizontal resolution of 6 km and comprises 40 vertical layers, covering a period of 23 years from 1995 to 2017. The dataset's high resolution is particularly beneficial for renewable energy analyses. It allows capturing meteorological processes at a regional scale, such as temporal variation in site assessment for wind power (Frank et al., 2020b; Henckes et al., 2018) and post-processing dataset of global horizontal irradiance for PV power applications (Frank et al., 2018).

COSMO-REA6 is a reanalysis dataset (REA) (Bollmeyer et al., 2015) developed based on the numerical weather prediction (NWP) model COSMO (Consortium for Small-scale Modeling¹). The initial and boundary conditions fed into COSMO-REA6 are provided by the global reanalysis dataset ERA-INTERIM (Dee et al., 2011), which has a coarser horizontal resolution of 80 km and 60 vertical layers. The gridded data of COSMO-REA6 conform to the CORDEX EURO-11² (Giorgi et al., 2009) specifications with a rotated pole projection, as shown in Fig 3.1. The reanalysis process in COMOS-REA6 uses the 4D-Var (4-dimensional variational) data assimilation technique (Navon, 2009). This technique adjusts (or nudge, Schraff (1997)) the model state variables towards the observations. In COSMO-REA6, these state variables are pressure, temperature, wind speed, and humidity. The observations assimilated into COSMO-REA6 are from the German Weather Service (DWD) operational database, including data from radiosondes, aircraft, wind profiler, and observations at the surface level (Bollmeyer et al., 2015). Note that no satellite data are directly assimilated into COSMO-REA6 but are indirectly incorporated through ERA-Interim.

In REM, the meteorological variables from COSMO-REA6 used are hourly 2 m-temperature, 10 m wind speed, wind speed at upper levels 36 and 37, equivalent to 116–178 m from sea level (DWD, 2022). Besides, data of hourly surface irradiance (direct and diffused short wave radiation), total cloud cover, and mean sea level pressure are also used for further analyses of the meteorological conditions associated with specific events of interest.

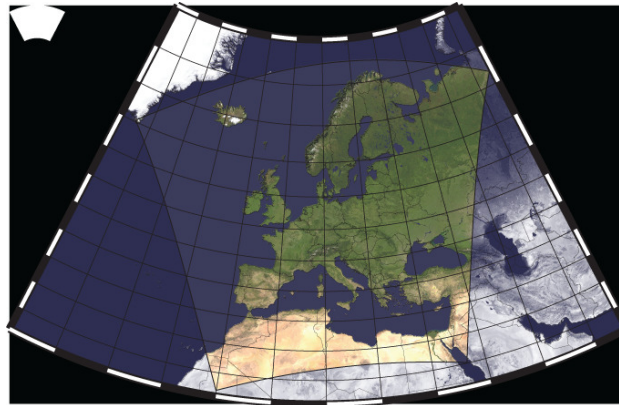


Figure 3.1: Model domain for COSMO-REA6 (Bollmeyer et al., 2015)

¹ www.cosmo-model.org

² www.euro-cordex.net/060378/

3.1.2 CLIMIX model

Information about the spatial distribution of PV and wind power installation is important in modelling their power production, as the impact of weather conditions varies across different regions. However, this information is not publicly available or is often provided at administrative levels, which are too large and heterogeneous to capture the nuances of weather variability. To address this issue, the CLIMIX (climate and energy mix) model, developed by Jerez et al. (2015a), was employed in REM.

CLIMIX offers a realistic gridded dataset representing a feasible spatial distribution of PV and wind power installations in Europe for both current (2012) and future (2050) scenarios (Jerez et al., 2015a). It achieves this by combining information on abundant resources for PV and wind power production, existing power plants, population density, and restricted areas. By using planned installations, CLIMIX extends its simulation to project future PV and wind power installations. One advantage of using CLIMIX is its consistent methodology for modeling both PV and wind power installations. The basic algorithm remains the same for both, but different assumptions are applied for on- and offshore wind power, and for large/centralised or small/decentralised PV power plants. These assumptions are summarised in Table 2.

The primary determinants of the spatial distribution of PV and wind power plants are the availability of resources and forbidden locations (see Table 2). Climate variables, such as 10-m wind speed and surface downward short-wave radiation, play a key role in estimating resource availability. They are derived from a regional climate simulation using the Weather Research and Forecast (WRF) model for the period 2000–2012 with a 0.44° horizontal resolution, nudged and driven by ERA-Interim (Dee et al., 2011). Additionally, a determining factor is integrated into CLIMIX to limit the installation in each grid cell to a maximum of 100%. CLIMIX also has an efficiency filter to ensure that determining factors must exceed certain thresholds for viable installations, see details in Table 2. Data for land use in CLIMIX, e.g. cities and forest, are based on the US Geological Survey's classification.

For PV power, large power plants are defined based on installed capacity, for instance, larger than 2 MW for Europe and 1 MW for France, while the remaining installations are classified as small power plants. The ratio of small to large PV power plants is 1.4:1, assumed to be proportional to population density for European countries and remaining constant over time. For wind power, separate assumptions are applied for offshore and onshore power plants. Their data are

Table 2: Summary of the main factors determining the spatial distribution of the renewable installations (adapted from Jerez et al. (2015a)). For a grid cell to be considered suitable for installation, the determining factors must exceed the threshold in the corresponding efficiency filter.

		Determining factor	Forbidden location	Efficiency filter [percentile]
PV power installations	Small	Resource x population	Forest Sea	30 th
	Large	Resource	Forest Cities Sea	30 th
Wind power installations	On-shore	Resource/population	Forest Cities Sea	30 th
	Off-shore*	Resource	Land	50 th

*Offshore wind power installations have one additional determining factor, namely the maximum distance to the coastline is one grid cell.

provided separately, see more in Table 2. For further details on the CLIMIX model, refer to Jerez et al. (2015a).

CLIMIX data were obtained through personal communication with the author of Jerez et al. (2015a). The dataset was provided for two scenarios 2012 and 2050 for EU-27 countries including the UK. However, the data for PV power installation in 2012 are incomplete, available for only nine European countries. Therefore, for consistency, only the scenario for 2050 was used to project PV and wind power in the future. This scenario projects a total installed capacity of 879 GW for PV power and 440 GW for wind power (on- and offshore). As of the time of this thesis (2023), this scenario is considered conservative. For instance, an outlook from the European Commission published in 2020 suggests a higher projected installations for European PV and wind power in 2030, with 872 GW and 620 GW, respectively (JRC, 2020).

3.1.3 Weather pattern classification

Analysing synoptic weather conditions is suitable to assess the anomalies of renewable energy at daily up to weekly time scale (Grams et al., 2017), given its spatial scale of 1000 km and temporal scale of several days. To evaluate the impact of synoptic weather conditions on

renewable energy, it is important to adopt an appropriate method for classifying these weather patterns³. The criteria include focusing on the Europe domain, offering a consistent method of classification, and being available for a substantial period of time. In this thesis, the objective weather pattern classification developed by James (2007) is selected as a well-established classification provided by the German Weather Service. It is built upon the *Grosswetterlagen* classification by Hess and Brezowsky (1969), but offers the advantage of an objective methodology and a broader domain over Europe and the North East Atlantic (James, 2007).

The weather pattern classification uses two meteorological variables: mean sea level pressure (MSLP) and geopotential height at 500 hPa (GH500) representing the steering flow. Climate composites are based on ERA40 reanalysis data (Uppala et al., 2005) from September 1957 to August 2002 and ECMWF operational analyses from August 2002 onward. To account for seasonal differences, the annual cycle is split into two halves according to the maximum and minimum anomalies of climatological means for MSLP and GH500. The winter part identified by this method is slightly longer than the summer part but for simplicity, the years are split equally into two half-year seasons, namely, winter from 16th October to 15th April (with maximum anomalies in mid-winter), and summer from 16th April to 15th October (with minimum anomalies in mid-summer). The composite means of MSLP and GH500 of the domain are then calculated separately for winter and summer. This weather pattern classification focuses on persistent conditions lasting at least two days and filters out transient conditions that last only one day.

The algorithm in the weather pattern classification uses two nested spatial domains, as illustrated in Fig 3.2. Within the initial domain 20°N–85°N, 84°W–75°E, the root mean square anomaly values of MSLP and GH500 are normalised against the mean values of the entire domain. The standard deviations of MSLP and GH500 for all weather patterns are weighted by their annual frequency of occurrence. These standard deviations were averaged across both winter and summer periods, then their 0.75 values are defined as the outer domain. The outer domain extends further to the north and west, covers parts of the Northern Atlantic, as depicted by the blue contour in Fig. 3.2. The inner domain was given double weight and was designed to cover regions that exhibit significant variances compared to the composite means of MSLP and GH500 (James, 2007). The result is a domain that covers all the regions within a distance of up to 1,500 km from Berlin, as depicted by the orange area in Fig. 3.2,

³ A detailed explanation on nomenclature of synoptic weather circulation, condition, regime, pattern, type can be found in Section 2.2.

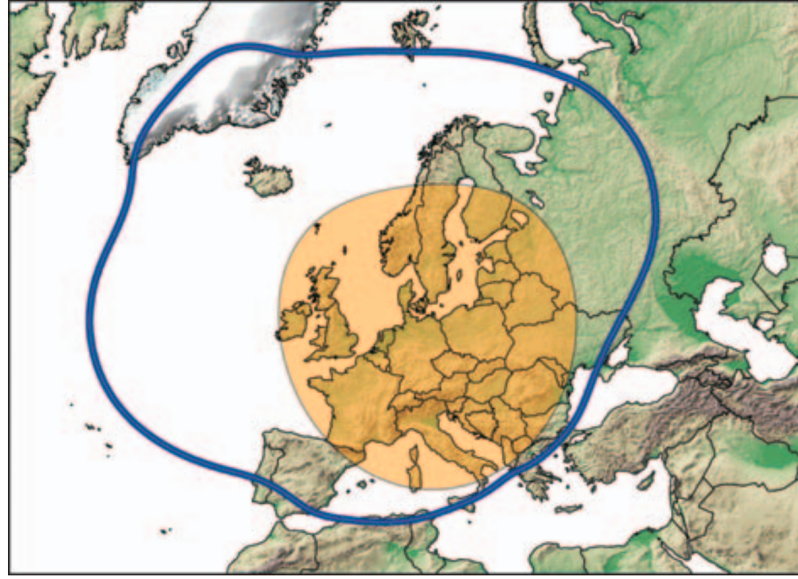


Figure 3.2: The inner (orange shade) and outer (blue circle) domain used to calculate MSLP and GH500 anomalies and to classify weather patterns from James (2007).

effectively capturing the main areas of Central Europe. MSLP and GH500 in the inner domain are used to distinguish between cyclonic and anticyclonic biases in each weather pattern (James, 2007).

The classification distinguishes weather patterns based on the circulation type (cyclonic or anticyclonic characteristic), the wind direction in the inner domain, and the location of the dominant air mass. James (2007) identified 29 types of weather patterns according to these criteria (Table 3). This well-established classification is provided and monitored by the German Weather Service (DWD). Its advantage arises from its capacity to capture the regional variability of meteorological processes in Central Europe (James, 2007), making it suitable to analyse the meteorological variability of PV and wind power production in this thesis. Note that the weather pattern classification provides one pattern every day across the entire Europe.

3.2 THE RENEWABLE ENERGY MODEL

The Renewable Energy Model (REM) is developed to investigate the impact of synoptic weather patterns on photovoltaic (PV) and wind power production in Europe at a finer temporal and spatial resolution than the conventional country-aggregated methods. REM uses the reanalysis dataset COSMO-REA6 (Bollmeyer et al., 2015) with a high horizontal resolution of 6 km and hourly temporal resolution. To reduce the computational time while preserving the high-resolution benefits, the energy output is generated at every 8th grid cells, re-

Table 3: Names of 29 weather patterns used in this thesis, adapted from James (2007)

	Weather pattern	English name	Characteristic
1	Wa	Anticyclonic Westerly	anticyclonic
2	Wz	Cyclonic Westerly	cyclonic
3	Ws	South-Shifted Westerly	cyclonic
4	Ww	Maritime Westerly (Block Eastern Europe)	cyclonic
5	Swa	Anticyclonic South-Westerly	anticyclonic
6	SWz	Cyclonic South-Westerly	cyclonic
7	NWa	Anticyclonic North-Westerly	anticyclonic
8	NWz	Cyclonic North-Westerly	cyclonic
9	HM	High over Central Europe	anticyclonic
10	BM	Zonal Ridge across Central Europe	anticyclonic
11	TM	Low (Cut-Off) over Central Europe	cyclonic
12	Na	Anticyclonic Northerly	anticyclonic
13	Nz	Cyclonic Northerly	cyclonic
14	HNa	Icelandic High, Ridge Central Europe	anticyclonic
15	HNz	Icelandic High, Trough Central Europe	cyclonic
16	HB	High over the British Isles	anticyclonic
17	TrM	Trough over Central Europe	cyclonic
18	NEa	Anticyclonic North-Easterly	anticyclonic
19	NEz	Cyclonic North-Easterly	cyclonic
20	HFa	Scandinavian High, Ridge Central Europe	anticyclonic
21	HFz	Scandinavian High, Trough Central Europe	cyclonic
22	HNFa	High Scandinavia-Iceland, Ridge Central Europe	anticyclonic
23	HNFz	High Scandinavia-Iceland, Trough Central Europe	cyclonic
24	SEa	Anticyclonic South-Easterly	anticyclonic
25	SEz	Cyclonic South-Easterly	cyclonic
26	Sa	Anticyclonic Southerly	anticyclonic
27	Sz	Cyclonic Southerly	cyclonic
28	TB	Low over the British Isles	cyclonic
29	TrW	Trough over Western Europe	cyclonic

sulting in the output at a 48 km resolution that effectively represents meteorological processes as in COSMO-REA6.

REM consists of two main components: a PV power simulation, based on the approach by Frank et al. (2020b), and a wind power estimation. The following sections describe how these two components simulate PV and wind power capacity factor (the ratio of power production to the installed capacity) and how they are integrated with the installation data to obtain hourly power production for PV and wind power in Europe. Additionally, evaluations of the model's output against two other datasets are also presented.

3.2.1 *The PV power simulation*

The photovoltaic (PV) simulation in this thesis was developed and described in detail by Frank (2019). This simulation uses the shortwave radiation data from COSMO-REA6 to compute the capacity factor in each grid cell. As summarised in Section 2.1.1, simulating PV power includes two steps: (1) the estimation of the solar irradiance received on PV panels⁴; and (2) the conversion of irradiance into power production within the PV panels. The PV simulation in this thesis focuses only on crystalline silicon modules as it is the most common technology in the current market, see Section 2.1.1.

For the first step, REM uses radiation data from COSMO-REA6, namely direct and diffused short-wave radiation at hourly temporal resolution. These radiation data from COSMO-REA6 exhibit a tendency to overestimate values in cloudy conditions and underestimate values in clear sky conditions, compared to the measurements from the Baseline Surface Radiation Network (BSRN) (Frank et al., 2018). An approach proposed by Frank et al. (2018) introduces a post-processing method with a transmissivity threshold for two regimes, "cloudy sky" and "clear sky", in order to reduce these systematic biases. However, to preserve the spatial distribution of the radiation across Europe and thereby of the PV power production, REM uses the original data of radiation from COSMO-REA6 without being undergoing post-processing.

The amount of irradiance reaching PV panels is influenced by two key factors: the orientation of the PV panels and the types of radiation coming to the PV panels. The panel orientation is characterised by two important angles: the tilt angle and the azimuth angle. The tilt angle included in this simulation is determined by maximising the PV power production to obtain the optimal tilt angle, then adjusted by a

⁴ The differences between PV cell, PV panel, PV module, PV array can be found in Section 2.1.1.

constant deviation factor of 0.7 (Saint-Drenan et al., 2018). This reduction in the tilt angle is primarily due to investors' considerations to minimise the shadow effect and maximise power production output per unit of surface (Frank, 2019). For computational reasons, the hourly optimal tilt angle is calculated by maximising the PV power production for the year 2014, before applied to all years in the period 1995–2017. The optimal title angle varies from 21° to 50° within the COSMO-REA6 domain. A sensitivity test concerning the effect of using a single year for tilt angle calculation yields a small difference of 0.35% (Frank, 2019). As for the azimuth angles, it is assumed that the PV panels constantly face southward to optimise the amount of irradiance received.

In terms of the type of incoming radiation, there are three parts of irradiance that can reach the plane of a tilted panel: (i) direct radiation Q_{dir} , which propagates in straight trajectory and is determined using geometric methods, e.g., from Quaschnig (1998); (ii) diffuse radiation Q_{dif} , which, on a titled plane, is calculated using analytic models such as from Klucher (1979); (iii) radiation reflected by the ground Q_R , which is calculated using an isotropic approach, i.e., equal distribution of radiation from all directions of the upper hemisphere. The value of Q_R depends on the global horizontal irradiance and the surface albedo. When the radiation reaches the plane of PV panels, some of it is reflected by the panel's surface. This reflection loss AL is estimated using the empirical method from Martin and Ruiz (2001). In this PV simulation, a constant coefficient of 0.16 (Martin and Ruiz, 2001) is assumed for AL calculations on silicon panels, as established by Urraca et al. (2018b). Consequently, the effective irradiance Q_{eff} available to convert into power within PV panels is calculated as follows:

$$Q_{eff} = (1 - AL) \cdot (Q_{dir} + Q_{dif} + Q_R) \quad (3.1)$$

The second step involves a conversion model for silicon PV panels to estimate the amount of power production converted from effective irradiance Q_{eff} . The efficiency of a PV panel depends on its temperature T_{panel} , which is a function of the ambient temperature, wind speed at the panel's elevation, and the incident irradiance (Faiman, 2008). The coefficients for silicon modules in this calculation is adopted from Koehl et al. (2011). The PV conversion model here was adapted from the empirical model from Huld et al. (2011). The instant deviation $\eta(Q', T')$ is calculated as in the equation 3.2. The main idea is to multiply the instant deviation $\eta(Q', T')$ to the theoretical power production in standard test conditions (STC) Q_{STC} , i.e., with the irradiance of 1000W/m^{-2} and the temperature at 25°C .

$$\eta(Q', T') = 1 + K_1 \ln(Q') + k_2 \left(\ln(Q') \right)^2 + k_3 T' + k_4 T' \ln(Q') + k_5 T' \left(\ln(Q') \right)^2 + k_6 T'^2 \quad (3.2)$$

where $Q' = Q_{\text{eff}}/Q_{\text{STC}}$ and $T' = T_{\text{panel}} - T_{\text{STC}}$.

k_1, k_2, \dots, k_6 are empirical coefficients estimated using a least-square optimisation: $k_1 = -0.17237, k_2 = -0.040465, k_3 = -0.004702, k_4 = 0.000149, k_5 = 0.000170, k_6 = 0.000005$.

Finally, the electricity losses from converters, shadows, snow, dust, and other factors, account for 10% of the total electricity yield (Pfenninger and Staffell, 2016). The final power production converted in PV panels $P(Q', T')$ is calculated as:

$$P(Q', T') = 0.9 \cdot P_{\text{STC}} \cdot Q' \cdot \eta(Q', T') \quad (3.3)$$

To be compatible with the output from REM, the PV power installation data from the CLIMIX dataset are converted from the original grid of 0.11° (approximately 12.5 km) to a 48 km resolution. This means around 4×4 data points from the original CLIMIX dataset fit into one grid cell of REM output. Then the sum of installed capacity in these data points is the installed capacity of PV power for each REM grid cell. The average installed capacity of PV power in REM grid cells is 510 MW. To obtain the PV power production for each new grid cell (48 km), this installed capacity is multiplied with the capacity factor at the corresponding grid cell. For more details on how different components were put together to simulate PV power capacity factor, see Frank (2019).

3.2.2 The wind power simulation

REM uses wind speed data from COSMO-REA6 at the vertical levels 36 and 37 (the 4th and the 3rd level from the ground), approximately at the height of 116 to 178 m above sea level (DWD, 2022). Data of wind speeds at hub height from COSMO-REA6 are shown to be beneficial for wind energy applications (Brune et al., 2021). To establish wind speeds at specific hub heights corresponding to CLIMIX wind turbines, linear interpolation is applied to wind speeds from levels 36 and 37, as shown in equation (3.4). Then the capacity factor for wind power is calculated by applying the cubic law to the wind speed at hub height, as shown in equation (3.5). The wind power production is calculated by multiplication with the installed capacity.

$$v_{\text{hub}} = \left(\frac{h_{\text{hub}} - h_{37}}{h_{36} - h_{37}} \right) (v_{36} - v_{37}) + v_{37} \quad (3.4)$$

where

- $h_{\text{hub}}, v_{\text{hub}}$ are hub height and wind speed at that height, $v < 0$ when $h_{\text{hub}} < h_{37}$
- $h_{36}, h_{37}, v_{36}, v_{37}$ are the heights of level 36 and 37 and their corresponding wind speed

$$\text{CF} = \frac{v_{\text{hub}}^3 - v_{\text{cut-in}}^3}{v_{\text{rated}}^3 - v_{\text{cut-in}}^3} \quad (3.5)$$

where

- CF is capacity factor
- v_{hub} is wind speed at the hub height
- $v_{\text{cut-in}}, v_{\text{cut-out}}, v_{\text{rated}}$ are the wind speeds at which a wind turbine starts operating, stops operating, and achieves maximum output (installed capacity). In REM, these parameters are 3.5, 25, and 13 m/s, respectively.

The CLIMIX dataset provides detailed information on the installed capacity and hub height of individual wind power plants at a horizontal resolution of 12.5 km. Unlike the aggregation approach for PV power, the CLIMIX dataset contains multiple wind turbine clusters (data points) within a single grid cell. Each cluster contains various wind power plants with different capacities and hub heights, making a straightforward sum or average in each cluster unsuitable. Instead, multiple layers of hub heights are identified from CLIMIX, resulting in 71 layers for the wind power installation in 2012, and one additional layer for the installation in 2050 (150 m for offshore wind power). Wind power capacity factors and associated power production are calculated individually for each layer, before summed up to obtain wind power production of that grid cell. This procedure was applied to the installed capacities in 2013 and 2050 separately, before summing them up to obtain the total wind power production in 2050. After aggregated into REM grid cells, the average hub height from CLIMIX is 99 m, and the average installed capacity is 187 MW.

3.2.3 Model evaluation

Data

In order to evaluate the performance of REM, comparative analyses are conducted with other renewable energy datasets obtained from Climate Data Store (CDS)⁵ and Renewables Ninja⁶. The CDS dataset (Copernicus Climate Change Service, 2020) uses the reanalysis dataset ERA5 (Hersbach et al., 2020) to simulate gridded data for capacity factor, energy, and mean power at a horizontal resolution of 0.25° , approximately 28 km, in Europe with an hourly temporal resolution available from 1979 to present. Note that for European domain, COSMO-REA6 and ERA5 have different domain borders and grid configurations, as shown in Fig. 3.3. ERA5 uses a reduced Gaussian grid (Hersbach et al., 2020), while COSMO-REA6 uses a rotated grid (Bollmeyer et al., 2015). The second dataset for evaluation, Renewables Ninja (Pfenninger and Staffell, 2016; Staffell and Pfenninger, 2016), simulates PV and wind power data using the global reanalysis dataset MERRA-2 (Gelaro et al., 2017) and satellite observations such as SARAHI (Müller et al., 2015). MERRA-2 has a horizontal resolution of 0.625° longitude and 0.5° latitude, translating to roughly 60 km in Europe. The Renewables Ninja dataset provides hourly time series of country-aggregated capacity factors for EU-28 countries plus Switzerland and Norway during the period 1980–2019.

To ensure a consistent evaluation of PV and wind power data across three datasets, potential capacity factors, ranging from 0 to 1, are used because they reflect the meteorological variability without influenced by different installed capacities in these datasets. Four countries—Norway, Germany, Czech Republic, and Spain—were selected for comparison due to their varying latitudes, resulting in diverse irradiance and wind regimes. Within each country, the potential capacity factors were spatially averaged on hourly basis, resulting in time series of hourly capacity factors for the period 1995–2017. The evaluation focuses on onshore wind power and excludes offshore wind power. In REM, the potential capacity factors for PV and wind power onshore are calculated in similar manners as described in Sections 3.2.1 and 3.2.2 without integrating installation data from CLIMIX. Corresponding variables from CDS include capacity factors for *Solar photovoltaic power generation* and *Wind power generation onshore*. Corresponding variables from Renewables Ninja include *PV national current* and *Wind national current* (or *Wind onshore current* in Germany and Spain).

⁵ <https://cds.climate.copernicus.eu/cdsapp#!/dataset/sis-energy-derived-reanalysis>

⁶ www.renewables.ninja

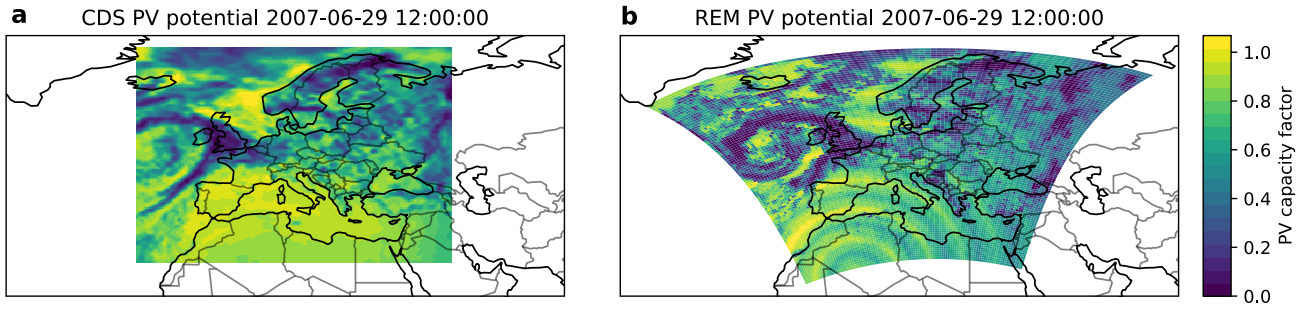


Figure 3.3: PV power capacity factor in European domain at 12:00 2007-06-29 from (a) CDS data, (b) REM data, plotted using the same projection conic and equal-area (PlateCarree). Note that the concentric circles appear at the bottom of (b) arised from sun position computation scheme. To save computational time, the sun position is defined in step of a few hours instead of hourly (Frank, 2019). This effect is canceled out when averaged over periods longer than a day.

The results of this comparative analysis are presented in Table 4, Fig. 3.5, 3.6, and 3.8.

The time sampling of the radiation data differ in COSMO-REA6, ERA5, and MERRA-2 datasets in terms of how the values are aggregated and the time coordinates are assigned. For instance, after averaging instantaneous short-wave radiation data during an interval of one hour from 16:00 to 17:00, in COSMO-REA6 the hourly data are assigned at 16:00 (DWD, 2022), while in ERA5 the hourly data are assigned at 17:00 (Hersbach et al., 2023), and in MERRA-2 the data are assigned at 16:30 (GES DISC, 2015). These time discrepancies are also shown in the PV power potential data in REM, CDS, and Renewables Ninja, illustrated by the differences in their zenith times on a clear-sky day in Fig. 3.4a. These temporal disparities are addressed through time offsets in order to compare the datasets at matching times. The time coordinates in REM are offset by a negative one-hour with respect to CDS data, and a negative half-hour with respect to Renewables Ninja data. After adjusting the time coordinates, the diurnal influence on the discrepancies across PV power data from REM, CDS and Renewables Ninja reduced significantly, as shown in Fig. 3.4c,e compared to the original data in Fig. 3.4b,d. Note that these time offsets were applied only for evaluations on PV power potential within this chapter, while the original data retained for other analyses throughout the thesis.

Luxembourg 1995--2017

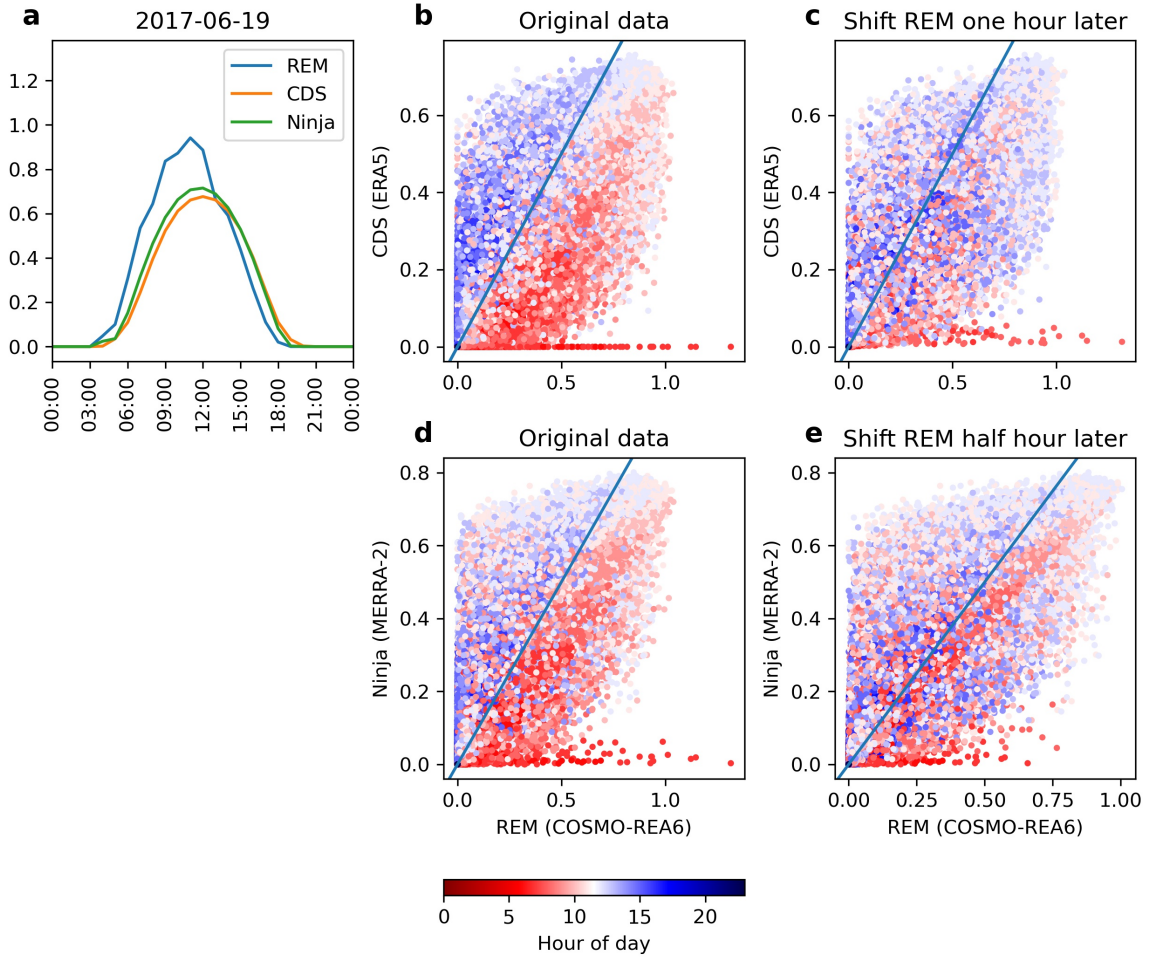


Figure 3.4: Offset in the time coordinates in PV power data illustrated for Luxembourg for the period 1995–2017 (a) Difference in zenith time in PV power potential between REM (using COSMO-REA6), CDS (using ERA5), and Renewables Ninja (using MERRA-2) on 2017-06-19; (b) Comparison PV power potential between REM and CDS; (c) similar to (b) but shifting REM data one hour later; (d) Comparison PV power potential between REM and Renewables Ninja; (e) similar but shifting REM data half hour later. Luxembourg was selected because its small size reduces the regional variation in its irradiance data.

Results

The three datasets—REM, CDS, and Renewables Ninja—show strong correlations (Fig. 3.5), with Pearson correlation coefficients between REM and CDS ranging from 0.88 to 0.91 for PV power, and slightly higher for wind power onshore, with values between 0.91 and 0.96. The Pearson correlation coefficients between REM and Renewables

Table 4: Temporally averaged potential capacity factors for PV and wind power onshore in four selected countries during 1995–2017 from REM, CDS, and Renewables Ninja. Values are rounded to two decimal digits. Compared to corresponding values from REM, lower values from CDS and Renewables Ninja are in red, equal values are in black, and higher values are in blue.

	REM		CDS		Renewables Ninja	
	PV	Wind onshore	PV	Wind onshore	PV	Wind onshore
Norway	0.11	0.26	0.09	0.20	0.10	0.27
Germany	0.13	0.28	0.10	0.30	0.13	0.19
Czech Rep.	0.13	0.22	0.11	0.25	0.13	0.22
Spain	0.18	0.21	0.16	0.18	0.17	0.27

Ninja are higher than with CDS data for PV power (0.95–0.98) but slightly lower for wind power onshore (0.75–0.94).

For PV power, REM consistently yields higher potential capacity factors compared to CDS and Renewables Ninja data for all four countries (Table. 4, Fig. 3.5). This is attributed to the higher values of capacity factors in REM, such as values larger than 0.75 for Spain, which are rare in the other two datasets (Fig. 3.5g). The discrepancy cannot be solely explained by the bias in irradiance data, as COSMO-REA6, used in REM, exhibits a negative bias when compared to ERA5 data used in CDS (Kenny and Fiedler, 2022; Niermann et al., 2019; Urraca et al., 2018a). Instead, the higher horizontal resolution of COSMO-REA6 is likely a contributing factor. At the resolution of 6 km, COSMO-REA6 is able to resolve the small-scale cloud schemes (Bollmeyer et al., 2015) that coarser resolutions do not provide, as in the case of ERA5 with a horizontal resolution of roughly 28 km for Europe. Moreover, smaller grid cells in COSMO-REA6 provide higher chances of cells with clear sky conditions, leading to greater PV power potential, see for instance in Fig. 3.4a. This effect is particularly pronounced in Southern countries with higher irradiance throughout the year, such as Spain (Fig. 3.6g). The systematical appearance of high values in REM’s PV power might also arise from using different modelling parameters (Copernicus Climate Change Service, 2020; Frank, 2019; Pfenninger and Staffell, 2016).

Further investigation of the diurnal and seasonal cycles of the differences across the three datasets show good agreement for PV power values smaller than 0.5 (Fig. 3.6). For capacity factor higher than 0.5, REM yields higher values than CDS from morning until early afternoon across all four countries, regardless of their latitudes (Fig. 3.6a,c,e,g). This discrepancy arises from COSMO-REA6 overestimat-

ing surface irradiance in cloudy conditions and underestimating it in clear-sky conditions compared to observations, due to its aerosol scheme (Niermann et al., 2019; Urraca et al., 2018a). However, this discrepancy cannot be solely attributed to irradiance data, as the countries do not consistently experience more clear-sky conditions in the morning and more cloudy conditions in the afternoon. The smaller grid cell of COSMO-REA6, leading to a higher likelihood of clear sky conditions, is likely a contributing factor. The overestimation from REM is particularly pronounced during the noon hours, coinciding with very high capacity factors associated with clear sky conditions (Fig. 3.6a,c,e,g). Discrepancies in PV power capacity factors between REM and Renewables Ninja data exhibit less dependency on diurnal cycles compared to CDS data (Fig. 3.7). Unlike the comparison with CDS data, REM yields smaller values before-noon time than Renewables Ninja data, except for Spain (Fig. 3.7g).

Regarding the seasonal cycle, the most notable differences arise during summer, with REM consistently yielding higher values than CDS and Renewables Ninja for all four countries (Fig. 3.6 and 3.7b,d,f,h). This seasonal discrepancy is more pronounced in Northern countries like Norway and less pronounced in Southern countries like Spain (Fig. 3.6b and h, respectively). Mismatches between high values from REM and near-zero values in CDS and Renewables Ninja are noticeable, shown as the lines of data points near the lower edges in Fig. 3.6 and 3.7, reminiscent of the irradiance bias observed in COSMO-REA6 when compared to observational data (Frank, 2019). These mismatches likely result from the fact that daylights are simulated in REM earlier than in CDS. For instance, on 15 September, 2017, the capacity factor of PV power in REM exceeded the threshold of 0.01 at 5:00, whereas CDS data exceeded it at 6:00. Conversely, at sunset, REM values fall below 0.01 sooner than CDS, as represented by the vertical lines of points at $x=0$ along the left y-axis (Fig. 3.6b,d,f,h and 3.7b,d,f,h).

For wind power onshore, the three datasets exhibit smaller discrepancies than in PV power, with capacity factors from REM consistently falling between CDS and Renewables Ninja data (Fig. 3.5b,d,f,h). The range of capacity factor values for wind power onshore is similar across all three datasets, except for Renewables Ninja in Norway (Fig. 3.5b). However, their mean values over time differ more significantly compared to PV power, especially for Germany and Spain (Table 4).

The discrepancies vary depending on the country. For instance, Norway and Spain share a similar pattern, where Renewables Ninja yields high capacity factors more frequently and low capacity factors less frequently than CDS data, while REM output falls in between the two

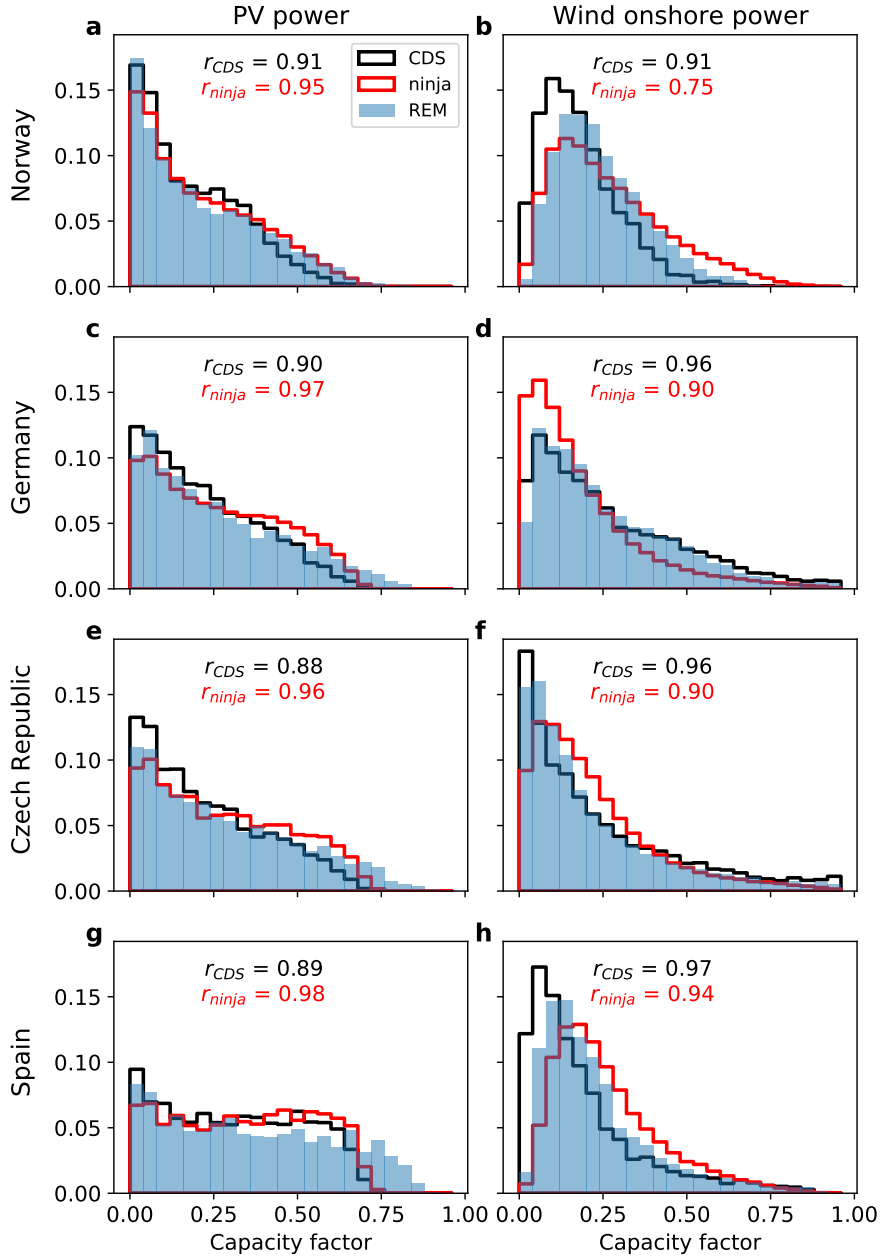


Figure 3.5: Probability density distribution of hourly capacity factors of PV power (first column) and wind power onshore (second column) obtained from REM (filled in blue) compared to CDS and Renewables Ninja data (solid lines in black and red) for four countries in a North to South order. A threshold of 0.01 is applied to filter out very low values of PV power during nighttime. The r -values in each box are the Pearson correlation coefficients between REM and CDS (Renewables Ninja) in black (red) for the period 1995–2017.

(Fig. 3.5b,h). This explains why Renewables Ninja yields larger mean capacity factors for wind onshore power, while CDS yields smaller mean values for these two countries (Table 4). Czech Republic exhibits a similar pattern for Renewables Ninja, but CDS yields very high capacity factors more frequently (Fig. 3.5f), leading to a larger average capacity factor from CDS compared to REM. In contrast, Germany displays a reverse pattern, where Renewables Ninja yields high values less frequently and low values more frequently compared to CDS, but REM output remains in between the two (Fig. 3.5d). These variations contribute to the disparities in average values across the three datasets, namely 0.28 from REM, 0.30 from CDS, and 0.19 from Renewables Ninja (Table 4). The variations in wind power onshore capacity factors likely arise from biases in estimating wind speed from the three reanalyses datasets. For instance, COSMO-REA6 may misrepresent low level jets, mountain and valley breezes compared to observational data (Brune et al., 2021).

In contrast to PV power, the discrepancies in capacity factors of onshore wind power across three datasets do not exhibit a clear dependency on the diurnal cycle (Fig. 3.8a,c,e,g). One exception is observed for Spain, where REM yields lower values in the afternoon and evening compared to CDS and Renewables Ninja (Fig. 3.8g and 3.9g). Similarly, no pronounced difference in three datasets are evidently from the seasonal cycle. All four countries produce higher capacity factors for wind power in winter. In Norway and Spain, REM yields lower capacity factors of wind power compared to CDS data but slightly higher values compared to Renewables Ninja data during the winter months (Fig. 3.8b,h). Whereas, in Germany and the Czech Republic, REM yields slightly higher values around 0.5 in early summer around May compared to CDS data (Fig. 3.8d,f). In Germany, REM yields lower values for the range of capacity factor from 0 to 0.7 in winter compared to Renewables Ninja data (Fig. 3.9d). These discrepancies can be attributed to the differences in wind speed data, as COSMO-REA6 underestimates wind speed compared to observational data and does not adequately represent phenomena like the valley breeze and low level jets (Brune et al., 2021).

3.3 MODEL ASSEMBLE

REM produces data for PV and wind power production by combining three main components: PV power simulation, wind power simulation, and their installed capacities from the CLIMIX dataset (Jerez et al., 2015a). Chapter 3 illustrates how this process is done. The output provides PV and wind power production at 48 km horizontal resolution for Europe at hourly temporal resolution for 23 years (1995–2007)

for all grid cells with available data from CLIMIX, see Fig. ??). Subsequently, REM output is paired with a weather pattern classification from James (2007) to examine the variations of European renewable energy by synoptic weather patterns. Given that the weather pattern classification is available at daily time resolution, the weather pattern data are expanded to hourly resolution by replicating 24 times before pairing them with PV and wind power production data. The REM output, combined with weather pattern classification, serves as the basis for further analyses in the subsequent chapters of this thesis.

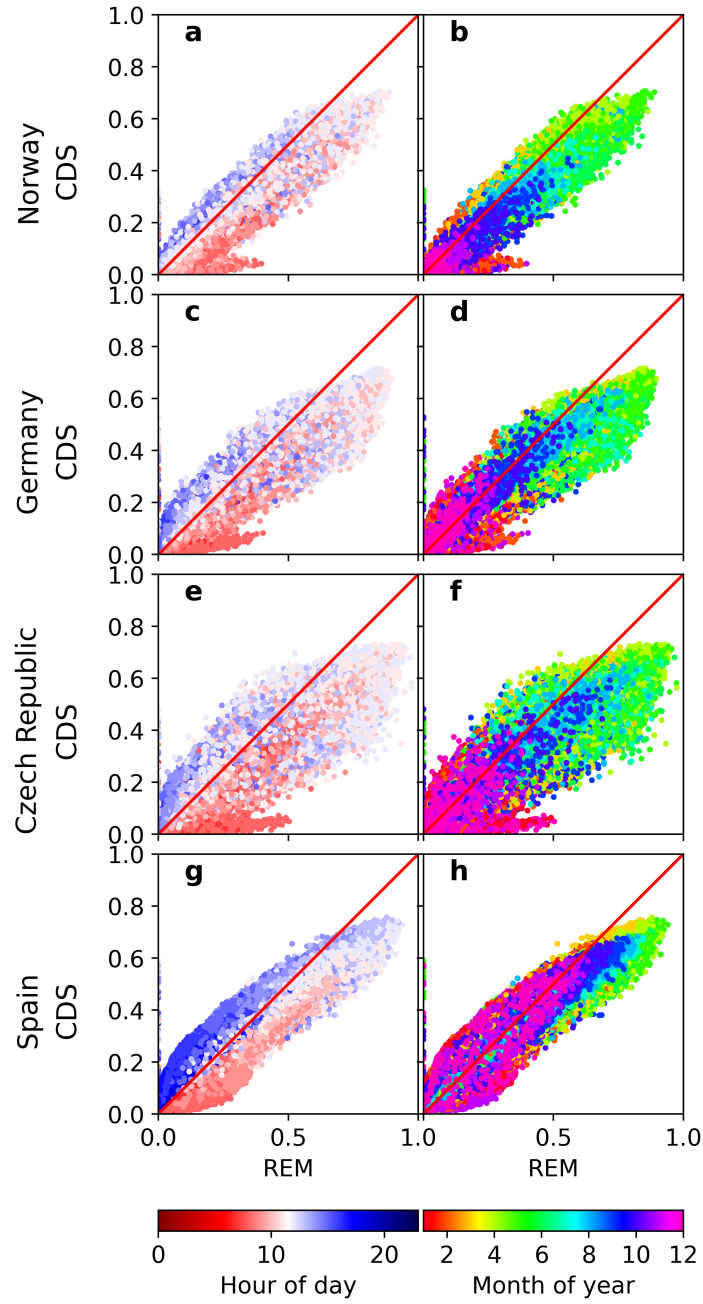


Figure 3.6: Comparison between the potential capacity factor from REM output (x-axis) and from CDS (y-axis) for PV power for four countries in order from North to South for the period 1995–2017. In red is $y = x$ line. Colours mark the hour of day (left column) and month of year (right column). The time coordinate in REM was offset to one hour later due to differences in aggregating radiation data, see details in the main text.

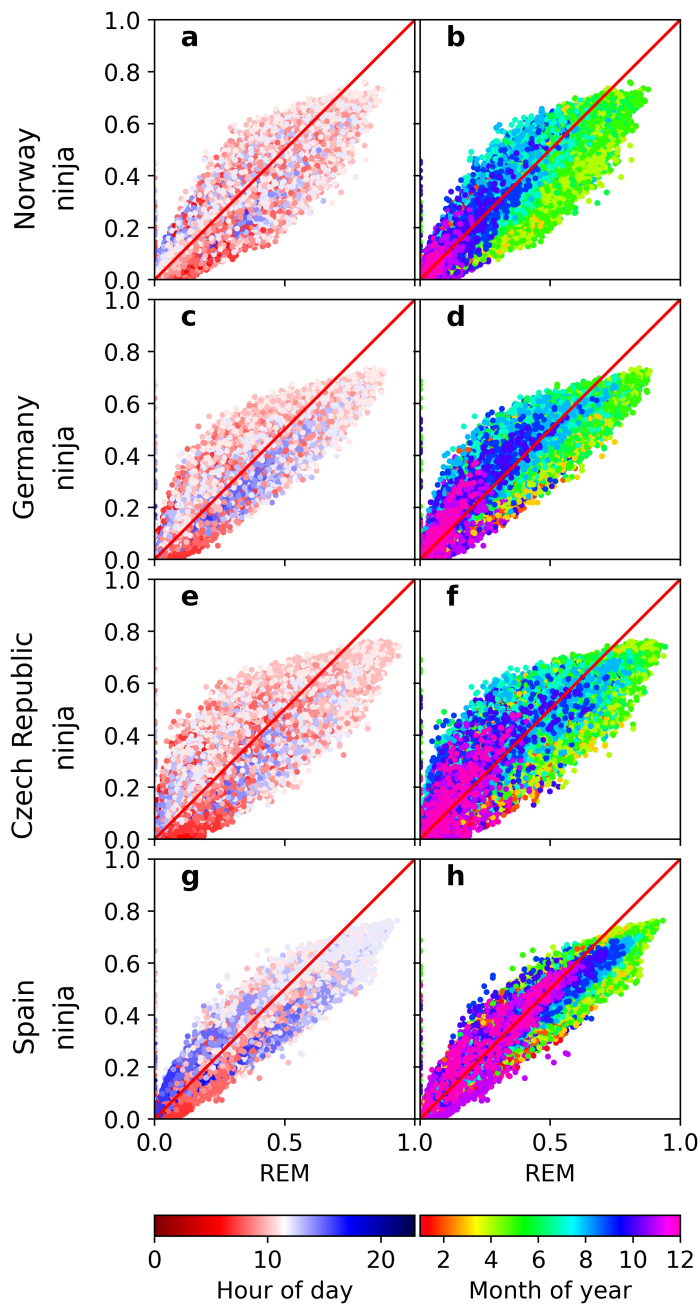


Figure 3.7: Similar to Fig. 3.6 but for Renewables Ninja PV power data against REM's. The time coordinate in REM was offset to half hour later due to differences in aggregating radiation data, see details in the main text.

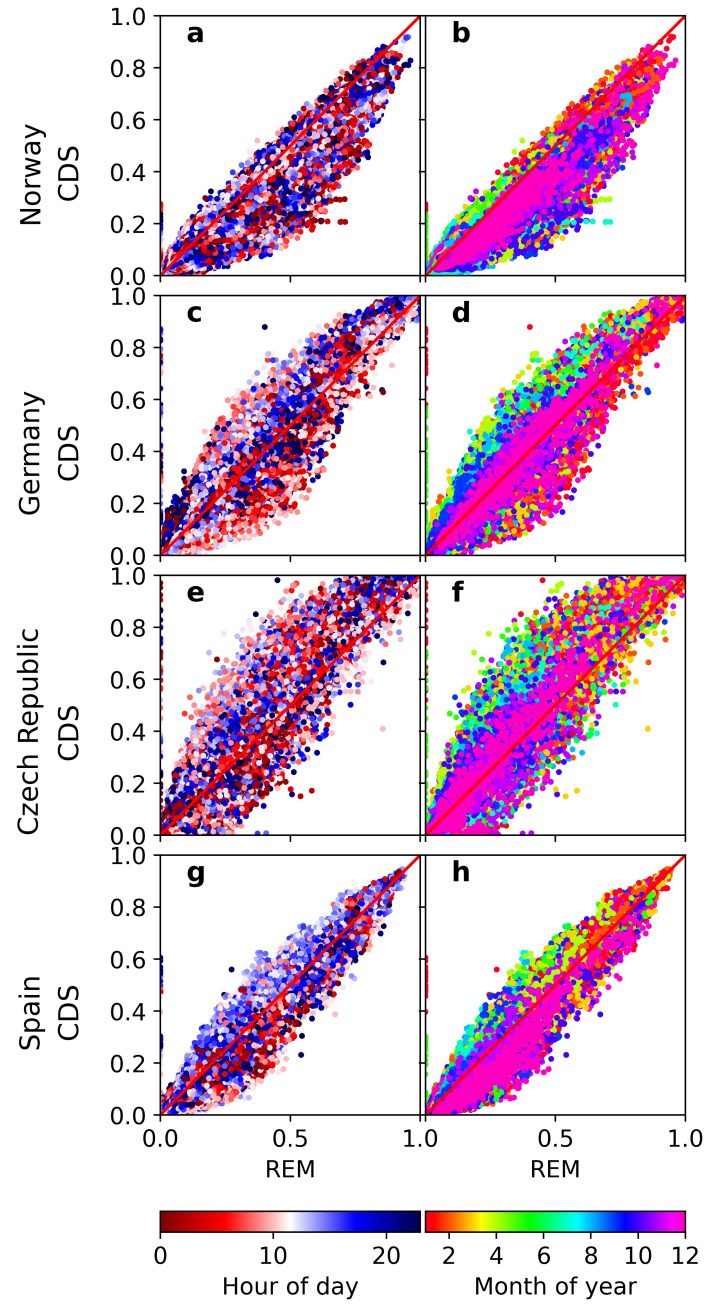


Figure 3.8: Similar to Fig. 3.6 but for wind onshore power in the period 1995–2005.

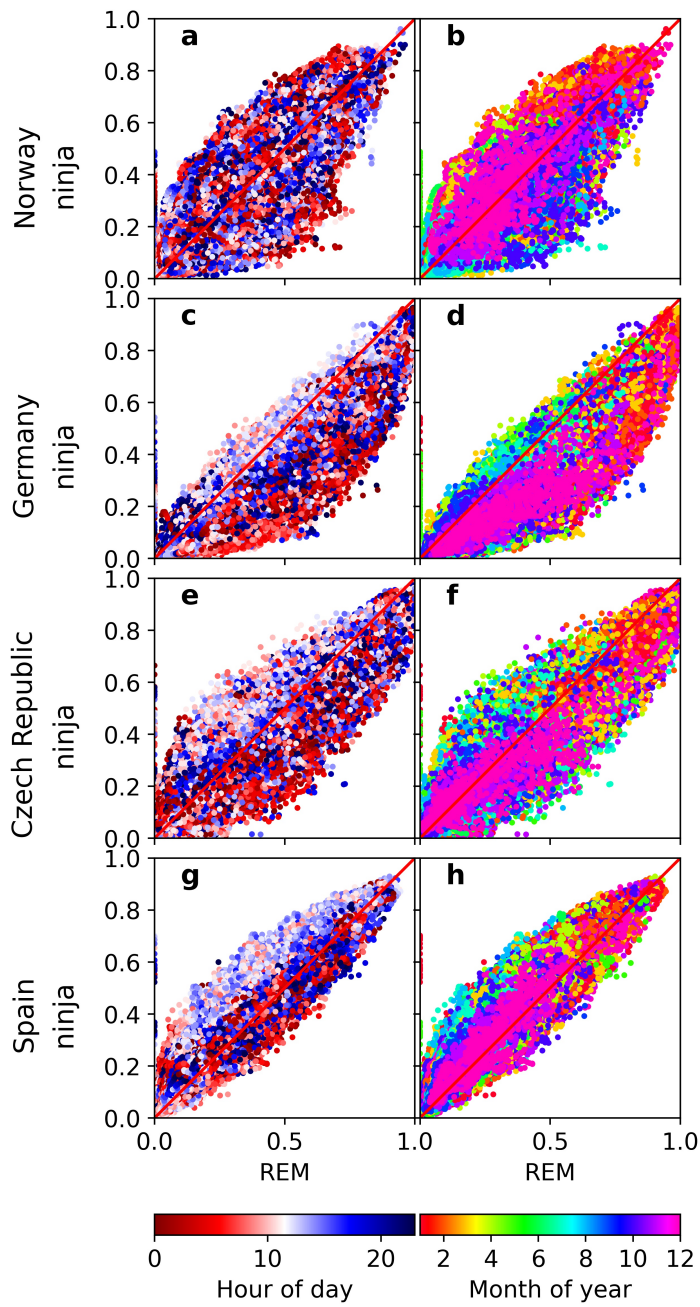


Figure 3.9: Similar to Fig. 3.6 but for wind onshore power Renewables Ninja data against REM's.

STUDIES

4.1 A CLIMATOLOGY OF WEATHER-DRIVEN ANOMALIES IN EUROPEAN PHOTOVOLTAIC AND WIND POWER PRODUCTION

The first study addresses the anomalies of wind and photovoltaic power production in Europe under different synoptic weather conditions and how they might change with future installed capacities. It features a climatology of these anomalies associated with a weather pattern classification of 29 types.


This study has been published as referenced below and is included subsequently in the journal layout. Its Supplementary material is included in the Appendices.

Ho-Tran, L. and Fiedler, S., 2024. A climatology of weather-driven anomalies in European photovoltaic and wind power production. *Communications Earth Environment*, 5(1), p.63.

The content of this section is published under a Creative Commons Attribution 4.0 International License.

Author contributions: L.H. designed and ran the model experiments, analysed the results, and created the figures. S.F. conceived the concept and led the study. Both authors wrote and reviewed the manuscript.

A climatology of weather-driven anomalies in European photovoltaic and wind power production

Linh Ho-Tran^{1,2}  & Stephanie Fiedler^{1,2,3}

Weather causes extremes in photovoltaic and wind power production. Here we present a comprehensive climatology of anomalies in photovoltaic and wind power production associated with weather patterns in Europe considering the 2019 and potential 2050 installations, and hourly to ten-day events. To that end, we performed kilometer-scale numerical simulations of hourly power production for 23 years and paired the output with a weather classification which allows a detailed assessment of weather-driven spatio-temporal production anomalies. Our results highlight the dependency of low-power production events on the installed capacities and the event duration. South-shifted Westerlies (Anticyclonic South-Easterlies) are associated with the lowest hourly (ten-day) extremes for the 2050 (both) installations. Regional power production anomalies can differ from the ones in the European mean. Our findings suggest that weather patterns can serve as indicators for expected photovoltaic and wind power production anomalies and may be useful for early warnings in the energy sector.

¹Institute of Geophysics and Meteorology, University of Cologne, Cologne, Germany. ²GEOMAR Helmholtz Centre for Ocean Research Kiel, Kiel, Germany.

³Faculty of Mathematics and Natural Sciences, Christian-Albrechts-University of Kiel, Kiel, Germany. ✉email: Lho@geomar.de

European countries are collectively facing pressing challenges in securing electricity supply with an increasing share of renewable energy. One of the challenges is the dependency of wind and solar power on the weather, which is especially critical when one or both power productions are anomalously low due to adverse weather conditions. The weather dependency is expected to increase in the future as the European Union plans to produce more energy from renewable sources to become climate-neutral by 2050¹. Therefore, it is important to study which weather conditions are related to extreme anomalies in wind and solar power production, and how their anomalies are spatially distributed across Europe. Such knowledge can help the electricity system operators to prepare counter-measures, e.g., with an adequate national and cross-border transmission grid for electricity^{2,3} that could make use of natural balancing effects arising from regional weather differences⁴.

Accounting for the weather impacts in energy system analyses has been attracting research contributions from the energy and meteorological perspectives. A few studies have addressed how synoptic weather conditions influence resources for wind and solar power production, but for past power installations or for a certain region only or limited to 1-day anomalies^{5–10}. The definition and classification of synoptic weather conditions varied across studies and often gave insights with some limitations as follows. According to a composite analysis based on sea level pressure, high-pressure systems over central Europe are associated with 1-day low power production¹¹. Others used up to seven weather regimes, i.e., synoptic weather systems that vary on weekly timescales^{7,12}, and show that European blocking high-pressure systems are associated with negative anomalies in renewable power production^{7,9}. Classifications of weather closer to 30 categories represent more details for the day-to-day variability and regional differences in the weather¹³. Higher spatial resolution and the analogy to meteorological charts make using weather patterns more applicable for electricity system operators. To the best of our knowledge, there is no study addressing this need with the necessary spatio-temporal detail using projected future installed capacities for photovoltaic (PV) and wind power production paired with a systematic assessment of power anomalies across Europe that have durations of one to up to ten days. Our study aims to contribute to filling this knowledge gap. The different duration of production anomalies is relevant since the security of supply depends not only on the daily power production but also on the load of storage capacities that are influenced by the sequence of weather over several days⁹, e.g., investigated with an energy-system model for Germany¹⁴.

This study presents to the best of our knowledge the first comprehensive kilometer-scale assessment of the effects of weather patterns on the spatiotemporal anomalies in PV and wind power production of different lengths for present and projected future installations in Europe. To that end, we have developed the Renewable Energy Model (REM) that simulates PV and wind power production using hourly meteorological data for 23 years (1995–2017) with an effective horizontal resolution of 6 km. We implemented gridded scenario data for installed capacities of PV and wind power for 2050¹⁵, which was not done for past assessments for power production anomalies associated with different weather patterns^{6,7,10}. Using gridded data is, however, important for assessments of weather and climate influences on the energy system¹⁶. Specifically, a kilometer-scale hourly resolution is important for the link between weather and power production because such an approach is substantially closer to the typical scales for energy applications, which cannot be accomplished with the often country-aggregated assessments in past studies^{4,6,7,10}. To investigate how power production anomalies are associated with different weather patterns and how the

dependency changes with the projected future power installations, we perform and inter-compare several REM simulations. Most of our results are based on the following two REM simulations (see Methods for details):

- Scenario-2050 is the REM simulation with the CLIMIX¹⁵ scenario for PV and wind power installations for 2050. This scenario reflects a substantial increase in the share of PV power production compared to 2019¹⁷. REM yields a share of the PV power production to the PV plus wind power production of 46%, which falls within the range of the suggested optimal share of 45–57% to minimize the spatial variability by changing weather and seasonal variability in power production^{4,18}.
- Scale-2019 is the REM simulation where we scale the installed capacities from scenario-2050 with constant values to match with the Europe-aggregated installed capacity of PV and wind power in 2019¹⁷. The ratio of PV to PV plus wind power production is 24%, which is about half of that in 2050 and similar to other calculations for present-day Western Europe¹¹. Our approach retains the spatial distribution of 2050 and decreases the magnitude of installations by multiplying scaling factors. This choice was made due to the lack of a gridded dataset for present-day installed capacity with a 6 km resolution. The results proved useful for our assessment and successfully reproduced past results for Germany with present-day capacities⁶.

The output of the REM simulations is paired with an established classification of 29 synoptic weather patterns from the German Weather Service¹⁹. This daily weather classification is based on an automated identification algorithm of patterns in charts of the mean sea-level pressure and the 500 hPa geopotential height. An expert control ensures the quality of the automatically identified weather pattern¹⁹. The classification data allows us to examine the weather dependency of future installed capacities for wind and PV power associated with different weather patterns for Europe using quality-controlled weather patterns of the past. Using synoptic weather patterns is desirable since this method is well established and routinely diagnosed as weather service. Our results point to specific weather patterns for anomalously low PV plus wind power production in Europe depending on the installation and event duration. For instance, the lowest hourly PV plus wind power productions are simulated during weather patterns with very regionally low wind speeds for the present-day installation while weather patterns for dark doldrums coincide with the lowest wind plus PV production for the 2050 installation, consistent with the higher share of PV power in 2050. Ten-day events with the lowest wind plus PV power production are associated with prolonged anticyclonic weather patterns for both installations. As such the weather pattern could give a first indication of whether power production anomalies are to be expected with the coming weather for a future PV and wind power installation—an aspect of growing importance when we move from primarily fossil fuel-based power technologies to an increasing share of renewable sources for climate change mitigation.

Results

European mean power production. We find substantial differences in the European PV plus wind power production (hereafter total production) depending on the weather pattern. Wind power production has a prevalent impact on the total output independent of the installed capacities with onshore and offshore installations typically having equal contributions. This can be

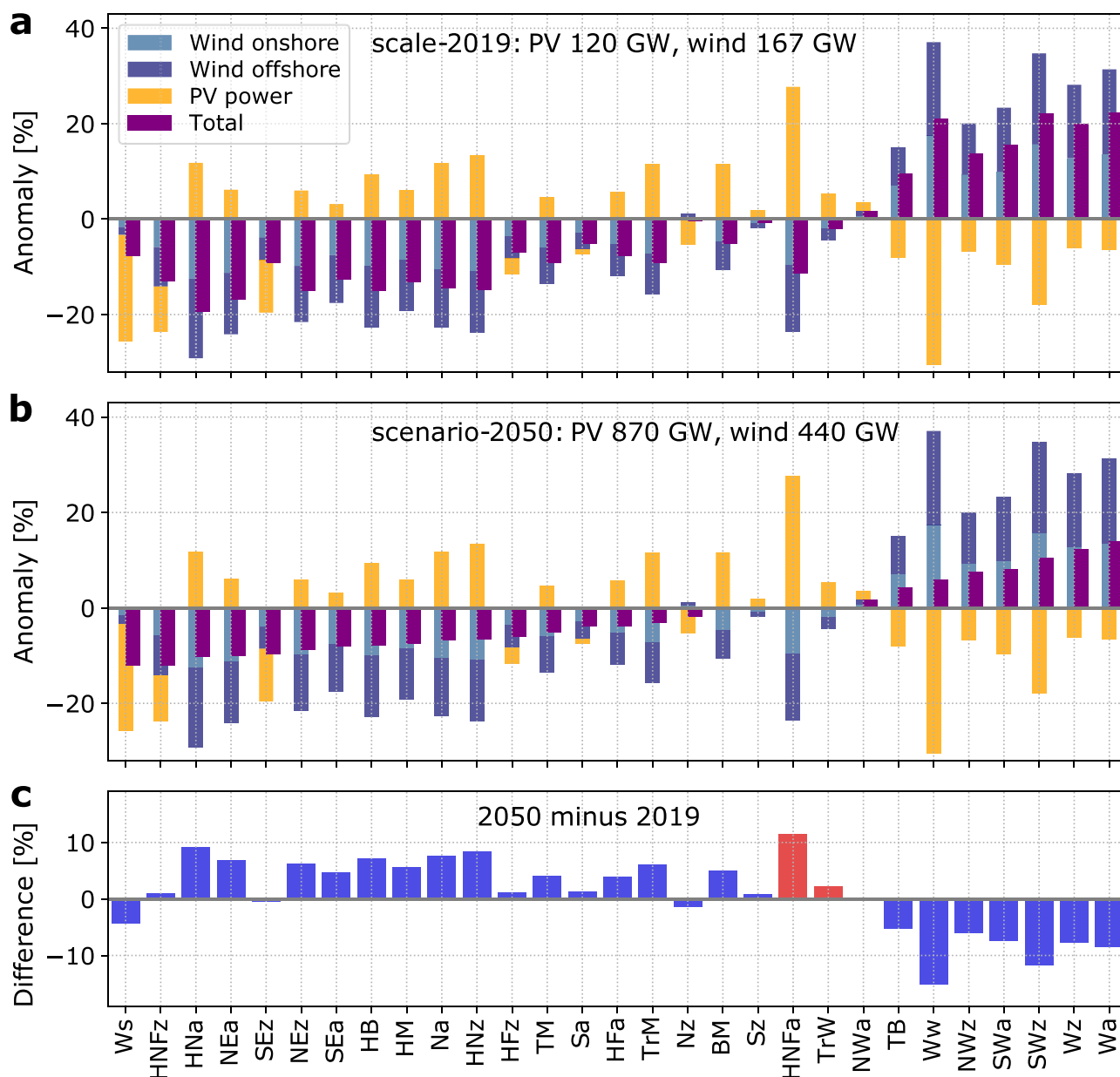


Fig. 1 Anomalies in power production associated with weather patterns in Europe. Anomalies in photovoltaic (PV), offshore, and onshore wind power production (stacked) as well as PV plus wind power (total) associated with weather patterns as simulated by (a). scale-2019 and (b). scenario-2050. Differences in the anomalies of total production associated with different installed capacities are shown as (c). scenario-2050 minus scale-2019. Red bars in (c). mark weather patterns where the sign of the anomaly depends on the installed capacities. Results in (a–c) are sorted by increasing total production from left to right based on scenario-2050 in (b).

seen from the similar behavior of anomalies in wind power production and total power production across weather patterns (Fig. 1a, b). Seven out of eight weather patterns with westerly winds, indicated by the letter W in the name, have a composite European total production higher than the climatological mean for 1995–2017 (Fig. 1a, b). The only exception is the South-Shifted Westerly pattern (Ws), which has the lowest European total production and will be discussed in detail later. Positive anomalies in PV power production have mostly northerly and northeasterly winds (with letters N and NE). The last character in their names refers to their cyclonic or anti-cyclonic characteristic, i.e., a low-pressure system with cyclonic flow indicated by the letter z (zyklonal in German) and a high-pressure system with anticyclonic flow marked with the letter a¹⁹. Nine out of thirteen weather patterns associated with anomalously high PV power

production have an anticyclonic characteristic, typically associated with anomalously high irradiance due to lower cloud cover (Fig. 1a, b). Values of power production anomalies associated with the weather patterns along with their names can be found in Supplementary Table S1.

Our results for scale-2019 installed capacities are consistent with earlier findings for Germany⁶. We see that the pattern of High pressure over Central Europe (HM) is associated with the lowest total production for Germany (see Supplementary Fig. S1). In the European mean, however, HM is associated with the 7th lowest total power production and is, therefore, less extreme when we assess a much larger area. From the European perspective, extremes in power production in single countries can theoretically be balanced with production in other countries in most cases⁴, and this is also true for production shortages in the German energy system¹⁴.

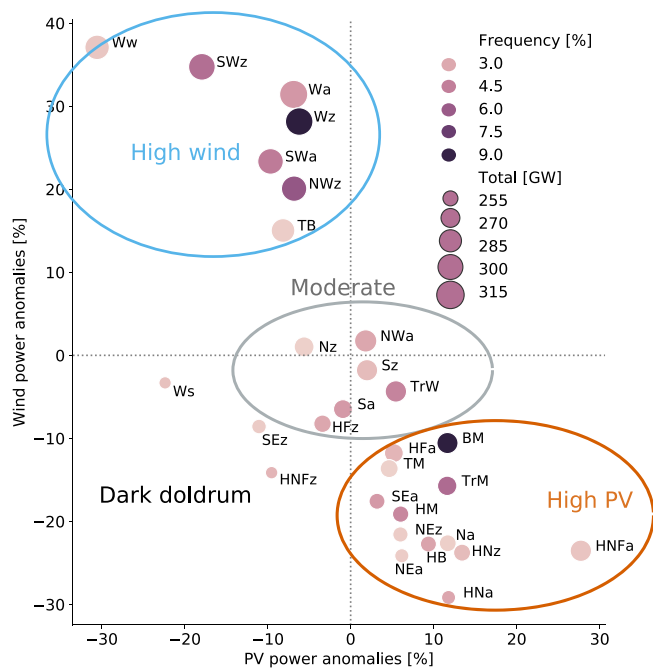


Fig. 2 Grouping of power production anomalies in Europe. Anomalies of wind power production against that of PV power production for each weather pattern based on scenario-2050. The color of the dots marks the frequency of occurrence and the size is proportional to the European mean total production in scenario-2050 installation. Circles mark the groups of weather patterns as used in the text. For the results of smaller sub-regions in Europe, refer to Supplementary Fig. S2.

For the majority of weather patterns, we see an anti-correlation between the European mean of the PV power production and wind power production, i.e., weather patterns associated with positive anomalies in wind power production typically coincide with negative anomalies in PV power production and vice versa (Fig. 2). This anti-correlation can be used to separate weather patterns into four groups of similar behavior determined by visual inspection of Fig. 2 for scenario-2050. The group High wind is the composite of anomalously high wind power production paired with anomalously low PV power production. All weather patterns in the group High wind have positive anomalies in the total power production and taken together occur 33% of the time. The group High PV summarizes weather patterns associated with anomalously low wind power production paired with anomalously high PV power production. Twelve out of thirteen weather patterns in the group High PV have negative anomalies in the total power production, consistent with the dominant influence of the negative wind power anomalies on the total production. This group covers the highest occurrence frequency of 43%. The group Moderate contains weather patterns associated with power production close to the climatological mean and together have an occurrence frequency of 18%. Taken together, weather patterns with below-average mean power production are the most frequent.

The group Dark doldrum occurs only during a small fraction of time (7%). Its weather patterns have simultaneously negative anomalies in PV and wind power production. This group contains three weather patterns: South-Shifted Westerly (Ws), Cyclonic South-Easterly (SEz), and High Scandinavia-Iceland, Trough Central Europe (HNFz), which are amongst the five patterns with the overall lowest total power production in scenario-2050. Although these weather patterns are rare, they are unique in the sense that there is no natural balancing of

anomalies in PV and wind power production as seen for the other groups. Since they lead to anomalously low power production, dark doldrums can potentially be a risk to the security of the power supply. Dark doldrums are therefore seen as extremes relevant for the energy sector but are substantially different from classical meteorological extremes, e.g., storms and floods, that are usually monitored in forecasts to issue warnings.

All European regions experience a dark doldrum at some point in time, but they are differently pronounced in magnitude and can occur with different weather patterns. We define four regions A–D, selected for their high installed capacity, high potentials for PV and wind power, or both (see Methods) to illustrate this point. Weather patterns for dark doldrums in Northern Germany and the North Sea (region B) are similar to those in the European mean. In contrast, in the Northernmost part of Scandinavia (region A), patterns in dark doldrum fall into the group High wind for the European mean, namely SWz, Wz, and NWz. Southern regions on the Iberia peninsula and in Eastern Europe (regions C and D) during winter have relatively larger PV power production than regions further North but can experience strong temporal variation in the wind power production due to the passage of weather systems. This means that in the Southern regions, weather patterns flagged as dark doldrum are more characteristic of a doldrum and are less dark than those occurring further North, e.g., SWa, HNa, Sa, and HFa (Supplementary Fig. S2).

Installation differences. The two different installations lead to changes in the ranking of weather patterns sorted by the magnitude of the associated total power production (Fig. 1a–c). In scale-2019, the ranking of total power production is almost identical to that of wind power, indicating a strong influence of wind power on total production. In scenario-2050, the dominant impact of wind power is still visible but less pronounced. Most weather patterns retain the sign of the power anomaly but the magnitude of the anomalies is weaker. One notable exception is High Scandinavia-Iceland with Ridge Central Europe (HNFa) with the highest change of total production anomaly, due to the larger influence from the highest anomaly of PV power (Fig. 1c).

Extremes in total production depend on both the weather pattern and the installed capacities when we assess the anomalously low hourly power production, but this is not true for anomalously high power production. The lowest total production for Europe is seen for the pattern Icelandic High, Ridge Central Europe (HNa, –19%) in scale-2019, primarily explained by the lowest anomaly in mean wind power production. For scenario-2050, however, the same weather pattern is now associated with the 9th lowest total power production for Europe. Instead, the lowest total production for scenario-2050 is seen for South-Shifted Westerlies (Ws, –12%) with an average wind power production paired with an anomalously low PV power production. It reflects the larger influence of PV power in the projected future power installations compared to 2019. The weather pattern for the largest total hourly production, Anticyclonic Westerly (Wa), is identical for the 2019 and 2050 installations. One could additionally expect more shortwave radiation at the surface in some future scenarios, e.g., as indicated by a future reduction in the aerosol optical depth, but other scenarios suggest little change or a slight increase in aerosol optical depth for 2050 against the present²⁰. In addition to direct irradiance, other meteorological factors also play a role in PV power production (see Methods), e.g., changes in clouds affecting the radiation transfer, as well as temperature and winds around the PV panel. As such it is difficult to infer from existing literature how PV power production would additionally change due to

future climate change, with an overview based on EURO-CORDEX experiments²¹. The impact of climate change on PV power production is not a focus of our study.

Natural balancing effects between PV and wind power production reduce the magnitude of anomalies in total power production, independent of the weather pattern and the installed capacities. This is seen by the consistently smaller anomaly in the total power production compared to either the anomaly in PV or wind power production (Fig. 1a, b). The range in anomalies across all weather patterns, i.e., the highest anomaly minus the lowest anomaly, in the total production in scenario-2050 (26%) is reduced by one-third compared to that of scale-2019 (42%). This reduction implies that a high share of PV power in scenario-2050 improves the potential for balancing effects in meteorological variability for the European energy system, previously suggested by other studies^{4,18}.

We test to what extent an even higher share of PV power installations could contribute to the balancing effect. To that end, we perform a sensitivity experiment with REM, where PV power installed capacity is five times larger than that of wind power, equivalent to a PV power contribution of 69% to the total production. This contribution of PV power is higher than the optimal share 45–57% of PV to PV plus wind power production that was estimated from weather and installations of the past^{4,18}. Increasing the installed capacities for PV power further reduces anomalies in total production associated with some of the weather patterns, e.g., HNa and HM have now near-average total production (Supplementary Fig. S3) in contrast to the below-average production of –10 and –8% in scenario-2050. There is, however, no large difference in the range of the total production anomalies with a slight increase by 3% compared to scenario-2050, consistent with the optimum being already reached for lower PV shares^{4,18}. This finding implies that there are benefits of an even higher share of PV power production during individual weather patterns, but it does not reduce the overall natural variability in power production for all weather patterns.

Seasonal differences. We assess the differences in anomalies in the total power production associated with different weather patterns for the winter and summer half-year (Fig. 3 and details for PV and wind power in Supplementary Fig. S4). We use here the same half-year definition as for the weather patterns¹⁹, i.e., 16 October to 15 April for winter, and 16 April to 15 October for summer.

The results highlight that weather patterns associated with above-average wind power production are good indicators for above-average total production for the 2019 and 2050 installations (group High wind in Fig. 3a, b). The group High wind dominates the weather during winter with an occurrence frequency of 60% (Fig. 3c). Looking at individual patterns in the group High wind suggests typically small seasonal differences in the associated total power production, compared to the group High PV. The seasonal differences are larger and not systematic across the patterns in the group High wind for scale-2019. For scenario-2050, however, most weather patterns in the same group High wind are associated with more production in the winter, except Low Pressure over the British Isles (TB, Fig. 3a, b). Result for smaller sub-regions of Europe can be different, e.g., SWz, Wz, and NWz in the group High wind for European power production show over region A the characteristics of a dark doldrum (see Supplementary Fig. S2).

Most weather patterns in group High PV typically have higher mean total production in summer than in winter (Fig. 3a, b), consistent with the naturally higher irradiance and lower wind power production during summer for these patterns (Fig. 2). This

is true for both installed capacities. Weather patterns from group High PV dominate the weather in summer with an occurrence frequency of 58%.

Interestingly, the lowest winter total production falls into the group High PV for both installations, namely Icelandic High with Ridge Central Europe (HNa). We find an anomaly of –24% in the total winter power production for HNa in scale-2019 with simultaneously below-average PV and wind power production (see Supplementary Fig. S4). During winter, HNa therefore has a characteristic behavior of a pattern in the dark doldrum explained by the lower irradiance and the potential fog formation during high-pressure influence in winter. This is different in summer when high pressure often leads to cloud-free skies allowing more irradiance consistent with the anomalously high PV power production for HNa in the annual mean (Fig. 1a, b). This finding points to a seasonal dependency of the dark doldrums characteristics.

In the group Dark doldrums, SEz has the largest seasonal differences. In the summer, it can lose the characteristic behavior of a dark doldrum due to near-average total production for both installations (Fig. 3a, b), primarily driven by above-average wind power production in the summer (Supplementary Fig. S4). On the other hand, patterns HNFz and Ws consistently show characteristics of a dark doldrum, with both PV and wind power production simultaneously below the average in both seasons and for both installations (Supplementary Fig. S4). For this reason, they have very small seasonal differences for total production, especially in the future installation. They produce the lowest all-year total production in scenario-2050 (Fig. 1b), although they are not associated with seasonal extremes, having the 4th and 11th lowest total production in the winter, respectively (Fig. 3b).

Spatial differences. We assess the spatial distribution of the most extreme anomalies in the mean all-year power production (Fig. 4). A complete pictorial atlas of spatial power anomalies associated with 29 weather patterns is given in Supplementary Fig. S5 along with statistical information (see Supplementary Table S1). We discuss here the patterns (1) HNa and Ws with the lowest total production in scale-2019 and scenario-2050, respectively, (2) Wa with the highest total production for both installations and (3) HNFa for the contrasting extremes in individual energy sources and the sensitivity to the installed capacities (Fig. 1b, c).

The pattern Icelandic High, Ridge Central Europe (HNa) (Fig. 4a–e) belongs to the group High PV with positive regional anomalies in PV power production and the lowest wind power production in the European mean (Fig. 1a). The ridge over Central Europe is associated with higher than average PV power production in Germany and Poland in contrast to weak winds around the North Sea, explaining the anomalously low wind power production with slightly more pronounced production reductions in offshore wind power compared to onshore in Europe (Fig. 1). Away from the ridge, the Iberian Peninsula receives relatively little irradiance and slightly above-average wind speeds. The combination of low wind power production around the North Sea and low PV power production in the Iberian Peninsula leads to anomalously low total power production in the European mean for scale-2019. A higher share of PV power in scenario-2050 helps the positive anomaly in PV power production over parts of Central and Northern Europe to better balance negative anomalies in wind power production in some areas in Germany and France. This effect is strong enough to increase the total power production associated with HNa, such that it does not have the lowest total production in scenario-2050.

The South-Shifted Westerly (Ws) belongs to the group Dark doldrums with simultaneously below-average PV and wind power

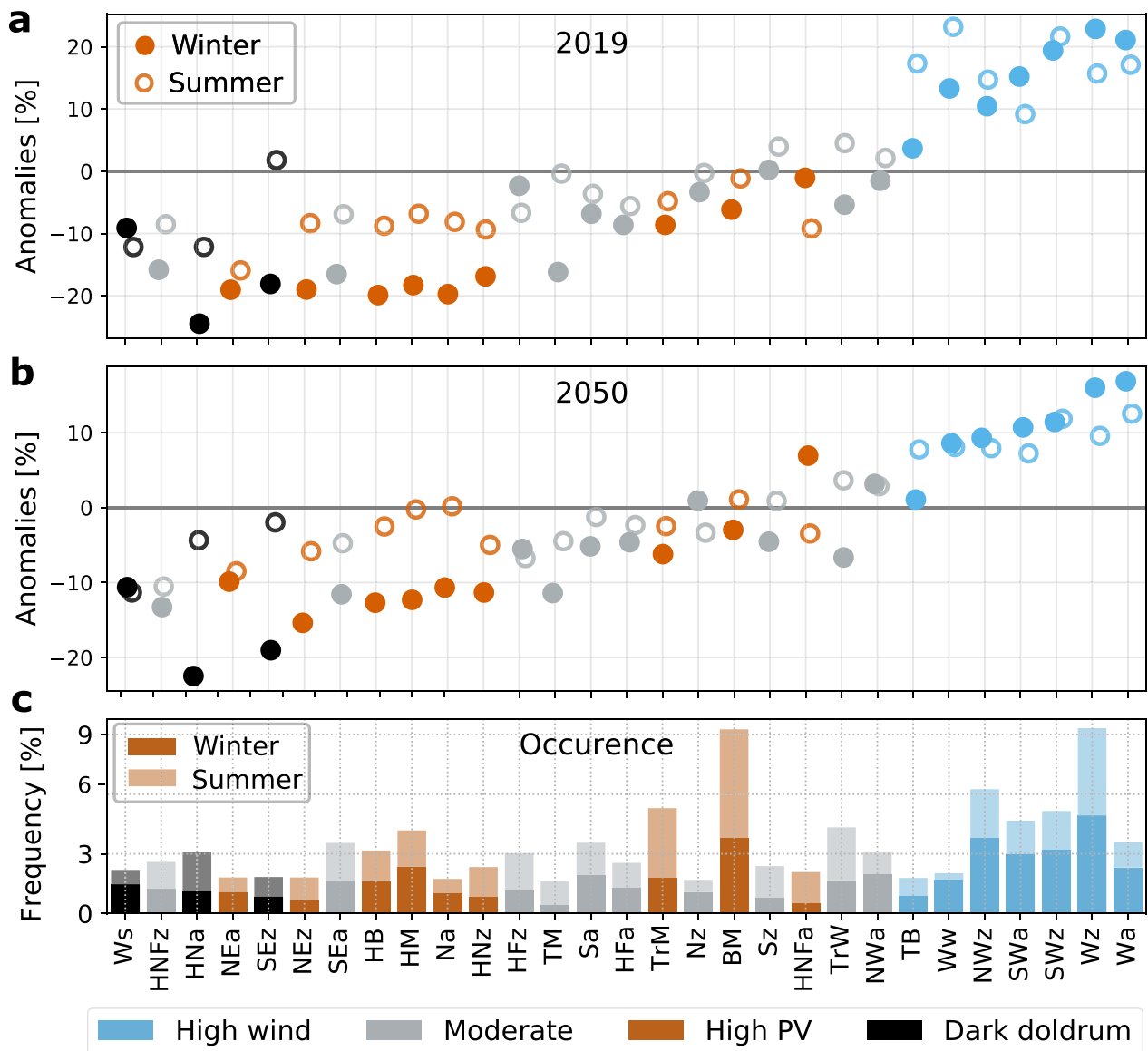


Fig. 3 Seasonal differences in power production anomalies. Total production anomalies in % as simulated by (a). scale-2019 and (b). scenario-2050, and (c). the seasonal frequency of the weather patterns (stacked), sorted by increasing magnitude of power production in scenario-2050 from left to right. The color-coded groups of weather patterns are marked as in Fig. 2. The seasons here are in half-year periods following the definition for the weather patterns¹⁹ with winter from mid-October to mid-April and summer from mid-April to mid-October. For the seasonal differences of PV and wind power production individually, refer to Supplementary Fig. S4.

production (Fig. 4f–j). PV power production is particularly low due to below-average irradiance across Europe along with a low-pressure system with the center over the North Sea. Wind speeds and hence the associated power production are anomalously high at the southern margin of the low-pressure system, i.e., across Central and Southern Europe. To the North, weak winds occur around the North Sea, the British Isles, and Scandinavia (Fig. 4a, d), leading to a slightly below-average wind power production for Ws for both installations (Fig. 1a, b). The combination of very low PV power production and the shortage of wind power production north of 51°N results in extremely low total power production across the northern regions for both installations (Fig. 4g, h). In scale-2019, south-western regions in Europe have slightly more areas with positive anomalies in total production, induced by a stronger influence of regionally high wind power production (Fig. 4g). The positive anomalies in these regions help

to better balance the negative anomalies in the northern regions, giving a total production for Europe with less negative anomaly than in scenario-2050 (Fig. 1a).

Anticyclonic Westerly (Wa) shows similar regional anomalies in total production for both installations that lead to the highest total production in the European mean. This result is mainly caused by the strong positive anomalies in wind power production in the North of Europe. The strong North-South pressure gradient between 49°N and 59°N causes strong westerly winds and therefore the anomalously high wind power production from the British Isles via the North Sea to the Baltic and the adjacent countries (Fig. 4k, o). The high wind power production explains the above-average total production for these regions which have large wind power plants. The pronounced regional impact of wind power gives Wa the highest total production in both seasons and for both installed capacities

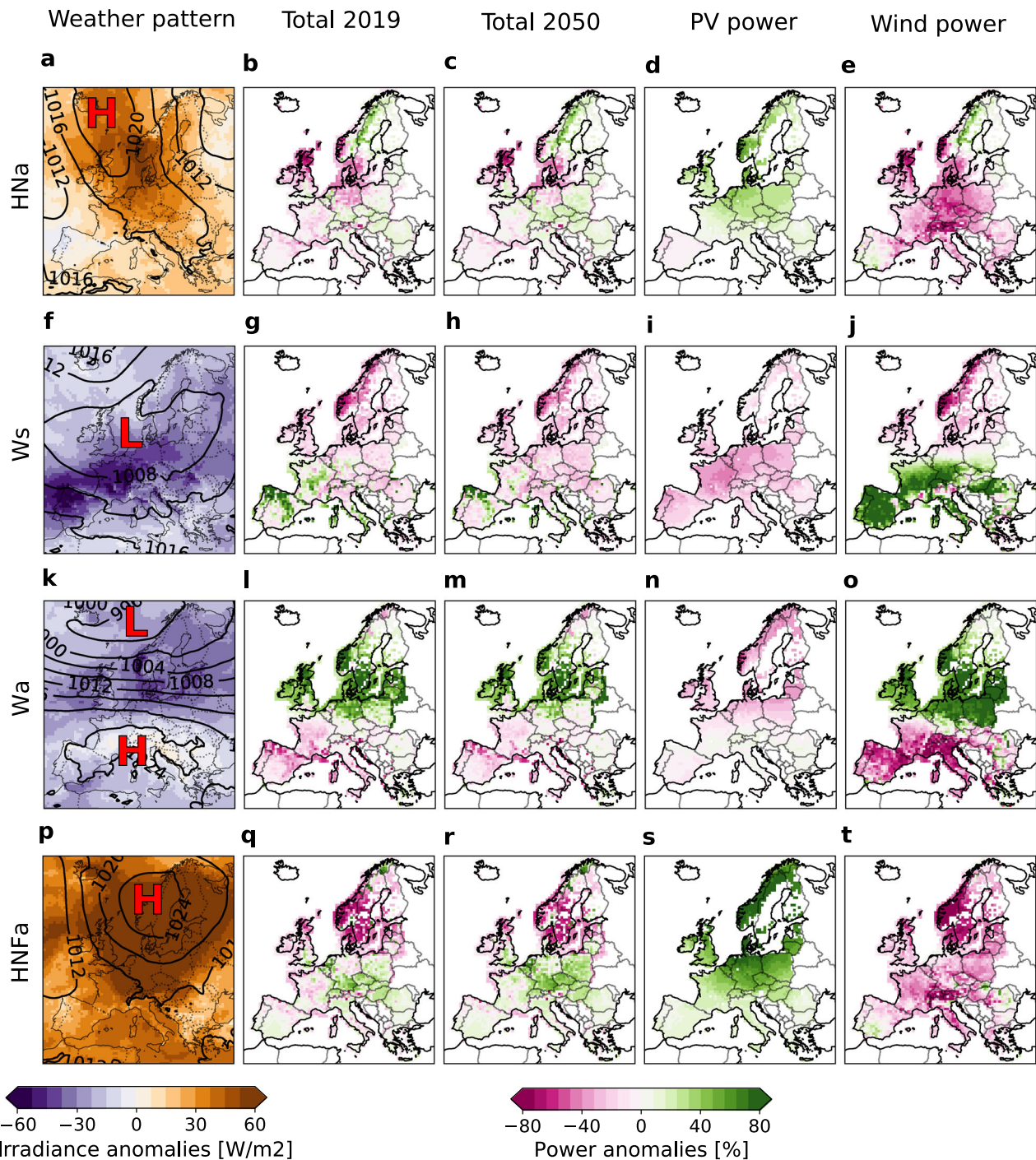


Fig. 4 Composite maps for production anomalies associated with four selected weather patterns. Spatial anomalies of power production associated with (a–e). HNa with the lowest total production simulated by scale-2019, (f–j). WS with the lowest total production in scenario-2050, (k–o). Wa with the highest total production in both simulations, (p–t). HNFA with anomalies of opposite signs for PV and wind power production in both simulations. The first column shows the composite maps of mean sea level pressure (contours) with 4 hPa increments and shading for the irradiance anomalies. The other columns (left to right) show the spatial distribution of anomalies in total production from scale-2019 and from scenario-2050 installations, as well as the contributions from PV and wind power production anomalies. The full Atlas of production anomalies associated with the individual 29 weather patterns is shown in Supplementary Fig. S5.

(Figs. 3a, b, 1a, b, 4l, m), despite the below-average wind power production in Southern regions and below-average PV power production across most of Europe (Fig. 4n, o).

Weather patterns High Scandinavia-Iceland, Ridge Central Europe (HNFA) are characterized by a high-pressure system over Scandinavia causing anomalously high PV but anomalously low wind power production across all of Europe (Fig. 4p–t). Taken

together, we see a strong North-South difference in the sign and magnitude of anomalies in the total power production independent of the installation (Fig. 4q, r). The change in sign of the regional anomalies occurs around the latitudes 45–55°N. This behavior points to the usefulness of building North-South electricity transmission lines to balance naturally occurring regional extremes in power production due to the weather, even during days when the

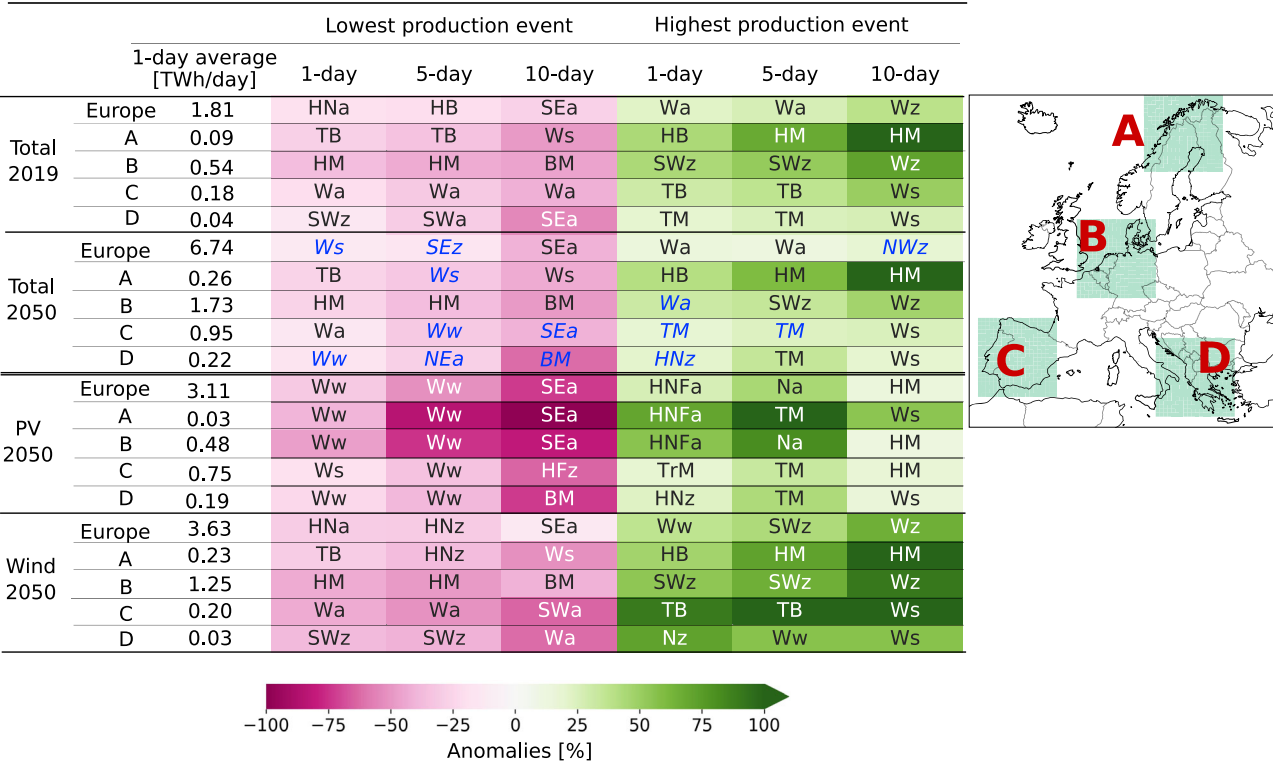


Fig. 5 Production extremes of different durations associated with weather patterns. Weather patterns associated with the lowest (magenta) and highest (green) production events that last at least one, five, and ten days for Europe and for the four regions marked on the map (A–D, see Methods). Blue marks where weather patterns leading to production extremes change from scenario-2050 to scale-2019. The results of sensitivity tests for intermediate event durations are shown in Supplementary Fig. S6.

weather has a similar influence on PV or wind power production for all of Europe.

Our results suggest that the balancing potentials strongly depend on the weather pattern and the installed capacity, such that the grid planning should not be based on coarse-grained data assessments. The regional differences such as in Wa specifically imply that aggregated power production for all of Europe or single countries is not always representative of all regions falling inside that area.

Duration differences. The impacts of an anomaly in power production are expected to be more severe the longer an event lasts. We conduct a quantitative assessment of the differences in power production associated with weather patterns prevailing for different numbers of days. To that end, we first identified events of consecutive days with the same weather pattern of at least one, five, and ten days, obtaining 8401, 443, and 19 events respectively during the period 1995–2017. We then identified from these events those that were associated with the lowest and highest daily power production, compared to the climatological daily mean shown in Fig. 5. We again use the same four regions (A–D marked in Fig. 5) to demonstrate how the impacts of extreme production events, measured on the European scale, vary spatially across several regions.

For individual energy sources, weather patterns associated with 1-day and 5-day extremes in power production are often similar, but this is not true for 10-day events (Fig. 5). With increasing duration, the impacts of the associated anomalies in power production are expected to increase. This is indeed seen in our result by the increasing magnitude of the power production anomaly when we go from 1-day to 10-day events, e.g., the largest absolute magnitude of an anomaly in wind power for 1-day

events is 90% (region C), and for 10-day events is 137% (region A). However, this effect is not seen for the high production events for PV power. Specifically, the anomalies in the 10-day highest production events for PV power are often smaller than for the shorter durations. This is because all 19 10-day events occur during winter (mid October–mid April) and are typically associated with an anticyclonic weather pattern that would fall into the category of atmospheric blockings. This puts more weight on the darker winter time in their 10-day means and thus decreases the average production of PV power compared to shorter events.

The lowest 10-day total power production for Europe is seen for Anticyclonic South-Easterly (SEa) with mean anomalies of –27% and –41% for scale-2019 and scenario-2050, respectively. Interestingly, SEa exhibits the characteristic of a dark doldrum in the winter in this event (25/11–04/12/2014), with the 10-day lowest production for both PV and wind power (–73% and –13%), but the same pattern is not associated with extremes in 1- and 5-day power production means.

Balancing potentials for total power production exist for both installations, even for extreme power production events with a duration of several days. For instance, the pattern High over Central Europe (HM) is associated with the 1-day and 5-day lowest total power production in region B, consistent with an assessment for Germany⁶. In region A, however, the same weather pattern leads to the 5- and 10-day highest total power production, pointing to the balancing potential between Scandinavia and Germany as seen earlier in a comprehensive power system simulation for Germany¹⁴. Another example of such balancing potentials is seen in regions C and D which have the highest 10-day total production associated with Ws, opposite to region A which has the lowest 10-day total production associated with the same weather pattern. Pattern Cyclonic South-Westerly

(SWz) brings the lowest wind power production in 1- and 5-day events in region D, but brings the highest wind power production with the same durations for region B, agreed with a previous study⁷. It implies that an efficient European electricity grid covering large distances across several country borders would be beneficial to reduce regional impacts of weather-induced shortages in power production from wind and irradiance.

The result is robust for events shorter than 2 days, i.e., the associated weather patterns are identical for 1-day and 2-day events (Supplementary Fig. S6). For longer similar event durations, the weather patterns associated with anomalies in production are not always identical, especially for low-production extremes, but the patterns have similar characteristics. For example, SEz and Ws are associated with 5-day and 4-day low-production events in Europe and both belong to the group Dark doldrum. Also, NWz and NWa are associated with the highest 10-day and 8-day production events and have similar patterns in wind directions. The largest differences in the weather patterns are seen for prolonged events of 8 days and 10 days, which is consistent with comparably few cases of such extremes. Specifically, there is a total of 19 10-day events in the period 1995–2017, compared to 69 events with 8-day duration.

Discussion

We provide a comprehensive analysis of PV and wind power differences and extremes associated with different synoptic weather patterns for Europe with an high level of detail. Using an hourly weather dataset with 6 km horizontal resolution, and future power installations, we simulate PV and wind power production and pair the results with a routinely used weather pattern classification. We identify weather patterns associated with extreme power production averaged for Europe. These cause extreme anomalies in PV or wind power production individually, e.g., Maritime Westerly, Block Eastern Europe (Ww), and High Scandinavia-Iceland, Ridge Central Europe (HNFa), and in some rare cases simultaneously low PV and wind power production which we refer to as dark doldrum, e.g., South-Shifted Westerly (Ws). For present-day installed capacity, the pattern Icelandic High, Ridge Central Europe (HNa) with low wind speeds across most of Europe is associated with the lowest mean hourly total production (PV plus wind power). However, with a higher share of PV power in the projected future installed capacity of 2050, Ws produces the lowest hourly average of total production primarily due to anomalously low irradiance. Weather patterns that lead to extremely high wind power production, such as Wa, produce the highest hourly total production, independent of the installed capacities. Interestingly, the relative share of anomalies in onshore and offshore wind power production for Europe is typically similar independent of the weather patterns, although the estimate of the European mean wind power production for 2050 is by about a factor of four larger offshore (155.8 MW) than onshore (37.1 MW). It suggests expanding on and offshore capacities is equally useful from a large-scale perspective on weather-driven production anomalies.

Increasing the duration of weather patterns from one to ten days leads to changes in the patterns that lead to extremes in PV and wind power production. The patterns HNa and Ws are associated with the lowest 1-day total production in present and future installation, similar to results for hourly production. But the pattern Anticyclonic South-Easterly (SEa) stands out as the 10-day event with the lowest PV, wind, and total power production for both the present-day and future installations. Different weather patterns are associated with different durations for extreme power production events. This suggests that adequate monitoring is needed for potential warnings in different

timescales for weather-induced production shortages in a climate-neutral energy system. In particular, the longer events might be critical, as they increase the burden on the security of the electricity supply due to continuous demand for electricity and a declining load of storage. Prolonged SEa thus can be considered as a multivariate compound event, one of the four types of compound weather and climate events²². Optimized spatial distribution of renewable power plants alone cannot substantially reduce the maxima in the total residual demand²³, but storage capacities and transmission of electricity could balance residual loads arising from anomalously low production¹⁴.

Prolonged SEa is one example of weather patterns with a high-pressure system that prevails over several days, commonly known as atmospheric blocking. Blocking events are known challenges for power production in energy systems of Europe^{7,24} and on other continents^{25,26}. The benefit of using the detailed weather pattern classification in our study compared to others^{7,9,11} stems from the ability to represent the location of the center of high-pressure systems, and therefore to see the regional differences in wind speed and irradiance at kilometer-scale resolution. For example, the two extreme weather patterns Ww and HNFa have a high-pressure system located over Eastern Europe and Scandinavia-Iceland. These two patterns yield European mean anomalies in PV and wind power production of opposite signs. Due to the high impacts of atmospheric blockings, accurately forecasting such events in terms of location and duration is a much-needed meteorological service for the renewable energy sector. Despite the importance, there are uncertainties in representing blockings in models for numerical weather predictions²⁷. Future climate projections suggest a reduction in frequency and duration of atmospheric blockings compared to the past^{27,28}, but rare high-impact events might be possible²⁷. It implies that blockings are also an increasing risk for future power production when we consider the impacts of climate change. Additionally, temporal sequences of different weather patterns leading to extremes can be addressed in future studies.

Our study indicates that synoptic weather patterns can be used to estimate the anomalies in PV and wind power production across Europe. An earlier study suggests that it is useful to forecast weather patterns with a focus on a daily time scale for wind power anomalies and a monthly time scale for PV power anomalies²⁹. Our results indicate that the monitoring of weather patterns associated with anomalies in both PV and wind power production can be useful across weather time scales, i.e., hours up to ten days. Such information is helpful for electricity system operators to replenish energy storage to balance an upcoming weather-induced shortage in power production. Weather pattern classifications like the one used here¹⁹ are already well established at meteorological services, e.g., it is monitored and reported by the German Weather Service. Using forecasts of weather patterns can therefore be a valuable meteorological service to quickly identify problematic weather conditions to inform stakeholders in energy system operation. This is possible without the need to routinely operate an energy system model and without the costly requirement to develop and implement a new warning index.

Methods

Modeling approach. The Renewable Energy Model (REM) simulates photovoltaic (PV) power, and both on- and offshore wind power production in Europe. Our simulation with REM uses 23 years of high-resolution meteorological data for 1995–2017 inclusively. The hourly meteorological data are taken from the COSMO-REA6 reanalysis dataset³⁰, namely 10-m wind speed, 2-m air temperature, and surface irradiance with a horizontal resolution of 6 km. COSMO-REA6 is a regional reanalysis dataset

based on the Consortium for Small-scale Modelling (COSMO, www.cosmo-model.org) model for numerical weather prediction. It has a horizontal resolution of 6 km and 40 vertical levels, with the initial and boundary conditions based on ERA-Interim reanalysis data³¹. Assimilated observational data include for instance radiosondes, wind profiler, aircraft, and station observations³⁰. This dataset was successfully used for renewable energy applications before for Europe and Germany^{14,32–37}. Note that the meteorological data has the same weather sequences as the data used in the weather pattern classification¹⁹ due to the assimilation of observations. In addition to the consistency with the weather patterns, our choice for using COSMO-REA6 is motivated by the proven skill for energy system assessments and the lack of a large ensemble of decadal predictions with a similarly high resolution for multiple European countries. COSMO-REA6 shows a negative bias of -1.4% in annual and spatial means of irradiance against satellite data but is one of the best gridded irradiance datasets currently available for this type of research³⁶. COSMO-REA6 is also known to reproduce characteristics of observed irradiance and wind speed in Germany³⁸ and often outperforms other observational products and reanalysis data in many metrics^{33,36,39}.

The combined process to produce the output for analyses is illustrated in Fig. 6a. To substantially speed up the simulation and retaining the meteorological accuracy of the original data, we calculate the power production in every eighth grid box, giving us information on the power production on a horizontal grid of 48 km but using the benefits of the 6 km resolution of the original meteorological input data at every grid point, following an earlier approach⁴. This choice is made to represent consistent meteorological developments in the power simulations free of artifacts that could be introduced through interpolation of the meteorological data to a coarser spatial resolution.

REM's PV power component was documented earlier^{4,36}. The locations of the PV power plants were obtained from www.wiki-solar.org (as of 2019-03-04). The effective irradiance, i.e., the

irradiance received on the tilted PV modules, is calculated from the direct and diffuse radiation fluxes using geometry and a model for transferring the diffuse irradiance from the horizontal to the plane of the array⁴⁰, as in previous studies^{4,36}. The optimal tilt angles were obtained by maximizing the PV power production based on irradiance data for 2014, resulting in tilt angles of 21° to 50° as we go from southern to northern Europe. An estimate of error derived from using one year of data (2014) compared to 20 years (1995–2014) for 10 stations in the Baseline Surface Radiation Network (BSRN) showed a maximum error of 0.35% ⁴¹. The optimal tilt angles are multiplied by a factor of 0.7 to reduce the shadow effects as investors typically make for economic reasons⁴². The azimuth angles were assumed to face south for all PV arrays. REM uses the power-rating model for crystalline silicon modules⁴³. The conversion rate is an empirical function based on ambient temperature, wind speed at the panel, and irradiance⁴³. Methods for PV power calculations like the one in REM were shown to have a good accuracy at a smaller computational burden, compared to other methods of power production estimates⁴⁴.

The wind power component uses a cubic power curve for calculating the wind power potential, following the method in previous studies^{11,45}. The potential capacity factor, denoted C , is calculated as in Eq. (1).

$$C = \begin{cases} 0 & \text{if } v_{hub} < v_{cut-in} \\ \frac{v_{hub}^3 - v_{cut-in}^3}{v_{rated}^3 - v_{cut-in}^3} & \text{if } v_{cut-in} \leq v_{hub} < v_{rated} \\ 1 & \text{if } v_{rated} \leq v_{hub} < v_{cut-out} \\ 0 & \text{if } v_{cut-out} \leq v_{hub} \end{cases} \quad (1)$$

where v_{hub} is the wind speed at hub height. v_{cut-in} and $v_{cut-out}$ are cut-in and cut-out wind speeds, defined as the threshold wind speeds for the onset and stop of producing power with the wind turbine, v_{rated} is the wind speed where the power production

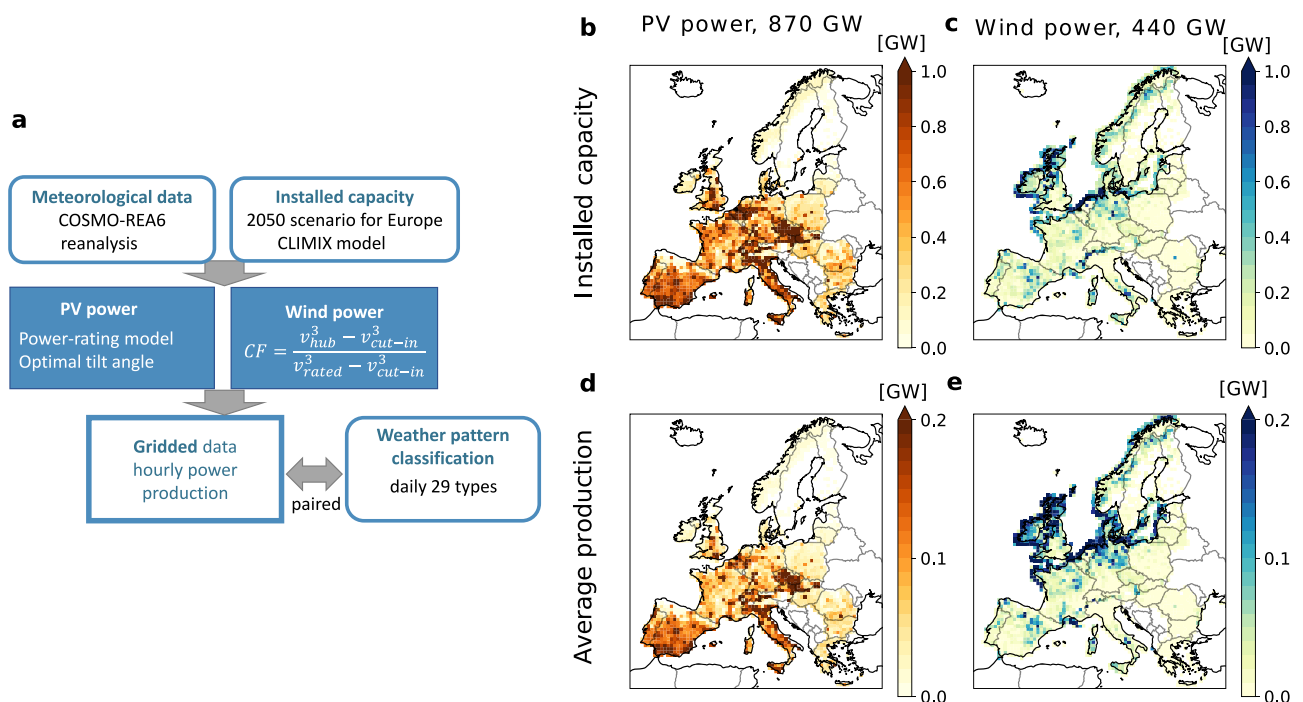


Fig. 6 Components of the Renewable Energy Model (REM). **a** Flow chart of REM used in this study. **b, c.** Installed capacity (GW) of PV and wind power in Europe in the scenario-2050 of the CLIMIX model¹⁵. **d, e.** Average hourly production (GW) of PV and wind power with the 2050 installation using weather of the period 1995–2017. All data is coarse-grained to a 48 km horizontal resolution, but is calculated using the original 6 km resolution such that the benefit of the high resolution for the meteorological data is retained.

reaches the maximum of production for which the turbine was designed, the so-called rated power.

REM simulates wind power production at a wind speed for v_{cut-in} , v_{rated} , $v_{cut-out}$ of 3.5, 13, 25 m s⁻¹ for all wind turbines, as in earlier wind power simulations^{4,15}. Turbine types have specific values for this wind power curve⁴⁶. We calculate v_{hub} from wind speeds at the two model levels 36 and 37 in COSMO-REA6 which corresponds to typical turbine hub heights from CLIMIX, e.g., 116 m and 178 m above mean sea level for mean meteorological conditions. Hub heights of the wind turbines in the CLIMIX model vary from 17 m to 150 m above ground level, but most are about 100 m above ground level and, therefore, fall within the layer between the chosen levels for a wind speed interpolation over land, and an extrapolation to some comparably few lower hub heights. Turbines in offshore regions are typically higher than on land, with values around 150 m in CLIMIX, and fall within the layer for interpolating the wind speeds from COSMO-REA6 output. Wind speed is the dominant driver of power differences, although air density also has an influence on the wind power output. In fact, the influence of variable air density on wind power production is two orders of magnitude smaller than the influence of wind on power production^{33,47}. For this reason and out of simplicity, REM uses a constant value of 1.2295 kg m⁻³ for air density in the wind power calculation, consistent with other studies^{4,45,47}.

We compare the REM output for the potentials of PV and wind power, i.e., calculated with irradiance and 100-m wind speed data. Data for validation are from the Climate Data Store (CDS)^{48,49} dataset Climate and energy indicators for Europe and from the website Renewables Ninja (www.renewables.ninja)^{50,51}. This is because the datasets for validation provide gridded data for potentials. The data for power production are provided at country-aggregated and with different installed capacities, and thus, not comparable. The REM output and the CDS data have different spatial resolutions and domain boundaries since they are based on different reanalysis datasets, namely COSMO-REA6³⁰, ERA5⁵², and MERRA-2⁵³. For this reason, we selected only grid cells inside four countries (Norway, Germany, Czech Republic, and Spain) to be comparable between the three datasets. For validation, we use potentials of PV and onshore wind power from REM. Wind power offshore was not calculated as country masks do not include the area of the offshore wind power plants. From CDS, we selected two variables: solar photovoltaic power generation and wind power generation onshore. From Renewables Ninja, we selected PV national current and Wind national current (Wind onshore current for Germany and Spain). We then spatially averaged these data to get their time series of potentials over the period 1995–2017. The temporal correlation coefficients between the hourly output of these datasets and our REM simulation with the scale-2019 installations for PV power range from 0.88 to 0.98 and for onshore wind power from 0.75 to 0.97, for the four selected countries shown in Supplementary Fig. S7. REM shows similar distributions of hourly PV and wind power production compared to the other datasets for the four countries and typically falls within the uncertainty in the distributions between CDS and Renewables Ninja. One noticeable difference is for PV power in Spain where REM simulates more high values compared to CDS and Renewables Ninja (Supplementary Fig. S7b). This is the benefit of the higher horizontal resolution of the meteorological data COSMO-REA6 in REM. It allows the simulation of clear and cloud-free skies in more grid cells which results in higher values of PV power production which is most noticeable in southern Europe with high irradiance. Comparing the average hourly potential, REM therefore also simulates larger average hourly potentials for PV power compared to CDS and Renewables Ninja (14%, 12%, and 13%, respectively). The average hourly potential for onshore wind power is comparable (24%,

23%, and 24%, respectively). Differences in the potentials between the datasets may arise from the different reanalysis data^{54,55}.

The model uses installed PV and wind power capacities projected for the year 2050 to account for the projected increase in renewable power plants that is expected for the coming years. The gridded data for the installed capacity for PV and wind power production stem from the 2050 scenario of the model on climate and energy mix (CLIMIX) with a horizontal resolution of 0.11°, approximately 12.5 km¹⁵ (Fig. 6b, c). CLIMIX integrates for instance information on the PV and wind power resource availability, forbidden locations (e.g., forest and sea for PV power and land for wind power offshore), and planned total installed capacities for the year 2050 from the 80% RES pathway for electricity production in the Roadmap 2050⁵⁶. Resource availability for PV and wind power in CLIMIX was determined based on surface irradiance and 10-m wind speed derived from a Weather Research and Forecast (WRF) model⁵⁷ simulation nudged to ERA-Interim³¹ reanalysis data for the period 2000–2012. CLIMIX does not explicitly consider hybrid plants but the grid cells typically contain both PV and wind power plants. The PV and wind power capacities do not change over time. Despite the static locations, CLIMIX data shows reasonable agreements between estimated power production and observed values for 2012¹⁵. Since the grid from CLIMIX (12.5 km) is finer than in REM (48 km), each REM grid cell contains several PV (wind) power plants from CLIMIX. The potential of an individual PV (wind) power plant was calculated and then multiplied by its corresponding installed capacity from CLIMIX to obtain its power production. Subsequently, the overall power production of one REM grid cell is the sum of the power production of all PV (wind) power plants inside that grid cell.

The installed capacities from CLIMIX are 870 GW for PV power and 440 GW for wind power, giving a ratio of PV-to-wind installed capacity of 2:1. The projected European total in onshore wind power is 259.8 GW and larger than the offshore capacity of 179.8 GW for 2050. Hub heights for onshore and offshore regions have a similar range but are in the mean larger offshore (121 m) than onshore (97.2 m). The total of PV and wind power capacities (1310 GW) is about 4.5 fold larger compared to the installed capacity in 2019 for Europe¹⁷, namely 287 GW including 120 GW of PV power and 167 GW of wind power installations resulting in a ratio of 0.7:1. The projected wind power in the CLIMIX model is conservative compared to, for example, another scenario for the European electricity in 2030 where the installed capacity of wind power is one-and-a-half times larger, namely 620 GW for wind power paired with 872 GW for PV power⁵⁸. Our choice of the CLIMIX model projection is motivated by the availability of gridded installations and the successful usage of the CLIMIX model to analyze the impacts of weather and climate change on renewable power in earlier studies^{11,21,59}.

With all the PV and wind power plants in the scenario-2050 installed capacities from CLIMIX (Fig. 6b, c), REM yields an average potential of 26% for wind power and 15% for PV power, which is comparable to other studies using installed capacities for 2015^{50,51}. The model yields a mean hourly production for Europe of 130 GW for PV power and 151 GW for wind power for the 2050 installed capacity, which gives a ratio of PV to PV plus wind power production of 46%. Our model captures regional differences in weather impacts accounting for the heterogeneous distribution of installed capacities. Some examples of regional clusters of high production are European cities with roof-top PV panels and offshore wind farms in the North Sea and around the British Isles (Fig. 6b, c).

Due to the lack of a comparable dataset of present-day installed capacity of PV and wind power, we simulate the present-day installed capacity (scale-2019) by scaling the gridded data for the

capacities of scenario-2050 such that they match the Europe-aggregated capacity for PV and wind power in 2019. The 2019 installed capacities aggregated over Europe are namely 120 GW of PV power and 167 GW of wind power¹⁷. The scaling approach decreases the installed capacity simultaneously across Europe at the same rate for individual energy sources, i.e., by about a factor of 0.14 (0.4) relative to the 2050 capacity for PV (wind) power, but retains the spatial distribution of installations of 2050. The regional capacity in scale-2019 thus does not necessarily reflect the current regional installed capacity because countries increase their capacities at different speeds and their future locations are not always the same as today. For example, the installed capacities for wind power in scale-2019 for Germany, France, and Italy are smaller, larger, and roughly equal compared to the results from a study using the capacities in 2015⁷ (in the same order: 12.6, 14.2, and 7.6 GW, compared to 31.5, 9.0, and 7.9 GW). In the absence of present-day gridded data for installed capacities with a high spatial resolution across Europe, differences in scientifically estimated capacities are to be expected. For instance, past studies had differences in the installed capacity of wind power in 2015 for Germany, with 31.5 GW⁷ and 40 GW⁶. Our approach successfully reproduces the ratio of PV to PV plus wind power from a previous study⁶. For example, from scale-2019 for Germany, the ratio of PV to PV plus wind power for installed capacity is 49% and for yearly production is 29%, comparable to the results from a previous study with 49% and 32%, respectively⁶. We also find that the pattern of High pressure over Central Europe (HM) is associated with the lowest total production for Germany in our 2019 simulation in agreement with a study using installed capacities of 2015⁶ (Supplementary Fig. S1). We further compared the temporal variability in hourly production from REM's scale-2019 simulation against actual production data from the ENTSO-E Transparency Platform (transparency.entsoe.eu)⁶⁰ for the year 2017, which is the last year for the meteorological data from COSMO-REA6. One cannot expect a close agreement with ENTSO-E for the hourly amount of country-aggregated power production due to differences in the installations and in the meteorological data. Nevertheless, REM's output has a similar temporal variability in the hourly PV and wind power production compared to the ENTSO-E data for 2017, with Pearson correlation coefficients of 0.95–0.97 for PV power and 0.56–0.69 for onshore wind power.

Analysis strategy. All results for power production associated with the weather patterns are calculated at an hourly time scale (unit GW), the same as the original output of the energy model to maintain its high temporal resolution. One exception is the daily production in the assessment of extremes of different duration namely 1, 5, and 10 days, all expressed in TWh per day. We calculate PV and wind power production for all time steps with valid data. We consider anomalies in terms of power production and do not simulate electricity demand or transmission. However, over- and underproduction would theoretically correspond to an over- or undersupply, if all else was equal.

We assess anomalies in PV and wind power production associated with different weather patterns. To that end, we use 29 different synoptic weather patterns for Europe from a dataset provided by the German Weather Service¹⁹. Each day is associated with one particular weather pattern for the whole of Europe. The names of the weather patterns follow the official definition¹⁹. To be compatible with the hourly output from REM, we assign the same weather pattern of a given day to all 24 hours of the same day. To get Europe-aggregated hourly mean production classified by weather patterns, we calculate the hourly mean across all time steps associated with the same weather pattern. The 1995–2017 mean is then subtracted from this composite of mean production per

weather pattern to determine the anomaly in power production. For seasonal differences, semi-annual division for seasons is defined as in the classification of weather pattern¹⁹ for consistency, i.e., winter refers to 16 October to 15 April, and summer to 16 April to 15 October. Seasonal anomalies are calculated in a similar manner but by selecting time steps for winter and summer mean production.

For spatial differences, to calculate the power production anomalies for each weather pattern, gridded data with the time steps corresponding to that weather pattern are selected and hourly averaged to compile composite data for each weather pattern. Then the 1995–2017 mean power production or meteorological data for Europe is subtracted from the composite means per pattern (e.g., Figs. 4, 6d, e). Anomalies in power production associated with weather patterns are calculated in percentage relative to the mean production, i.e., subtracted and then divided by the mean for all-year or the season for the period 1995–2017 from the same simulation. Note that the different installed capacities for PV and wind power in the simulations imply different absolute power productions even when relative anomalies of individual energy sources are identical between the simulations.

Four regions, marked in Fig. 5, are chosen for an assessment of spatially averaged anomalies in power production considering different durations. The regions cover 20 x 20 grid boxes each and are selected for the following reasons. The northernmost part of Scandinavia (around 67.6°N, 20.1°E) is selected because of the contrast in the power production anomaly compared to Western Europe, e.g., Fig. 4b, c. Northern Germany paired with the North Sea (around 53.1°N, 7.0°E) is assessed due to the large number of installed wind power plants. The Iberia peninsula (around 39.9°N, 5.0°W) is investigated due to the high potential for PV power production. The Balkans and surrounding areas (40.3°N, 20.8°E) are analyzed due to the contrast in wind power production relative to Western Europe⁷.

To identify weather patterns associated with extremes in PV and wind power production of different durations, we first identify sets of consecutive days that have the same weather pattern for at least 1, 5, and 10 days, referred to as 1-, 5-, and 10-day events. One day is a typical time frame used in past studies and chosen here for the comparability to past results. Ten days is a typical time period for the limit of weather forecasting beyond which the predictability of the weather strongly declines. We additionally choose five days to assess one interim point in time. We obtained 8401, 443, and 19 events with 1-, 5- and 10-day duration, respectively. The year-to-year differences in the event occurrence can be large, e.g., zero to four events for 10-day events, but there is no perceptible strong long-term trends (see Supplementary Fig. S8). In each region, we compute the composite of 1-day means for the same weather pattern and subtract the 1-day mean for 1995–2017 to obtain the anomalies. The weather patterns associated with the lowest and highest power production are identified per duration and region (Fig. 5).

Data availability

COSMO-REA6 data is freely available at https://opendata.dwd.de/climate_environment/REA/COSMO_REA6/. The CLIMIX data was acquired from the author¹⁵. The output of REM and the source data for figures are available⁶¹ at https://www.wdc-climate.de/ui/entry?acronym=DKRZ_LTA_1198_ds00003.

Code availability

The code of REM and custom codes to reproduce the figures are available⁶¹ at https://www.wdc-climate.de/ui/entry?acronym=DKRZ_LTA_1198_ds00003.

Received: 23 February 2023; Accepted: 16 January 2024;

Published online: 01 February 2024

References

1. The European Commission. Stepping up Europe's 2030 climate ambition - Investing in a climate-neutral future for the benefit of our people. Communication from the commission to the European Parliament, the council, the European economic and social committee and the committee of the regions. <https://eur-lex.europa.eu/legal-content/EN/TXT/?uri=CELEX:52020DC0562> (2020).
2. European association for the cooperation of transmission system operators (TSOs) for electricity (ENTSO-E). ENTSO-E grid map 2015. <https://www.entsoe.eu/data/map/downloads/>. Accessed 24 Apr 2022.
3. Ten-Year Network Development Plan (TYNDP) 2022. Opportunities for a more efficient European power system in 2030 and 2040 <https://eepublicdownloads.blob.core.windows.net/public-cdn-container/tyndp-documents/TYNDP2022/public/system-needs-report.pdf> (2022). version for public consultation, Accessed: 15 Dec 2022.
4. Frank, C., Fiedler, S. & Crewell, S. Balancing potential of natural variability and extremes in photovoltaic and wind energy production for European countries. *Renew. Energy* **163**, 674–684 (2020).
5. Brayshaw, D. J., Troccoli, A., Fordham, R. & Methven, J. The impact of large scale atmospheric circulation patterns on wind power generation and its potential predictability: a case study over the UK. *Renew. Energy* **36**, 2087–2096 (2011).
6. Drücke, J. et al. Climatological analysis of solar and wind energy in Germany using the Grosswetterlagen classification. *Renew. Energy* **164**, 1254–66 (2020).
7. Grams, C. M., Beerli, R., Pfenninger, S., Staffell, I. & Wernli, H. Balancing Europe's wind-power output through spatial deployment informed by weather regimes. *Nat. Clim. Change* **7**, 557–562 (2017).
8. Couto, A., Costa, P., Rodrigues, L., Lopes, V. V. & Estanqueiro, A. Impact of weather regimes on the wind power ramp forecast in Portugal. *IEEE Trans. Sustain. Energy* **6**, 934–942 (2014).
9. van der Wiel, K. et al. The influence of weather regimes on European renewable energy production and demand. *Environ. Res. Lett.* **14**, 094010 (2019).
10. Bloomfield, H. C., Brayshaw, D. J. & Charlton-Perez, A. J. Characterizing the winter meteorological drivers of the European electricity system using targeted circulation types. *Meteorol. Appl.* **27** (2019).
11. van der Wiel, K. et al. Meteorological conditions leading to extreme low variable renewable energy production and extreme high energy shortfall. *Renew. Sustain. Energy Rev.* **111**, 261–275 (2019).
12. Michelangeli, P.-A., Vautard, R. & Legras, B. Weather regimes: recurrence and quasi stationarity. *J. Atmos. Sci.* **52**, 1237–1256 (1995).
13. Huang, W. T. K. et al. Weather regimes and patterns associated with temperature-related excess mortality in the UK: a pathway to sub-seasonal risk forecasting. *Environ. Res. Lett.* **15**, 124052 (2020).
14. EWI (Energiewirtschaftliches Institut an der Universität zu Köln). dena pilot study "Towards climate neutrality". Climate neutrality 2045—Transformation of final energy consumption and the energy system (2021). Published by the German Energy Agency GmbH (dena).
15. Jerez, S. et al. The CLIMIX model: a tool to create and evaluate spatially-resolved scenarios of photovoltaic and wind power development. *Renew. Sustain. Energy Rev.* **42**, 1–15 (2015).
16. Maimó-Far, A., Homar, V., Tantet, A. & Drobinski, P. The effect of spatial granularity on optimal renewable energy portfolios in an integrated climate-energy assessment model. *Sustain. Energy Technol. Assessments* **54**, 102827 (2022).
17. Audrey Errard, F. D.-A. & Goll, M. Electrical capacity for wind and solar photovoltaic power—statistics. https://ec.europa.eu/eurostat/statistics-explained/index.php?title=Electrical_capacity_for_wind_and_solar_photovoltaic_power_-_statistics#Increasing_capacity_for_wind_and_solar_over_the_last_decades (2021). Accessed: 2022-02-08.
18. Heide, D. et al. Seasonal optimal mix of wind and solar power in a future, highly renewable Europe. *Renew. Energy* **35**, 2483–2489 (2010).
19. James, P. An objective classification method for Hess and Brezowsky Grosswetterlagen over Europe. *Theor. Appl. Climatol.* **88**, 17–42 (2007).
20. Fiedler, S. et al. First forcing estimates from the future CMIP6 scenarios of anthropogenic aerosol optical properties and an associated Twomey effect. *Geosci. Model Dev.* **12**, 989–1007 (2019).
21. Jerez, S. et al. The impact of climate change on photovoltaic power generation in Europe. *Nat. Commun.* **6**, 1–8 (2015).
22. Zscheischler, J. et al. A typology of compound weather and climate events. *Nat. Rev. Earth Environ.* **1**, 333–347 (2020).
23. Zappa, W. & Van Den Broek, M. Analysing the potential of integrating wind and solar power in Europe using spatial optimisation under various scenarios. *Renew. Sustain. Energy Rev.* **94**, 1192–1216 (2018).
24. Sillmann, J. & Croci-Maspoli, M. Present and future atmospheric blocking and its impact on European mean and extreme climate. *Geophys. Res. Lett.* **36** (2009).
25. Gibson, P. B. & Cullen, N. J. Synoptic and sub-synoptic circulation effects on wind resource variability—a case study from a coastal terrain setting in New Zealand. *Renew. Energy* **78**, 253–263 (2015).
26. Ohba, M., Kadokura, S. & Nohara, D. Impacts of synoptic circulation patterns on wind power ramp events in East Japan. *Renew. Energy* **96**, 591–602 (2016).
27. Woollings, T. et al. Blocking and its response to climate change. *Curr. Clim. Change Rep.* **4**, 287–300 (2018).
28. Dorrington, J., Strommen, K., Fabiano, F. & Molteni, F. CMIP6 models trend toward less persistent European blocking regimes in a warming climate. *Geophys. Res. Lett.* **49**, (2022).
29. Bremen, L.V. Large-Scale Variability of Weather Dependent Renewable Energy Sources. In: *Management of Weather and Climate Risk in the Energy Industry*, (ed Troccoli, A.) 189–206 (Springer Netherlands, 2010).
30. Bollmeyer, C. et al. Towards a high-resolution regional reanalysis for the European CORDEX domain. *Q. J. Roy. Meteorol. Soc.* **141**, 1–15 (2015).
31. Dee, D. P. et al. The ERA-Interim reanalysis: Configuration and performance of the data assimilation system. *Q. J. Roy. Meteorol. Soc.* **137**, 553–597 (2011).
32. Frank, C. W. et al. Bias correction of a novel European reanalysis data set for solar energy applications. *Sol. Energy* **164**, 12–24 (2018).
33. Frank, C. W. et al. The added value of high resolution regional reanalyses for wind power applications. *Renew. Energy* **148**, 1094–1109 (2020).
34. Henckes, P., Knaut, A., Obermüller, F. & Frank, C. The benefit of long-term high resolution wind data for electricity system analysis. *Energy* **143**, 934–942 (2018).
35. Kaspar, F. et al. Regional atmospheric reanalysis activities at Deutscher Wetterdienst: review of evaluation results and application examples with a focus on renewable energy. *Adv. Sci. Res.* **17**, 115–128 (2020).
36. Kenny, D. & Fiedler, S. Which gridded irradiance data is best for modelling photovoltaic power production in Germany? *Sol. Energy* **232**, 444–458 (2022).
37. Weide Luiz, E. & Fiedler, S. Spatio-temporal observations of nocturnal low-level jets and impacts on wind power production. *Wind Energy Sci. Discussions* 1–28 (2022).
38. Camargo, L. R., Gruber, K. & Nitsch, F. Assessing variables of regional reanalysis data sets relevant for modelling small-scale renewable energy systems. *Renew. Energy* **133**, 1468–1478 (2019).
39. Borsche, M., Kaiser-Weiss, A. K. & Kaspar, F. Wind speed variability between 10 and 116 m height from the regional reanalysis COSMO-REA6 compared to wind mast measurements over Northern Germany and the Netherlands. *Adv. Sci. Res.* **13**, 151–161 (2016).
40. Klucher, T. M. Evaluation of models to predict insolation on tilted surfaces. *Sol. Energy* **23**, 111–114 (1979).
41. Frank, C. W. *The Potential of High Resolution Regional Reanalyses Cosmo-rea for Renewable Energy Applications*. Ph.D. thesis, University of Cologne, Germany (2019).
42. Saint-Drenan, Y.-M., Wald, L., Ranchin, T., Dubus, L. & Troccoli, A. An approach for the estimation of the aggregated photovoltaic power generated in several European countries from meteorological data. *Adv. Sci. Res.* **15**, 51–62 (2018).
43. Huld, T. et al. A power-rating model for crystalline silicon PV modules. *Sol. Energy Mater. Sol. Cells* **95**, 3359–3369 (2011).
44. Dittmann, S. et al. Results of the 3rd modelling round robin within the European project "PERFORMANCE"—comparison of module energy rating methods. *Presented at the 25th European Photovoltaic Solar Energy Conference and Exhibition*, 4333–4338 (Valencia, Spain 2010).
45. Henckes, P., Frank, C., Küchler, N., Peter, J. & Wagner, J. Uncertainty estimation of investment planning models under high shares of renewables using reanalysis data. *Energy* **208**, 118207 (2020).
46. Wang, Y., Hu, Q., Li, L., Foley, A. M. & Srinivasan, D. Approaches to wind power curve modeling: a review and discussion. *Renew. Sustain. Energy Reviews* **116**, 109422 (2019).
47. Tobin, I. et al. Assessing climate change impacts on European wind energy from ENSEMBLES high-resolution climate projections. *Clim. Change* **128**, 99–112 (2015).
48. Copernicus Climate Change Service. Climate and energy indicators for Europe from 1979 to present derived from reanalysis <https://cds.climate.copernicus.eu/cdsapp#!/dataset/sis-energy-derived-reanalysis?tab=form> (2020). Data retrieved from Climate Data Store (CDS), Accessed 3 June 2021.
49. Dubus, L. et al. C3S Energy: A climate service for the provision of power supply and demand indicators for Europe based on the ERA5 reanalysis and ENTSO-E data. *Meteorol. Appl.* **30**, e2145 (2023).
50. Staffell, I. & Pfenninger, S. Using bias-corrected reanalysis to simulate current and future wind power output. *Energy* **114**, 1224–1239 (2016).
51. Pfenninger, S. & Staffell, I. Long-term patterns of European PV output using 30 years of validated hourly reanalysis and satellite data. *Energy* **114**, 1251–1265 (2016).
52. Rohrer, M., Martius, O., Raible, C. & Brönnimann, S. Sensitivity of blocks and cyclones in ERA5 to spatial resolution and definition. *Geophys. Res. Lett.* e2019GL085582 (2019).
53. Gelaro, R. et al. The modern-era retrospective analysis for research and applications, version 2 (MERRA-2). *J. Clim.* **30**, 5419–5454 (2017).
54. Urraca, R. et al. Evaluation of global horizontal irradiance estimates from ERA5 and COSMO-REA6 reanalyses using ground and satellite-based data. *Sol. Energy* **164**, 339–354 (2018).

55. Niermann, D., Borsche, M., Kaiser-Weiss, A. K. & Kaspar, F. Evaluating renewable-energy-relevant parameters of COSMO-REA6 by comparison with satellite data, station observations and other reanalyses. *Meteorologische Z.* **28**, 347–360 (2019).
56. European Climate Foundation. Roadmap 2050: a practical guide to a prosperous, low carbon Europe. *Brussels: ECF* (2010).
57. Skamarock, W. C. et al. A description of the advanced research WRF version 3. *NCAR Techn. Note* **475**, 113 (2008).
58. European Commission, Joint Research Centre (JRC). Global Energy and Climate Outlook 2020: Energy, Greenhouse gas and Air pollutant emissions balances. *Dataset* <https://data.jrc.ec.europa.eu/dataset/1750427d-afd9-4a10-8c54-440e764499e4> (2020). Accessed 24 Apr 2022.
59. Tobin, I. et al. Climate change impacts on the power generation potential of a European mid-century wind farms scenario. *Environ. Res. Lett.* **11**, 034013 (2016).
60. Hirth, L., Mühlenpfordt, J. & Bulkeley, M. The ENTSO-E transparency platform—a review of Europe’s most ambitious electricity data platform. *Appl. Energy* **225**, 1054–1067 (2018).
61. Ho, L., Fiedler, S. & Wahl, S. PV and Wind power dataset for Europe. https://www.wdc-climate.de/ui/entry?acronym=DKRZ_LTA_1198_ds00003 (2023).

Acknowledgements

This study has been conducted in the framework of the Hans-Ertel-Centre for Weather Research funded by the German Federal Ministry for Transportation and Digital Infrastructure (grant number BMVI/DWD 4818DWD5A). We thank the German Weather Service for providing COSMO-REA6 data, P. James for the data for the weather patterns, C. Frank for the code for photovoltaic power simulations, and S. Jerez for the CLIMIX data.

Author contributions

L.H. designed and ran the model experiments, analyzed the results, and created the figures. S.F. conceived the concept and led the study. Both authors wrote and reviewed the manuscript.

Funding

Open Access funding enabled and organized by Projekt DEAL.

Competing interests

The authors declare no competing interests.

Additional information

Supplementary information The online version contains supplementary material available at <https://doi.org/10.1038/s43247-024-01224-x>.

Correspondence and requests for materials should be addressed to Linh Ho-Tran.

Peer review information *Communications Earth & Environment* thanks Linyue Gao and Merlinde Kay for their contribution to the peer review of this work. Primary Handling Editors: Ana Teresa Lima, Clare Davis and Martina Grecequet. A peer review file is available.

Reprints and permission information is available at <http://www.nature.com/reprints>

Publisher’s note Springer Nature remains neutral with regard to jurisdictional claims in published maps and institutional affiliations.



Open Access This article is licensed under a Creative Commons Attribution 4.0 International License, which permits use, sharing, adaptation, distribution and reproduction in any medium or format, as long as you give appropriate credit to the original author(s) and the source, provide a link to the Creative Commons license, and indicate if changes were made. The images or other third party material in this article are included in the article’s Creative Commons license, unless indicated otherwise in a credit line to the material. If material is not included in the article’s Creative Commons license and your intended use is not permitted by statutory regulation or exceeds the permitted use, you will need to obtain permission directly from the copyright holder. To view a copy of this license, visit <http://creativecommons.org/licenses/by/4.0/>.

© The Author(s) 2024

4.2 MORE SUMMERTIME LOW-POWER PRODUCTION EXTREMES IN GERMANY WITH A LARGER SOLAR POWER SHARE

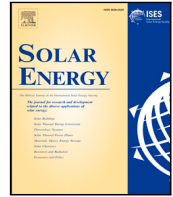
The second study addresses the seasonality of prolonged low production events in wind and photovoltaic power production in Germany. It shows that in these events are associated with stationary weather patterns and such events might occur more in the summer, especially in May, with the future installed capacities.

This study has been published as referenced below and is included subsequently in the journal layout. Its Supplementary material is included in the Appendices.

Ho-Tran, L. and Fiedler, S., 2024. More summertime low-power production extremes in Germany with a larger solar power share. *Solar Energy*, 283, p.112979.

The content of this section is published under a Creative Commons Attribution 4.0 International License.

Author contributions: Linh Ho-Tran: Writing – review editing, Writing – original draft, Visualization, Validation, Software, Methodology, Investigation, Formal analysis, Data curation, Conceptualization. Stephanie Fiedler: Writing – review editing, Supervision, Resources, Project administration, Funding acquisition, Conceptualization.



More summertime low-power production extremes in Germany with a larger solar power share

Linh Ho-Tran^{a,b,c,*}, Stephanie Fiedler^{a,b,d,1}

^a Institute of Geophysics and Meteorology, University of Cologne, Cologne, Germany

^b GEOMAR Helmholtz Centre for Ocean Research Kiel, Kiel, Germany

^c Faculty of Technology, Policy and Management, Delft University of Technology, Delft, Netherlands

^d Institute of Environmental Physics (IUP), Heidelberg University, Heidelberg, Germany

ARTICLE INFO

Dataset link: https://www.wdc-climate.de/ui/entryacronym=DKRZ_LTA_1198_ds00003

Keywords:

Extremes power production

Stationary weather pattern

Seasonality

ABSTRACT

The share of renewable energy in Germany is increasing to meet the climate-neutral targets in 2050. Weather-driven anomalies in renewable power production thus can pose greater challenges in balancing electricity supply and demand. This study investigates the seasonal differences in extreme events in photovoltaic (PV) plus wind power production in Germany for installed capacities for the present and 2050. The results indicate an increase in such extreme events in the summer half-year, mostly pronounced in May. Extremely low production with a duration of 14 days in winter is associated with atmospheric blocking, with very low wind power production anomalies of up to -37% . Summertime extremely low production is associated with stationary cyclonic weather patterns, with similar reductions in both energy sources of up to -19% . Case studies illustrate the dependency of the benefits of cross-border electricity transmission lines on the prevailing wind direction. North–South transmission lines are beneficial when an anticyclone moved from the Northwest to Germany, whereas West–East transmission lines are beneficial when a cyclone moved from the Southwest to Germany. The results imply an increased risk of extremely low power production during future summers in Germany and suggest monitoring sequences of different weather patterns for the energy sector.

1. Introduction

European countries are rapidly increasing the share of power production from renewable sources to reach the 2050 climate-neutral targets [1]. As part of this goal, the German government has set its target to increase the share of renewable sources in electricity generation to 80% and in gross energy consumption (including electricity, heating, cooling, and transport) to 60% by 2050 [2,3], compared to 49.6% and 20.4% in 2022 [4]. Wind and solar power are the two fastest-growing renewable sources in Germany. In 2022, wind and solar power (mainly photovoltaic) contributed 26% and 12% to electricity production in Germany [5]. The total installed capacities of onshore wind power and solar power in Germany have almost doubled over 10 years with 58 GW and 67 GW in 2022, compared to 31 GW and 33 GW in 2012. Particularly, German offshore wind power capacities have strongly increased from 0.3 GW in 2012 to 8 GWM in 2022 [6].

The high shares of renewable power sources make the electricity system susceptible to adverse weather conditions. One such challenge arises when both photovoltaic (PV) and wind power produce less than

the expected amount for a prolonged period of up to 14 days [7]. Such low production events can be challenging with the currently available storage capacities for electricity in Germany, e.g., with 5.6 GW for battery [8] and 6.7 GW for pump storages [9]. Prolonged low production events can be especially problematic when they co-occur with an increased demand, e.g., for heating during cold spells [10].

Previous studies have primarily focused on anomalously low power production events occurring in winter [7,11,12], mostly caused by a reduction in wind power production [13]. However, extreme events in the energy system can also occur in summer. Summertime irradiance is larger than in winter making weather-driven extremes in power production more sensitive to potential reduction in PV power production. This dependency can increase in the future because the projected ratio of PV to wind power capacity for Europe is larger than today, e.g., 2:1 in 2050 [14] compared to 0.7:1 in 2019 [15]. Moreover, European PV power anomalies show a more homogeneous spatial distribution across seasonal to multidecadal weather variability in comparison to wind power in various installed capacity scenarios [16]. In consequence, an event of low PV power production can affect relatively large regions resulting in little opportunity for cross-border electricity transmission

* Corresponding author at: GEOMAR Helmholtz Centre for Ocean Research Kiel, Kiel, Germany.

E-mail address: Lho@geomar.de (L. Ho-Tran).

¹ formerly: Institute of Geophysics and Meteorology, University of Cologne, Cologne, Germany.

of neighboring countries [13]. In addition, climate change leads to more frequent, intense, and prolonged heatwaves [17,18], which may increase the future electricity demand for cooling, akin to the demand for heating during cold spells in winter.

A study by [13] has identified synoptic weather conditions associated with low PV plus wind power production, hereafter referred to as total production in Europe, using the weather pattern classification from [19]. Specifically, using the European installed capacity projected for 2050, the pattern South-Shifted Westerly is associated with the lowest 1-day total production, while Anticyclonic South-Easterly is associated with the lowest 10-day total production event. The number of such weather patterns lasting for more than 10 days is limited with 19 events during the period 1995–2017. However, an energy system assessment points to the importance of sequences of several different weather patterns for anomalously low power production in Germany [10]. To what extent events composed of several weather patterns are more extreme in comparison to prolonged events with the same prevailing weather pattern has not been systematically studied in light of future capacities. The present study aims at helping to fill this knowledge gap.

We examine prolonged extremes in total power production in Germany with a focus on their seasonal differences. By performing PV and wind power simulations and pairing the results with a synoptic weather classification, this study provides evidence that there might be more prolonged low-production events in summer for the 2050 installation. Our study contributes to filling the gap in knowledge of how summertime low-production events differ from wintertime events, in terms of how PV and wind power production vary and what weather patterns drive extremes in production. Such knowledge is important for electricity system operators to issue warnings when the weather conditions associated with extreme events are forecasted. Moreover, the knowledge helps to mitigate potential impacts, e.g., by installing storage and suitable transmission lines for electricity to balance regional differences in production during extremes.

Detailed descriptions of the data and methods used in the analyses are provided in Section 2. The results first show the seasonal differences of events with anomalous PV and wind power production in Germany (Section 3.1). Section 3.2 compares the cyclonic and anticyclonic characteristics of weather patterns that are associated with extreme events occurring in winter and summer. To further examine prolonged low production events, ten low production events of a duration of 14 days were selected and examined (Section 3.3), and two case studies are analyzed in detail in Section 3.4. Finally, the discussion and conclusion of the results are presented in Sections 4 and 5.

2. Methods

2.1. Data

Our analysis of extremes in total production (PV plus wind power production) is based on simulations with the Renewable Energy Model (REM), which has been described and used in an earlier article [13]. REM was developed to simulate PV and wind power production using meteorological and power installation data for Europe. In REM, the meteorological data are from the reanalysis dataset COSMO-REA6 [20] with a high horizontal resolution of 6 km. Validation tests of REM output against Renewables Ninja [21,22] and CDS data [23] show good temporal correlations of 0.88–0.98 for PV power and 0.75–0.97 for wind power onshore, and potential capacity factors in agreement for PV power (in the range of 12% to 14%) and wind power onshore (around the value of 24%) for four selected countries in 1995–2017 [13]. The potential capacity factors (potentials) of PV and wind power production were calculated based on COSMO-REA6 data using a power-rating method with effective irradiance, including direct and diffused radiation, on crystalline silicon PV modules [24] with the azimuth angles facing south and the optimal tilt angles of 21° to 50° for European

countries [25] multiplied by 0.7 as investors usually opt for lower tilt angles to reduce the shadow effects [26]. The potentials of wind power were calculated using a cubic power curve with the cut-in, rated, and cut-out wind speeds of 3.5, 13, and 25 m/s. Wind speeds were taken from COSMO-REA6 data at the two model levels 36 and 37 with average heights of 116 m and 178 m over the European domain.

The potentials were then multiplied by the installed capacities from CLIMIX to get power production of wind and PV power. The data on power installation in REM include the spatial distribution and installed capacity of PV and wind power in Europe at a horizontal resolution of 11 km from the model CLIMIX (CLimate and energy MIX) by [14]. CLIMIX allocates the installed capacities of PV and wind power reported for present-day and planned for 2050 from each country into a grid of 0.11° based on criteria such as resource availability, population, and restricted areas. The output of REM is the hourly production of PV and wind power in every eight grid box, i.e., at a horizontal resolution of 48 km but with an effective resolution of 6 km for the meteorological processes. Our study is based on one scenario of installed capacity projected for 2050 from the CLIMIX model [14]. The results can vary depending on the ratio of PV and wind power and the future spatial distribution of their installation. CLIMIX is shown to be conservative for wind power, e.g., 440 GW for Europe in 2050 compared to another projection of 620 GW [27]. A higher ratio of PV to wind installed capacity, e.g. 5:1, would decrease the total power anomalies in individual weather patterns but not the overall anomalies across all patterns [13].

To assess the dependency of power production anomalies on the installed capacity, we performed and compared the following two experiments with the same meteorological data for 1995–2017 and different installed capacities.

- scenario-2050: REM simulation for a future installation using the scenario for 2050 obtained from the CLIMIX model [14]
- scale-2019: REM simulation for a present-day installation derived by scaling the scenario-2050 installation to match the European installed capacity in 2019 [15]

The scaling for obtaining the scale-2019 installation was necessary due to the lack of a suitable gridded data set covering all of Europe. We used country-aggregated installations of the year 2019 [15] for the scaling. The corresponding REM experiment scale-2019 yields a ratio of the annual PV to wind power production and total installed capacities for Germany that closely aligns with data reported for 2015 [12]. Moreover, the experiment scale-2019 reproduces the weather pattern associated with the lowest total power production for Germany [12,13]. See [13] for more details on the methods and underlying data. Note that the scaling method retains the same spatial distribution of installed capacities between the two examined scenarios. The future spatial distribution of PV and wind power installation can differ from scenario-2050 depending on the countries' plans and implementation. However, we perceive scenario-2050 as a plausible future scenario since CLIMIX has taken into account the resource availability and countries' plans for future investments. The scenario 2050 from the CLIMIX model has been used in several publications before to assess renewable power production variability [7,28–31]. Validation of CLIMIX model shows reasonable agreement to past power production records for most countries [14], albeit with larger values due to the overestimation of the model simulation [32] and assumptions that all planned power plants operate and function well at the same time [14]. Maps of PV and wind power installed capacity in scenario-2050 is shown in [13].

To examine the impact of synoptic weather conditions on PV and wind power production, we pair each day in the timeseries from REM output with a weather pattern from the classification comprising 29 patterns [19]. In this classification, the weather patterns are distinguished based on the position of dominant pressure systems, their cyclonic or anticyclonic characteristics, and the prevailing wind

direction over Central Europe [19]. We further assessed the 2 m temperature, mean-sea-level pressure, and downward direct and diffuse short-wave radiation from COSMO-REA6 to characterize the meteorological developments during extreme events in total power production.

2.2. Analysis strategy

In this study, we define extreme events based on the time series of total power production in Germany. These time series are derived by taking the mean values of PV and wind power production across all grid cells with available data within Germany from the REM output. The grid cells were selected using a pre-defined shapefile [33]. We selected PV power and onshore wind power production in Germany for the analyses of our experiments. The installed capacities for Germany are 88.5 (12.2) GW for PV power and 33.1 (12.6) GW for onshore wind power in scenario-2050 (scale-2019), resulting in a ratio of PV to wind power installation of about 2.5:1 (1:1). The analysis includes only wind power onshore in Germany inside the shapefile (Supplementary Fig. S1). Wind power offshore could reach 45–70 GW in Germany in 2050, decreasing the ratio of PV to wind power installation to between 1.2:1 and 2.3:1 [34], still within the range of ratio between scale-2019 and scenario-2050 installations. The lower ratio means the influence of PV power on total production anomalies would reduce and the influence of wind power would be further enhanced, the overall effect on the total production anomalies would be similar to scenario-2050 but with lower magnitudes.

Wind power has a strong influence on total production in scale-2019 and is higher in winter than in summer [13], while PV power produces a larger amount during summer than in winter. To account for the seasonality of production, we calculate normalized power production anomalies time series to represent deviations from the climatological mean power production for a given time of year. We first calculated hourly anomalies of power production against the climatological mean with the same hour, day and month of every year for the entire period. Then we summed the hourly data to obtain daily time series to be comparable with weather pattern data and analyze 1-, 7-, and 14-day events.

We statistically analyze prolonged anomalously high and low production events associated with weather patterns. Our selection of the 50 most extreme total production events for each category, i.e., for the lowest and highest total production, and each duration of 1, 7, and 14 days. We defined prolonged low production events with a duration of 14 days because German energy deficits increase monotonically up to 14 days [35]. The time windows of 1 and 7 days were selected to represent the short and medium length of events, as used in a previous study for Europe [7]. Tests of other time windows in the context of power production anomalies associated with weather patterns show similar results amongst events with duration differences of up to two days [13]. For instance, to define the 50 lowest total production events with a 14-day duration, we used the time series of daily anomalies for the period 1995–2017 to first calculate the moving average over 14-day time windows. Then, we select the 50 dates with the lowest moving average. These 50 dates are assigned as the central dates of the 14-day events with extremely low production. When two events have their central dates closer than 14 days to each other, one of the events was removed before further analyses to avoid counting the same event more than once. During 7- and 14-day events the sequences of weather patterns can contain a mix of cyclonic and anticyclonic patterns depending on how the weather conditions develop.

Monthly statistics are calculated based on the central dates of the events for each event duration, namely the first, fourth, and eighth days of the duration 1-, 7-, and 14-day, respectively. The statistics for the weather patterns were computed per event, i.e., considering all dates during the duration of the events. For each category of highest or lowest power production, we selected the 50 most extreme events per duration, with 50 days for 1-day events, 350 days for 7-day events, and

700 days for 14-day events, resulting in 2200 days in total. To account for a higher frequency of occurrence of some weather patterns, the frequencies of patterns for extreme production events were normalized by the climatological mean of the frequency of occurrence of the weather patterns (1995–2017) separately for winter and summer. For the seasonal division, we adopted the same two half-year seasons to be consistent with the weather pattern classification as in [19], namely summer from April 16th to October 15th and winter from October 16th to April 15th.

We aim to better understand the seasonal differences in the power production anomalies in Germany from a meteorological perspective. To that end, we first investigate the anomalies in total power production associated with different weather patterns separated into cyclonic and anticyclonic characteristics. Out of 29 weather patterns, 16 are cyclonic patterns denoted by the letter *z* for *zyklonal* in German or *T* for *Trough* or *Tief* (low) in German, and 13 are anticyclonic patterns denoted by the letter *a* or *H* for high pressure [19]. Fig. 3 shows the frequency of occurrence of cyclonic and anticyclonic patterns associated with the 50 most extreme production events for each duration of 1, 7, and 14 days. To further examine the seasonal differences between prolonged low production events in winter and summer, we also select the two most extreme 14-day events to perform two case studies, based on the weather in December 2007 and May 2016 to analyze in detail the co-development of power anomalies and weather conditions.

3. Results

3.1. Seasonal differences

The experiment scenario-2050 shows four times more summer events with extremely low total power production over Germany compared to scale-2019. Namely, out of all 150 lowest production events with 1-, 7-, and 14-day durations, 22% occurred in summer compared to 5% in scale-2019 (Fig. 1a,c). The largest difference is seen for the 14-day lowest production events in summer, with 25% (5%) of the 50 lowest production events in scenario-2050 (scale-2019). None of the 50 lowest production events with 1-day duration occurs in summer for scale-2019, but 14% are seen in summer in scenario-2050. For 7-day lowest production events, the occurrence more than doubles with the future installed capacities with 6% in scale-2019 to 15% in scenario-2050. Nevertheless, the most extreme low production events occur more frequently in winter (Fig. 1), consistent with previous studies with various durations of events for Germany [12] and Europe [7]. Most extreme production anomalies are seen around December and January for both installations (Fig. 1c), which is two months later than in [7]. The difference might be due to their assessment of Western Europe, whereas we focus here on Germany.

May has of all months the largest increase of extremely low power production events in scenario-2050 for all durations with 2–3.3% of the 150 most extreme events falling into this month, in comparison to no extreme events in scale-2019 (Fig. 1a,c). This increase in the occurrence of extremes in May is due to its higher frequencies of weather patterns with anomalously low irradiance and thus low PV power production, e.g., Cyclonic North-Easterly (NEz), Icelandic High, Trough Central Europe (HNz), and Low Cut-Off over Central Europe (TM) (Fig. 2). The full list of names of the weather patterns is given in Supplementary Table S1. One example is the 14-day event on 8–21 May 1996, of which eight days had the pattern NEz. A strong extra-tropical cyclone with a center over the south of Italy and a core pressure of 998 hPa (Supplementary Fig. S2) led to anomalously high cloud cover over Germany reducing irradiance at the surface. As a result, an extremely low PV power production was simulated with up to –36% on 11 May which was very low compared to the composite mean for the NEz pattern of –2% for Germany [13]. The extremely low PV power production has a higher influence on total production in scenario-2050

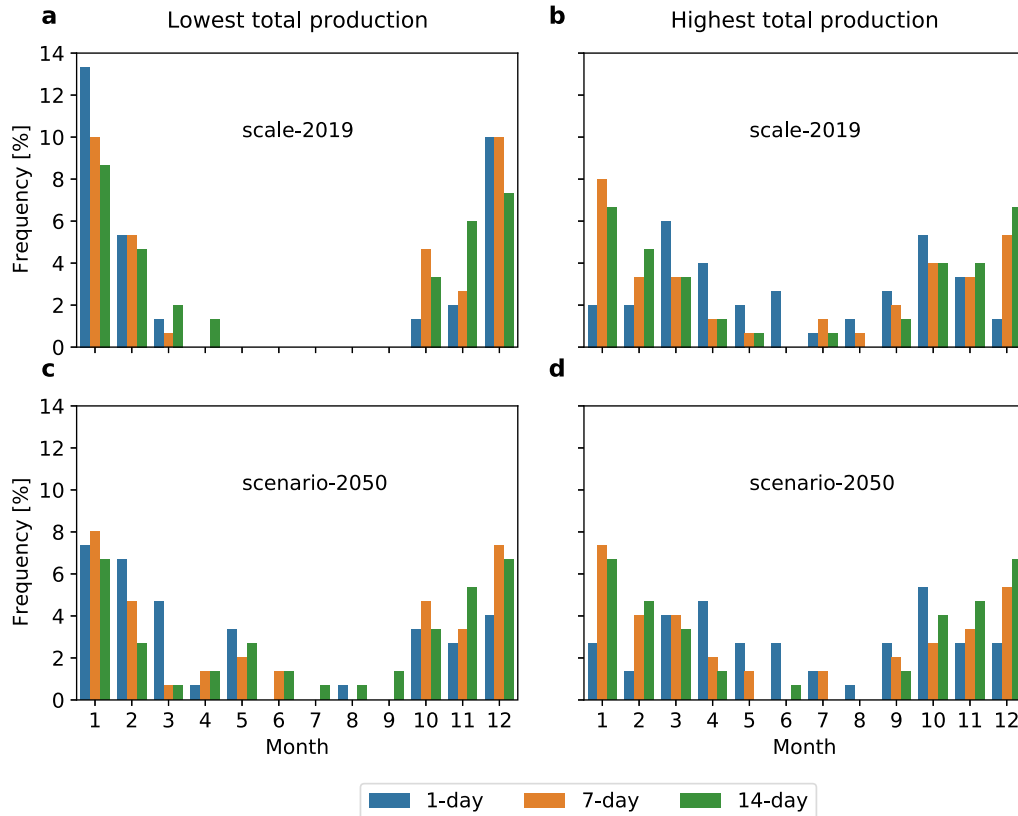


Fig. 1. Monthly distribution of the most extreme power production events. Shown are the 50 most extreme events color-coded for each duration of 1, 7, and 14 days for the lowest total power production (left) and the highest total power production (right) aggregated for Germany, simulated with scale-2019 (top) and scenario-2050 (bottom) installed capacities. (For interpretation of the references to colour in this figure legend, the reader is referred to the web version of this article.)

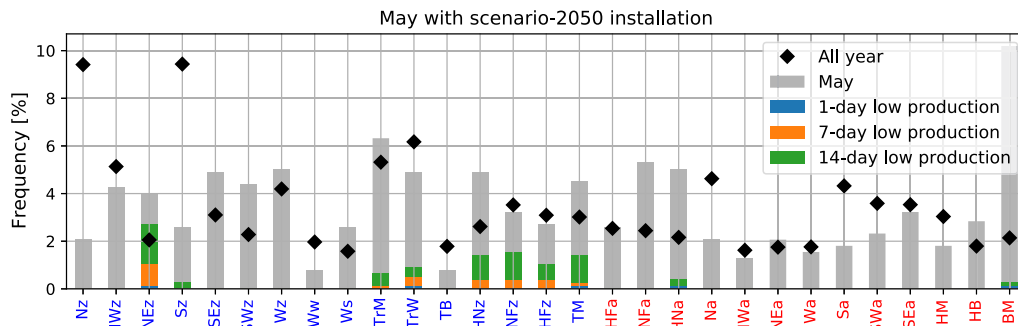


Fig. 2. Frequency of co-occurring weather patterns and lowest power production events in May. Shown are the relative frequency of weather patterns occurring in May (gray bars) and the whole year (black diamonds) over the period 1995–2017. Included in the gray bars are the percentages of days with extremely low total production events in May co-occurring with the weather patterns (5, 3, and 4 events with the duration 1, 7, and 14 days, respectively) simulated in scenario-2050. Weather patterns written in blue have cyclonic characteristics, while weather patterns written in red have anticyclonic characteristics. (For interpretation of the references to color in this figure legend, the reader is referred to the web version of this article.)

due to a higher share of PV power installations compared to scale-2019. Consequently, this event had the sixth lowest total production in scenario-2050 in summer but was not in the top 50 lowest production events in scale-2019.

Most of the highest production events also occur in winter in the experiment scale-2019, with 82% of 150 events with high extremes compared to 95% of the low extremes (Fig. 1a,b). For the high extremes in power production, changes in the seasonal differences are moderate between the two installations, with percentages of events occurring in summer increasing up to 3% for each duration (Supplementary Table S2). For both installations, the 7- and 14-day high extremes occur most frequently in January due to winter cyclones associated with strong winds. For 1-day high extremes, the simulations show later maxima in the occurrence of extremes, with a shift of the maximum from March to

April when we go from scale-2019 to scenario-2050 (Fig. 1b,d). Again, this is due to the higher share of PV in scenario-2050 such that the influence of the stronger irradiance towards spring has a larger effect on the total power production.

3.2. Cyclonic and anticyclonic characteristics

Most events with low extremes are associated with anticyclonic weather patterns for all durations in scale-2019 explaining 60%–66% of all events (Fig. 3a–c). In scenario-2050, anticyclonic patterns also explain 52%–54% of events with a duration of 7 and 14 days, but less than half (42%) of the 1-day extreme events (Fig. 3a). Consequently, cyclonic patterns show an increase in association with 1-day lowest

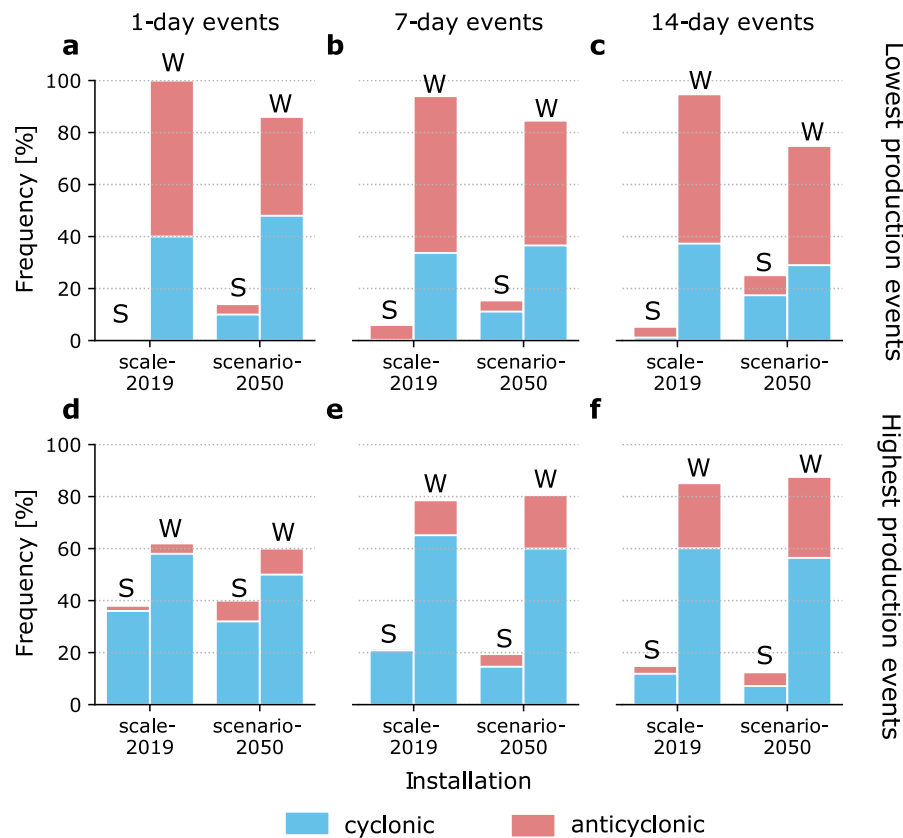


Fig. 3. Frequency of co-occurrence of power production extremes with cyclonic and anticyclonic weather patterns in winter and summer. Shown are the number of cyclonic (blue) and anticyclonic (red) weather patterns associated with the 50 lowest (a–c) and highest (d–f) total power production events in summer (S) and winter (W) half-years for each duration 1, 7, and 14 days, calculated in percentage of day for scale-2019 and scenario-2050 installations with weather data of 1995–2017 in Germany. Quantitative statistics are listed in Supplementary Table S2. (For interpretation of the references to color in this figure legend, the reader is referred to the web version of this article.)

production events from scale-2019 to scenario-2050, both in winter (from 40% to 48%) and summer (from 0 to 10%). The higher frequency of cyclonic patterns on the lowest production events in scenario-2050 is due to their low irradiance and the higher influence of low PV power anomalies on total production, particularly in summer (Fig. 3a). Similar increases in the frequencies of cyclonic patterns are also seen in summer for 7-day events from 0 to 11% and for 14-day from 1% to 17% (Fig. 3b,c, Supplementary Table S2). However, weather patterns leading to the largest number of extremely low production events show cyclonic characteristics, specifically the pattern Cyclonic South-Easterly (SEz) for all three durations 1, 7, and 14 days (Supplementary Table S1 and Fig. S3). The weather pattern SEz is known as Dark doldrum pattern for Europe, associated with simultaneously low production in PV and wind power [13].

In contrast to the prevalence of anticyclonic patterns in the 50 lowest power production events, the highest power production events are predominantly associated with cyclonic patterns independent of the event durations and season, explaining namely 72%–94% of the extreme events in scale-2019 and 63%–82% in scenario-2050 (Fig. 3d–f, Supplementary Table S2). In particular, the events with the highest 1-day production coincide mostly with cyclonic weather patterns, namely 94% (82%) of the cases in scale-2019 (scenario-2050), and have relatively less pronounced seasonal differences than the longer events (Fig. 3d). High production events are characterized by westerly winds over Central Europe and the North Sea, e.g., Wz, SWz, and NWz (Supplementary Fig. S4), consistent with findings for Europe [13]. Noticeably, the pattern Scandinavia-Iceland (HNFa), which is not related to high production events in scale-2019, sees a substantial increase in the number of extreme events in scenario-2050 (Supplementary Fig. S4), primarily in winter. The pattern shows a ridge over Central Europe

that leads to anomalously high irradiance and therefore amplifies the impact of the higher future PV power share in Germany.

3.3. Prolonged low production events

We compare the meteorological conditions during the 14-day lowest production events between winter and summer using ten events for each half-year season (Fig. 4). Overall, 14-day lowest production events in winter are associated with anticyclonic patterns (59% of days), while those in summer are more likely associated with cyclonic patterns (66% of days). There are no particularly repeating weather pattern sequences during these lowest production events, but rather the low production comes from combinations of several weather patterns with low PV and/or wind power production.

In certain years, such as 1996, 2007, and 2016, extremely low power production events occurred in both winter and summer. Noticeably, three out of the five lowest total production 14-day events occurred for the weather of summer 2016. This might be linked to the anomalous activity of the Rossby waves in 2016 [36]. Under certain conditions, Rossby waves favor blocking which is linked to the development of heat waves and cold spells [37], e.g., the unusual heatwaves across Western Europe in 2016 [36]. This blocking in summer 2016 also resulted in prolonged periods of anomalously low wind speeds which caused the reduction in wind power production in Germany in May, June, and July 2016 (Fig. 4).

Stationary weather patterns play a substantial role in prolonged low-production events, e.g., a blocking high-pressure system like during 2016. Here we define stationary weather patterns when the same pattern occurs for at least five consecutive days, following the criteria for an atmospheric blocking [38]. Specifically, 13 of the 20 lowest

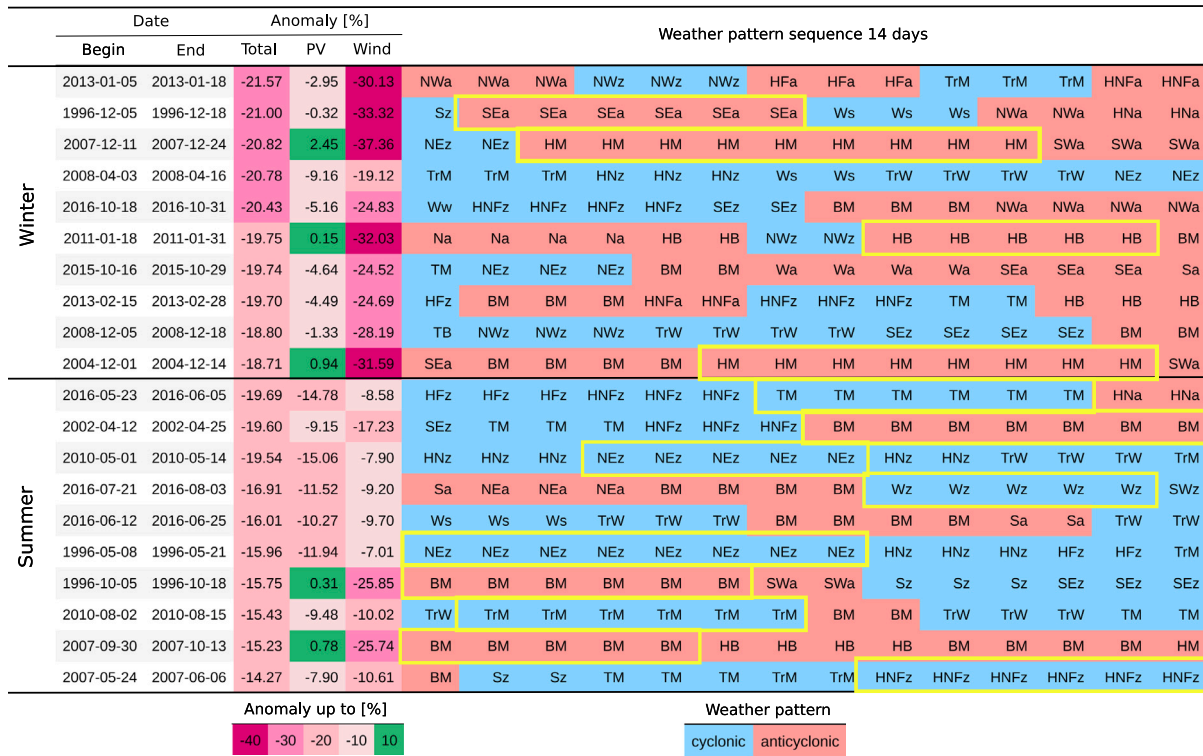


Fig. 4. Weather patterns in 20 lowest 14-day power production events in Germany, including 10 events in winter and 10 events in summer. The beginning and ending dates (inclusive) and anomalies (moving average 14 days). Half-year winter is 16 Oct–15 Apr, and half-year summer is 16 Apr–15 Oct. Anomalies are as deviations from their climatological means (see Methods). The color denotes anomalies in intervals of 10%. Weather patterns colored in blue (red) have cyclonic (anticyclonic) characteristics. Sequences with stationary weather patterns that last at least five days are highlighted in bright yellow rectangles. (For interpretation of the references to color in this figure legend, the reader is referred to the web version of this article.)

power production events of a duration of 14 days are characterized by a stationary weather pattern for five or more consecutive days, marked by yellow rectangles in Fig. 4. The characteristics of the stationary weather patterns depend on the season of the event. Nine of ten events in summer contain a stationary weather pattern, six among which are associated with cyclonic patterns, e.g., TM, NEz, Wz, TrM, HNFz (Fig. 4). These events are characterized by relatively low production in both PV and wind power, simultaneously contributing to the anomalously low total production, e.g., events in May 2016, May 1996, August 2010, and April 2002 with anomalies in PV and wind power production of up to -11.7% and -17.2% .

Four of ten lowest production events in winter (December 1996, December 2007, January 2011, December 2004) are associated with stationary anticyclonic weather patterns, e.g., SEa, HM, HB, identified as atmospheric blocking with a known link to weather extremes, e.g., cold spells, heat waves, and droughts [39]. These events involve stationary high-pressure systems, resulting in low wind speeds and cloud covers ranging from 60% to 72% over Germany, close to the climatological winter mean for 1995–2017 (65%). The PV power production was therefore close to the seasonal average (-0.3 to 2.5%). Anomalously low total production is explained by the low wind speeds which led to extremely low wind power production during these blocking events, with anomalies an order of magnitude lower than that of PV power (up to -37%) (Fig. 4). High pressure over Central Europe (HM) occurred as two blocking events in December 2007 and December 2004, consistent with the role of HM in low production for events with a duration 120 h (5 days) in Germany as reported in a previous study [12]. Additionally, Anticyclonic South-Easterly (SEa) was a stationary weather pattern in the December 1996 event, a pattern known for 10-day low production events for both present-day and future installations in Europe [13].

Some events occurring during the transitional times between the winter and summer half-year exhibited the characteristics of events

in the other season. The transitional times are typically two weeks around the dates of seasonal division, i.e. 15 April and 15 October [19]. For example, one event in late winter (April 2008) shares similar characteristics with summer events with relatively low production in both PV and wind power (-9% and -19% , respectively), whereas two events in late summer (October 1996 and October 2007) share similar characteristics with winter events with very low wind power production (up to -26%) and slightly above average PV power production (up to 1%) (Fig. 4).

3.4. Case studies

Two case studies were selected for further analysis of how the meteorological development influenced the power production of PV and wind power over time in Germany: (1) The event in December 2007 represents the third lowest 14-day total production event in winter with a significant impact in the simulation of Germany's electricity system [10]; (2) the event in May 2016 was selected because of its representative meteorological conditions during summer events with the lowest anomaly of total production (19.7% , Fig. 4). Figs. 5 and 7 show the sequences of weather patterns, the development of the meteorological variables 2m-temperature, mean sea level pressure, 10m-wind speed, and surface irradiance, and the associated anomalies in the power production. We show the development for seven days before and seven days after the central date of the events, resulting in a total of 28 days. It allows us to assess the weather conditions ahead of the extreme events and the subsequent recovery of the production. To explore the possibility of importing electricity during shortages in Germany, we include time series of the corresponding power production anomalies in the neighboring countries France and Denmark, two of the countries trading energy with Germany most frequently [8]. Similar figures for the ten lowest production events for each season (as in Fig. 4) are shown in Supplementary Figs. S5 and S6.

3.4.1. Winter event: December 2007

On December 8, 2007, a low-pressure system formed in the North Atlantic, resulting in increased Westerly wind and cloud cover (72%) over Germany, leading to higher wind power (44%) and slightly lower PV power production (−3%, Fig. 5). The system moved southeastward with the center located over Germany, decreasing wind power production in Germany (−13%), initiating the 14-day low production event on December 10 (Fig. 6c). This system formed a cyclonic flow with Northeasterly wind (NEz) over the eastern coast of Great Britain, increasing wind power production in the southwestern tip of Germany, France, and the northern part of Spain (Fig. 6d). Additionally, from December 12 the Northeasterly wind directed cold air from the Arctic to Germany, increasing the energy demand for heating [10] (Fig. 5a). Simultaneously, a ridge formed in the south of Europe, with an axis extending from the west coast of Spain to Iceland (Fig. 6c). A stationary high-pressure system formed over Central Europe (HM) lasting from December 13 to 22. The high-pressure system was associated with slightly higher PV power production up to 10% on December 15 due to less cloudiness (cloud cover of 63%). However, the seasonally lower irradiance in winter did not compensate for the very low wind power production of up to −54% on December 14, resulting in an overall very low total production of up to −25% on December 14.

In the middle of the event, on December 17, 2017, a small cyclonic system formed in the Mediterranean. At its intersection with the existing high pressure over Central Europe, wind speeds increased in southwest Germany, while low wind power production persisted in the northeast of the country (Fig. 6g). A temporary increase in wind power in southern Germany alleviated the power shortage on the 17th but this recovery was short. Given that southern Germany currently has a lower number of batteries and pumped storage compared to the north [40], this brief recovery might not have been sufficient to replenish storage during the prolonged low production event. By December 18, the cyclonic system in the Mediterranean weakened and the influence of the high-pressure system dominated in Central Europe, reducing wind power production again on the 19th (Fig. 5).

The high-pressure system had a core pressure of more than 1025 hPa and had the core over Central and Southern Europe. It weakened on the 21st (Fig. 5) when a low-pressure system formed near Iceland. It resulted in strong Southwesterly winds over the North Sea (Fig. 6k), increasing wind power production in Germany on the 25th. This increased wind power production spread from the northwestern coast (Fig. 6l) to the rest of the country the following days, reaching the most positive anomalies of total production on the 29th (37%, Fig. 5) before decreasing again with the new weather condition (BM). The Southwesterly wind brings milder temperatures above zero degrees Celsius from the south of Europe to Germany. The higher temperatures would have also reduced the energy demand for heating, further alleviate the stress on the German electricity provision.

3.4.2. Summer event: May 2016

The meteorological development of the summer event in May 2016 was characterized by cyclonic weather patterns with a surface low-pressure system over Central Europe, including a stationary Cut-Off Low over Central Europe (TM) for six days from May 29 to June 3, along with Scandinavian High, Trough Central Europe (HFz) and High Scandinavian-Iceland, Trough Central Europe (HNFz) (Fig. 7).

On May 21, a low-pressure system north of Great Britain moved southeastward, weakened, and formed a trough over Germany on May 22. At the same time, a high-pressure system located in Eastern Europe (Fig. 8c). The pressure gradient between the two pressure systems increased the wind speeds, leading to higher wind power production in the north and west of Germany. The regional above-average production balanced the low wind power production in eastern Germany (Fig. 8d), resulting in a German wind power production close to the climatological mean on May 22 (Fig. 7e). Also along the pressure gradient between two pressure systems, increased cloud cover led to reduced

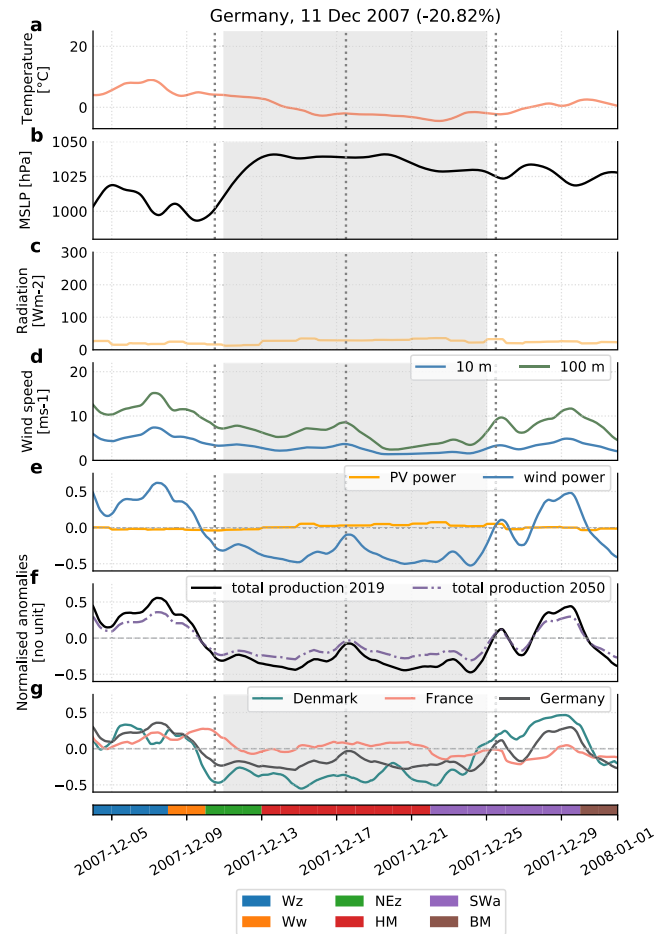


Fig. 5. Meteorological development during the 14-day low production event in Germany in the winter 11–24 December 2007. Shown are meteorological variables including 2-m temperature (a), mean sea level pressure (MSLP) (b), wind speed at 10 m and 100 m (c), and irradiance (downward short-wave direct and diffused radiation) (d), and normalized anomalies of energy variables including PV, wind power onshore (e), total production for *scale-2019* and *scenario-2050* installations (f), and total production of Germany and two neighboring countries Denmark and France (g). The figures are shown with moving averages of 24 h to smooth the diurnal variation. Vertical dotted lines mark three selected times to show the spatial variations of meteorological conditions and power production anomalies in Fig. 6. (For interpretation of the references to colour in this figure legend, the reader is referred to the web version of this article.)

surface irradiance and hence below-average PV power production in France on May 22 (Fig. 8a,b). In the following days, the area between two pressure systems moved eastward, affecting Germany, leading to a very low PV power production with daily anomalies of up to −48% on May 25. The positive anomaly of wind power production (20%) did not balance the very low PV power production, resulting in a very low total production anomaly of −73% on May 24. By May 26, the trough dissolved with a higher pressure area arriving from the west of Germany, and PV power returned closer to the climatological mean at −11% (Fig. 7).

In the middle of this 14-day low production event, the German total production temporarily increased on May 30. This was caused by a cut-off low-pressure system over Central Europe (TM) on May 29 (Fig. 8b). This low-pressure system remained stationary until June 4. Its strong pressure gradients led to high wind speeds and therefore high wind power production along the North Sea and the border of Germany near France, balancing the low wind power production in the southern parts of Germany (Fig. 8g,h) and leading to an above average wind power production in Germany on May 30 (Fig. 7). Cloudy

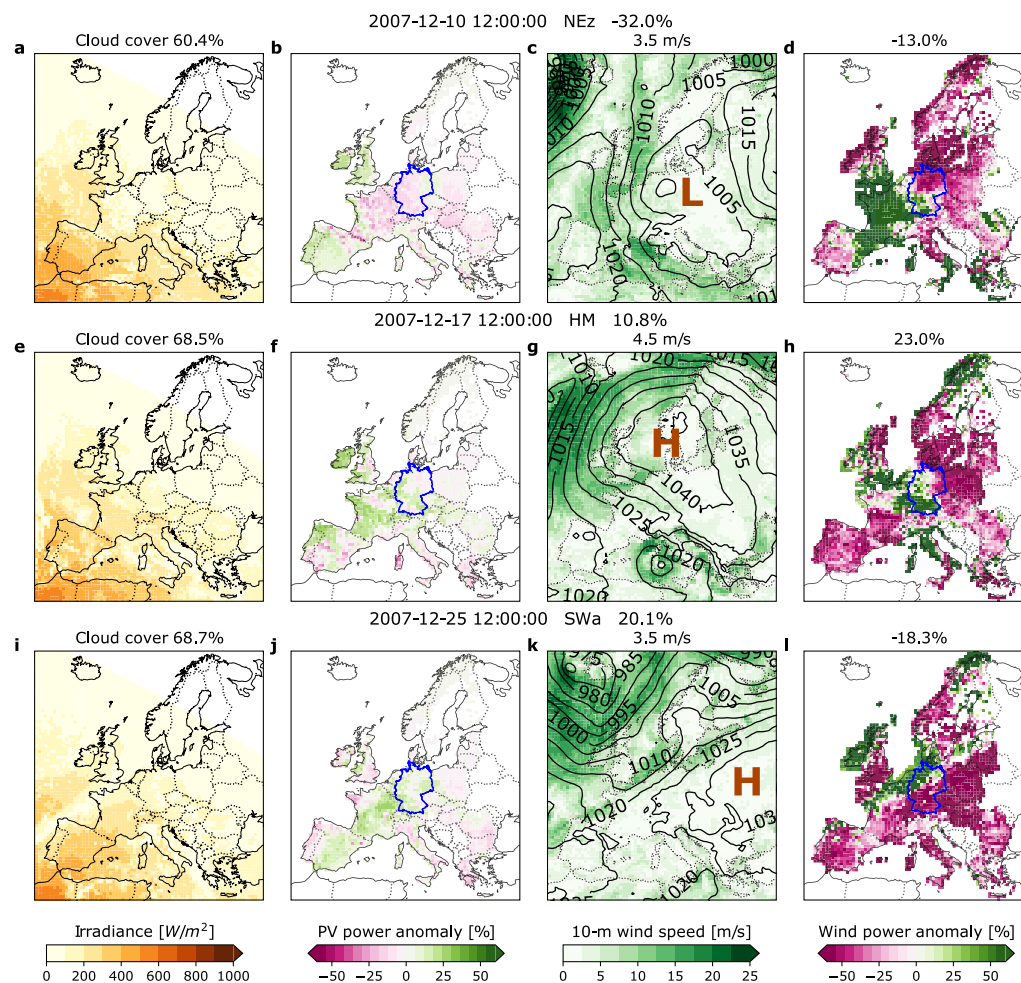


Fig. 6. Meteorological conditions in three selected times during the winter event December 2007 marked by dotted lines in Fig. 5. Four columns show (left to right) surface irradiance (%), anomalies of PV power production (%), wind speed at 10m (shaded) with mean sea level pressure (contour), and anomalies of wind power onshore production (%). The numbers shown on top of the first-column panels are mean cloud cover (%) for Germany. The other numbers show the corresponding mean values for Germany. The title for each row shows the weather patterns and the anomalies of total power production of Germany at 12:00 on that day. (For interpretation of the references to colour in this figure legend, the reader is referred to the web version of this article.)

conditions associated with the low-pressure system reduced the PV power production across Germany below average and dampened the effect of increased wind power production on May 30, thus the total production was still below average in scenario-2050. In the following days, the low-pressure system moved westward and dissolved on June 4, again reducing the wind power production in Germany leading to the continuation of the prolonged low production event (Fig. 7).

The extreme event ended on June 4, when a high-pressure system formed over Iceland with a ridge extending over Central Europe (HNa), resulting in reduced cloudiness (53%) and increased surface irradiance. PV power increased accordingly, starting from northern Germany on June 5 (Fig. 8j) and affecting the entire country until June 10. Wind power production remained nevertheless relatively low during this period with anomalies of up to -22% on June 7.

4. Discussion

The regional differences in power production anomalies have implications for the future possibility of the transmission and storage of electricity. The direction of a pressure system development influences the spatial distribution of power production anomalies in Germany and the neighboring countries, here shown with the example of France and Denmark. The winter event in December 2007 (and the start of the May 2016 event) began with a high (low) pressure system forming over the

North Atlantic in the northwest of Germany. In both cases, the pressure systems moved southeastward to Germany before continuing eastward over land and eventually dissolved. Following these developments, the negative anomalies of wind (PV) power production initiated in the northwest of Germany first, then expanding to Denmark, while France maintained an average power production in these cases (Fig. 5g and 7b). The tempo-spatial development of the power production anomalies poses a challenge since the west of Germany has industrial areas with high electricity demand and storage [40]. The North-South electricity transmission would be less useful in this case, particularly when wind power production in the North Sea and Denmark is simultaneously below average (Fig. 5g, 6d,h). Instead, the West-East electricity transmission line between France and Germany would be more helpful in balancing the extremes in power production.

In contrast, the Cut-off low-pressure system (TM) from May 29 to June 3, 2016, moved from the southwest to Germany. Negative anomalies of PV power production initiated in the south of Germany and France, while wind speeds increased in Denmark in the north of the Cut-off Low. Consequently, from May 29 to June 5, Germany and France had similar negative anomalies in total production, while Denmark had positive anomalies due to high wind power production on May 30 before returning to the climatological mean. In such situations, the North-South electricity transmission lines in Germany could be beneficial by importing surplus electricity from Denmark to the regions with electricity shortages in the south.

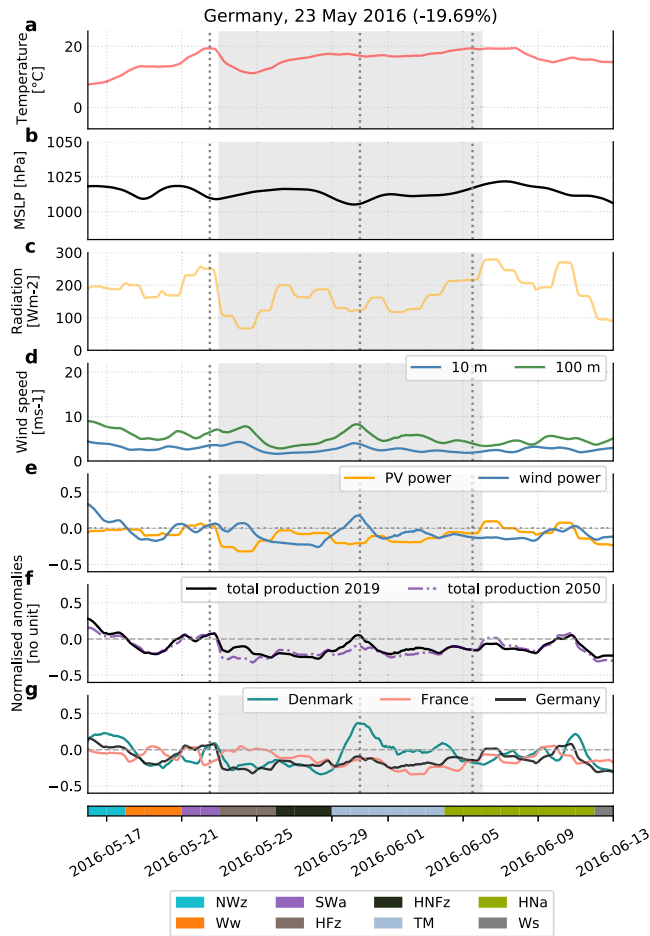


Fig. 7. Meteorological progression during a low production event in May 2016. Similar to Fig. 5 but for 14-day low production event in the summer, May 2016 (May 23 to June 5). (For interpretation of the references to colour in this figure legend, the reader is referred to the web version of this article.)

Interestingly, amongst 20 extreme events in Fig. 4, the winter event in Dec 2004 characterized the pattern HM from Dec 4–6, similar to the event in Dec 2007, but the low pressure system north of Great Britain moved southeastward made the North–South transmission lines from Denmark to Germany more beneficial (Supplementary Fig. S7a–d). On the contrary, the summer event in May 2007 characterized TM on May 30 to June 1, similar to the event in May 2016, but the low pressure system formed in France moved northeastward made the West–East transmission line from France to Germany more beneficial (Supplementary Fig. S7e–h). Nevertheless, the other 16 events did not include similar weather development and therefore, it is difficult to draw a definite conclusion. More studies with a larger number of events and weather conditions are thus required to understand the relationship between weather development and the role of transmission lines.

The total production in scenario-2050 may experience an alleviation of extremely low power production intensity during winter events but an exacerbation during summer events, relative to scale-2019. Over the 14 days of the winter event in December 2007, the anomalies of total production in scenario-2050 were moderate (closer to zero) compared to scale-2019 (Fig. 5). This stands in contrast to the summer event May 2016, where the total production in scenario-2050 has lower anomalous values than in scale-2019 due to the stronger impact from reduced PV power production on May 25 and 30 (Fig. 7). The need for battery storage during low production events in summer therefore increases in the future, as inflow for pumped storage is projected to decrease in summer due to reduced Alpine snow melt in future climate

change [41]. This may be especially critical for the electricity provision since blocking high-pressure systems in summer may coincide with the development of heat waves. Heat waves can lead to an increase in the electricity demand for cooling during such low-power production episodes, and both the frequency and intensity of heat waves are projected to further increase with future global warming [18].

A notable observation is that the anomalies of total production did not remain consistently low throughout the entire 14-day low power production events. There were instances where wind speeds recovered to near or slightly above the climatological mean in the middle of the assessed events, such as around December 18, 2007, and May 30, 2016 (Fig. 5, 7). Similarly short increases in total production can be seen in other 14-day low production events for each season in Supplementary Fig. S5 and S6. However, these temporary increases in total production anomalies rarely exceed 10% above the climatological means, indicating that electricity shortages could be alleviated but not fully recovered. Two exceptions are in December 1996 and May 2007 with positive anomalies of up to 20%. The variations in total production during these events underscore the need to monitor weather conditions to prepare electricity storage for an extended period of low power production, even when the total production appears to recover briefly. Including more offshore wind power would enhance the effect of wind power. Therefore during these short recovery time from low wind speeds, the total production might more quickly increase and reach regional values that exceed the average total production values, which would allow to store or transmit the surplus electricity to alleviate low production days elsewhere.

5. Conclusion

We present a comprehensive comparison of extreme events for PV and wind power production in winter and summer in Germany. To that end, we simulated PV and wind power using present-day and future installations, defined with an increased ratio of PV to wind power installed capacity from 0.7:1 for the present-day installation (scaled-2019) to 2:1 for the future installation (scenario-2050) in Europe, which corresponds to an increase from 1:1 to 2.5:1 in Germany. We identified extreme anomalies in power production and compared the meteorological conditions associated with these extreme events using synoptic weather pattern classification with 29 patterns [19] for Germany.

The results show distinct characteristics in weather patterns associated with the lowest and highest total production events. High production events are predominantly associated with cyclonic weather patterns with 77% and 68% for present-day and 2050 installations, respectively. In particular, Cyclonic Westerly (Wz) and Cyclonic North-Westerly (NWz) account for half of the days with high production events with a total of 51% in present-day installation. The seasonal differences in high-production events show no clear dependence on the installations, suggesting that conclusions for future high-production events can be drawn from results with present-day installations. In contrast, low production events are mainly associated with anticyclonic weather patterns with 63% in the present-day installation and are more influenced by an increased share of PV power installation. With the simulated future installation, low production events occur almost equally frequently with anticyclonic (53%) and cyclonic weather patterns (47%). This is due to the increase in the frequency of low production events occurring in summer associated with cyclonic patterns, driven by the higher influence of anomalously low PV power production on the total production.

Our analysis indicates an increased likelihood of extremely low production occurring in summer, rising from 5% to 25% of the total of 150 extreme events when we go from the present-day to the 2050 installation. In addition, the 14-day summer event in May 2016 shows lower anomalies in total production in the future installation compared to the present-day installation, indicating a potential exacerbation of

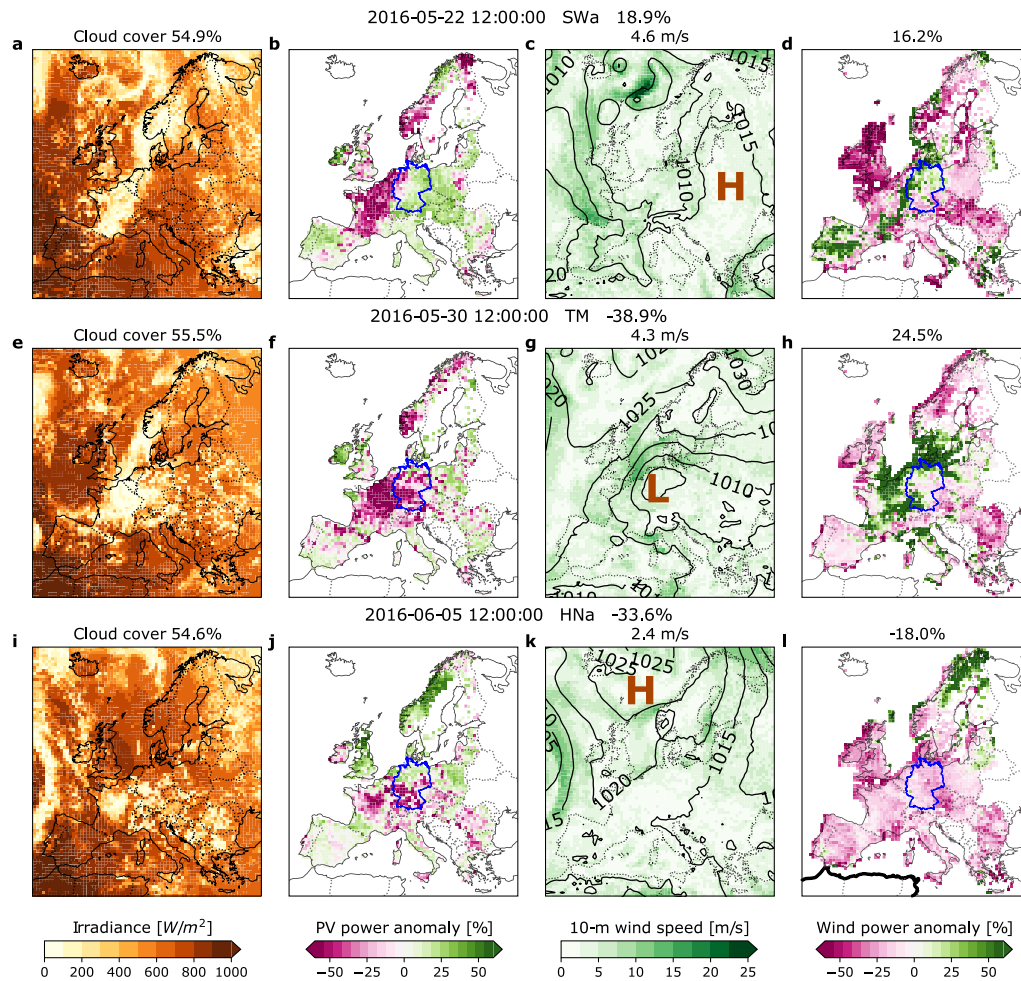


Fig. 8. Meteorological conditions in three selected times during low production event in May 2016. Similar to Fig. 6 but for the summer event May 2016 at three times marked in dotted lines in Fig. 7. (For interpretation of the references to colour in this figure legend, the reader is referred to the web version of this article.)

extremely low production events in summer in the future. With climate change, the peak demand for cooling in summer will define the annual maximum load in Germany by 2100 [41]. The combination of low power production and high electricity demand in summer can therefore pose extra stress on the energy supply system.

There are distinct differences between the 14-day low-production events in winter and summer. In terms of the magnitude of anomalies, summer events have relatively low PV and wind power production, with a lowest PV power anomaly of -15% and a lowest wind power anomaly of -19% . In contrast, during winter events, PV power produces slightly below the climatological mean up to -9% , while wind power produces much lower amounts with anomalies up to -37% . In terms of meteorological conditions, the majority (13 of 20) of 14-day lowest production events are associated with stationary weather patterns that lasted at least five days, with stationary anticyclonic patterns being more prevalent in winter events, while stationary cyclonic patterns being more prevalent in summer events. There are no repeating sequences of weather patterns during these prolonged low production events; rather, the extremely negative anomalies come from combinations of several patterns with low PV and/or low wind power production. There are great uncertainties on how stationary cyclonic and anticyclonic conditions vary with climate change in terms of frequency, intensity, and duration [42,43]. How future changes in stationary weather patterns can affect prolonged low-production events can be explored in future studies. There is an increased persistence of weather patterns compared in the 20th century (since 1881), especially in the 1970s-80s [44]. However, for climate projections in the

future, studies show high uncertainty on how atmospheric blockings might change due to differences in definition and in representation in numerical weather prediction models [43]. While the frequency and duration of atmospheric blockings might decrease [42,43], rare but high impact blockings such as those with extremely high intensity (strong pressure gradient) and long duration are possible [43]. The implication thus differs for the statistical 20 most extreme events and for the most extreme events, i.e., the overall number of low-power production events might decrease, but the most extreme low-wind power production events would be intensified in terms of duration and severity.

How these weather systems move during these events influences which transmission lines between Germany and neighboring countries Germany could be more helpful in electricity shortage. Our case studies indicate that both North-South and West-East transmission lines are needed during production shortfalls in Germany due to the different propagation directions of the production anomalies during the developments of different weather conditions.

Our findings highlighted that extreme events in PV and wind power production, especially low power production events, may become more frequent and more severe in summer for a plausible future power installations in Germany. The results provide first insights for planning the future energy system. To support the energy transition, future studies need to explore extreme events in renewable power production with additional simulations of the electricity demand and storage, such as from hydropower and batteries, and the electricity transmission from neighboring countries in Europe and elsewhere. To do so, more

plausible future projections for PV and wind power production sites are needed, since gridded data for installations are scarce and currently hinder the advancement of the understanding of weather impacts on renewable power systems.

CRedit authorship contribution statement

Linh Ho-Tran: Writing – review & editing, Writing – original draft, Visualization, Validation, Software, Methodology, Investigation, Formal analysis, Data curation, Conceptualization. **Stephanie Fiedler:** Writing – review & editing, Supervision, Resources, Project administration, Funding acquisition, Conceptualization.

Declaration of competing interest

The authors declare that they have no known competing financial interests or personal relationships that could have appeared to influence the work reported in this paper.

Data availability

The CLIMIX data was acquired from the author [14]. The code of the Renewable Energy Model (REM) is available at [45]. The data of REM are available at https://www.wdc-climate.de/ui/entry{a}cronym=DKRZ_LTA_1198_ds00003.

Acknowledgments

This study has been conducted in the framework of the Hans-Ertel-Centre for Weather Research funded by the German Federal Ministry for Transportation and Digital Infrastructure, Germany (grant number BMVI/DWD 4818DWDPA5A). We thank the German Weather Service for providing COSMO-REA6 data, P. James for the data for the weather patterns, C. Frank for the code for photovoltaic power simulations, and S. Jerez for the CLIMIX data.

Appendix A. Supplementary data

Supplementary material related to this article can be found online at <https://doi.org/10.1016/j.solener.2024.112979>.

References

- [1] European Commission, European green deal : delivering on our targets, 2021, Directorate-General for Communication, <https://data.europa.eu/doi/10.2775/373022>, (Accessed: 2023-03-21).
- [2] BMBF, Federal Ministry of Education and Research, German energy transition, 2019, URL https://www.bmbf.de/bmbf/en/research/energy-and-economy/german-energy-transition/german-energy-transition_node.html. (Accessed: 2023-08-07).
- [3] Umweltbundesamt, Energy target 2050: 100% renewable electricity supply, 2010, https://www.umweltbundesamt.de/sites/default/files/medien/378/publikationen/energieziel_2050_kurz.pdf, (Accessed: 2023-04-12).
- [4] BMWK, Bundesministerium für Wirtschaft und Klimaschutz, Entwicklung der erneuerbaren Energien in Deutschland im Jahr 2022, 2023, URL https://www.erneuerbare-energien.de/EE/Navigation/DE/Service/Erneuerbare_Energien_in_Zahlen/Entwicklung/entwicklung-der-erneuerbaren-energien-in-deutschland.html. (Accessed: 2023-08-07).
- [5] ISE, Net electricity generation in Germany in 2022: Significant increase in generation from wind and PV, 2023, Press Release <https://www.ise.fraunhofer.de/en/press-media/press-releases/2023/net-electricity-generation-in-germany-in-2022-significant-increase-in-generation-from-wind-and-pv.html>, (Accessed: 2023-04-12).
- [6] Energy-Charts, Installierte Netto-Leistung zur Stromerzeugung in Deutschland in 2022, 2022, URL https://energy-charts.info/charts/installed_power/chart.html?l=de&c=DE&chartColumnSorting=default&year=2022. (Accessed: 2023-08-07).
- [7] K. van der Wiel, L.P. Stoop, B. Van Zuijlen, R. Blackport, M. Van den Broek, F. Selden, Meteorological conditions leading to extreme low variable renewable energy production and extreme high energy shortfall, *Renew. Sustain. Energy Rev.* 111 (2019) 261–275.
- [8] B. Burger, Öffentliche Nettostromerzeugung in Deutschland im Jahr 2022, 2023, Presentation https://www.energy-charts.info/downloads/Stromerzeugung_2022.pdf, (Accessed: 2023-04-12).
- [9] G.E.A. dena, Pumped-storage integrates renewable energy into the grid, 2015, URL <https://www.dena.de/en/topics-projects/energy-systems/flexibility-and-storage/pumped-storage/>. (Accessed: 2023-08-07).
- [10] EWI (Energiewirtschaftliches Institut an der Universität zu Köln), dena pilot study “Towards climate neutrality”. Climate neutrality 2045 - Transformation of final energy consumption and the energy system, 2021, Published by the German Energy Agency GmbH (dena).
- [11] C.M. Grams, R. Beerli, S. Pfenninger, I. Staffell, H. Wernli, Balancing Europe's wind-power output through spatial deployment informed by weather regimes, *Nat. Clim. Chang.* 7 (8) (2017) 557–562.
- [12] J. Drücke, M. Borsche, P. James, F. Kaspar, U. Pfeifroth, B. Ahrens, J. Trentmann, Climatological analysis of solar and wind energy in Germany using the Grosswetterlagen classification, *Renew. Energy* (2020).
- [13] L. Ho-Tran, S. Fiedler, A climatology of weather-driven anomalies in European photovoltaic and wind power production, *Commun. Earth Environ.* 5 (1) (2024) 63.
- [14] S. Jerez, F. Thais, I. Tobin, M. Wild, A. Colette, P. Yiou, R. Vautard, The CLIMIX model: a tool to create and evaluate spatially-resolved scenarios of photovoltaic and wind power development, *Renew. Sustain. Energy Rev.* 42 (2015) 1–15.
- [15] Eurostat, Eurostat renewable energy statistics, 2020, https://ec.europa.eu/eurostat/statistics-explained/index.php?title=Renewable_energy_statistics#Share_of_renewable_energy_more_than_doubled_between_2004_and_2020. (Accessed: 2022-04-14).
- [16] J. Wohland, D. Brayshaw, S. Pfenninger, Mitigating a century of European renewable variability with transmission and informed siting, *Environ. Res. Lett.* 16 (6) (2021) 064026.
- [17] S. Perkins, L. Alexander, J. Nairn, Increasing frequency, intensity and duration of observed global heatwaves and warm spells, *Geophys. Res. Lett.* 39 (20) (2012).
- [18] V. Masson-Delmotte, P. Zhai, A. Pirani, S.L. Connors, C. Péan, S. Berger, N. Caud, Y. Chen, L. Goldfarb, M. Gomis, et al., Climate change 2021: the physical science basis, *Contrib. Work. Group I Sixth Assess. Rep. Intergov. Panel Clim. Chang.* 2 (1) (2021) 2391.
- [19] P. James, An objective classification method for Hess and Brezowsky Grosswetterlagen over Europe, *Theor. Appl. Climatol.* 88 (1–2) (2007) 17–42.
- [20] C. Bollmeyer, J. Keller, C. Ohlwein, S. Wahl, S. Crewell, P. Friederichs, A. Hense, J. Keune, S. Kneifel, I. Pscheidt, et al., Towards a high-resolution regional reanalysis for the European CORDEX domain, *Q. J. R. Meteorol. Soc.* 141 (686) (2015) 1–15.
- [21] S. Pfenninger, I. Staffell, Long-term patterns of European PV output using 30 years of validated hourly reanalysis and satellite data, *Energy* 114 (2016) 1251–1265.
- [22] I. Staffell, S. Pfenninger, Using bias-corrected reanalysis to simulate current and future wind power output, *Energy* 114 (2016) 1224–1239.
- [23] L. Dubus, Y.-M. Saint-Drenan, A. Troccoli, M. De Felice, Y. Moreau, L. Ho-Tran, C. Goodess, L. Sanger, C3S energy: A climate service for the provision of power supply and demand indicators for Europe based on the ERA5 reanalysis and ETSO-E data, *Meteorol. Appl.* 30 (2023) e2145.
- [24] T. Huld, G. Friesen, A. Skoczek, R.P. Kenny, T. Sample, M. Field, E.D. Dunlop, A power-rating model for crystalline silicon PV modules, *Sol. Energy Mater. Sol. Cells* 95 (12) (2011) 3359–3369.
- [25] C.W. Frank, S. Wahl, J.D. Keller, B. Pospichal, A. Hense, S. Crewell, Bias correction of a novel European reanalysis data set for solar energy applications, *Sol. Energy* 164 (2018) 12–24.
- [26] Y.-M. Saint-Drenan, L. Wald, T. Ranchin, L. Dubus, A. Troccoli, An approach for the estimation of the aggregated photovoltaic power generated in several European countries from meteorological data, *Adv. Sci. Res.* 15 (2018) 51–62.
- [27] European Commission, Joint Research Centre (JRC), Global energy and climate outlook 2020: Energy, greenhouse gas and air pollutant emissions balances, 2020, *Dataset* <https://data.jrc.ec.europa.eu/dataset/1750427d-afd9-4a10-8c54-440e764499e4>. (Accessed: 2022-04-24).
- [28] K. van der Wiel, H.C. Bloomfield, R.W. Lee, L.P. Stoop, R. Blackport, J.A. Screen, F.M. Selden, The influence of weather regimes on European renewable energy production and demand, *Environ. Res. Lett.* 14 (9) (2019) 094010.
- [29] I. Tobin, S. Jerez, R. Vautard, F. Thais, E. Van Meijgaard, A. Prein, M. Déqué, S. Kotlarski, C.F. Maule, G. Nikulin, et al., Climate change impacts on the power generation potential of a European mid-century wind farms scenario, *Environ. Res. Lett.* 11 (3) (2016) 034013.
- [30] I. Tobin, W. Greuell, S. Jerez, F. Ludwig, R. Vautard, M. Van Vliet, F. Breón, Vulnerabilities and resilience of European power generation to 1.5 C, 2 C and 3 C warming, *Environ. Res. Lett.* 13 (4) (2018) 044024.
- [31] W. Zappa, M. Van Den Broek, Analysing the potential of integrating wind and solar power in Europe using spatial optimisation under various scenarios, *Renew. Sustain. Energy Rev.* 94 (2018) 1192–1216.
- [32] R. Vautard, F. Thais, I. Tobin, F.-M. Bréon, J.-G.D. De Laverne, A. Colette, P. Yiou, P.M. Ruti, Regional climate model simulations indicate limited climatic impacts by operational and planned european wind farms, *Nature communications* 5 (1) (2014) 3196.

- [33] GISCO: Geographical Information and Maps, EuroGeographics for the administrative boundaries, 2020, <https://ec.europa.eu/eurostat/web/gisco/geodata/reference-data/administrative-units-statistical-units>. (Accessed: 2020-03-23).
- [34] T. Klaus, C. Vollmer, K. Lehmann, K. Müschen, R. Albert, M. Bade, T. Charissé, F. Eckermann, R. Herbener, U. Kaulfersch, G. Knoche, K. Kuhnenn, C. Lohse, C. Loreck, U. Lorenz, B. Lünenbürger, M. Memmler, C. Mordziol, A. Ostermeier, B. Westermann, 2050 Energy Target: 100% Renewable Electricity Supply, Umweltbundesamt, 2010.
- [35] O. Ruhnau, S. Qvist, Storage requirements in a 100% renewable electricity system: extreme events and inter-annual variability, *Environ. Res. Lett.* 17 (4) (2022) 044018.
- [36] P. Zschenderlein, G. Fragkoulidis, A.H. Fink, V. Wirth, Large-scale Rossby wave and synoptic-scale dynamic analyses of the unusually late 2016 heatwave over Europe, *Weather* 73 (9) (2018) 275–283.
- [37] M. Röthlisberger, L. Frossard, L.F. Bosart, D. Keyser, O. Martius, Recurrent synoptic-scale rossby wave patterns and their effect on the persistence of cold and hot spells, *J. Clim.* 32 (11) (2019) 3207–3226.
- [38] D. Barriopedro, R. García-Herrera, A.R. Lupo, E. Hernández, A climatology of northern hemisphere blocking, *J. Clim.* 19 (6) (2006) 1042–1063.
- [39] L.-A. Kautz, O. Martius, S. Pfahl, J.G. Pinto, A.M. Ramos, P.M. Sousa, T. Woollings, Atmospheric blocking and weather extremes over the Euro-Atlantic sector—a review, *Weather Clim. Dyn.* 3 (1) (2022) 305–336.
- [40] J. Figgenger, C. Hecht, D. Haberschusz, J. Bors, K.G. Spreuer, K.-P. Kairies, P. Stenzel, D.U. Sauer, The development of battery storage systems in Germany: A market review, 2023, <https://battery-charts.rwth-aachen.de/>.
- [41] G. Totschnig, R. Hirner, A. Müller, L. Kranzl, M. Hummel, H.-P. Nachtnebel, P. Stanzel, I. Schicker, H. Formayer, Climate change impact and resilience in the electricity sector: the example of Austria and Germany, *Energy Policy* 103 (2017) 238–248.
- [42] T. Shaw, M. Baldwin, E.A. Barnes, R. Caballero, C. Garfinkel, Y.-T. Hwang, C. Li, P. O’gorman, G. Rivièrè, I. Simpson, et al., Storm track processes and the opposing influences of climate change, *Nat. Geosci.* 9 (9) (2016) 656–664.
- [43] T. Woollings, D. Barriopedro, J. Methven, S.-W. Son, O. Martius, B. Harvey, J. Sillmann, A.R. Lupo, S. Seneviratne, Blocking and its response to climate change, *Curr. Clim. Chan. Rep.* 4 (3) (2018) 287–300.
- [44] J. Kysely, P. Domonkos, Recent increase in persistence of atmospheric circulation over europe: comparison with long-term variations since 1881, *Int. J. Climatol.* 26 (4) (2006) 461–483.
- [45] L. Ho, S. Fiedler, S. Wahl, PV and Wind Power Dataset for Europe, 2023, URL https://www.wdc-climate.de/ui/entry?acronym=DKRZ_LTA_1198_ds00003.

4.3 EXTREMES IN ENERGY DEMAND SECTOR - THE DENA STUDY

The following section is part of the study from EWI (2021). Here I summarise the meteorological perspective that I contributed to that study, translated into English from the original document in German in EWI (2021).

The study from EWI (2021) examines critical situations that can challenge the electricity system in Germany. It was developed in cooperation between the Institute of Energy and Economics (EWI) and the Institute of Geophysics and Meteorology (IGM), University of Cologne. In this study, the energy system model includes different types of energy sources, e.g., coal power plants, PV and wind power, hydropower pump storage, and trading with neighbouring countries. The critical situations are defined with residual load, i.e., the electricity demand minus the electricity generated. An event with high residual load means the electricity supply could not meet the demand and requires electricity transmission from other countries.

This study identifies two events with the highest residual load for the period of 168h (7 days) and 336h (14 days). Their central dates are on 1997-01-08 and 2007-12-17, respectively. PV and wind power in Germany produced very low amounts during these two events. Fig. 4.1a,b illustrate the potential capacity factors of these two energy sources during the two events, and their climatological mean for three winter months (DJF) during the period 1995–2014 for reference (Fig. 4.1a). The potential capacity factor for PV power is calculated for Standard Test Condition (STC, 25°C, 1000W/m²), while estimated for wind power using wind speed at 100 m.

In the synoptic weather conditions for Europe, winter typically features a westerly wind with isobars parallel to the latitudes (EWI, 2021). The cold and dry air masses are usually over the North and East of Europe, in contrast with the warm temperatures in the Mediterranean region. The contrast creates distinctly different characteristics between the north and south of Europe, and partially in Germany (Fig. 4.1a). Specifically, Europe has high wind power potential (with a capacity factor $CF > 0.5$) in the Northern part, and moderate potential for wind and PV power in the Southern half ($0.25 \leq CF_{wind} \leq 0.5$, $0.15 \leq CF_{PV} \leq 0.3$).

The 7-day extreme weather condition from 1997 is a *Dark doldrum* event over the large part of Europe, i.e., both PV and wind power produced significantly low amounts compared to the climatological mean ($CF_{PV} \leq 0.15$, $CF_{wind} \leq 0.25$) (Fig. 4.1b). From January 5th, a stationary ridge of high pressure lay over the northern part of Central Europe, directing cold air masses from the Arctic to Central Europe (Fig. 4.2a). The ridge brought significant "doldrum" with a regional

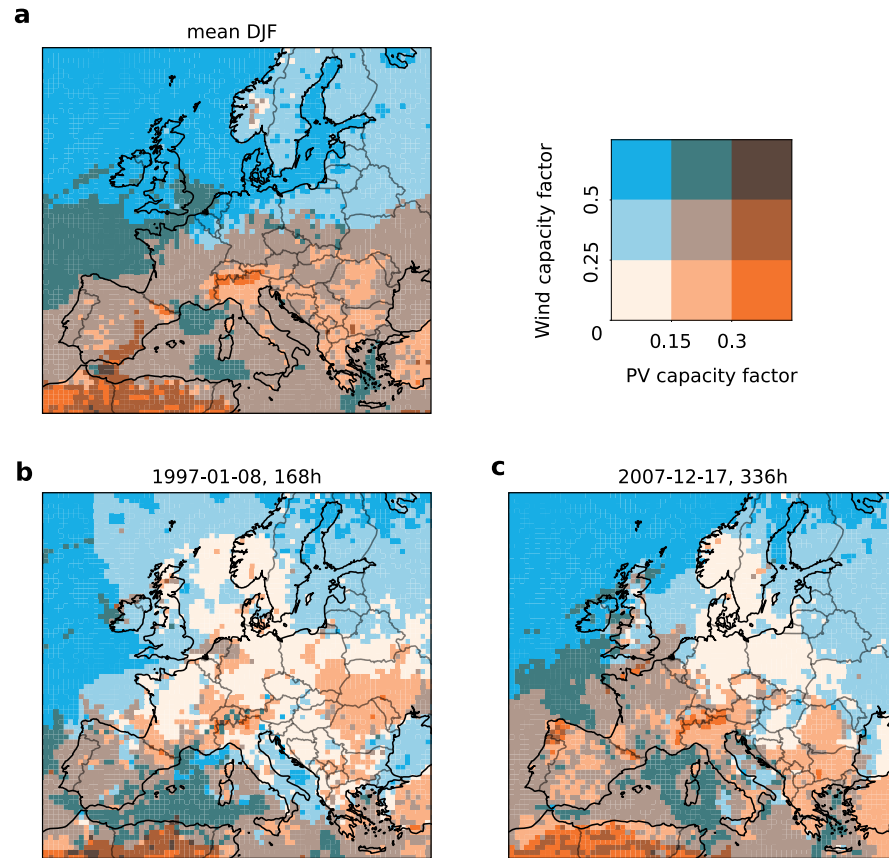


Figure 4.1: The potential capacity factor of PV and wind power hourly mean for (a) the winter (DJF) 1995–2014, (b) for the event in January 1997 (7 days), (c) for the event December 2007 (14 days). Figure from [EWI \(2021\)](#).

wind speed anomaly as low as -9 ms^{-1} on average for Jan 4–11th, 1997 (Fig. 4.2a). The estimates of wind energy potential show negative anomalies in wind power in Germany, France, the United Kingdom, the North Sea and Baltic Sea, and in parts of Eastern Europe and the southern part of Scandinavian countries. Southern Europe and Northern Scandinavia showed relatively higher wind speeds than average. The anomaly in irradiance occurred mainly in southern Europe (Fig. 4.2a) due to increased cloud cover. The irradiance was slightly above average in the northeastern part of Germany, while below average for the rest of Germany. The stationary cold air resulted in a prolonged cold spell, leading to a 2-m temperature negative anomaly of up to -10°C compared to the long-term winter mean, see details in [EWI \(2021\)](#). The simultaneous cold weather and low power production in

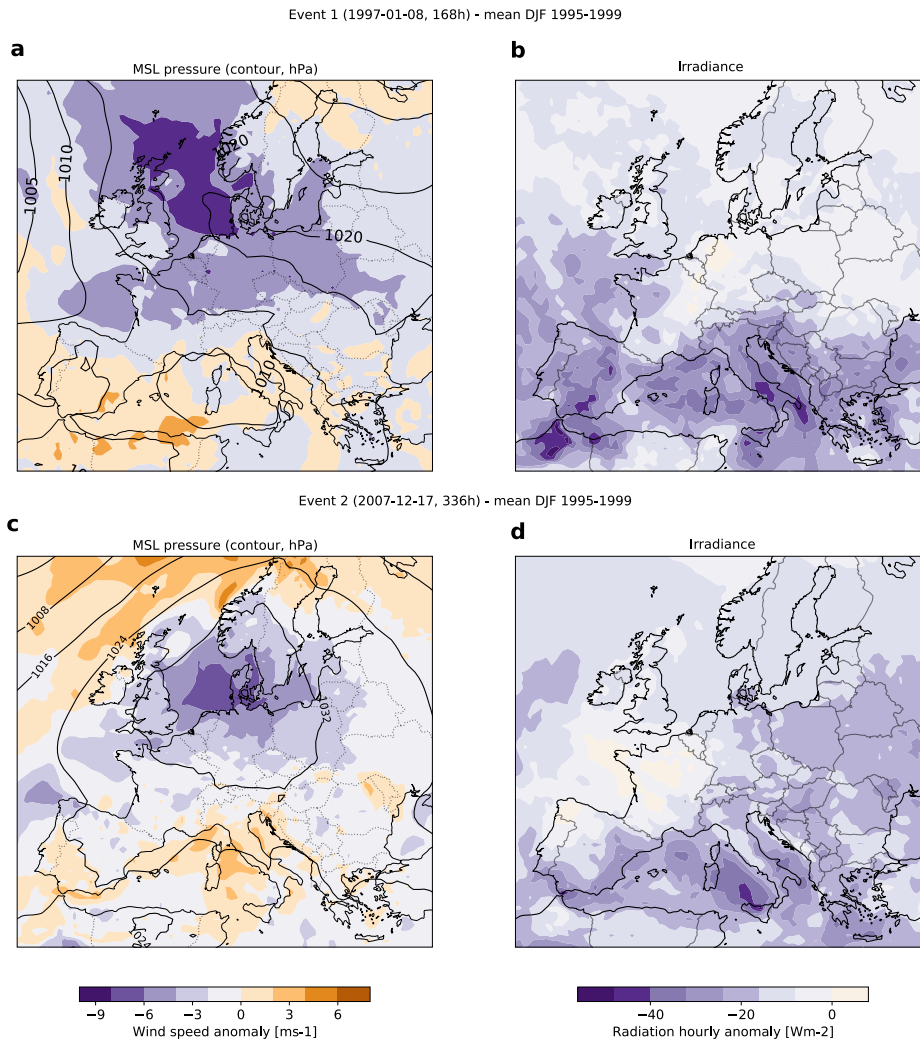


Figure 4.2: Wind speed anomalies at 100 m (shadding), compared to the winter mean (DJF) and the mean sea level pressure (contour) and irradiance anomalies compared to the winter mean 1995–2014, for two extreme events in (a,b) January 1997 (7 days), (c,d) December 2007 (14 days). Figure from [EWI \(2021\)](#).

western Germany characterises this event as a distinctive "cold dark doldrum".

The weather condition during the 14-day event in December 2007 show a similar picture as in January 1997. A stationary high pressure system formed over Central Europe during the period 13–21st December 2007 (Fig. 4.2c). The result was weak winds over the North Sea and northern Germany, with the anomalies up to -8 ms^{-1} . Potential wind power is significantly lower than expected for the winter months. The solar irradiance for Germany in this period was also lower than usual for the winter mean (Fig. 4.2d), especially in south-

ern Europe, similar to the January 1997 event. The differences compared to the 1997 event are the higher values of positive anomalies in wind speed and irradiance over France and parts of Eastern Europe. This situation favoured energy availability for importing to Germany.

DISCUSSION AND CONCLUSION

Increasing the share of renewable energy is an important measure to achieve Europe's climate-neutral goals by 2050. Solar and wind power production heavily relies on the availability of irradiance and wind speed at specific locations. The temporal and spatial variability of these two variables are extensively studied from a meteorological perspective. However, their integration into the energy sector is limited due to disparities in methods and purposes between the two fields.

This thesis bridges the gap by examining the associations between synoptic weather patterns and anomalous power production in photovoltaic (PV) and wind energy in Europe. To achieve this, the Renewable Energy Model (REM) was developed at a 48 km horizontal resolution, utilising the COSMO-REA6 reanalysis dataset. COSMO-REA6 has two benefits in PV and wind power simulations. First, it provides suitable meteorological variables to simulate both PV and wind power with temporal and spatial consistency, which is necessary to combine them into total power production in Europe. Second, the high spatial resolution of 6 km in COSMO-REA can represent more regional variation of meteorological processes (Bollmeyer et al., 2015), which is important in assessing the spatial variability of anomalies in total power production (Frank et al., 2020a, 2018). The gridded data output from REM also incorporates spatial distribution of PV and wind power installations from the CLIMIX model. This approach has the advantage of showing finer spatial variation of power anomalies that approaches using country-aggregated values lack of. The weather pattern classification used in REM is well-established and routinely monitored from the German Weather Service.

In the following sections, the main findings of this thesis are summarized, highlighting two studies examining Europe and Germany. Next, the assumptions and uncertainties relevant to these studies are discussed. Finally, the significance of this thesis in applying meteorological insights to the energy sector is presented, followed by an outlook on future research possibilities to expand understanding in this field.

5.1 SUMMARY

5.1.1 *Study I - A climatology of weather-driven anomalies in European photovoltaic and wind power production*

Study I (Section 4.1) addresses the first and second objectives of this thesis (Section 1.2). Therein, it first conducts a comprehensive analysis of weather patterns associated with both anomalously low and high power production for PV, wind power, and their total production in Europe. Second, the study explores various perspectives, including different event durations, seasons, regions in Europe, comparing between present-day and future installations.

The research questions posed in the Introduction (Section 1.3) are addressed as follows:

1. *Which weather patterns are associated with extremely anomalous power production in PV and wind power in Europe?* The study shows a clear anti-correlation relationship between the two sources. High wind power production is linked to westerly wind and/or cyclonic characteristics, while high PV power production is associated with anticyclonic characteristics. For instance, for hourly European power production, the weather pattern Maritime Westerly, Block Eastern Europe (Ww, cyclonic) exhibits the highest wind power production and the lowest PV power production. In contrast, the pattern High Scandinavia-Iceland, Ridge Central Europe (HNFa, anticyclonic) displays the highest PV power production and the fourth lowest wind power production.
2. *Are there any common characteristics in weather patterns associated with extreme events in power production with different event durations and seasons?* The anti-correlation between PV and wind power dampens the anomalies of their total production compared to individual energy type. Specifically, the absolute values of anomalies in total production (up to 22.4% for present-day installation) are smaller than those observed for PV (up to 30.5%) or wind power (up to 34.7%) across all 29 weather patterns. This effect is stronger in the future installation, with anomalies up to 13.9% for total production, indicating improved balancing between PV and wind power with a 2:1 installation ratio compared to the present-day ratio of 0.7:1. Weather patterns associated with the most anomalous total production are similar to those for wind power in the present-day installation, but differ in the future installation. The weather patterns associated with the most anomalous total production differ from those of individual energy types. The Wa (Anticyclonic Westerly) pattern exhibits the highest total hourly production, ranked third in wind power production, and has a slightly

negative anomaly in PV power production. The pattern with the lowest total production for the present-day installation is HNa, which also has the lowest wind power production. However, for the future installation, the pattern Ws (South-Shifted Westerly) is associated with the lowest total production, having the second lowest PV power production and a slightly negative anomaly in wind power production, indicating the greater impact of PV power in the future installation. Ws belongs to the group *Dark doldrum*, characterised by low PV and wind power production simultaneously, as described in Study I (Section 4.1).

3. *How are the anomalies of power production distributed spatially during these weather patterns* For the patterns HNFa (High Scandinavia-Iceland, Ridge Central Europe) and HNa (Icelandic High, Ridge Central Europe), the anomalies in PV and wind power have the same sign but vary in magnitude almost across Europe, except for regions in Northern Scandinavia and the Southern tip of Iberia. However, the total production anomalies exhibit a highly variable spatial distribution across Europe, particularly in countries such as Germany, France, and the Netherlands. For patterns Ws and Wa, the low PV power production exhibits a similar spatial distribution across Europe but with different magnitudes. However, wind power anomalies show distinct North-South differences for European regions with the opposite sign of anomaly. This results in a strongly varying spatial distribution of anomalies in total production for regions with high wind power production, namely the Southern part of Europe during Ws, and the Northern part of Europe during Wa. A comprehensive catalog of the spatial distribution of anomalies in PV, wind, and total production for both present-day and future installations in all 29 weather patterns is provided in Supplementary of Study I.
4. *How sensitive are the results to the installation with different ratio of PV to wind power installed capacities?* For low total production, the associated weather patterns strongly depend on the ratio of installed capacity of PV to wind power. In the present-day installation, total production anomalies rank similarly to wind power production due to the prevalent contribution of wind power. However, in the future installation, three out of five patterns with the lowest total production belong to the *Dark doldrum* group, including Ws, HNFz (High Scandinavia-Iceland with Trough Central Europe), and SEz (Cyclonic South-Easterly). Additionally, the associated patterns vary with the event duration. For events with the same weather pattern lasting 10 days, SEa (Anticyclonic South-Easterly) is associated with the lowest total production for Europe in both present-day and future installations (-27% and -41% , re-

spectively). On the contrary, for high total production, the associated weather patterns remain consistent regardless of durations and installations, characterised by cyclonic and westerly wind patterns, such as Wz (Cyclonic Westerly) and NWz (Cyclonic North-Westerly). Weather patterns associated with anomalous power production for half-year winter and summer are similar to those observed in the whole-year analyses. However, the values of anomalies for low production events show larger differences between summer and winter half-year means compared to that of high production events.

5.1.2 *Study II - More summertime low-power production extremes in Germany with a larger solar power share*

Study II (Section 4.2) addresses the third and fourth objectives of this thesis (Section 1.2). Thereby, it investigates the differences in winter and summer events with extremely anomalous PV plus wind power production in Germany.

The findings in Study II address the questions posed in the Introduction (Chapter 1.1) as follows:

1. *Do seasonal differences in extreme events in renewable energy change between the present-day and future installation?* Both the lowest and highest production events occur more frequently in winter in both present-day and future installations (95% and 78% for low production events, and 82% and 84% for high production events). The seasonal difference is more pronounced for the lowest production events. Noticeably, in the future installation, there is an increase in the lowest production events occurring in summer (22%), compared to the present-day installation (5%). May exhibits the most significant increase in the frequency of 7- and 14-day lowest production events, attributed to higher frequencies of weather patterns associated with low production in summer, such as NEz (Cyclonic North-Easterly) and HNFz (High Scandinavia-Iceland, Trough Central Europe). However, the highest production events do not display a change in seasonal differences based on installation, with slightly more high production events occurring in winter in the future installation compared to the present-day installation (84% and 82%, respectively).
2. *Are there different characteristics in weather patterns that involve extreme events between winter and summer?* For lowest production events, cyclonic and anticyclonic weather patterns are nearly equally associated in the present-day installation (51% and 49%, respectively). In the future installation, the increase in likelihood these events

occurring in summer are mostly associated with cyclonic patterns. Winter events also show an increase in associating with cyclonic patterns and a decrease in associating with anticyclonic patterns. The overall effect is an increase in association with cyclonic patterns in lowest production events in the future installation at 66%. The highest production events are mainly associated with weather patterns with a cyclonic characteristic but this association decreases in the future installation (77% and 68% of the days, respectively). Highest production events in winter occur more frequently with anticyclonic patterns in the future installation (24%, compared to 11% in present-day installation).

3. *Is there a difference in meteorological conditions when prolonged low power production events progress in winter and in summer?* There are differences in meteorological conditions during prolonged low power production events in winter and summer. 14-day lowest production events in the winter half-year are primarily associated with blocking anticyclonic weather patterns. During these events, PV power is produced close to the climatological mean (with anomalies up to -9%), while wind power production is significantly reduced (up to -37%). In contrast, typical summer events are mainly associated with stationary cyclonic weather patterns, during which PV and wind power are relatively low (up to -15% and -19% , respectively). The seasonal divisions of extreme events in renewable energy in Germany (beginning of April and October) occur approximately two weeks earlier than the weather pattern classification (mid-April and mid-October). Additionally, 14-day lowest production events in both winter and summer experience a short period of around one day in the middle of the event, where wind power production temporarily increased close to the climatological mean, briefly alleviating stress on the electricity supply.

5.2 METHODOLOGICAL LIMITATIONS AND UNCERTAINTIES

There are three main sources that can contribute to the uncertainty of the results from this thesis. They can arise from (1) the biases in data used in simulations, (2) the decisions made while simulating PV and wind power in REM, and (3) the impact of climate change on the meteorological variables used.

In terms of data, reanalysis data used in the simulations have known biases in radiation and wind speed (Borsche et al., 2015; Brune et al., 2021; Camus et al., 2019; Frank et al., 2020a, 2018; Niermann et al., 2019). Radiation data from COSMO-REA6 show an overestimation in cloudy conditions (by around 15 Wm^{-2}) and an underestimation in clear sky conditions (by around -50 Wm^{-2} compared to observa-

tional data (Frank et al., 2018). Efforts have been made to mitigate radiation data biases through post-processing methods (Frank et al., 2018), but this algorithm alters the spatial patterns of irradiance data. Thereby, the original data for short-wave direct and diffused radiation from COSMO-REA6 are retained in REM to preserve spatial variation in PV power. In terms of wind speed data, COSMO-REA6 underestimates wind speed at night in all terrains due to misrepresenting low level jets, mountain and valley breezes (Brune et al., 2021). Additionally, challenges arise in weather pattern classification regarding consistency, as similar meteorological conditions may be classified differently (James, 2007). Certain patterns exhibit considerable similarity and are grouped together, such as High pressure over Scandinavia-Iceland with Trough (HNFz) or Ridge (HNFa) over Central Europe, while some patterns with westerly flow lack distinct differentiation (James, 2007). Such inconsistencies pose challenges in associating specific weather patterns with extreme PV and wind power production events.

The simulation of energy production introduces further uncertainties. The simulation of PV power is based on empirical methods, leading to parameter definition uncertainties (Frank, 2019). The simulation of wind power in REM uses the cubic law to convert wind speed into wind power production. However, the actual power produced is greatly influenced by manufacturer's specifications for wind turbine (Lydia et al., 2014). Furthermore, different energy models include various components such as electricity demand and other energy sources such as coal power plant, nuclear energy, and hydropower. Consequently, the definition of extreme events in renewable energy may vary depending on the specific energy model employed. Nevertheless, the studies in this thesis show agreement with some studies using different models, indicating a coherence in certain aspects of the analysis. For example, the pattern High pressure over Central Europe (HM) is associated with very low PV plus wind power production in Germany (Drücke et al., 2020), as shown in Section 4.1.

Another source of uncertainty is using past data. The reanalysis dataset COSMO-REA6 is produced using data assimilation between regional climate model and observational data for the period 1995–2017 (Bollmeyer et al., 2015). This past dataset does not take into account the impact of climate change on renewable sources in the future. Changes in solar irradiance and wind speed due to climate change can significantly influence PV and wind power production, which vary regionally and affect how synoptic weather patterns interact with energy production. For example, PV power potential from solar irradiance can increase in Southern Europe in the future (Jerez et al., 2015b), while wind speed can decrease (Vautard et al., 2010). Additionally, weather pattern clas-

sification relies on historical data since 1948 (James, 2007) to define clusters of 29 patterns. Future changes in meteorological variables (mean sea level pressure and geopotential height at 500 hPa) can result in changes in the frequency of occurrence of weather patterns in the future. As a result, the association between extreme events in renewable energy and weather patterns may differ in the future compared to the associations defined in this thesis.

5.3 SIGNIFICANCE AND OUTLOOK

Motivated by the increasing interest in applying meteorological knowledge to the renewable energy sector, this thesis aims to identify synoptic weather patterns that may pose challenges to the renewable energy system. The approach combines gridded data for PV and wind power simulation with a well-established weather pattern classification. The combination allows analyses in extreme power production events associated with weather patterns at various spatial and temporal scales.

The significance of this study lies in its comprehensive analysis of the impacts of synoptic weather patterns on PV and wind power production in Europe. The research highlights that the pairs of weather pattern–low production events are more sensitive to changing the installed capacity and the length of the event duration, whereas weather patterns associated with high production events have consistent westerly wind direction. Furthermore, it draws attention to the increased concerns in the future energy system regarding *Dark doldrum* weather patterns, during which both PV and wind power produce below average amount. Additionally, it identifies Anticyclonic Southeasterly as associated with the lowest 10-day production events for both present-day and future installations.

This thesis also shows the new threat in the renewable energy system: an increased frequency of low production events occurring in summer in the future installation. Study II shows that the meteorological processes involved in such summer events are different from those in the winter, with low production in both PV and wind power up to -19% and associated with stationary cyclonic weather patterns. While current literature primarily focuses on winter events, the study emphasizes the importance of investigating these summer events, particularly considering the potential rise in heat waves due to climate change. Such heat waves could lead to higher electricity demand for cooling, potentially resulting in energy shortfalls during the summer when electricity supply cannot meet the demand.

One valuable product from this project is the catalogue presenting the spatial anomalies of power production associated with 29 weather patterns. This catalogue allows for quick identification of expected anomalies for specific weather patterns, locations, and neighboring areas without the need for complex energy modeling. Classification of weather pattern is routinely provided and monitored by the German Weather Service, with the potential to provide with weather patterns in the up-coming days. A combination between this weather pattern classification and the look-up catalogue can enable an early warning of potential extreme situation in renewable energy.

For future research, it would be valuable to understand how weather patterns change with climate change in terms of frequency, pressure gradient, and seasonal differences. Investigating the extent to which these changes impact the influence of weather patterns on renewable energy, compared to the findings in this thesis, could be interesting in further studies.

Additionally, considering various possible future scenarios for European renewable energy installations is essential, especially in terms of spatial distribution and total capacities. This thesis uses the scaling factor method to simulate the present-day installation from the future installation. This approach highlights changes in weather dependence with different ratios of PV and wind power installed capacity. However, the regional impact of weather patterns can vary greatly depending on the allocation of PV and wind power plants in different scenarios. For example, having more wind power offshore plants in the North Sea, beyond the one-grid-cell limit in CLIMIX, could amplify the impact of strong westerly winds on the renewable energy system.

Furthermore, it would be interesting to examine if the impacts of weather pattern influence simultaneously or have delay in time across European countries. Such knowledge could guide neighboring countries in understanding how long problematic events may persist in their regions, when to import or export electricity during extreme events, and whether to prioritize energy storage or transmission based on specific meteorological developments.

Part I

SUPPLEMENTARY OF STUDY I

Supplementary information for manuscript

A climatology of weather-driven anomalies in European photovoltaic and wind power production

Authors: Linh Ho-Tran and Stephanie Fiedler

Table S1. Anomalies (%) of PV and wind power and their total production as in Fig. 1 in the main text.

Anomalies (%) of PV and wind power production apply to both scale-2019 and scenario-2050 because the two installed capacities are related by constant scale factors.

Group	Weather pattern	Full name	Mean anomalies in hour production [%]			
			Total 2019	Total 2050	PV power	Wind power
High wind	Wa	Anticyclonic Westerly	22.3	13.9	-6.6	31.4
	Wz	Cyclonic Westerly	20.0	12.3	-6.2	28.2
	SWz	Cyclonic South-Westerly	22.2	10.4	-17.9	34.7
	SWa	Anticyclonic South-Westerly	22.4	8.1	-9.7	23.4
	NWz	Cyclonic North-Westerly	13.7	7.7	-6.8	20.1
	Ww	Maritime Westerly (Block Eastern Europe)	21.0	5.9	-30.5	37.1
	TB	Low over the British Isles	9.5	4.3	-8.1	15.0
Mode-rate	NWa	Anticyclonic North-Westerly	1.8	1.8	1.8	1.7
	TrW	Trough over Western Europe	-2.1	0.2	5.4	-4.3
	Sz	Cyclonic Southerly	-0.9	-0.1	2.0	-1.8
	Nz	Cyclonic Northerly	-0.5	-1.9	-5.3	1.1
	Sa	Anticyclonic Southerly	-5.2	-3.9	-0.9	-6.5
	HFz	Scandinavian High, Trough Central Europe	-7.1	-6.0	-3.4	-8.2
High PV	HNFa	High Scandinavia-Iceland, Ridge Central Europe	-11.4	0.1	27.7	-23.5
	BM	Zonal Ridge across Central Europe	-5.3	-0.3	11.7	-10.6
	TrM	Trough over Central Europe	-9.3	-3.1	11.6	-15.7
	HFa	Scandinavian High, Ridge Central Europe	-7.6	-3.8	5.7	-11.9
	TM	Low (Cut-Off) over Central Europe	-9.3	-5.2	4.6	-13.6
	HNz	Icelandic High, Trough Central Europe	-15.0	-6.6	13.4	-23.7
	Na	Anticyclonic Northerly	-14.5	-6.8	11.7	-22.6
	HM	High over Central Europe	-13.2	-7.5	6.0	-19.1
	HB	High over the British Isles	-15.1	-7.9	9.4	-22.7
	SEa	Anticyclonic South-Easterly	-12.7	-8.0	3.2	-17.6
	NEz	Cyclonic North-Easterly	-15.1	-8.9	6.0	-21.6
	NEa	Anticyclonic North-Easterly	-16.9	-10.2	6.2	-24.1
	HNa	Icelandic High, Ridge Central Europe	-19.5	-10.3	11.8	-29.2
Dark doldrum	SEz	Cyclonic South-Easterly	-9.2	-9.7	-11.0	-8.6
	HNFz	High Scandinavia-Iceland, Trough Central Europe	-13.1	-12.0	-9.5	-14.1
	Ws	South-Shifted Westerly	-7.9	-12.1	-22.3	-3.3

Figure S1. As Figure 1 but for Germany. Shown are anomalies of photovoltaic (PV), wind power (stacked) and their total production associated with weather patterns for Germany from (a) scale-2019 and (b) scenario-2050. Differences in anomalies of total production by different installed capacities are shown in (c) for scenario-2050 minus scale-2019 installation. Red in (c) marks weather patterns where the signs of anomaly depend on the installed capacity. All three plots are sorted by increasing magnitude of total production in Germany in scenario-2050 (b) from left to right. Note here the larger range on the y-axis compared to Fig. 1 in the manuscript.

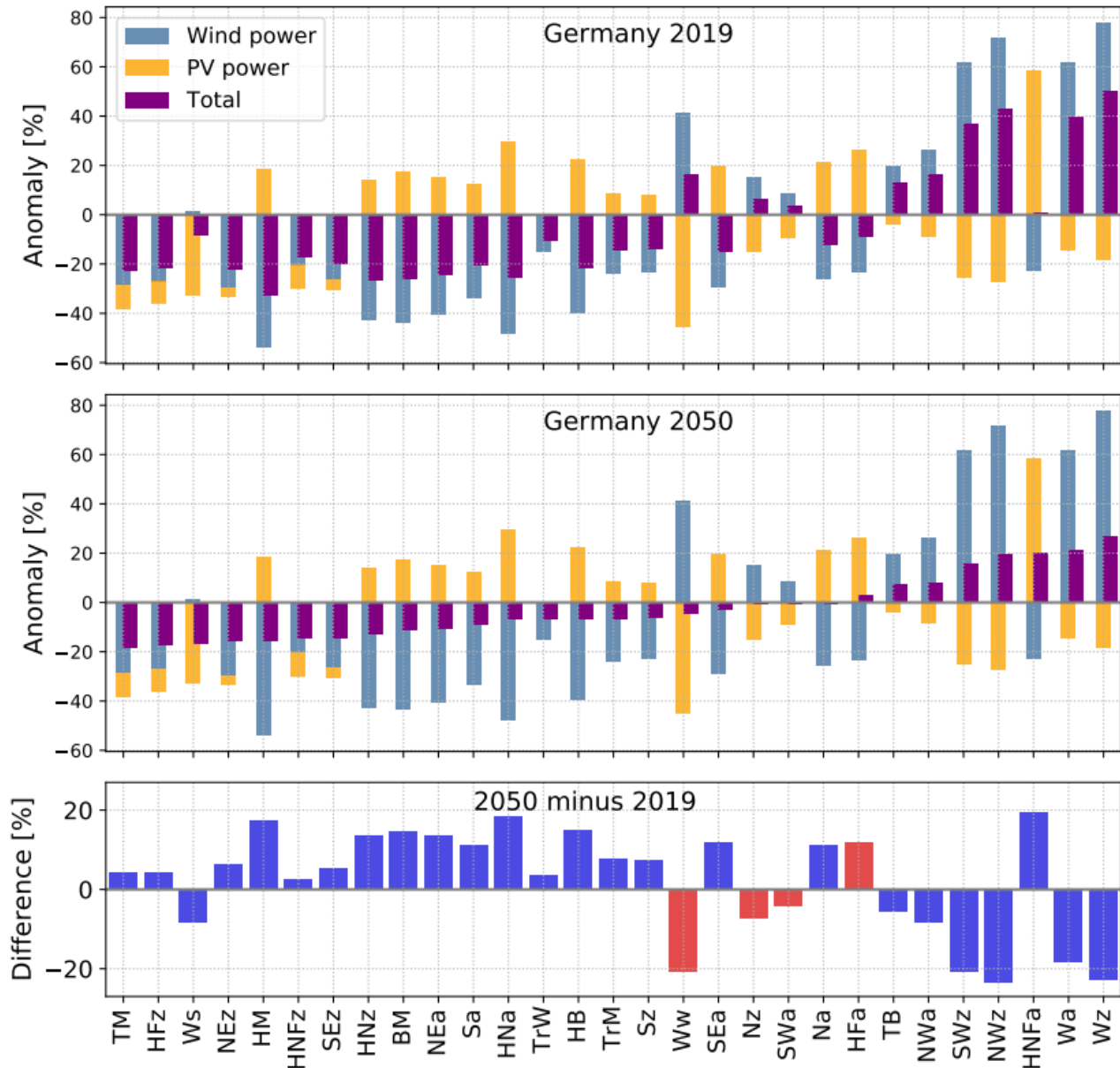
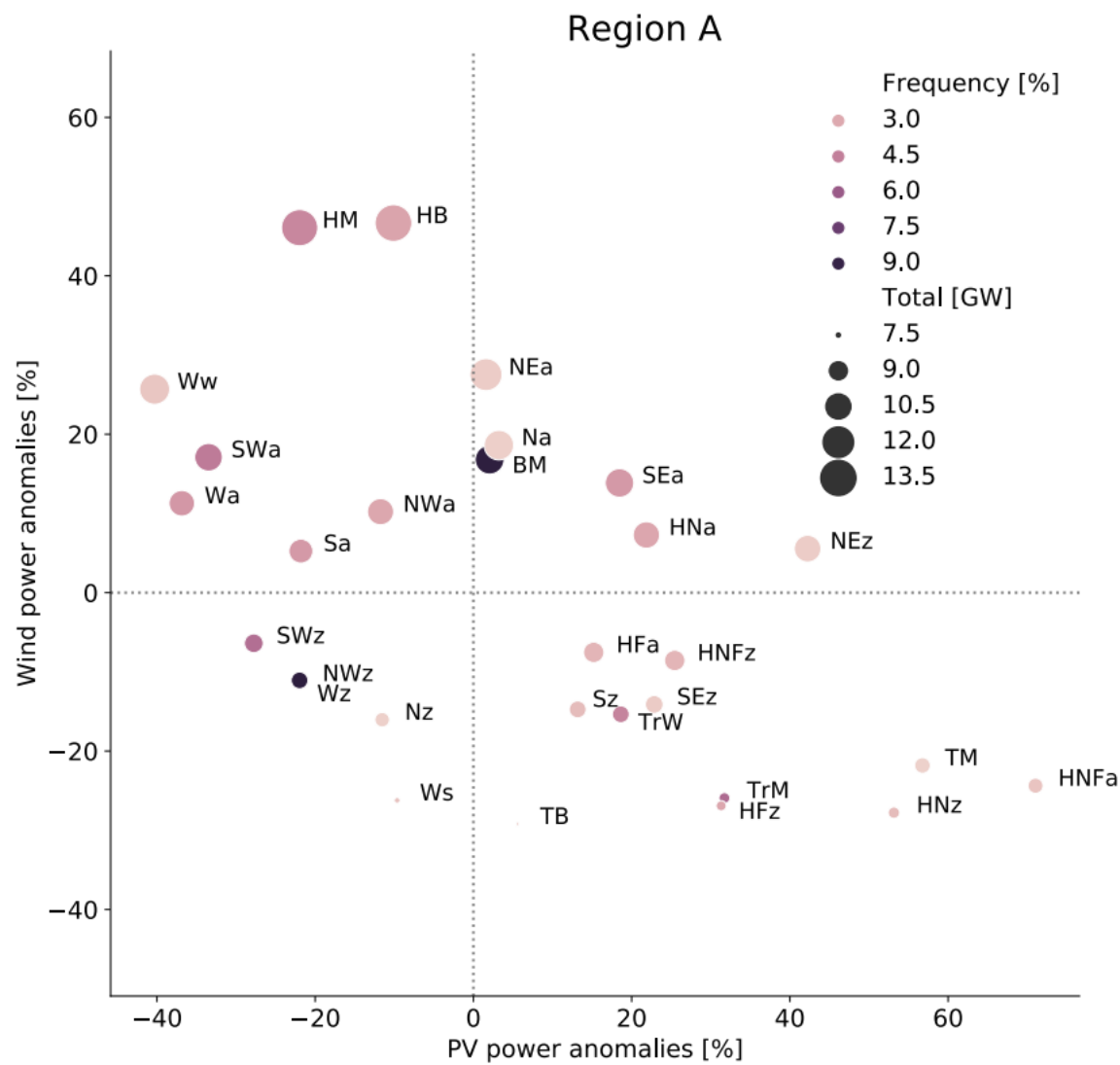
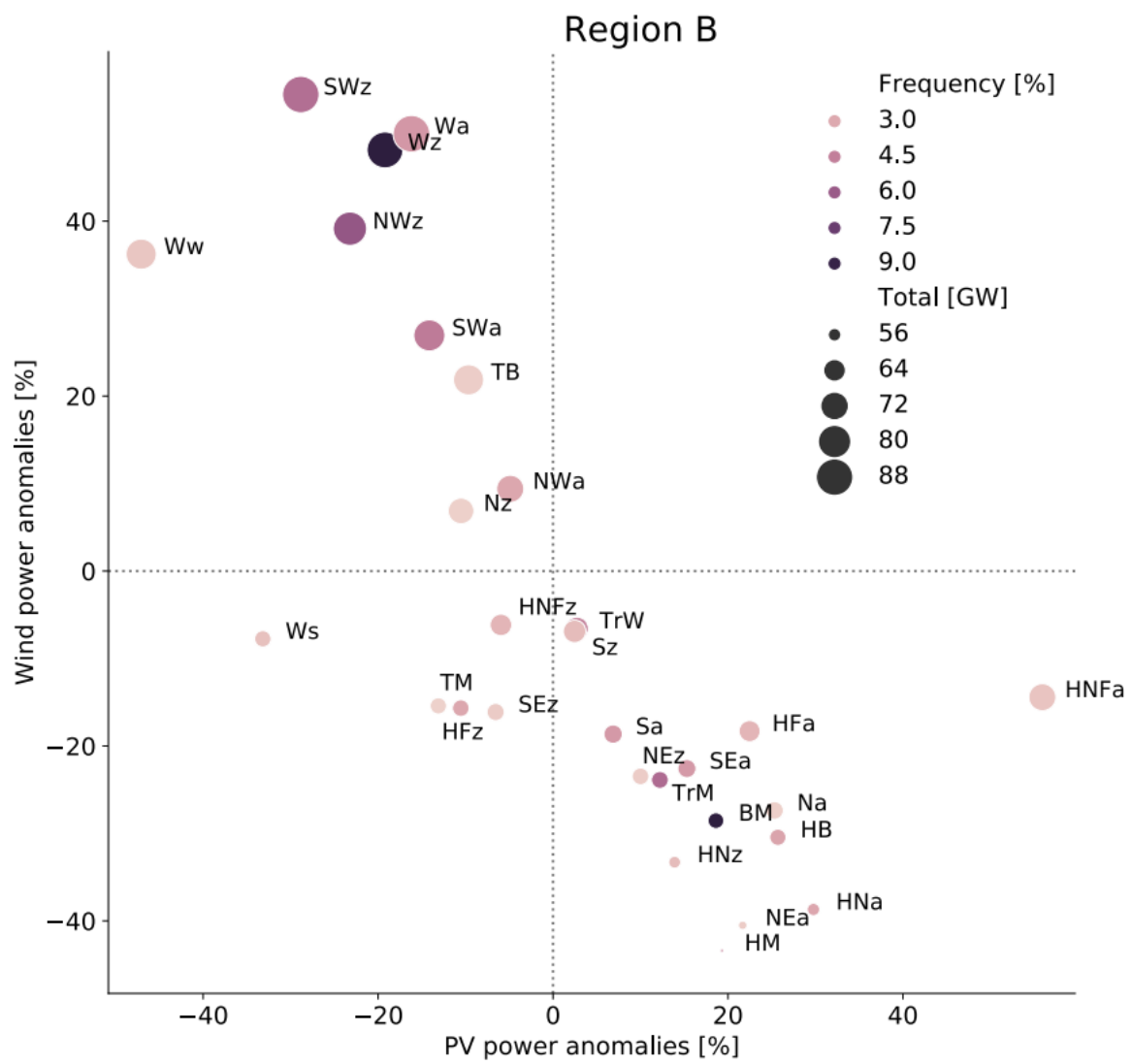
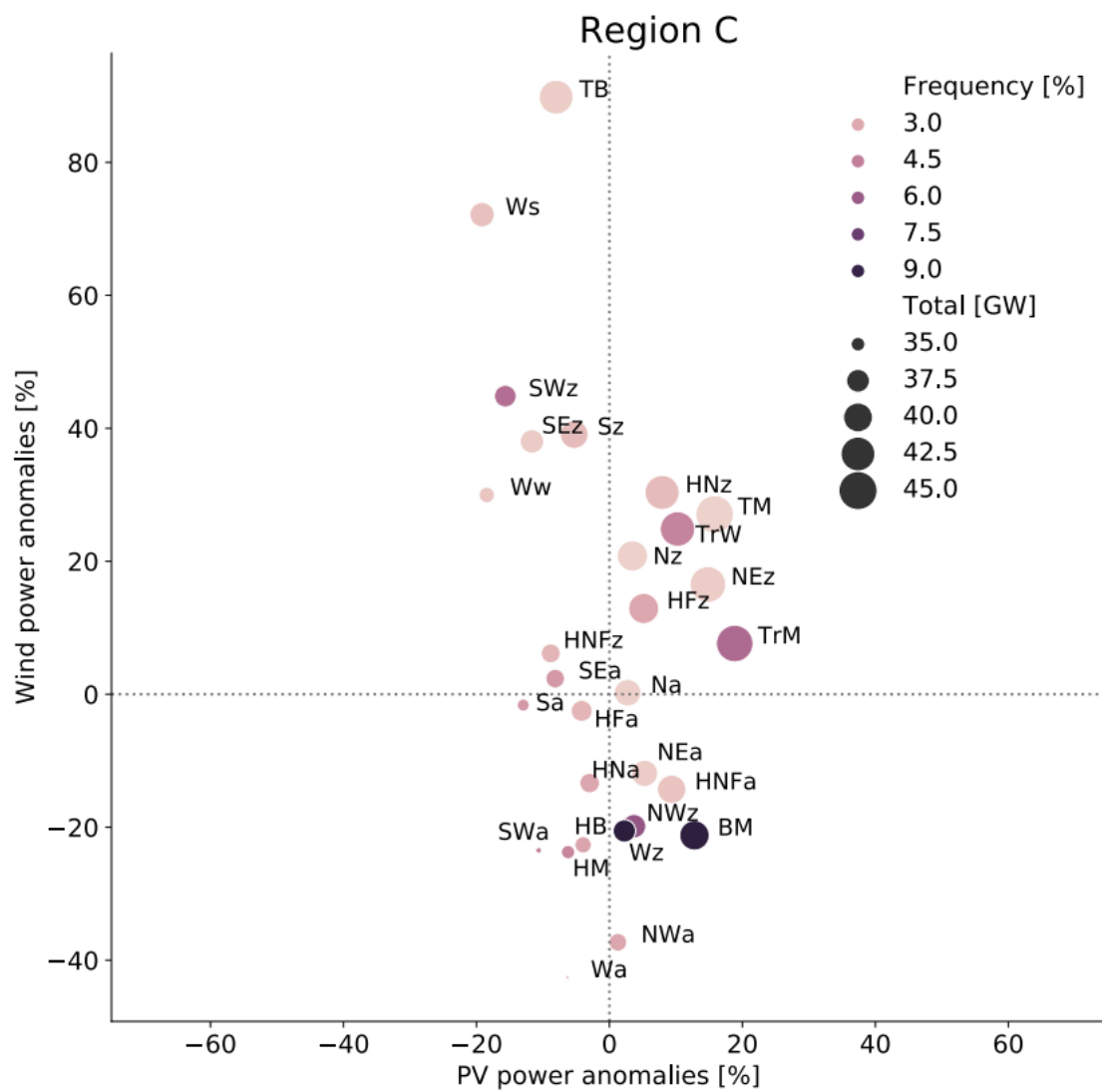


Figure S2. As Figure 2 in the manuscript but for the four selected regions A—D shown in Figure 5.







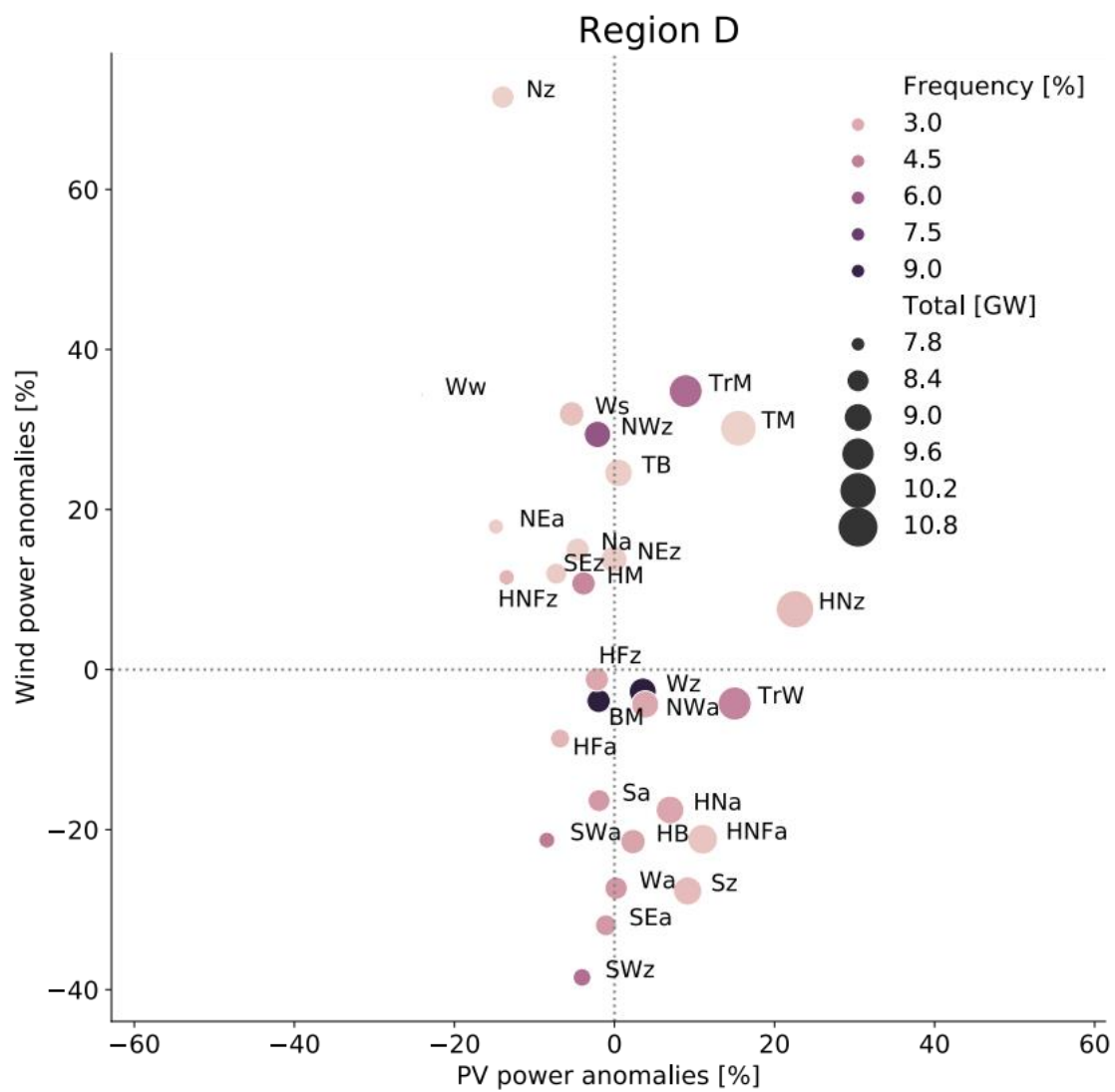


Figure S3. As Figure 1 but for a high-share PV power experiment for Europe, namely the installed capacity of PV power is more than 5-fold that of wind power with the Europe-aggregated installed capacity of PV power of 870 GW and wind power of 167 GW. Shown are PV and wind power production anomalies (stacked) and their total production anomalies (%) relative to their climatological mean for 1995–2017 associated with weather patterns.

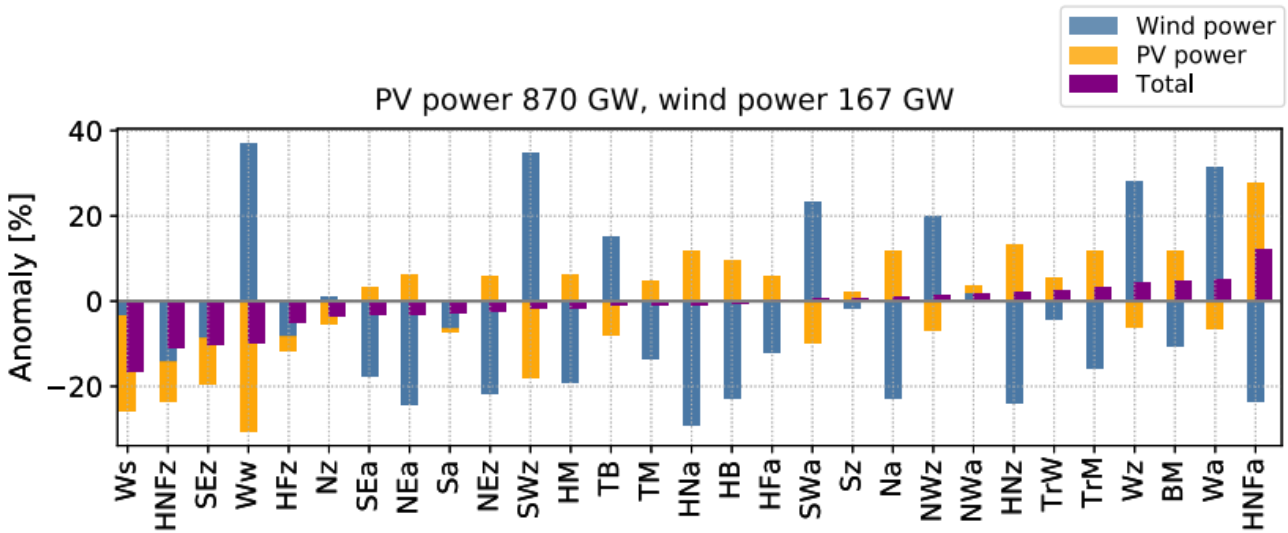


Figure S4. Seasonal differences (%) of European PV and wind power production, sorted by increasing total production from scenario-2050 in Fig. 1b. Anomalies for individual power sources are calculated relative to the climatological mean from scale-2019 and scenario-2050 installations.

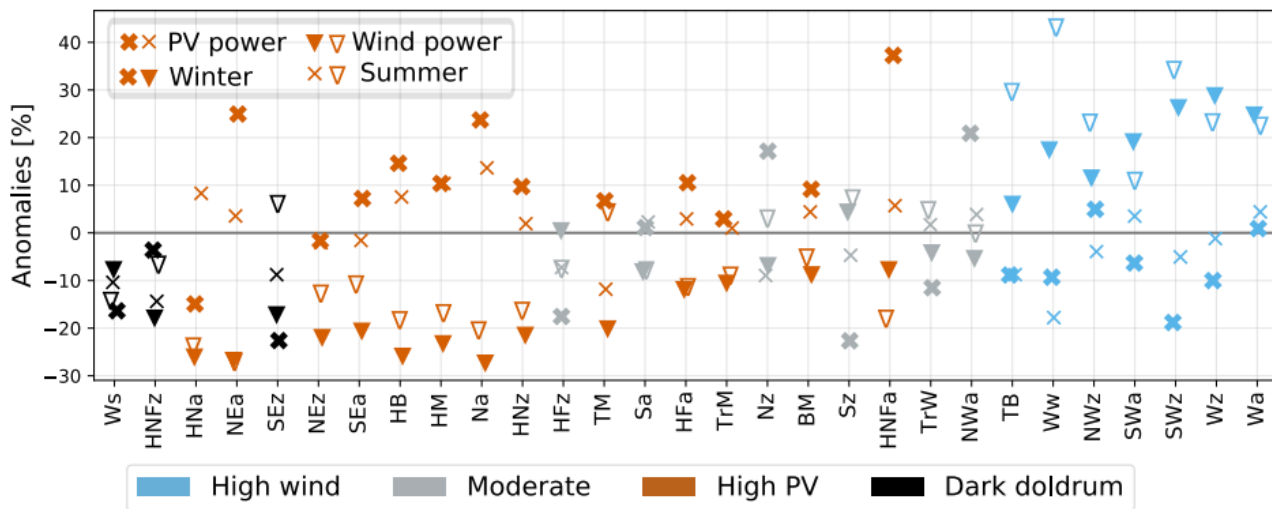
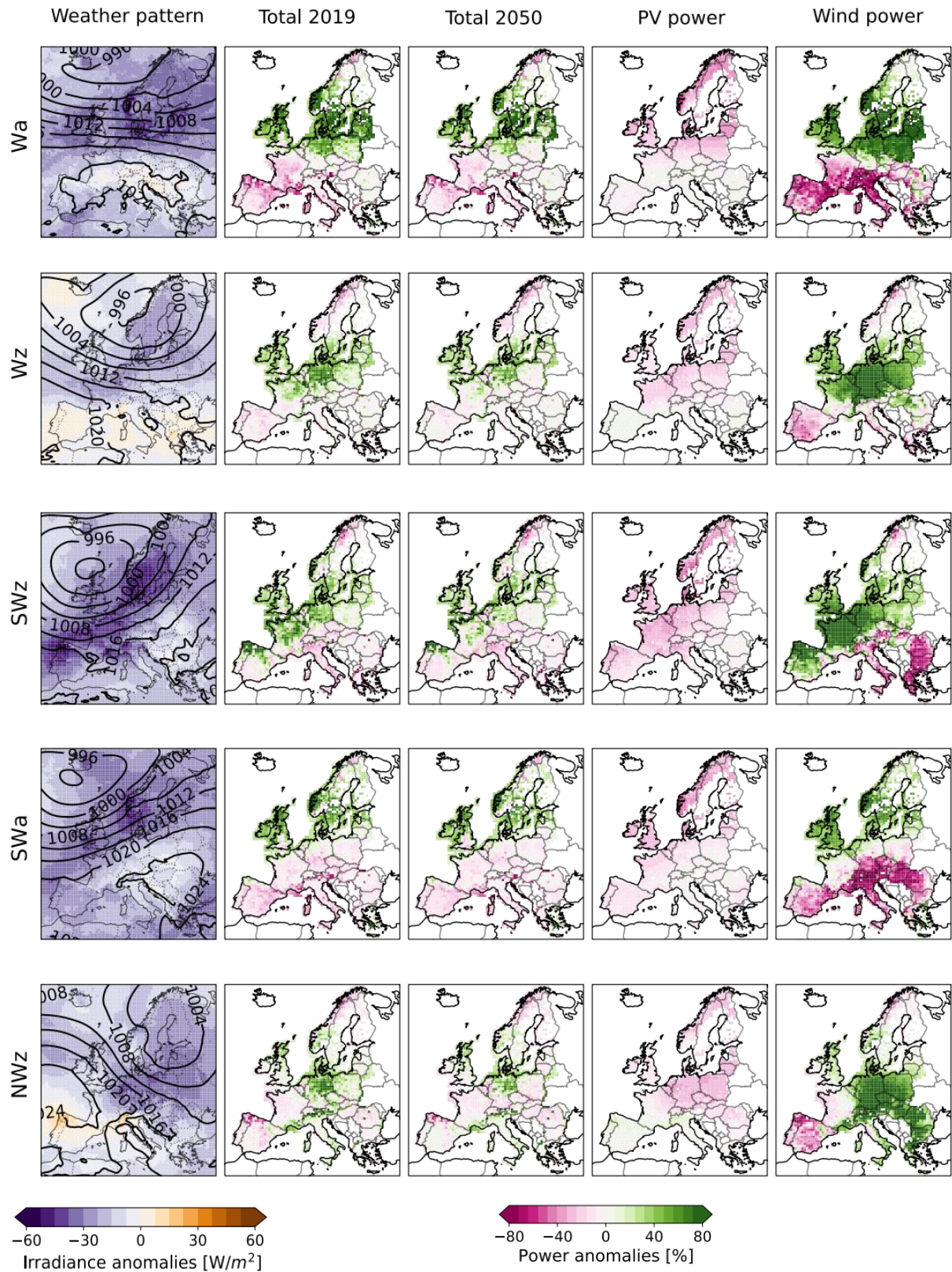
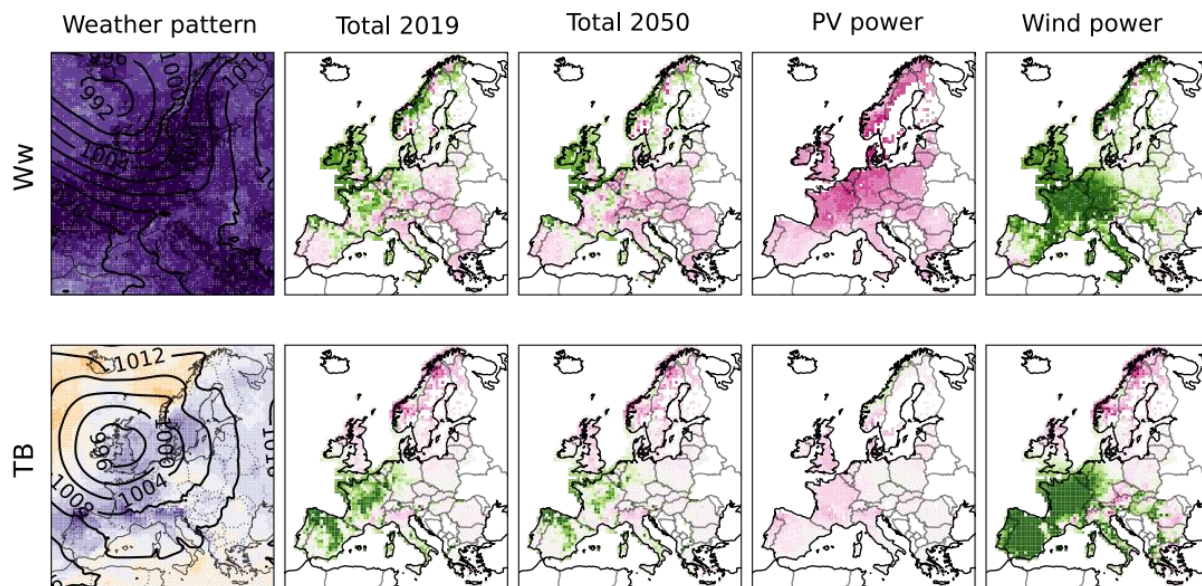


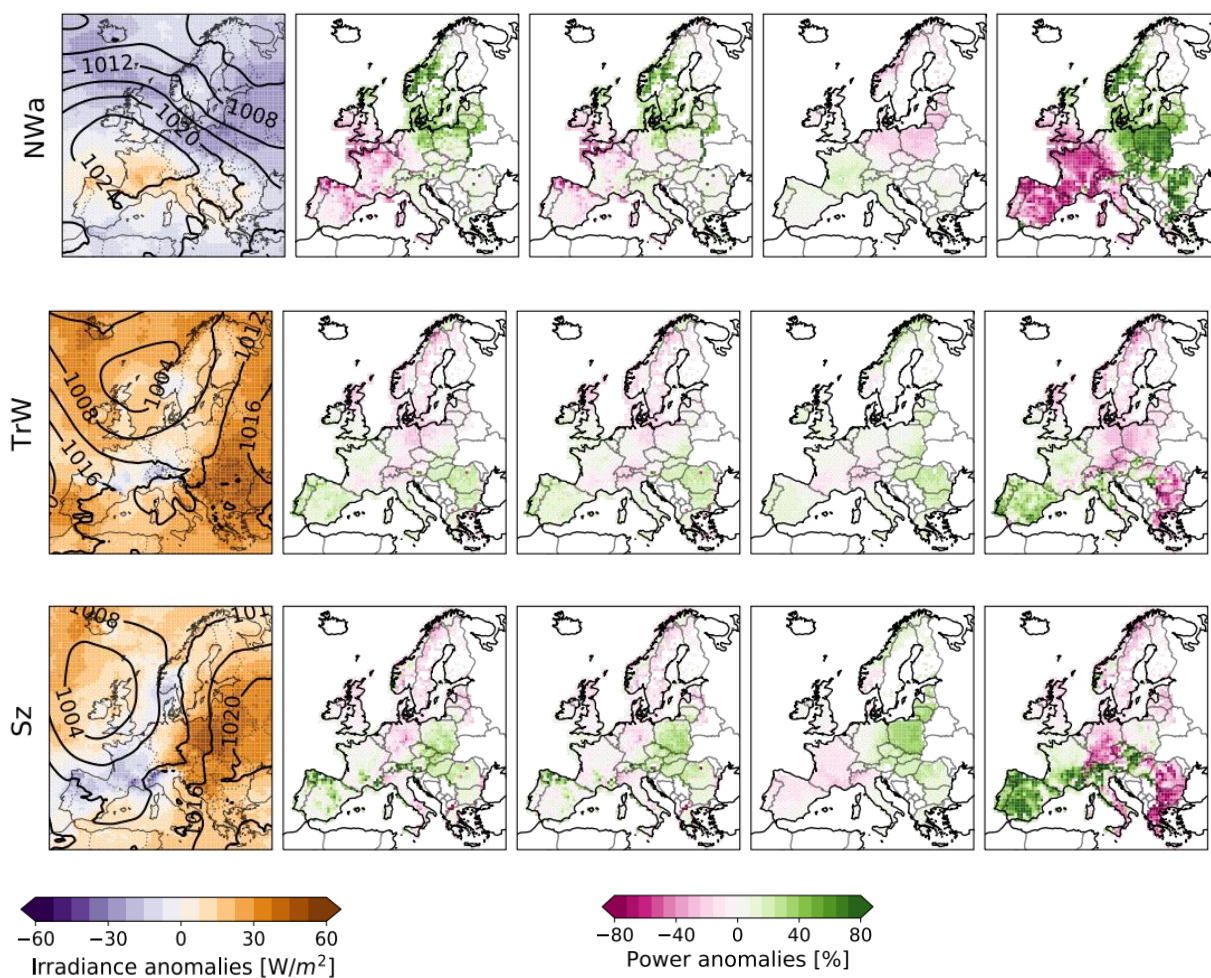
Figure S5. Composite maps for 29 weather patterns in the same order as in Table S1: First column is the composite mean of meteorological conditions with contours for mean sea-level pressure with 4 hPa increments and shading for surface irradiance anomalies. Four following columns are their composite anomalies (%) of total production from scale-2019 and scenario-2050, PV and wind power production. Anomalies (%) of PV and wind power production apply to both scale-2019 and scenario-2050 because the two installed capacities are related by constant scale factors.

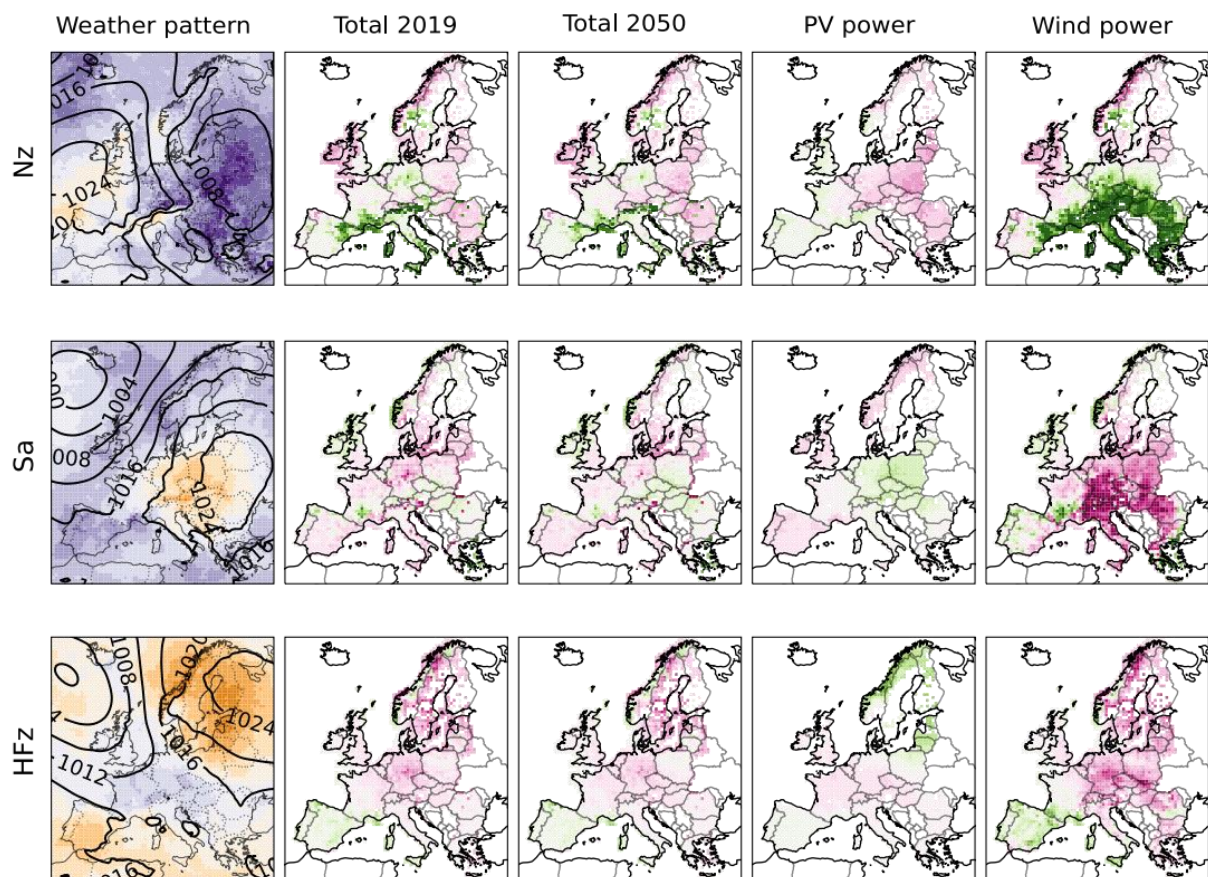
Group High wind



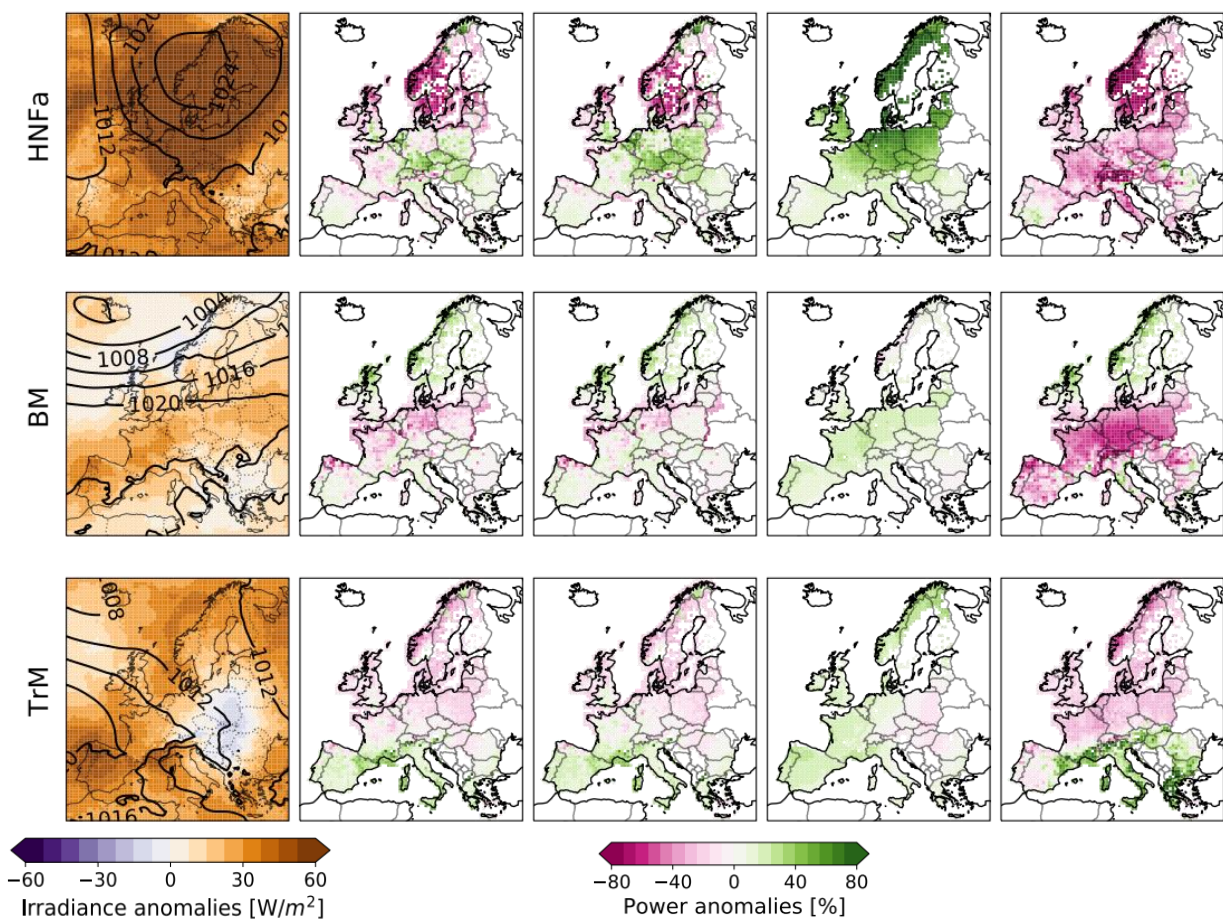


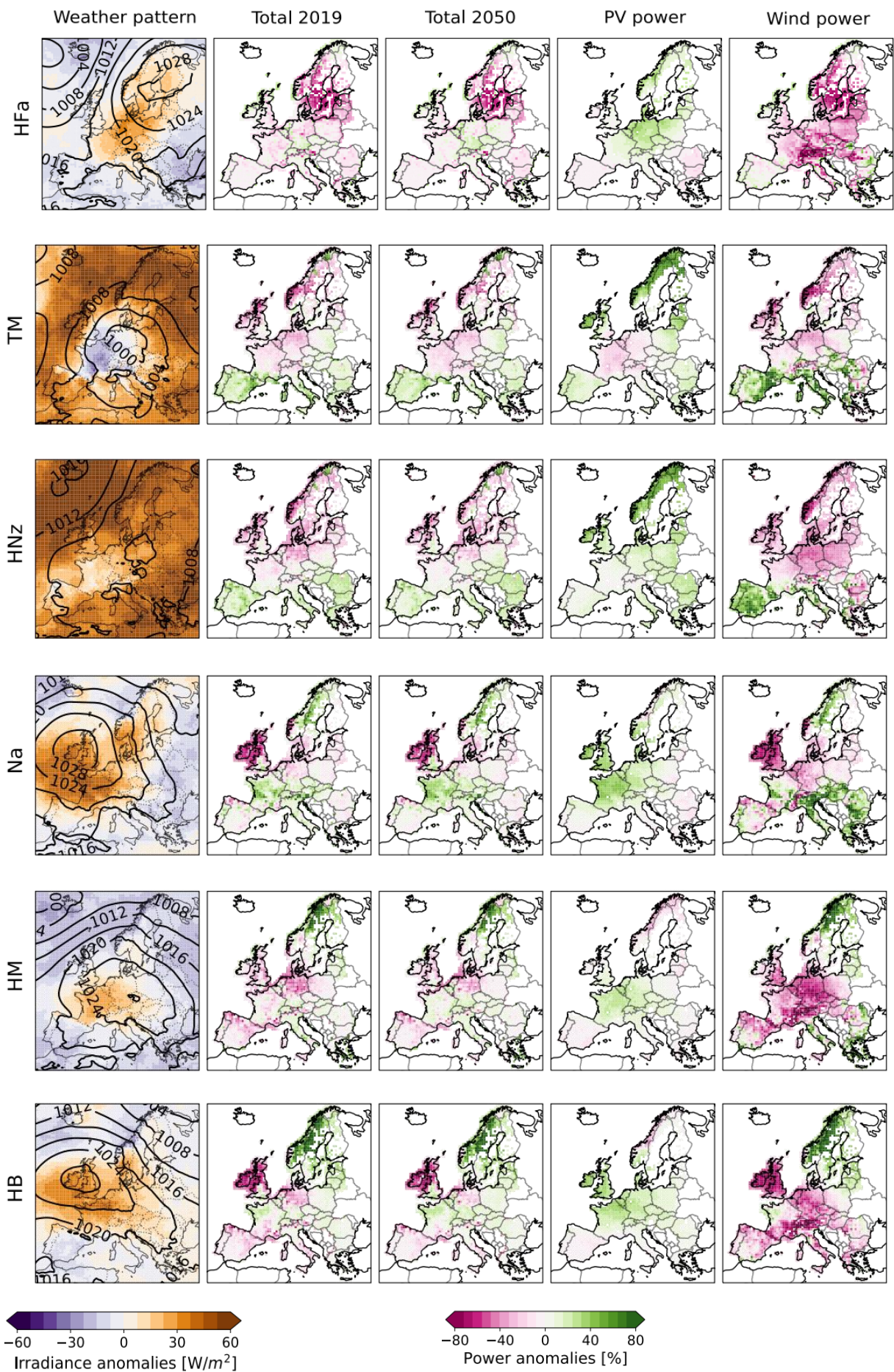
Group Moderate

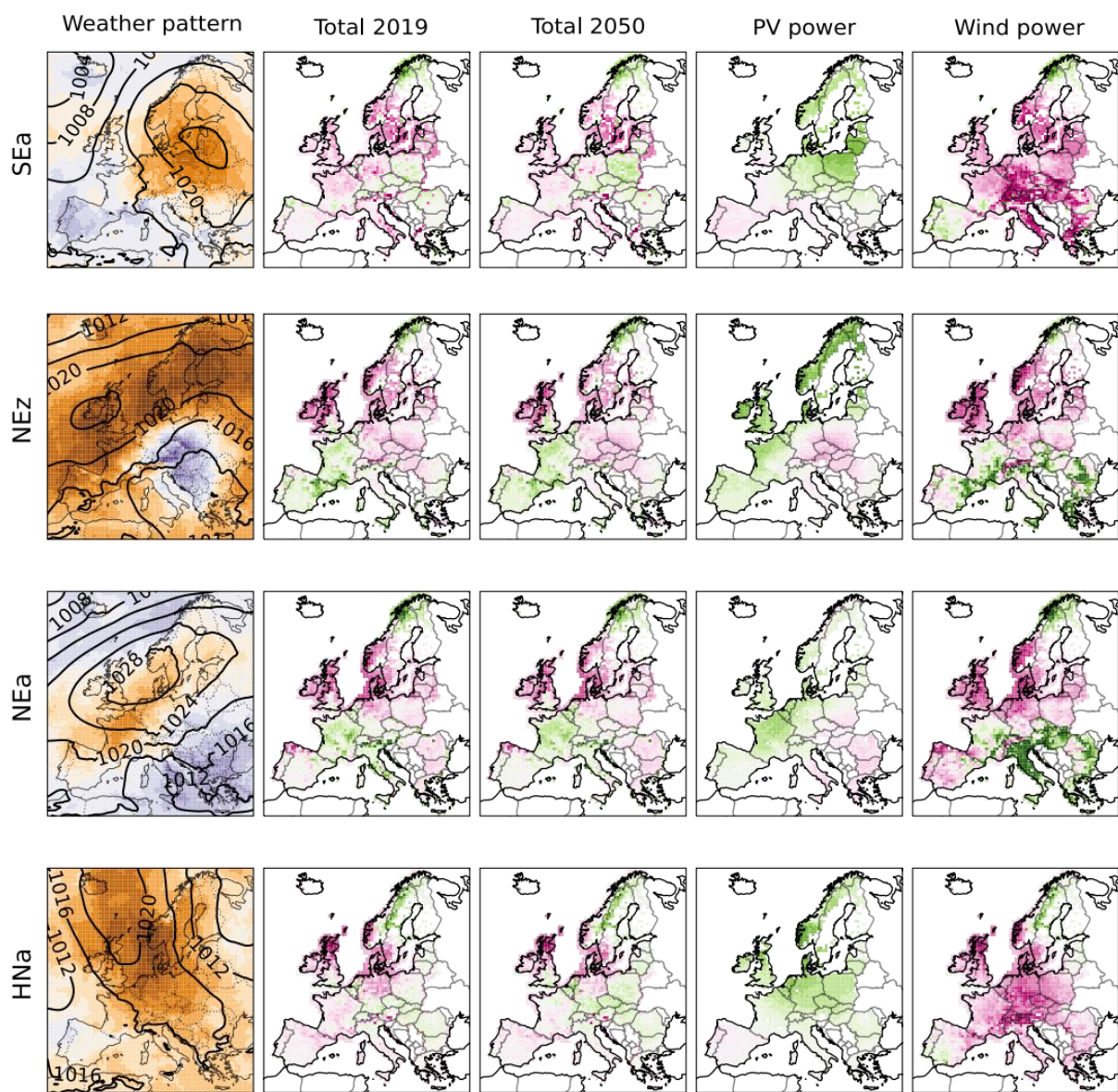




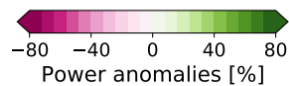
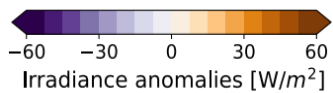
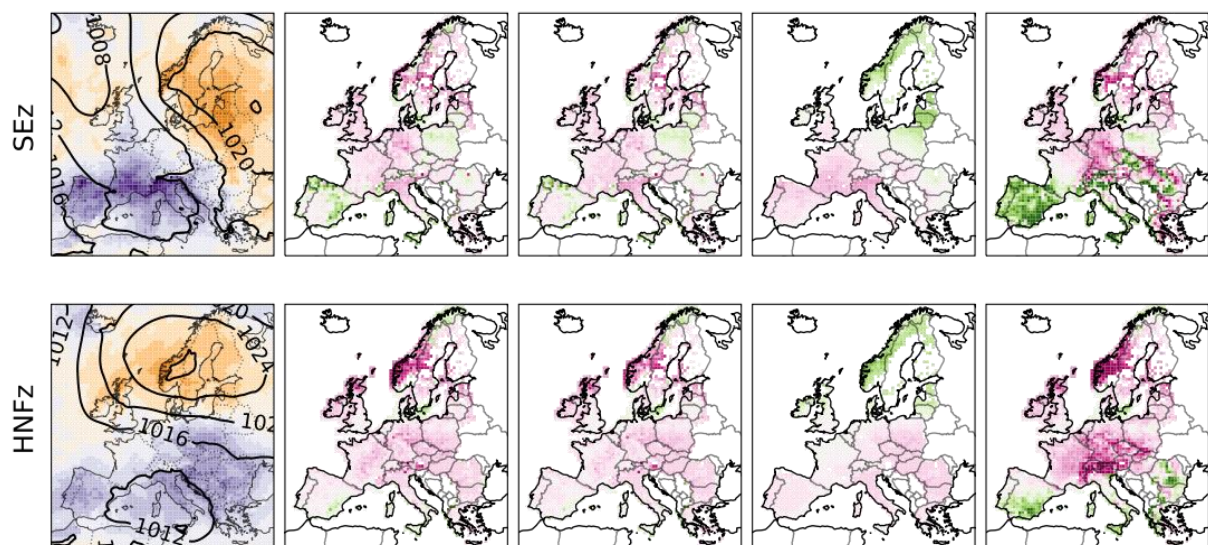
Group High PV







Group Dark doldrum



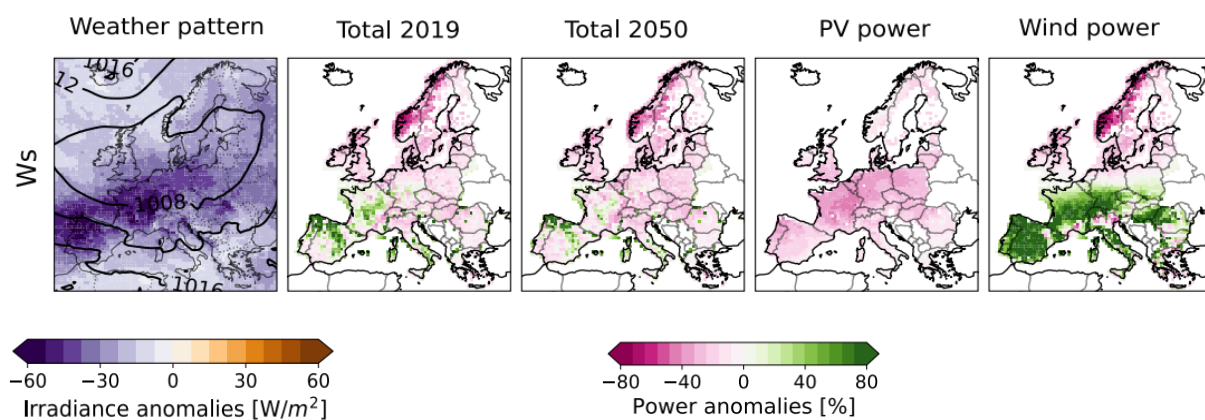


Figure S6. As Figure 5 but for the lowest and highest production extremes with the same weather patterns that last at least for 2, 4, and 8 days. Blue marks weather patterns that are different between 2-,4-, and 8-day compared to 1-, 5-, and 10-day durations in the manuscript, e.g., 1-day and 2-day durations are identical, but 8-day and 10-day extremes are often associated with different weather patterns.

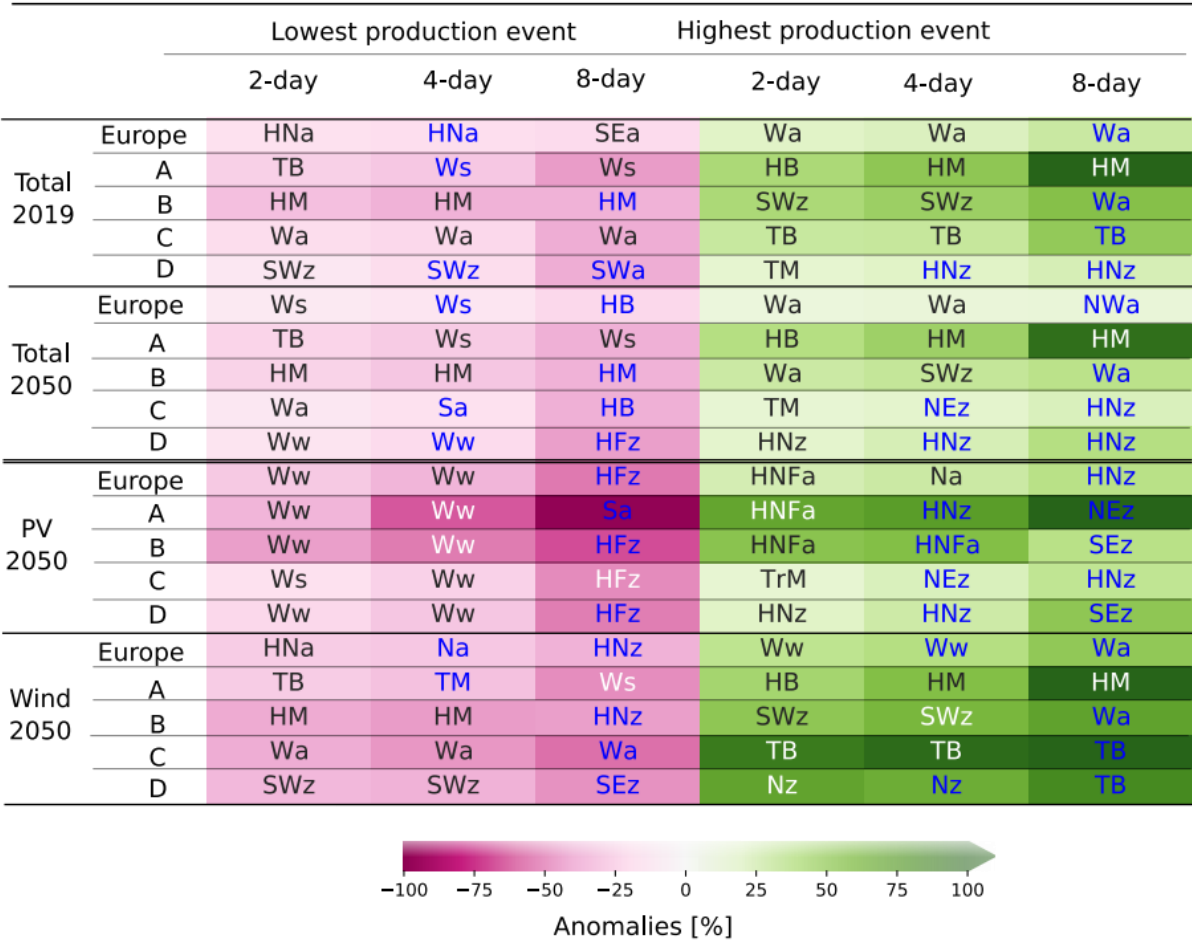


Figure S7. Probability density distribution of hourly capacity factors of PV power (first column) and wind power onshore (second column) for the period 1995–2017, showing REM (filled in blue) compared to CDS and Renewables Ninja (solid lines in black and red) for four European countries in a North-to-South order. A threshold of 0.01 was applied to filter out very low values of PV power during nighttime. The r-values in each box are the corresponding Pearson correlation coefficients between REM and CDS (Renewables Ninja) in black (red).

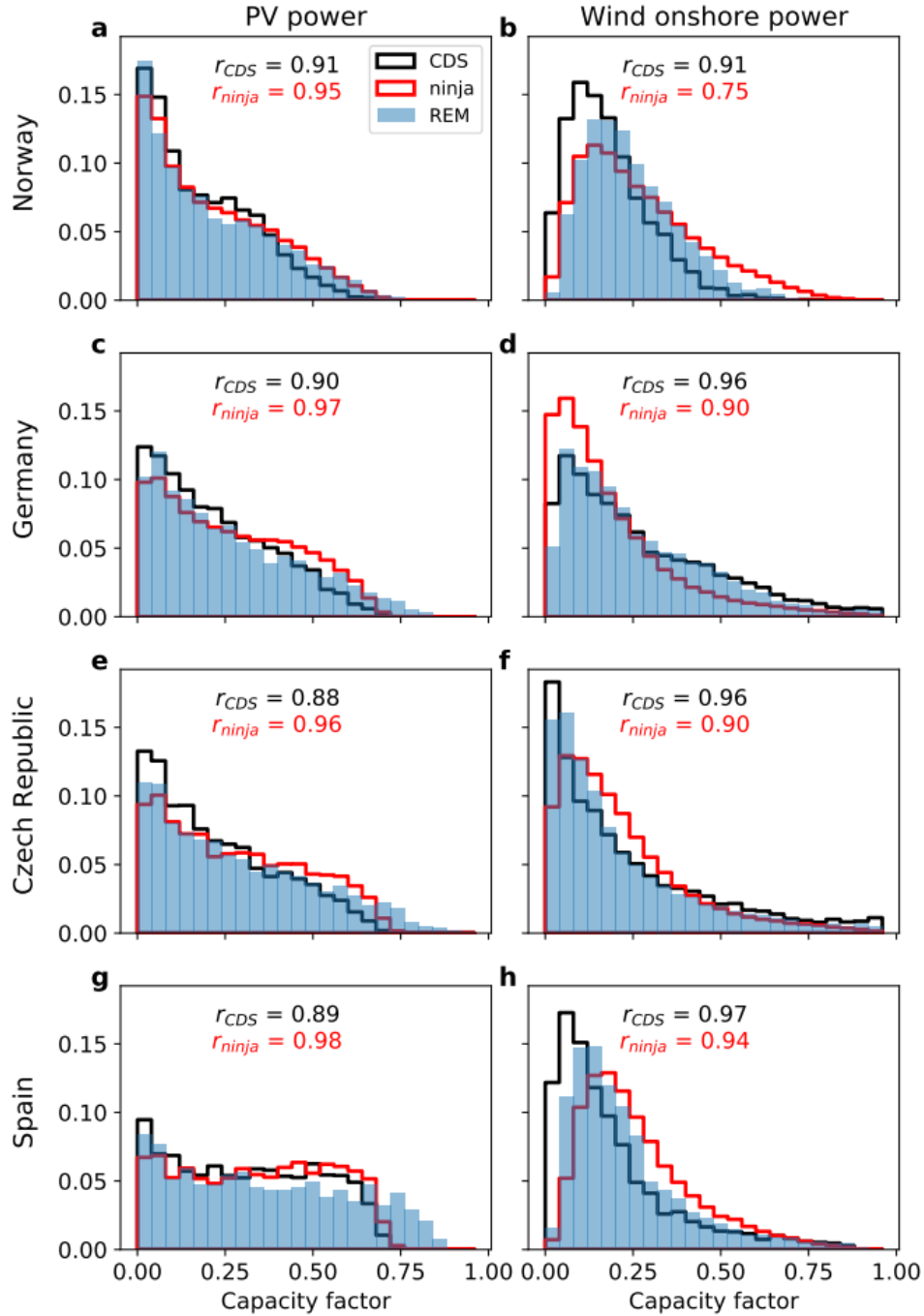
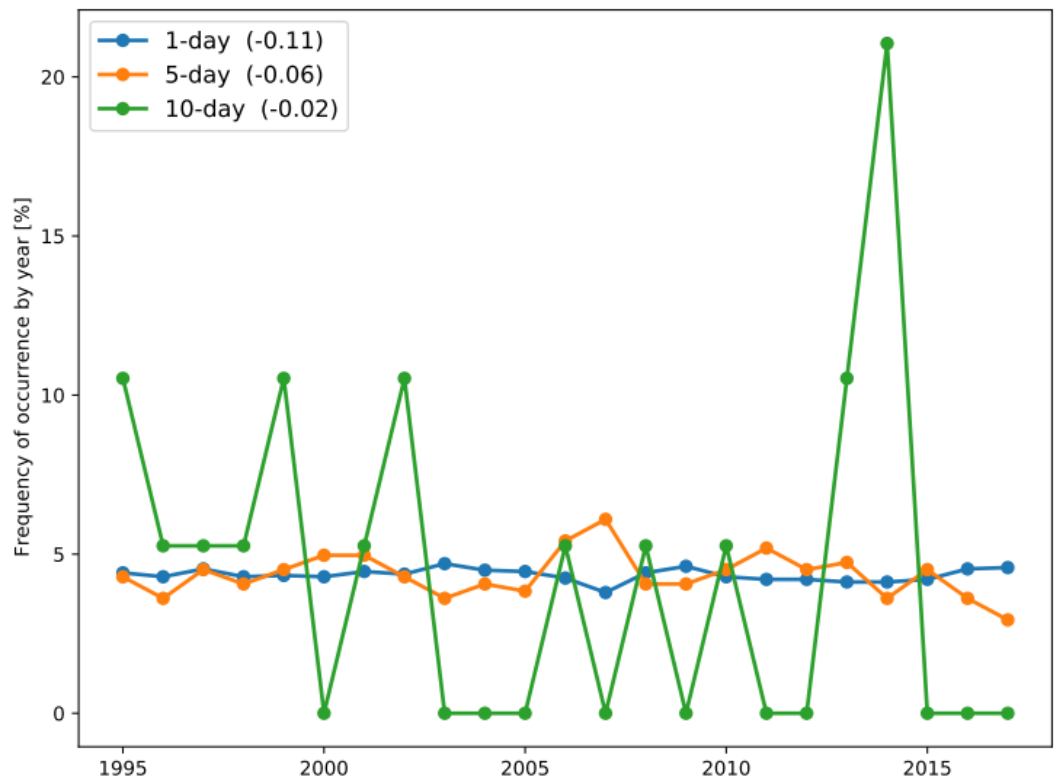


Figure S8. Frequency of yearly occurrence of events with the same weather patterns that last for 1, 5, and 10 days over the period 1995–2017. The trends calculated from linear regression are listed in brackets in the legend. There is a total of 8401, 443, and 19 events of 1-, 5- and 10-day duration. There is a large year-to-year changes in 10-day duration with none to four events (in 2014) in a year.



Part II

SUPPLEMENTARY OF STUDY II

Supplementary material for manuscript

More summertime low-power production extremes in Germany with a larger solar power share

Authors: Linh Ho-Tran and Stephanie Fiedler

Fig S1. (a) Spatial distribution of wind power in Europe for the scenario-2050 installation from CLIMIX model (Jerez et al., 2015); (b) similar but masked for Germany, used in the manuscript; (c) Installation of wind power without the masked area for Germany, shows wind power offshore that was not included in the calculation for Germany in the manuscript.

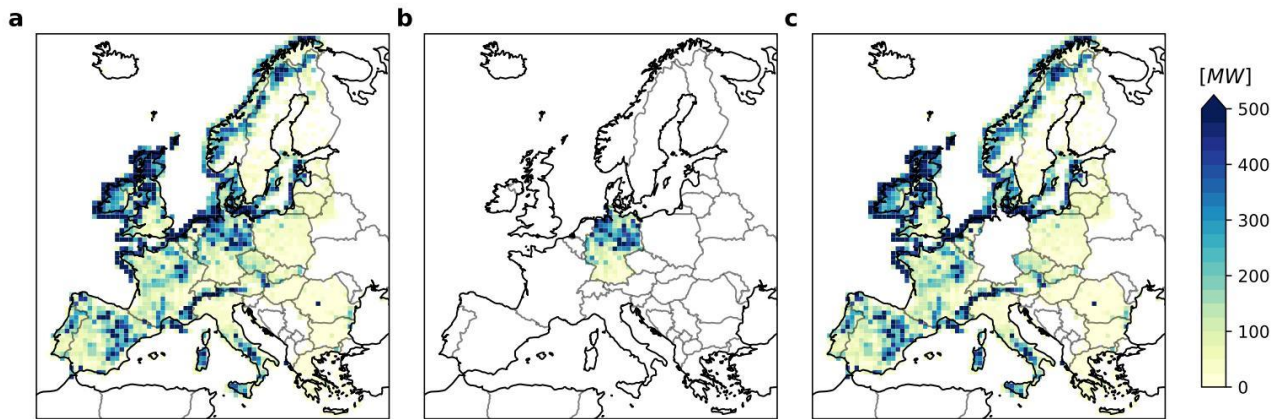


Table S1. Names of 29 weather patterns (James, 2007) and their three frequencies of occurrence associated with extreme events with 1-, 7-, 14-day durations respectively, normalized by their respective frequencies of occurrence over the period 1995—2017. For each weather patterns, the percentages on the upper rows (in grey) are for winter and lower rows (in white) are for summer. The statistics method is described in the Method section in the main text.

	Weather pattern	Full name	Low extremes		High extremes	
			Scale-2019	Scenario-2050	Scale-2019	Scenario-2050
Cyclonic	Nz	Cyclonic Northerly	0.9, 0.3, 0.3	0, 0, 0	2.8, 0.1, 0.5	1.8, 0.1, 0.5
			0, 0, 0	0, 0, 0	0, 0.5, 0.7	0, 0, 0.3
	NWz	Cyclonic North-Westerly	0.3, 0, 0.2	0.3, 0.2, 0.4	2.9, 1.4, 1.1	1.6, 1.1, 1.0
			0, 0, 0	0, 0, 0	2.9, 1.2, 0.4	2.0, 0.5, 0.4
	NEz	Cyclonic North-Easterly	1.5, 1.9, 2.4	3.0, 2.4, 1.7	0, 0, 0.4	0, 0, 0
			0, 0, 0.1	0.9, 0.9, 1.2	0, 0, 0	0, 0, 0
	Sz	Cyclonic Southerly	0, 0.9, 1.4	1.3, 0.9, 0.7	0, 0, 0.1	0, 0, 0.4
			0, 0, 0.1	0, 0, 0.4	0, 0, 0	0, 0, 0
	SEz	Cyclonic South-Easterly	5.9, 4.0, 3.1	8.3, 3.4, 3.1	0, 0, 0.2	0, 0, 0
			0, 0, 0	0, 0, 0.1	0, 0, 0.1	0, 0, 0
	SWz	Cyclonic South-Westerly	0, 0.1, 0.1	0.3, 0.1, 0.1	0.6, 1.5, 2.4	0.9, 1.5, 2.4
			0, 0, 0	0, 0, 0	0.5, 0.9, 0.8	0, 0.7, 0.3
	Wz	Cyclonic Westerly	0, 0, 0	0.2, 0, 0	2.6, 4.1, 3.0	2.8, 3.9, 2.7
			0, 0, 0	0, 0, 0.1	1.8, 0.8, 0.4	1.4, 0.6, 0.3
	Ww	Maritime Westerly (Block Eastern Europe)	0, 0.7, 0.3	0, 0.6, 0.2	0, 0.5, 0.3	0, 0.1, 0.3
			0, 0, 0	0, 0, 0	0, 0, 0	0, 0, 0
	Ws	South-Shifted Westerly	2.1, 0.9, 1.2	2.1, 0.7, 0.5	0, 0.2, 0.4	0, 0.2, 0.1
			0, 0, 0	0, 0.6, 0.3	0, 0, 0.1	0, 0, 0
	TrM	Trough over Central Europe	0.6, 0.6, 0.6	0, 0.8, 0.6	0, 0, 0.1	0, 0, 0.1
			0, 0, 0	0.3, 0.2, 0.4	0, 0.1, 0.1	0.3, 0, 0
	TrW	Trough over Western Europe	2.4, 1.1, 0.9	1.8, 1.6, 0.9	0, 0.3, 0.3	0, 0.3, 0.5
			0, 0, 0	0.4, 0.5, 0.4	0.8, 0.5, 0.2	1.1, 0.5, 0
	TB	Low over the British Isles	0, 0, 0.3	0, 0, 0.2	0, 0, 0.7	0, 0, 0.8
			0, 0, 0	0, 0, 0	0, 0, 0.2	0, 0, 0.2
	HNz	Icelandic High, Trough Central Europe	1.2, 0.7, 1.5	1.2, 1.2, 1.5	0, 0.2, 0.1	0, 0.2, 0.1
			0, 0, 0	0, 0.3, 0.5	0, 0, 0	0, 0, 0
	HNFz	High Scandinavia-Iceland, Trough Central Europe	1.6, 2.2, 1.9	0.8, 2.2, 1.7	0, 0, 0	0, 0.2, 0
			0, 0, 0.2	0.7, 0.6, 0.6	0, 0, 0	0, 0.2, 0.1
	HFz	Scandinavian High, Trough Central Europe	0.9, 1.6, 1.8	1.7, 1.2, 0.5	0, 0, 0.1	0, 0.2, 0.1
			0, 0, 0	0, 0.2, 0.5	0, 0, 0	0, 0.1, 0
	TM	Low (Cut-Off) over Central Europe	0, 0.3, 1.9	2.4, 2.1, 1.4	0, 0, 0	0, 0, 0
			0, 0.1, 0	0.8, 0.4, 0.7	0, 0, 0	0.8, 0, 0

Anticyclonic	HFa	Scandinavian High, Ridge Central Europe	1.6, 1.6, 2.0	0.8, 1.0, 1.1	0, 0, 0	0.8, 0.6, 0.5
			0, 0, 0	0, 0, 0	0, 0, 0	0, 0.4, 0.1
	HNFa	High Scandinavia-Iceland, Ridge Central Europe	0, 0.3, 0.6	0, 0.8, 0.6	0, 0, 0.6	1.9, 1.7, 0.1
			0, 0, 0	0, 0, 0	0, 0, 0.3	0, 0.5, 0.3
	HNa	Icelandic High, Ridge Central Europe	3.6, 2.8, 2.2	0.9, 2.3, 1.7	0, 0, 0	0, 0, 0.1
			0, 0, 0	0.5, 0.1, 0.1	0, 0.1, 0	0, 0.1, 0.1
	Na	Anticyclonic Northerly	2.0, 1.0, 1.1	2.0, 1.0, 0.6	0, 0, 0.2	0, 0, 0.2
			0, 0, 0	0, 0, 0	0, 0, 0.1	0, 0, 0.1
	NWa	Anticyclonic North- Westerly	0, 0, 0.6	0, 0, 0.5	0.5, 0.5, 0.8	1.0, 0.7, 1.1
			0, 0, 0	0, 0, 0	0.9, 0, 0.2	1.9, 0.4, 0.6
	NEa	Anticyclonic North- Easterly	0.9, 1.7, 2.2	0.9, 1.2, 1.7	0, 0, 0	0, 0, 0
			0, 0, 0	0, 0, 0.3	0, 0, 0	0, 0, 0
	Wa	Anticyclonic Westerly	0, 0, 0.2	0, 0, 0.2	0.4, 1.7, 2.1	0.4, 2.2, 2.5
			0, 0, 0	0, 0, 0	0, 0, 0.3	0.8, 0, 0.3
	Sa	Anticyclonic Southerly	2.1, 1.6, 1.2	0.5, 1.0, 0.7	0, 0, 0.3	0, 0, 0.3
			0, 0.4, 0	0, 0.4, 0.1	0, 0, 0.1	0, 0, 0.1
	SWa	Anticyclonic South- Westerly	0.3, 0.4, 0.4	0.3, 0.4, 0.5	0, 0.4, 1.1	0, 0.5, 1.3
			0, 0.2, 0.1	0, 0.2, 0.1	0, 0, 0.1	0, 0.3, 0.3
	SEa	Anticyclonic South- Easterly	1.8, 1.8, 1.3	0.6, 1.5, 0.8	0, 0, 0	0, 0, 0
			0, 0, 0	0, 0, 0.2	0, 0, 0	0.5, 0, 0
	HM	High over Central Europe	1.7, 3.0, 2.2	0.4, 1.9, 1.9	0, 0, 0.2	0, 0, 0.2
			0, 0, 0.1	0, 0, 0	0, 0, 0	0, 0, 0
	HB	High over the British Isles	1.2, 1.5, 1.7	1.9, 1.8, 1.6	0, 0.1, 0.1	0, 0.2, 0.1
			0, 0.3, 0.2	0, 0, 0.3	0, 0, 0	0, 0, 0
	BM	Zonal Ridge across Central Europe	1.9, 1.4, 1.2	1.9, 1.2, 1.1	0, 0.1, 0.4	0, 0.1, 0.5
			0, 0.3, 0.3	0.2, 0.2, 0.4	0, 0, 0	0, 0, 0

Figure S2. Meteorological condition and anomalies of PV and wind power on 1996-05-11. Percentages are average values for Germany.

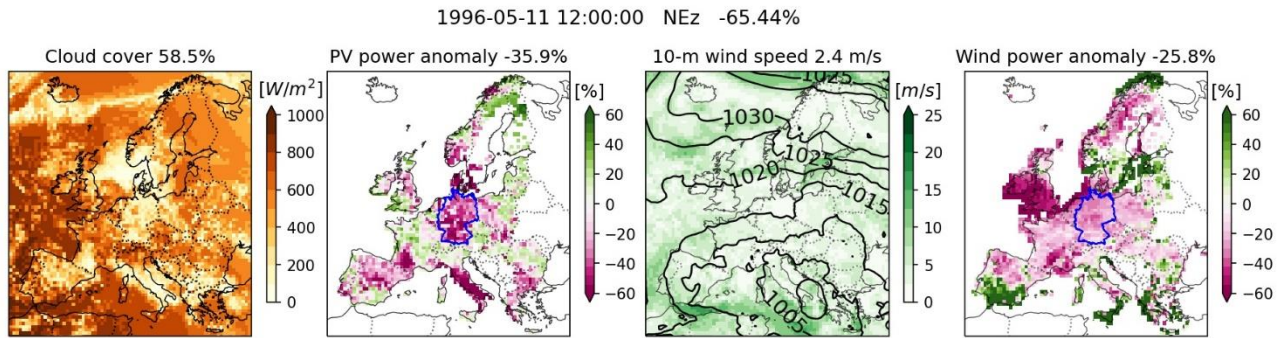


Table S2. Percentage of 50 lowest and highest total production events for Germany in proportion of cyclonic (C) and anticyclonic (A), 3 numbers in order for 1-, 7-, 14-day events as shown in **Fig. 3**. The percentages were calculated by the number of days with that pair of characteristics, e.g., cyclonic and summer, against the number of days in 50 events (50, 350, and 700 days, respectively).

		Lowest production events		Highest production events	
Installation		Scale-2019	Scenario-2050	Scale-2019	Scenario-2050
Summer	Cyclonic	0 – 0 – 1	10 – 11 – 17	36 – 21 – 12	32 – 15 – 7
	Anticyclonic	0 – 6 – 4	4 – 4 – 8	2 – 1 – 3	8 – 5 – 5
Winter	Cyclonic	40 – 34 – 37	48 – 37 – 29	58 – 65 – 60	50 – 60 – 56
	Anticyclonic	60 – 60 – 57	38 – 48 – 46	4 – 13 – 25	10 – 21 – 31

Figure S3. Frequency of occurrence of lowest total production events associated with 29 weather patterns normalised by the corresponding frequency of patterns during the period 1995--2017. 50 lowest production events were selected for each duration 1, 7 and 14 days in winter half-year (in full colours) and summer half-year (in pale colours, stacked). Result is shown for scale-2019 (a), and scenario-2050 installation (b), and the different between scenario-2050 minus scale-2019 installations in winter (c) and summer (d).

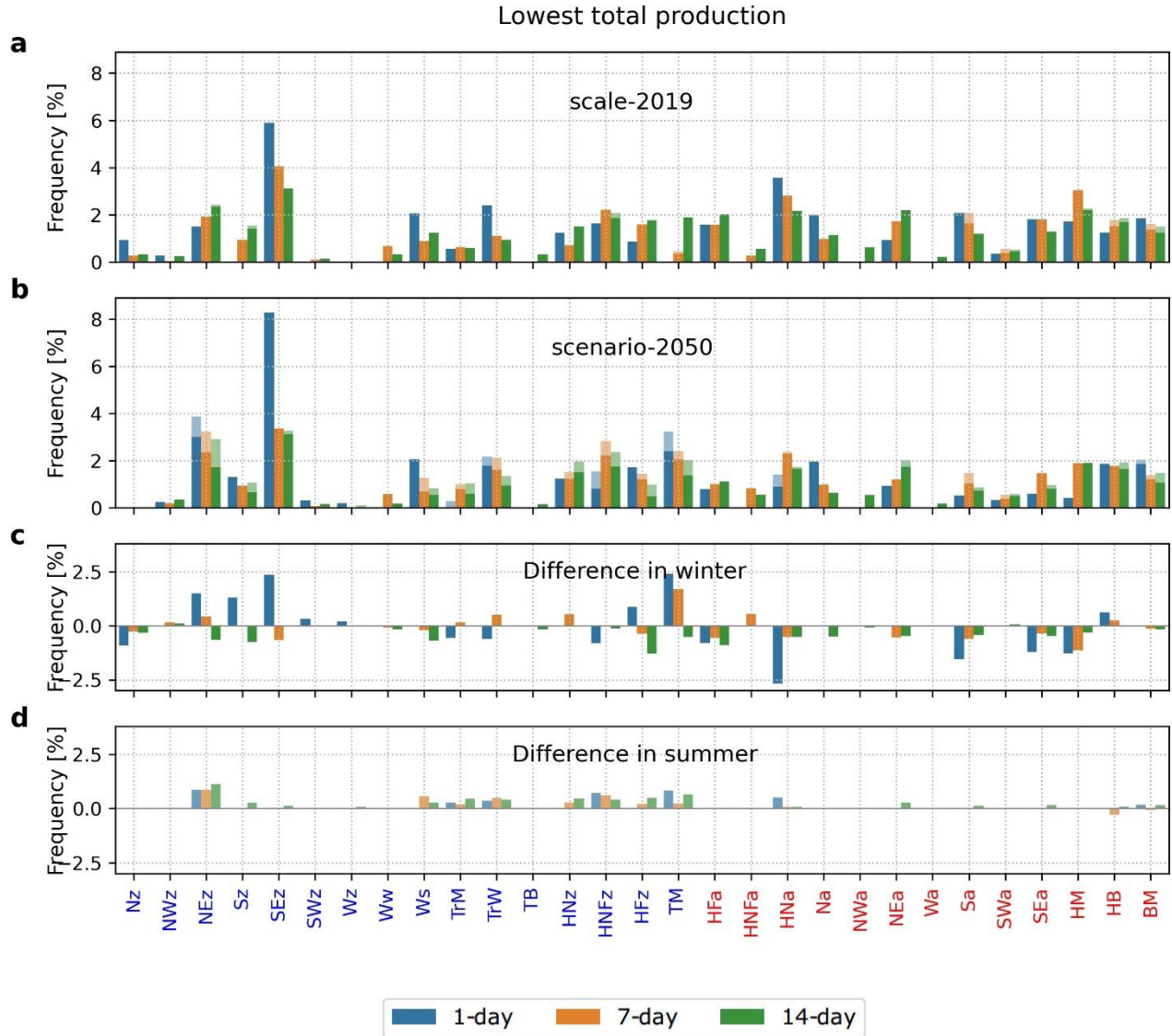


Figure S4. Same as Figure S2 but for 50 highest production events.

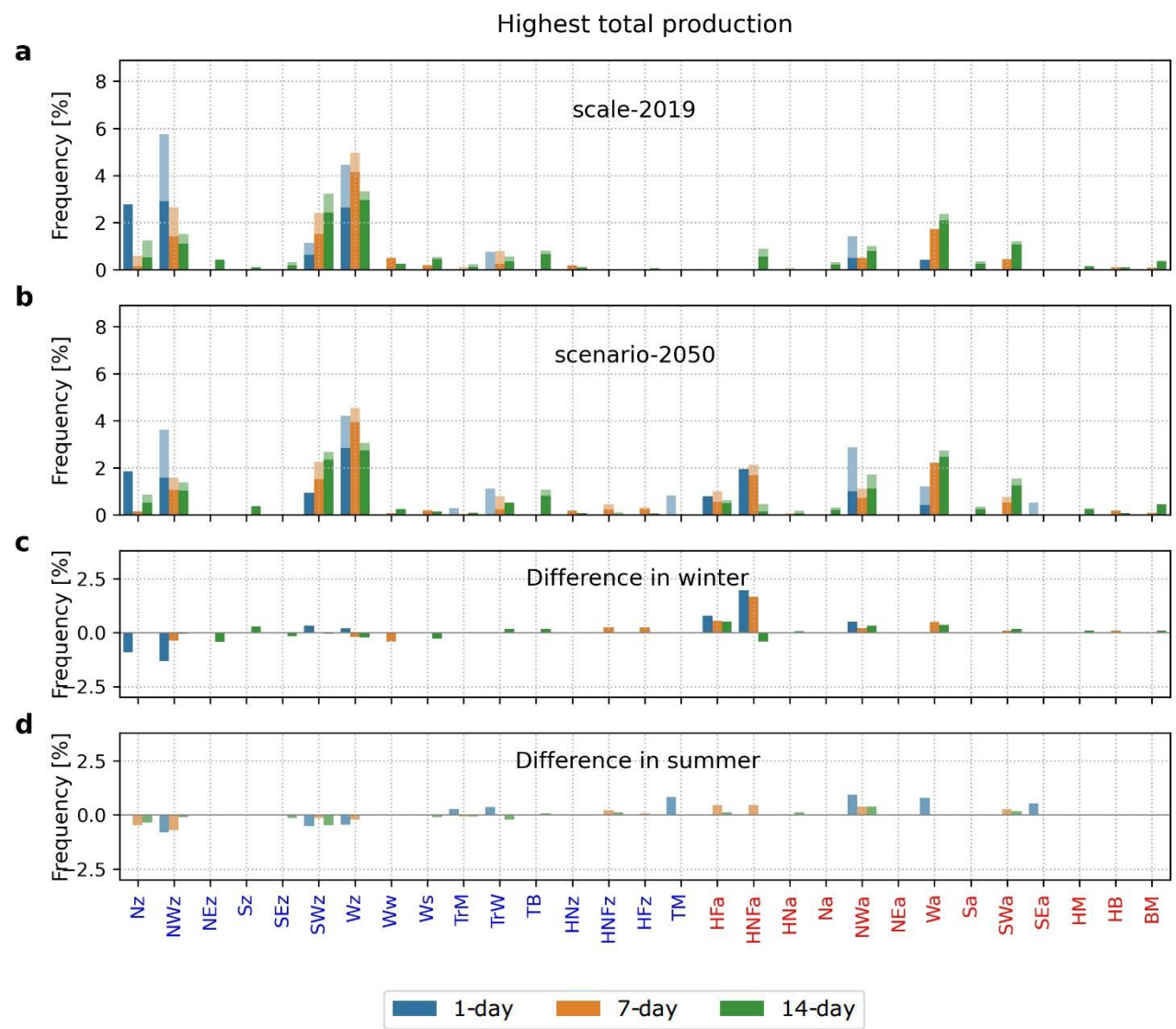
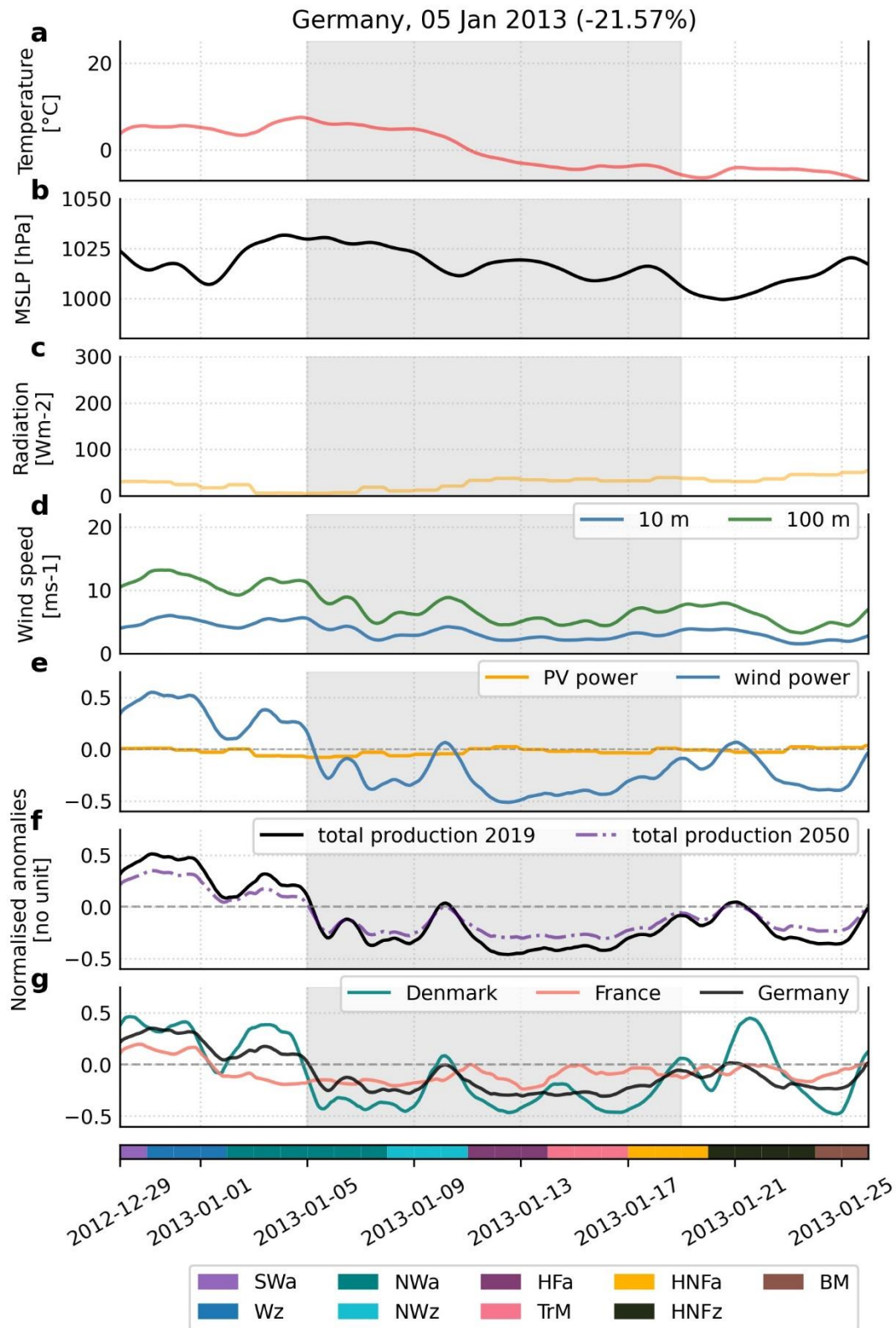
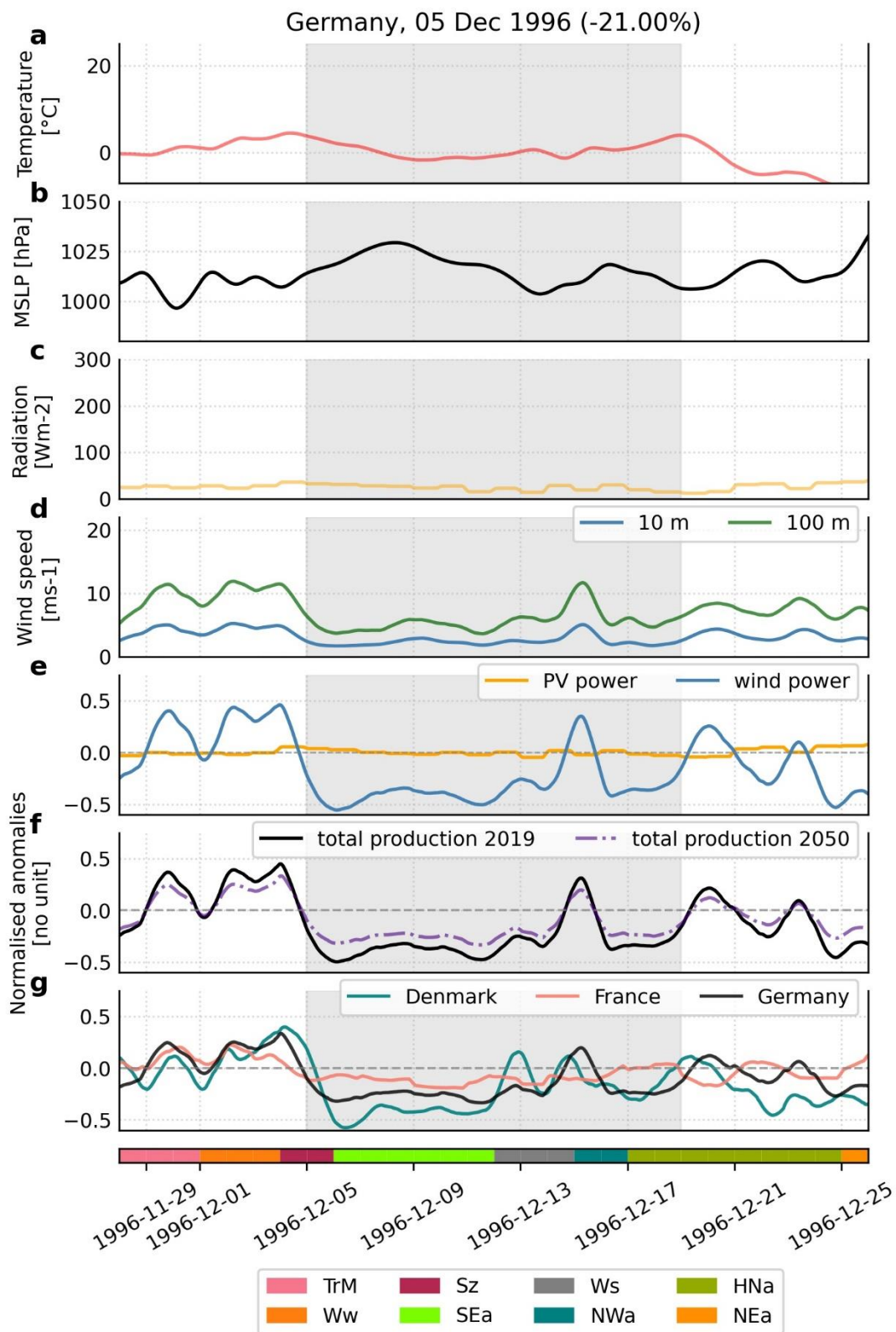
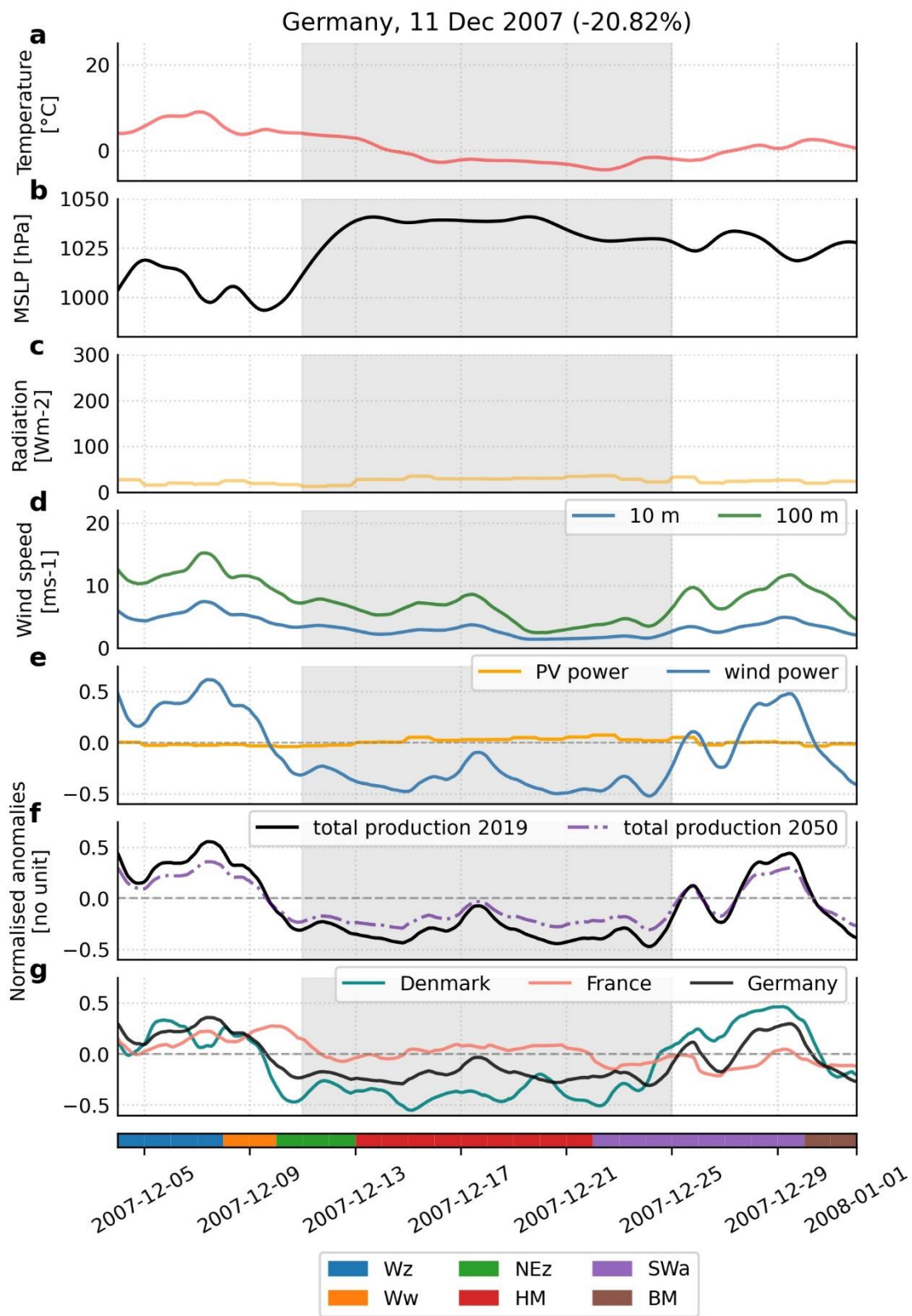
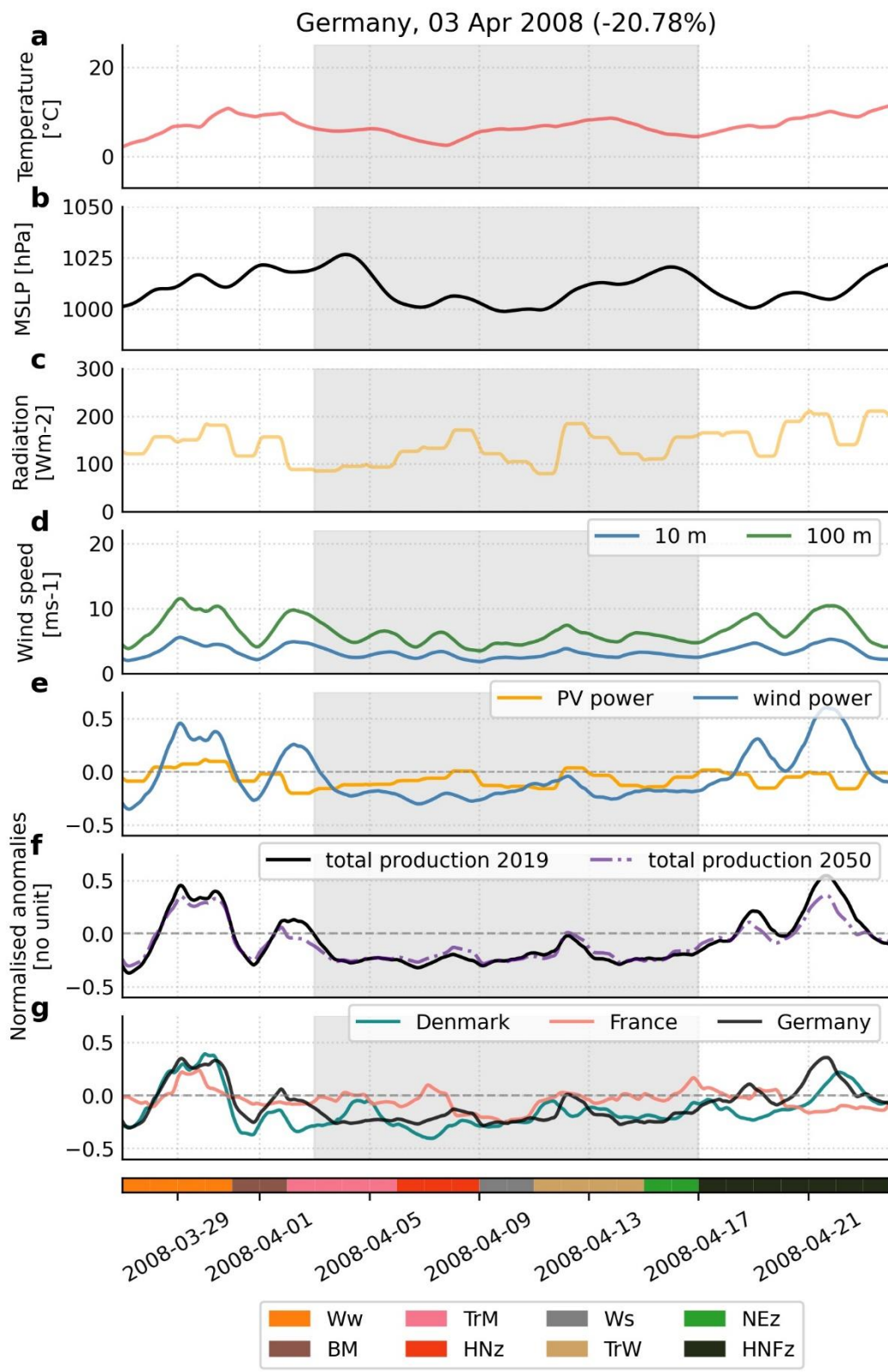


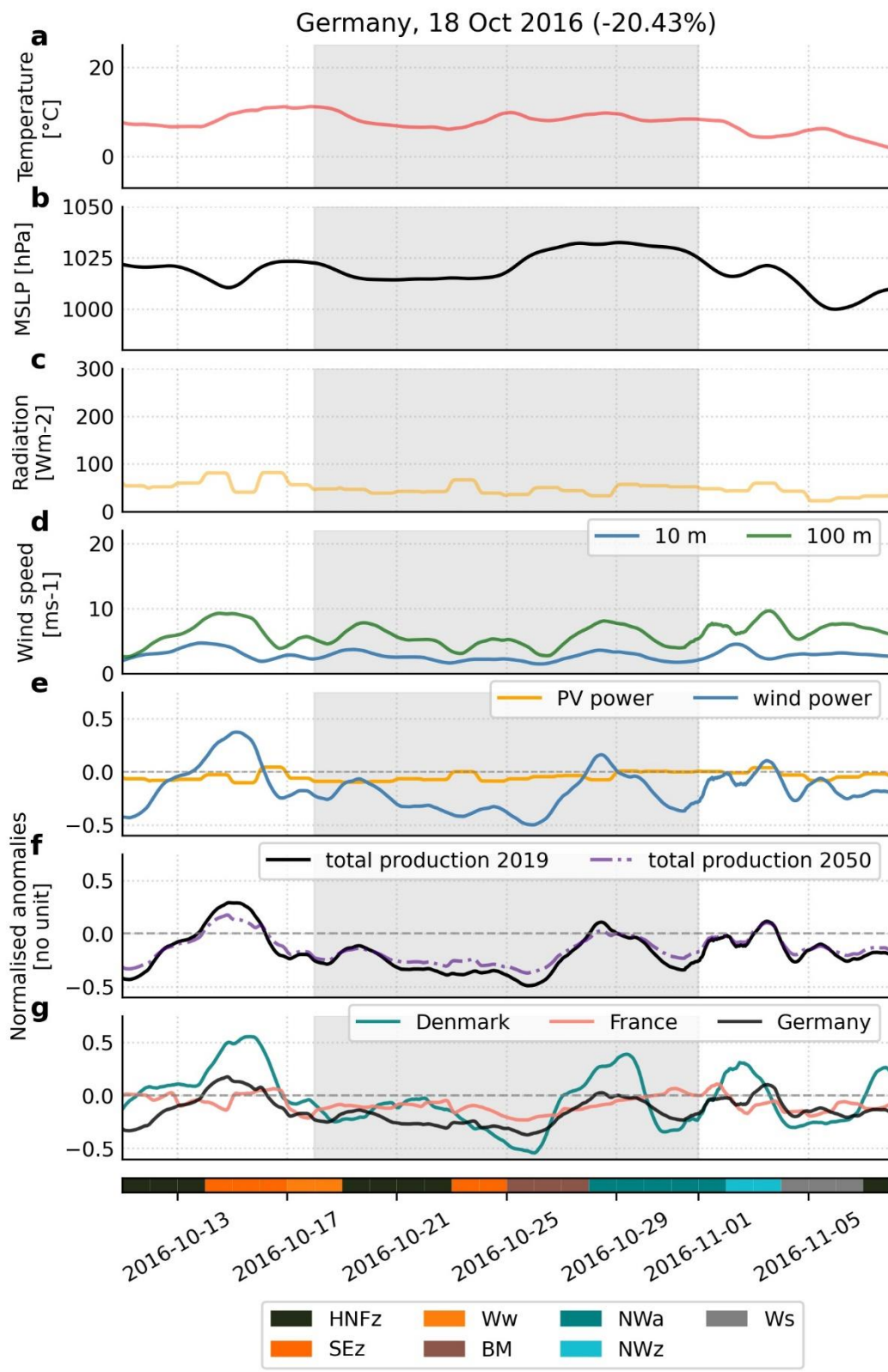
Figure S5. Meteorological progression during ten events of 14-day low total production in Germany in winter (including the event in the manuscript) that listed in Table 1 in the manuscript. Their central dates at 00:00 UTC of the 8th days of the events are marked by vertical dotted lines.

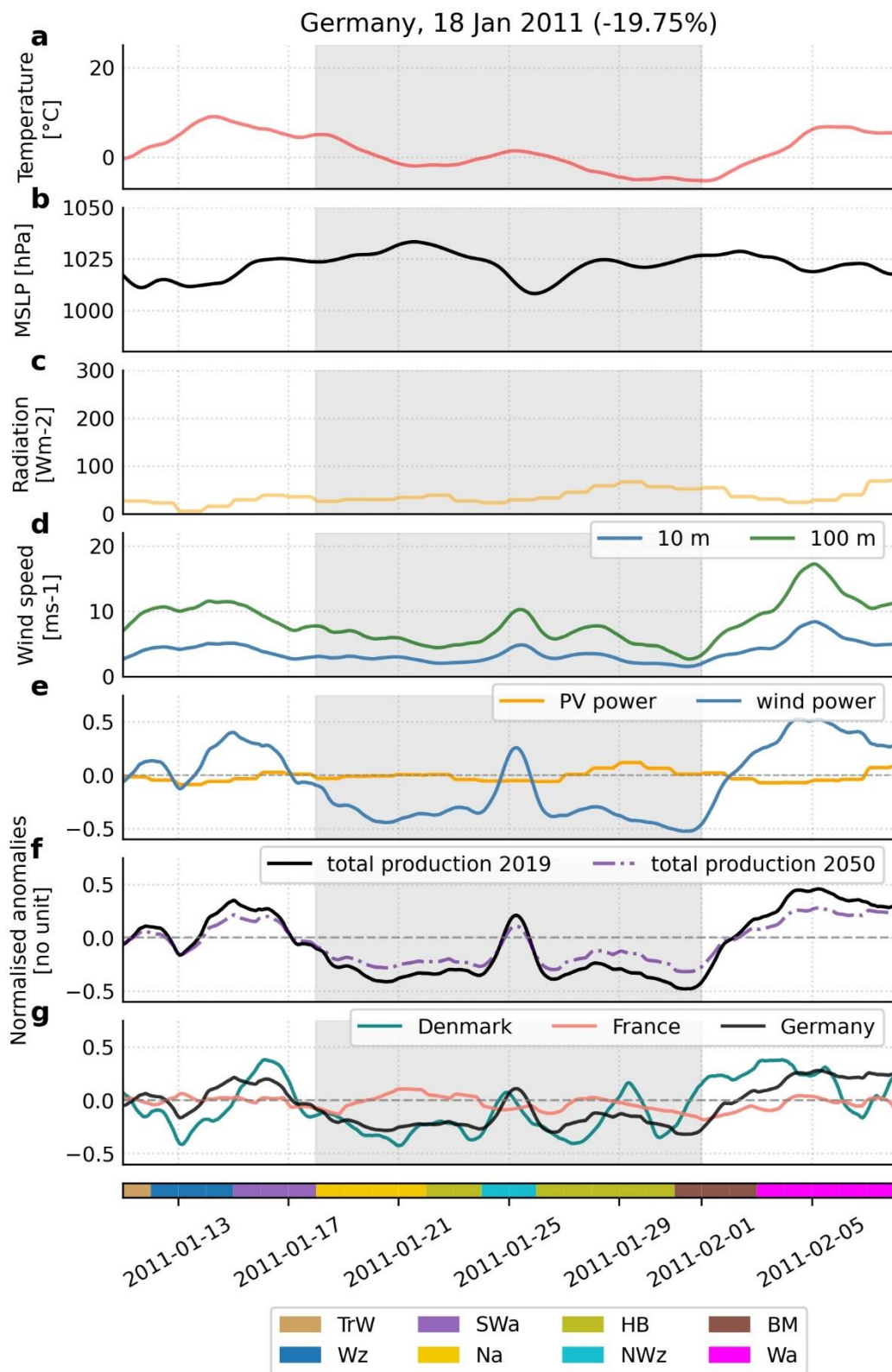


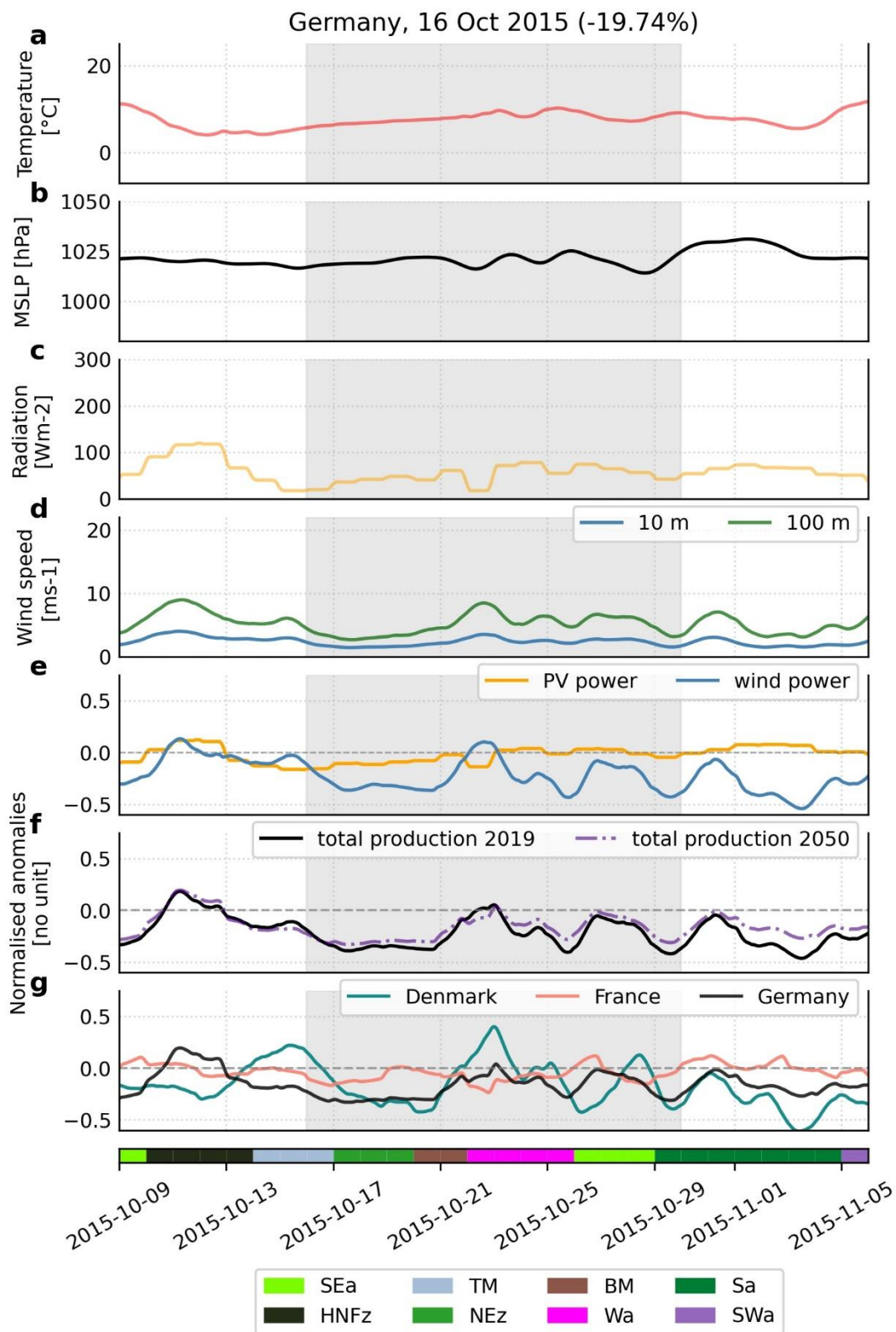


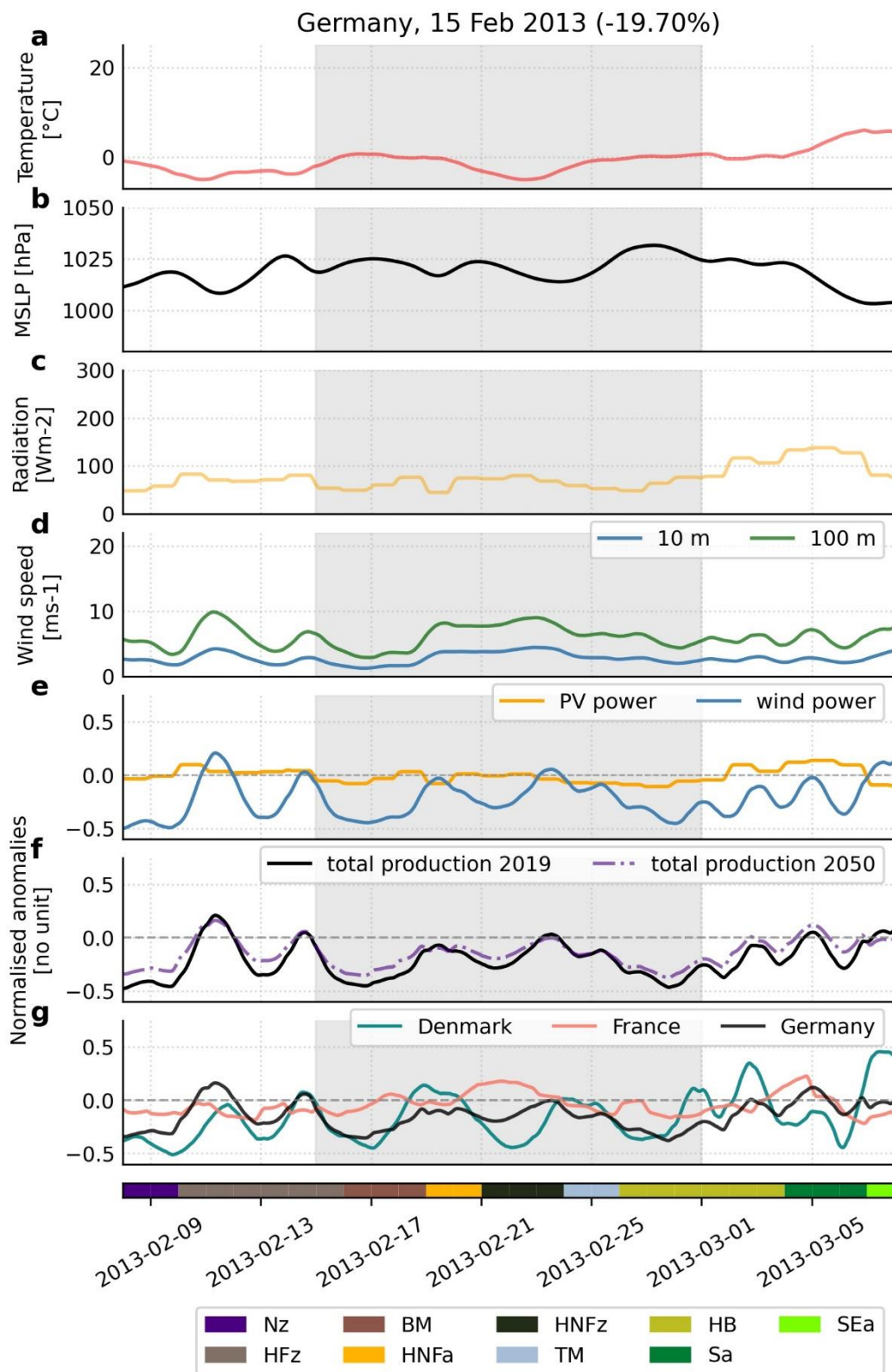


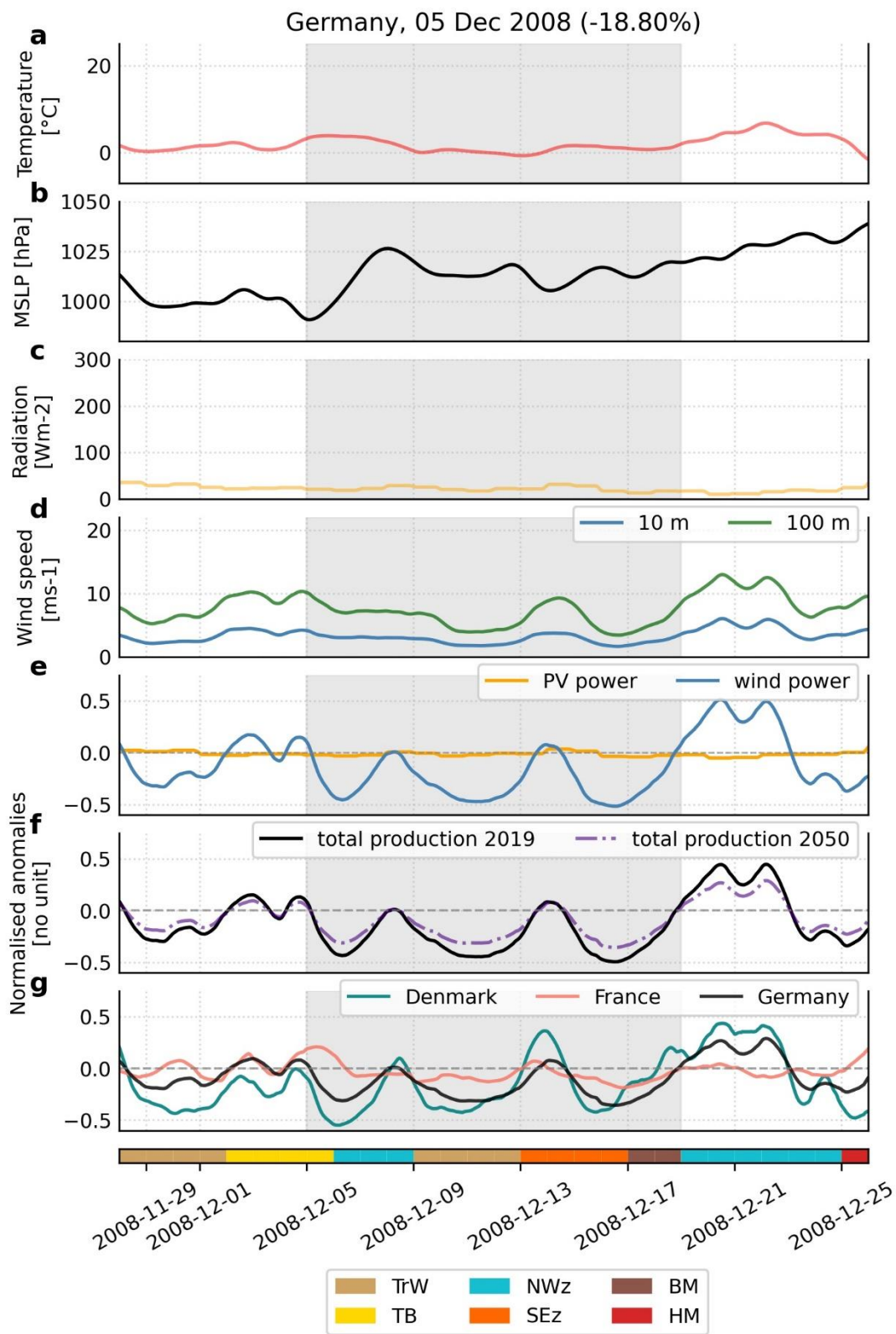












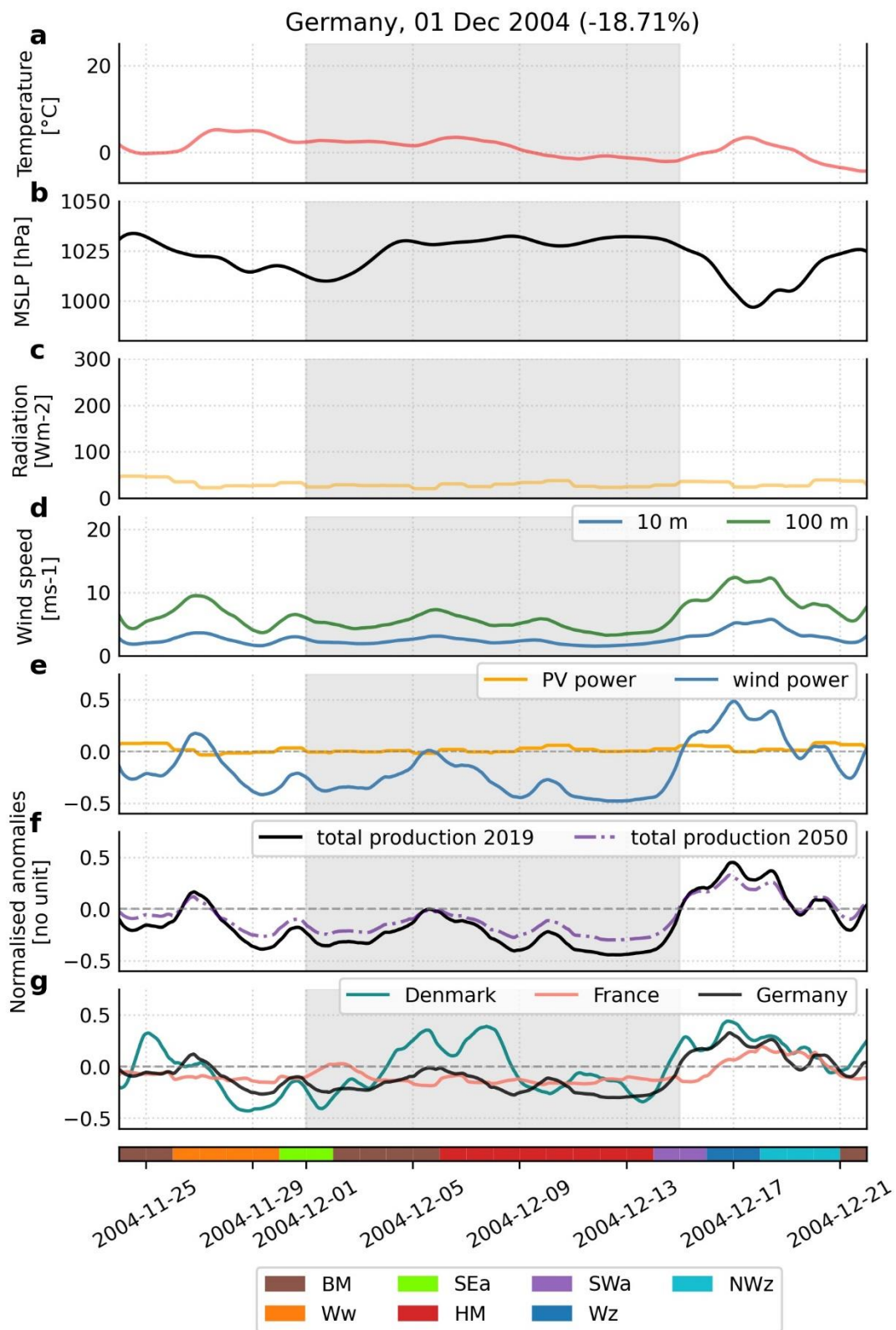
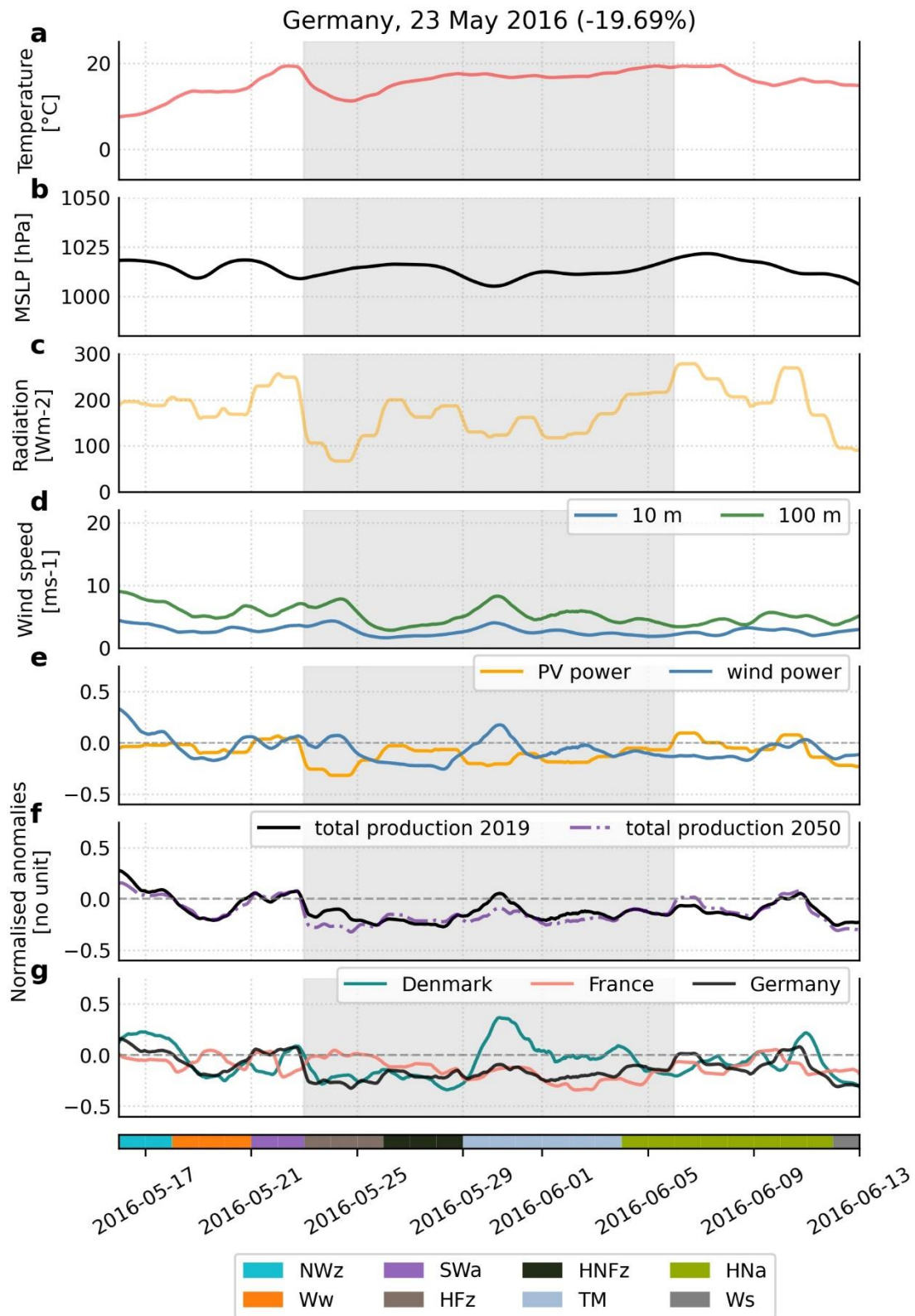
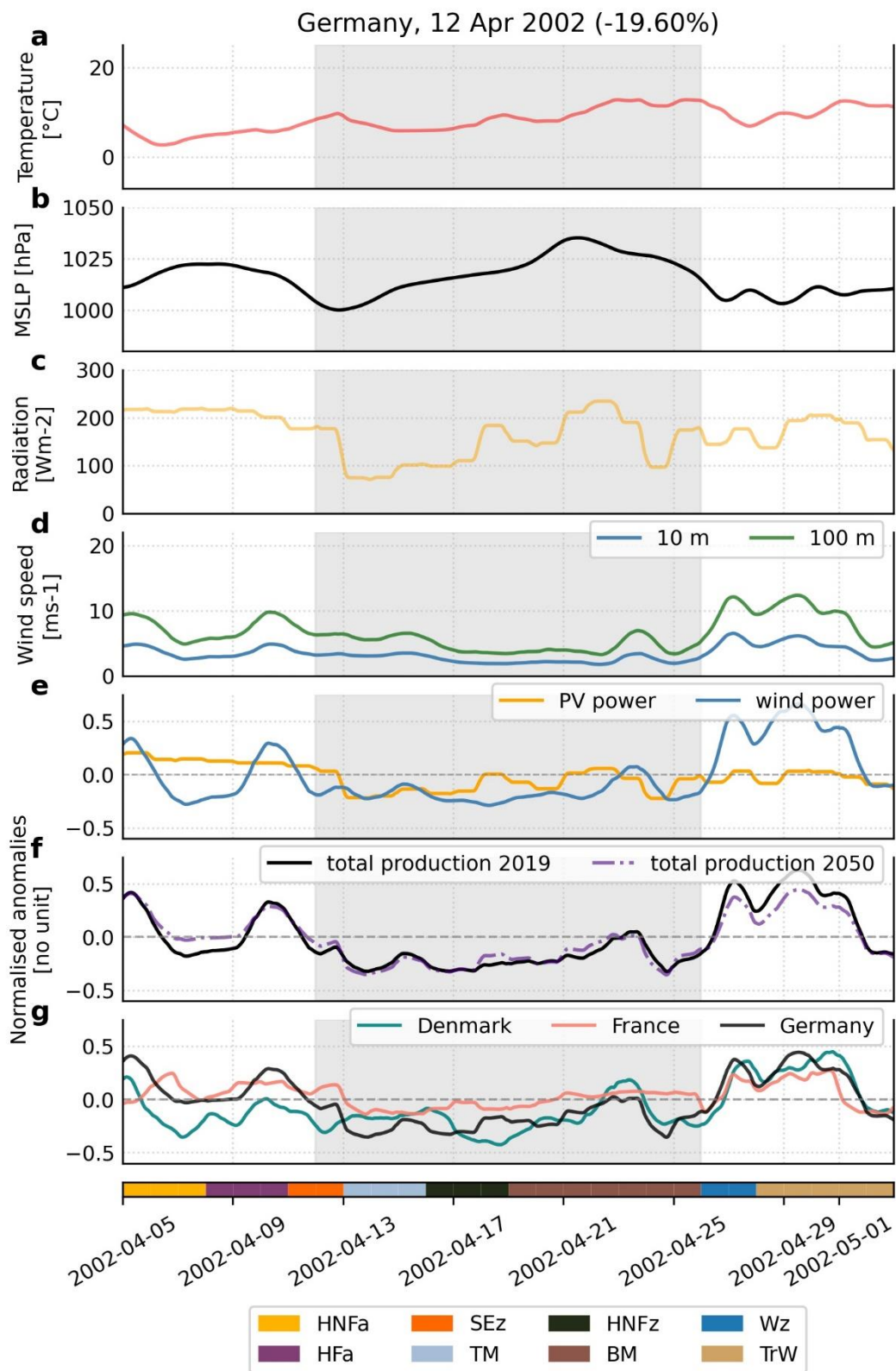
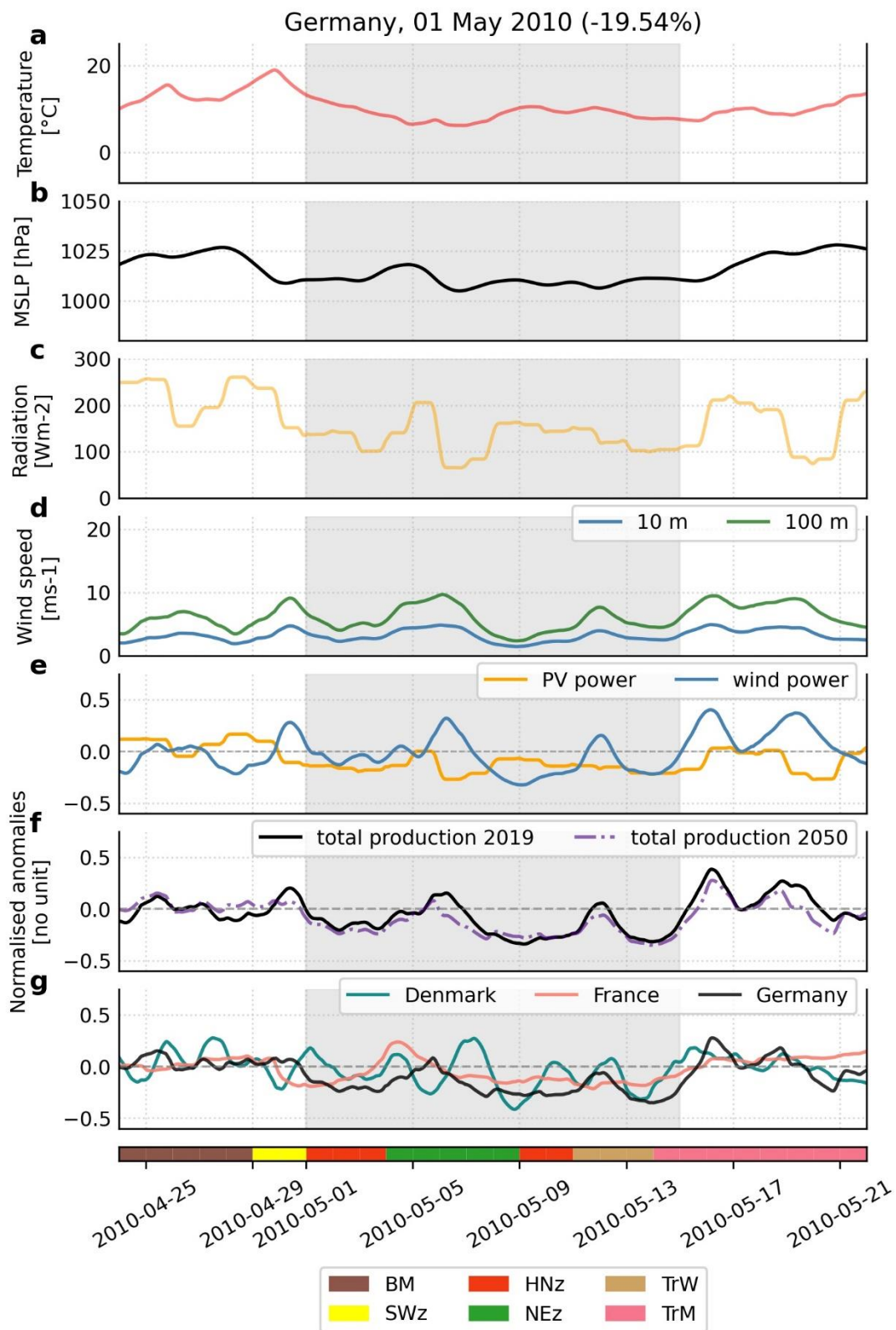
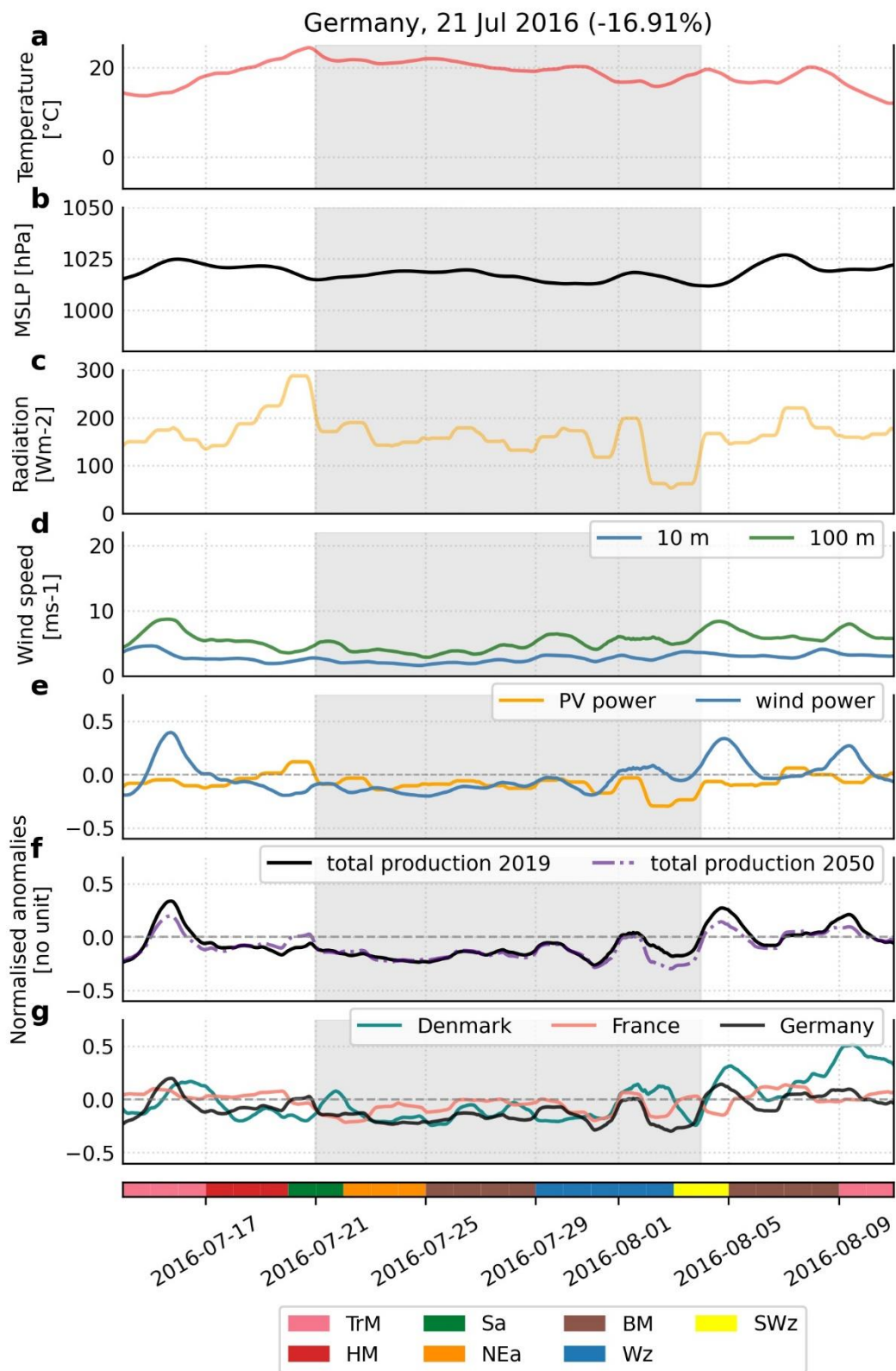


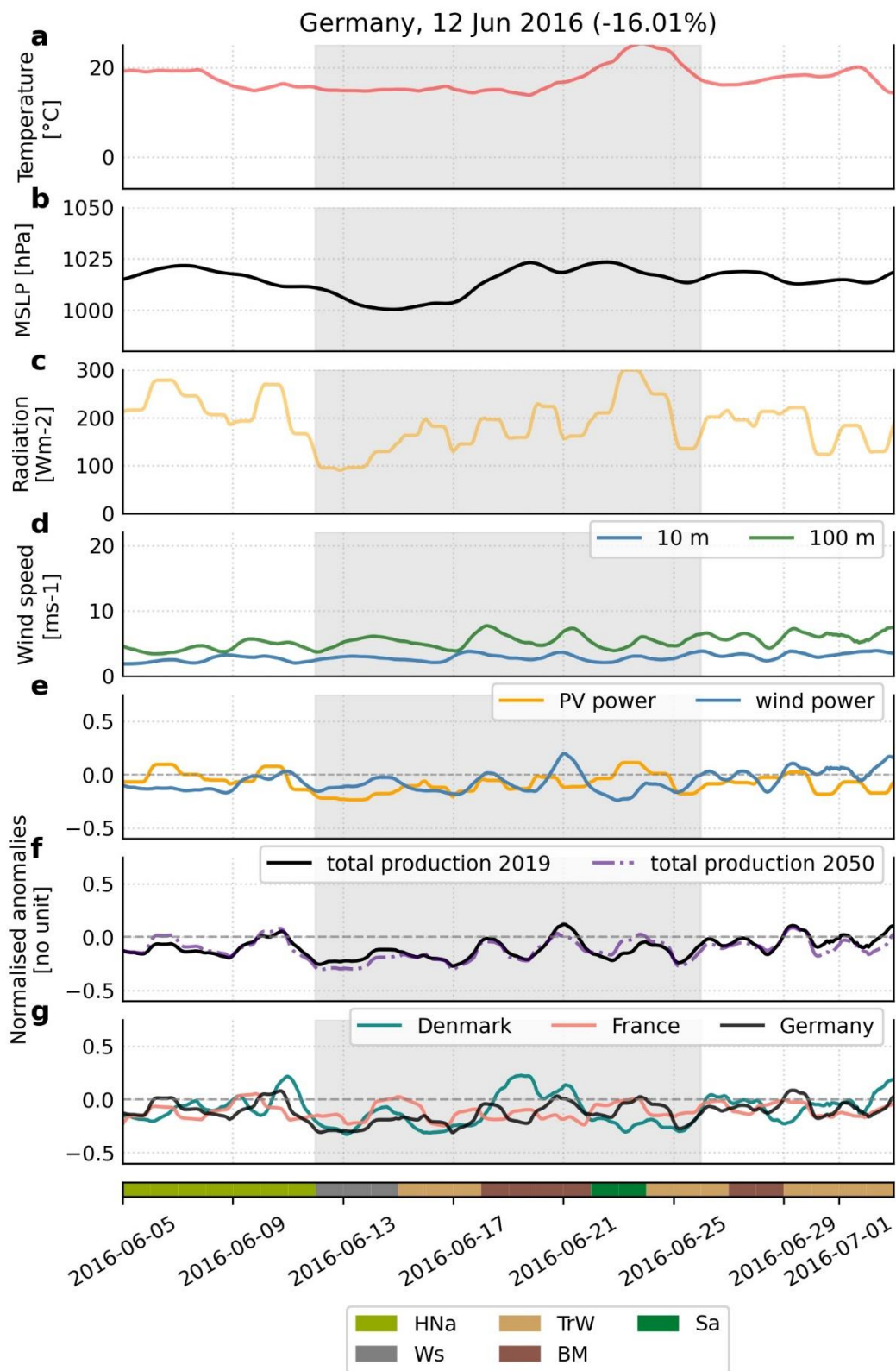
Figure S6. Similar to Fig. S6 but for ten events of 14-day low total production in summer including the event in the manuscript. Note that there are missing data on 1996-05-04 to 05.

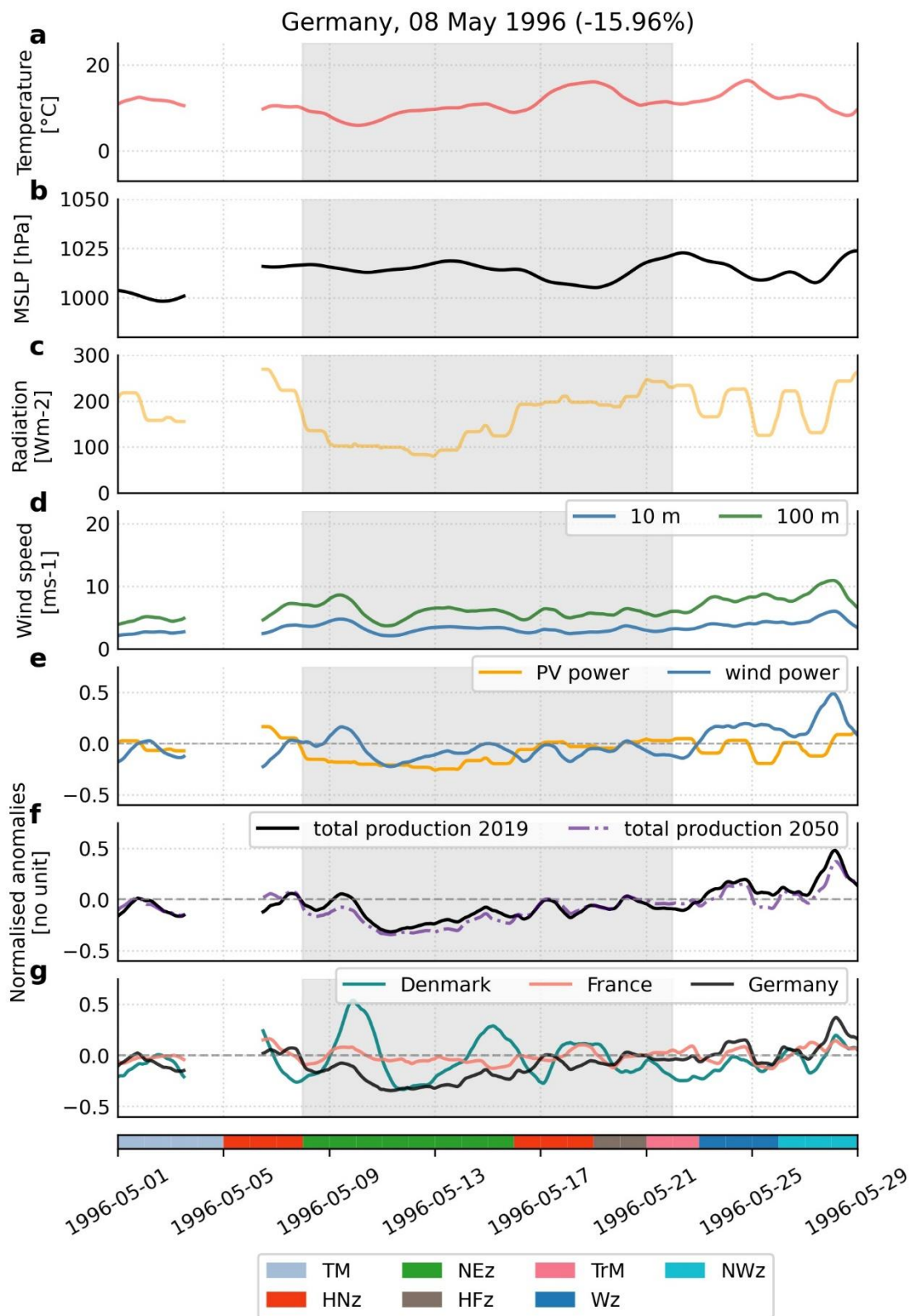


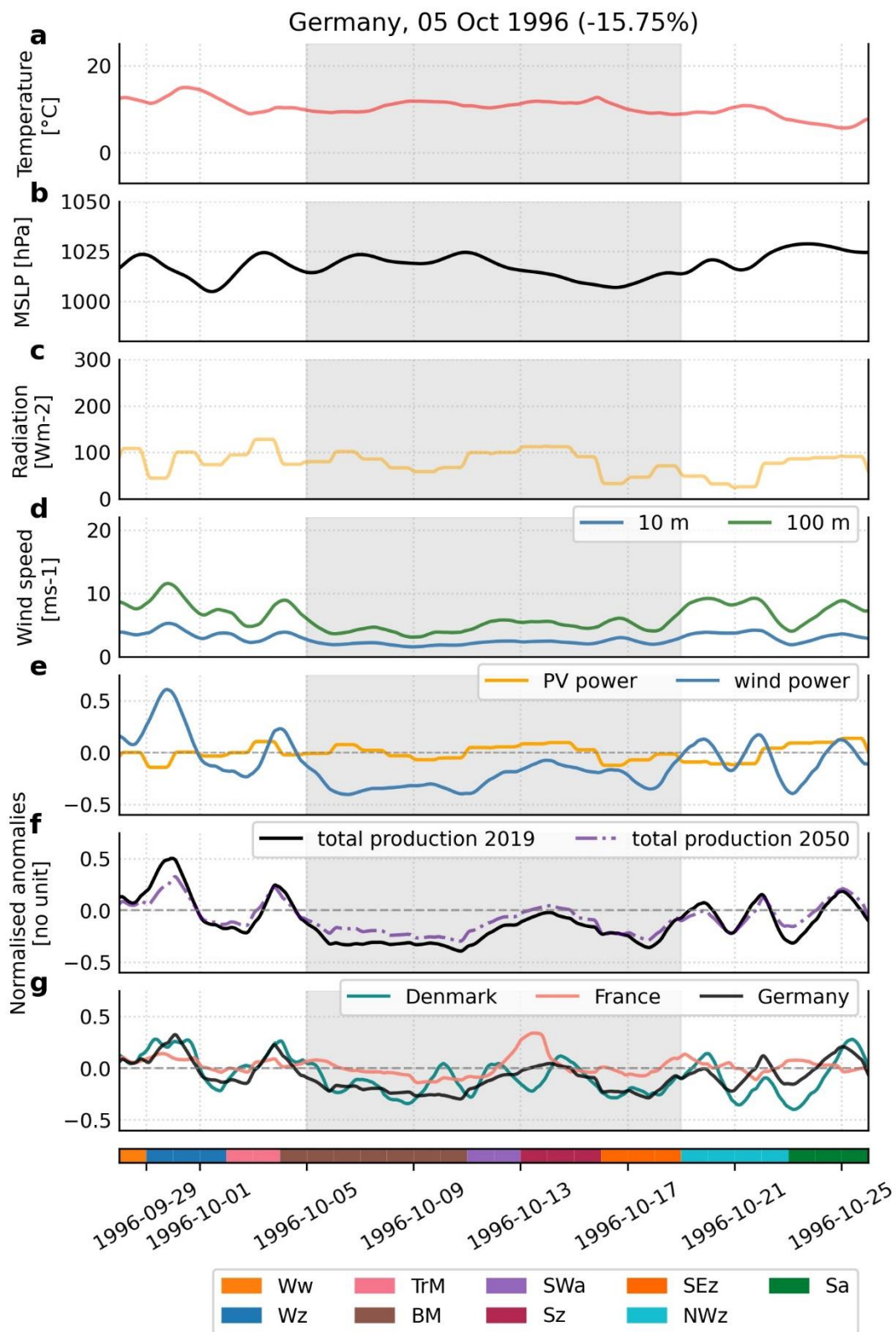


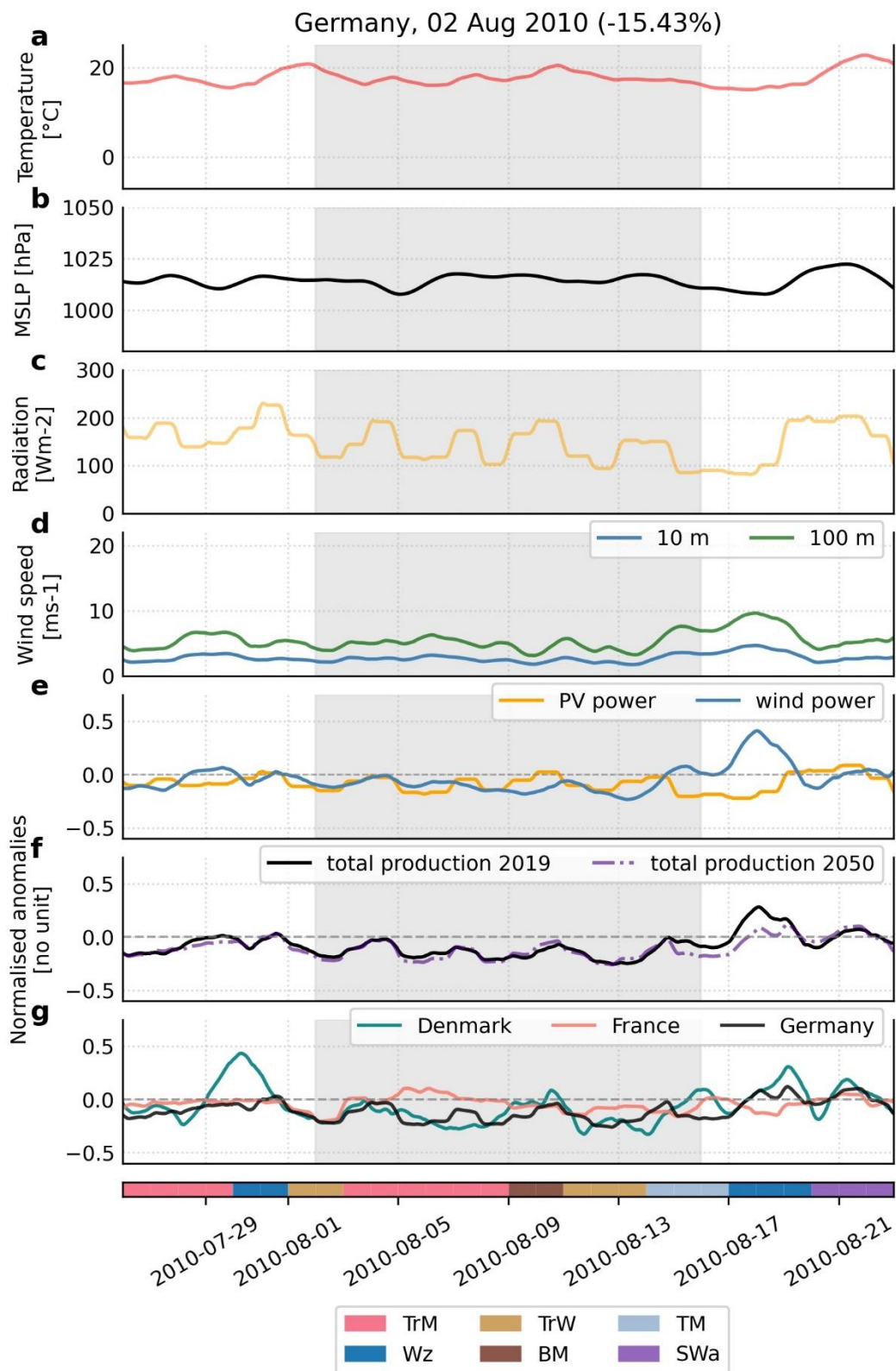


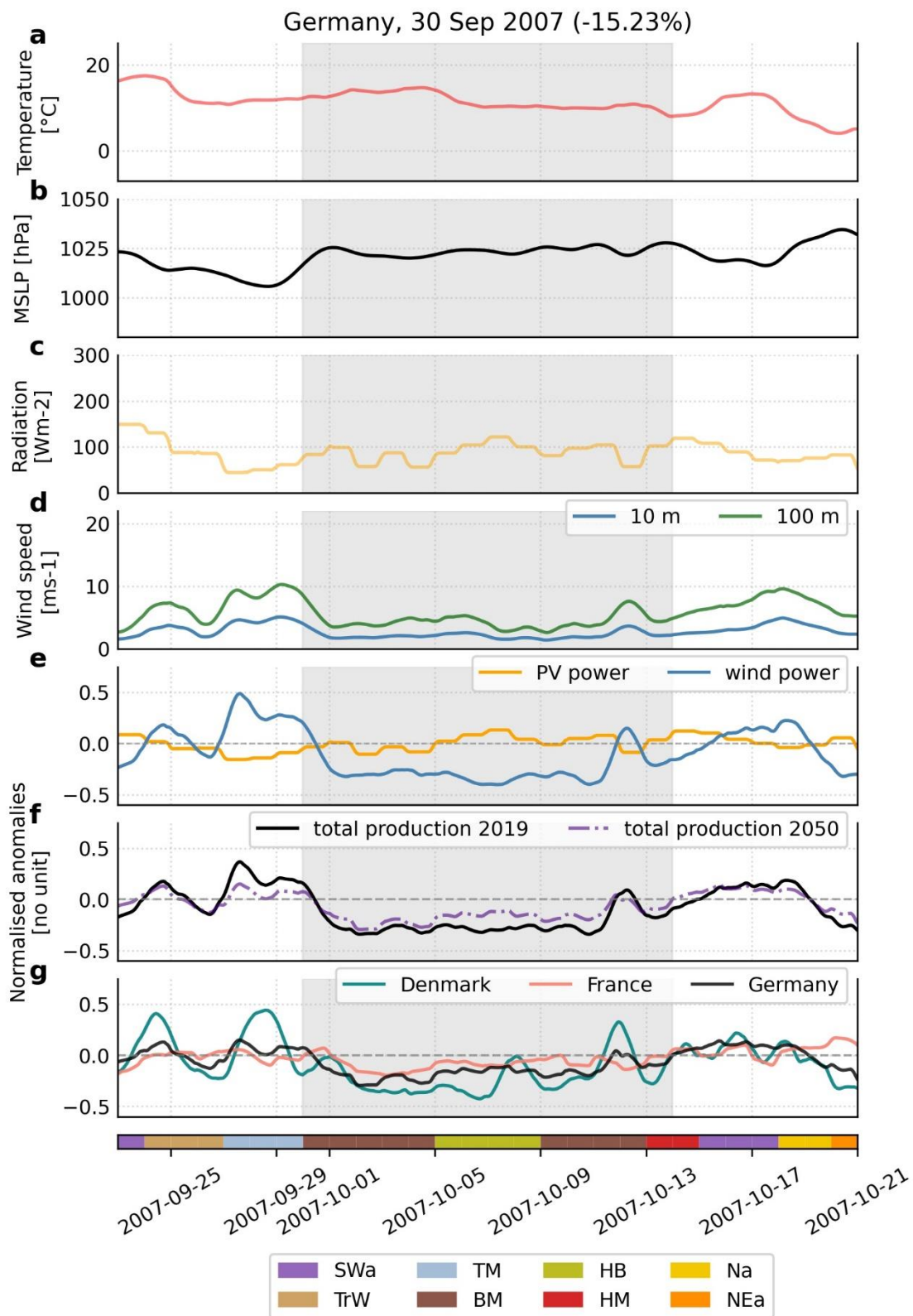












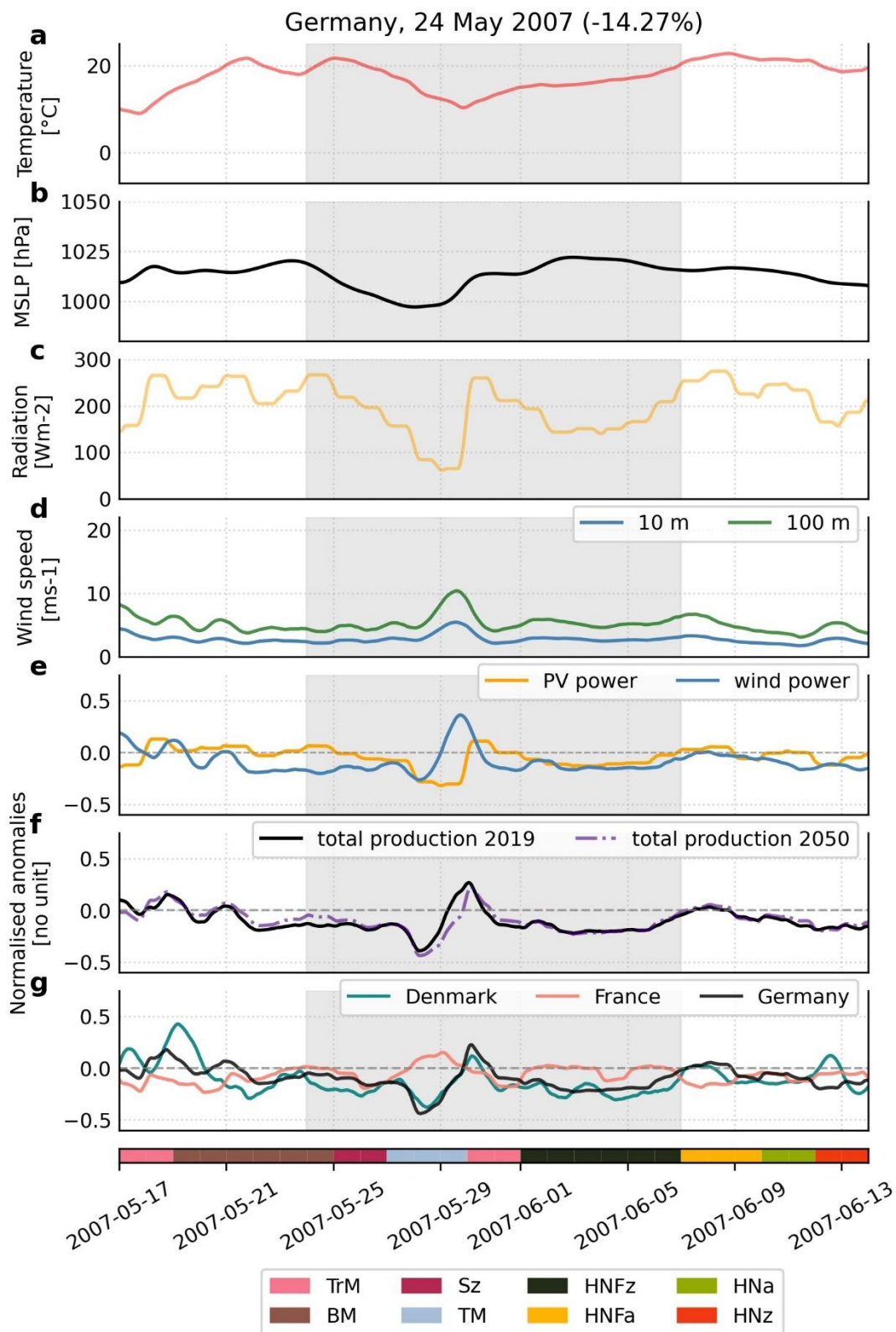
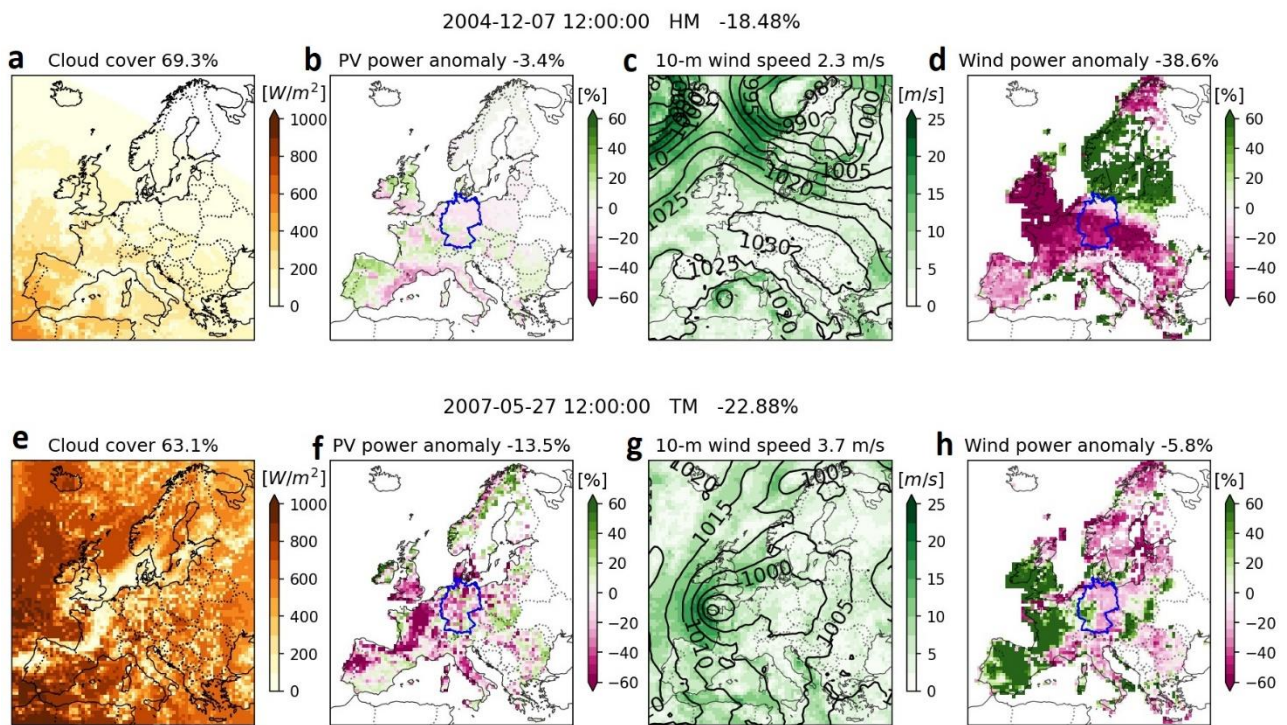


Fig. S7. Weather conditions during the event December 2004 (a--d) and May 2007 (e--h)



BIBLIOGRAPHY

- Ahmed, R., V Sreeram, Y Mishra, and M. Arif (2020). "A review and evaluation of the state-of-the-art in PV solar power forecasting: Techniques and optimization." In: *Renewable and Sustainable Energy Reviews* 124, p. 109792.
- Ahrens, C. D. (2015). *Meteorology today: an introduction to weather, climate, and the environment*. Cengage Learning Canada Inc.
- Akhtar, N., B. Geyer, B. Rockel, P. S. Sommer, and C. Schrum (2021). "Accelerating deployment of offshore wind energy alter wind climate and reduce future power generation potentials." In: *Scientific reports* 11.1, p. 11826.
- Alzahrani, A., P. Shamsi, C. Dagli, and M. Ferdowsi (2017). "Solar irradiance forecasting using deep neural networks." In: *Procedia Computer Science* 114, pp. 304–313.
- Armaroli, N. and V. Balzani (2011). "Towards an electricity-powered world." In: *Energy & Environmental Science* 4.9, pp. 3193–3222.
- Beerli, R. and C. M. Grams (2019). "Stratospheric modulation of the large-scale circulation in the Atlantic–European region and its implications for surface weather events." In: *Quarterly Journal of the Royal Meteorological Society* 145.725, pp. 3732–3750.
- Bloomfield, H. C., D. J. Brayshaw, P. L. Gonzalez, and A. Charlton-Perez (2021). "Sub-seasonal forecasts of demand and wind power and solar power generation for 28 European countries." In: *Earth System Science Data* 13.5, pp. 2259–2274.
- Bodini, N., J. K. Lundquist, and P. Moriarty (2021). "Wind plants can impact long-term local atmospheric conditions." In: *Scientific reports* 11.1, p. 22939.
- Boer, G. (2003). "Predictability as a function of scale." In: *Atmosphere-ocean* 41.3, pp. 203–215.
- Bollmeyer, C, J. Keller, C Ohlwein, S Wahl, S Crewell, P Friederichs, A Hense, J Keune, S Kneifel, I Pscheidt, et al. (2015). "Towards a high-resolution regional reanalysis for the European CORDEX domain." In: *Quarterly Journal of the Royal Meteorological Society* 141.686, pp. 1–15.
- Borsche, M, A. Kaiser-Weiss, P. Undén, and F Kaspar (2015). "Methodologies to characterize uncertainties in regional reanalyses." In: *Advances in Science and Research*. Vol. 12, pp. 207–218.
- Brayshaw, D. J., A. Troccoli, R. Fordham, and J. Methven (2011). "The impact of large scale atmospheric circulation patterns on wind

- power generation and its potential predictability: A case study over the UK." In: *Renewable Energy* 36.8, pp. 2087–2096.
- Brune, S., J. D. Keller, and S. Wahl (2021). "Evaluation of wind speed estimates in reanalyses for wind energy applications." In: *Advances in Science and Research* 18, pp. 115–126.
- Büeler, D., R. Beerli, H. Wernli, and C. M. Grams (2020). "Stratospheric influence on ECMWF sub-seasonal forecast skill for energy-industry-relevant surface weather in European countries." In: *Quarterly Journal of the Royal Meteorological Society* 146.733, pp. 3675–3694.
- Büeler, D., L. Ferranti, L. Magnusson, J. F. Quinting, and C. M. Grams (2021). "Year-round sub-seasonal forecast skill for Atlantic–European weather regimes." In: *Quarterly Journal of the Royal Meteorological Society* 147.741, pp. 4283–4309.
- Camus, C., P. Offermann, M. Weissmann, C. Buerhop, J. Hauch, and C. J. Brabec (2019). "Site-specific assessment of mechanical loads on photovoltaic modules from meteorological reanalysis data." In: *Solar Energy* 188, pp. 1134–1145.
- Cassou, C. (2008). "Intraseasonal interaction between the Madden–Julian oscillation and the North Atlantic Oscillation." In: *Nature* 455.7212, pp. 523–527.
- Changmai, P., S. Deka, S. Kumar, T. S. Babu, B. Aljafari, and B. Nastasi (2022). "A Critical Review on the Estimation Techniques of the Solar PV Cell's Unknown Parameters." In: *Energies* 15.19, p. 7212.
- Charlton-Perez, A. J., L. Ferranti, and R. W. Lee (2018). "The influence of the stratospheric state on North Atlantic weather regimes." In: *Quarterly Journal of the Royal Meteorological Society* 144.713, pp. 1140–1151.
- Connolly, D., H. Lund, B. V. Mathiesen, and M. Leahy (2010). "A review of computer tools for analysing the integration of renewable energy into various energy systems." In: *Applied energy* 87.4, pp. 1059–1082.
- Copernicus Climate Change Service (2020). *Climate and energy indicators for Europe from 1979 to present derived from reanalysis*. data retrieved from Climate Data Store (CDS), <https://cds.climate.copernicus.eu/cdsapp#!/dataset/sis-energy-derived-reanalysis?tab=form>, Accessed: 2021-06-03. DOI: 10.24381/cds.4bd77450.
- Couto, A., P. Costa, L. Rodrigues, V. V. Lopes, and A. Estanqueiro (2014). "Impact of weather regimes on the wind power ramp forecast in Portugal." In: *IEEE Transactions on Sustainable Energy* 6.3, pp. 934–942.
- Crippa, P., M. Alifa, D. Bolster, M. G. Genton, and S. Castruccio (2021). "A temporal model for vertical extrapolation of wind speed and wind energy assessment." In: *Applied Energy* 301, p. 117378.

- DWD (2022). *COSMO-REA6 Start help*. https://opendata.dwd.de/climate_environment/REA/COSMO_REA6/help_COSMO_REA6/COSMO_REA6_start_help.pdf. Accessed: 2023-02-07.
- De Vos, A. (1980). "Detailed balance limit of the efficiency of tandem solar cells." In: *Journal of Physics D: Applied Physics* 13.5, p. 839.
- Dee, D. P., S. M. Uppala, A. J. Simmons, P. Berrisford, P. Poli, S. Kobayashi, U. Andrae, M. Balmaseda, G. Balsamo, d. P. Bauer, et al. (2011). "The ERA-Interim reanalysis: Configuration and performance of the data assimilation system." In: *Quarterly Journal of the royal meteorological society* 137.656, pp. 553–597.
- Drücke, J., M. Borsche, P. James, F. Kaspar, U. Pfeifroth, B. Ahrens, and J. Trentmann (2020). "Climatological analysis of solar and wind energy in Germany using the Grosswetterlagen classification." In: *Renewable Energy*.
- Emeis, S. and S. Frandsen (1993). "Reduction of horizontal wind speed in a boundary layer with obstacles." In: *Boundary-layer meteorology* 64, pp. 297–305.
- Emeis, S. and M. Turk (2007). "Comparison of logarithmic wind profiles and power law wind profiles and their applicability for offshore wind profiles." In: *Wind Energy: Proceedings of the Euromech Colloquium*. Springer, pp. 61–64.
- Energiewirtschaftliches Institut an der Universität zu Köln (2021). *dena pilot study "Towards climate neutrality". Climate neutrality 2045 - Transformation of final energy consumption and the energy system*. Published by the German Energy Agency GmbH (dena).
- Engeland, K., M. Borga, J.-D. Creutin, B. François, M.-H. Ramos, and J.-P. Vidal (2017). "Space-time variability of climate variables and intermittent renewable electricity production—A review." In: *Renewable and Sustainable Energy Reviews* 79, pp. 600–617.
- European Commission, Joint Research Centre (JRC) (2020). *Global Energy and Climate Outlook 2020: Energy, Greenhouse gas and Air pollutant emissions balances*. Dataset <https://data.jrc.ec.europa.eu/dataset/1750427d-afd9-4a10-8c54-440e764499e4>. Accessed: 2022-04-24.
- European Commission (2021). *European green deal : delivering on our targets*. Directorate-General for Communication, <https://data.europa.eu/doi/10.2775/373022>, Accessed: 2023-03-21. Publications Office of the European Union.
- European Commission, S. (2018). *Statement/18/4155, "Europe leads the global clean energy transition: Commission welcomes ambitious agreement on further renewable energy development in the EU"*. https://ec.europa.eu/commission/presscorner/detail/en/STATEMENT_18_4155. Accessed: 2020-03-23.

- Eurostat (2022). *Renewable energy on the rise: 37% of EU's electricity*. <https://ec.europa.eu/eurostat/web/products-eurostat-news/-/ddn-20220126-1>. Accessed: 2023-02-02.
- Fabiano, F., V. L. Meccia, P. Davini, P. Ghinassi, and S. Corti (2021). "A regime view of future atmospheric circulation changes in northern mid-latitudes." In: *Weather and Climate Dynamics* 2.1, pp. 163–180.
- Faiman, D. (2008). "Assessing the outdoor operating temperature of photovoltaic modules." In: *Progress in Photovoltaics: Research and Applications* 16.4, pp. 307–315.
- Ferranti, L, L Magnusson, F Vitart, and D Richardson (2019). "A new product to flag up the risk of cold spells in Europe weeks ahead." In: *ECMWF Newsletter* 158, pp. 15–20.
- Fischereit, J., R. Brown, X. G. Larsén, J. Badger, and G. Hawkes (2022). "Review of mesoscale wind-farm parametrizations and their applications." In: *Boundary-Layer Meteorology* 182.2, pp. 175–224.
- Frank, C. W., B. Pospichal, S. Wahl, J. D. Keller, A. Hense, and S. Crewell (2020a). "The added value of high resolution regional reanalyses for wind power applications." In: *Renewable Energy* 148, pp. 1094–1109.
- Frank, C. W., S. Wahl, J. D. Keller, B. Pospichal, A. Hense, and S. Crewell (2018). "Bias correction of a novel European reanalysis data set for solar energy applications." In: *Solar Energy* 164, pp. 12–24.
- Frank, C. W. (2019). "The potential of high resolution regional reanalyses COSMO-REA for renewable energy applications." PhD thesis. University of Cologne, Germany.
- Frank, C., S. Fiedler, and S. Crewell (2020b). "Balancing potential of natural variability and extremes in photovoltaic and wind energy production for European countries." In: *Renewable Energy* 163, pp. 674–684.
- Friesen, G, R Gottschalg, H. Beyer, S. Williams, W. van Sark, A Guérin de Montgareuil, N Van Der Borg, T Huld, B Müller, A. De Keizer, et al. (2007). "Intercomparison of different energy prediction methods within the European project" performance"-results of the 1st round robin." In: *22nd European Photovoltaic Solar Energy Conference*. WIP-Renewable Energies, pp. 2659–2663.
- Gallego-Castillo, C., A. Cuerva-Tejero, and O. Lopez-Garcia (2015). "A review on the recent history of wind power ramp forecasting." In: *Renewable and Sustainable Energy Reviews* 52, pp. 1148–1157.
- Garud, K. S., S. Jayaraj, and M.-Y. Lee (2021). "A review on modeling of solar photovoltaic systems using artificial neural networks, fuzzy logic, genetic algorithm and hybrid models." In: *International Journal of Energy Research* 45.1, pp. 6–35.

- Gelaro, R., W. McCarty, M. J. Suárez, R. Todling, A. Molod, L. Takacs, C. A. Randles, A. Darmenov, M. G. Bosilovich, R. Reichle, et al. (2017). "The modern-era retrospective analysis for research and applications, version 2 (MERRA-2)." In: *Journal of climate* 30.14, pp. 5419–5454.
- Ghigo, A., L. Cottura, R. Caradonna, G. Bracco, and G. Mattiazzo (2020). "Platform optimization and cost analysis in a floating offshore wind farm." In: *Journal of Marine Science and Engineering* 8.11, p. 835.
- Gibson, P. B. and N. J. Cullen (2015). "Synoptic and sub-synoptic circulation effects on wind resource variability—A case study from a coastal terrain setting in New Zealand." In: *Renewable Energy* 78, pp. 253–263.
- Giorgi, F., C. Jones, G. R. Asrar, et al. (2009). "Addressing climate information needs at the regional level: the CORDEX framework." In: *World Meteorological Organization (WMO) Bulletin* 58.3, p. 175.
- Global Modeling And Assimilation Office, and Pawson, S. (2015). *MERRA-2 avg_{12d} and dx : 2d, 1 – Hourly, Time – Averaged, Single – Level, Assimilation, RadiationDiagnosticsV5.12.4[Dataset]*. DOI: 10.5067/Q9QMY5PBNV1T. Accessed: 2023-08-07.
- González-Longatt, F., P. Wall, and V. Terzija (2012). "Wake effect in wind farm performance: Steady-state and dynamic behavior." In: *Renewable Energy* 39.1, pp. 329–338.
- Graham, R. M., J. Browell, D. Bertram, and C. J. White (2022). "The application of sub-seasonal to seasonal (S2S) predictions for hydropower forecasting." In: *Meteorological Applications* 29.1, e2047.
- Grams, C., L. Ferranti, and L. Magnusson (2020). "How to make use of weather regimes in extended-range predictions for Europe." In: *ECMWF Newsletter* 165, pp. 14–19.
- Grams, C. M., R. Beerli, S. Pfenniger, I. Staffell, and H. Wernli (2017). "Balancing Europe's wind-power output through spatial deployment informed by weather regimes." In: *Nature climate change* 7.8, pp. 557–562.
- Gualtieri, G. (2019). "A comprehensive review on wind resource extrapolation models applied in wind energy." In: *Renewable and Sustainable Energy Reviews* 102, pp. 215–233.
- Henckes, P., C. Frank, N. Küchler, J. Peter, and J. Wagner (2020). "Uncertainty estimation of investment planning models under high shares of renewables using reanalysis data." In: *Energy* 208, p. 118207.
- Henckes, P., A. Knaut, F. Obermüller, and C. Frank (2018). "The benefit of long-term high resolution wind data for electricity system analysis." In: *Energy* 143, pp. 934–942.
- Herceg-Bulić, I., B. Mezzina, F. Kucharski, P. Ruggieri, and M. P. King (2017). "Wintertime ENSO influence on late spring European cli-

- mate: the stratospheric response and the role of North Atlantic SST." In: *International Journal of Climatology* 37, pp. 87–108.
- Hersbach, H. et al. (2023). *ERA5 hourly data on single levels from 1940 to present*. DOI: 10.24381/cds.adbb2d47. Accessed: 2023-08-07.
- Hersbach, H., B. Bell, P. Berrisford, S. Hirahara, A. Horányi, J. Muñoz-Sabater, J. Nicolas, C. Peubey, R. Radu, D. Schepers, et al. (2020). "The ERA5 global reanalysis." In: *Quarterly Journal of the Royal Meteorological Society* 146.730, pp. 1999–2049.
- Hess, P. and H. Brezowsky (1969). "Katalog der grosswetterlagen Europas." In.
- Honrubia, A, A Vingueras-Rodriguez, E. G. Lazaro, D Rodriguez, M Mejias, and I Lainez (2010). "The influence of wind shear in wind turbine power estimation." In: *measurements* 2, p. 9.
- Huang, W. T. K., A. Charlton-Perez, R. W. Lee, R. Neal, C. Sarran, and T. Sun (2020). "Weather regimes and patterns associated with temperature-related excess mortality in the UK: a pathway to sub-seasonal risk forecasting." In: *Environmental Research Letters* 15.12, p. 124052.
- Huber, M., D. Dimkova, and T. Hamacher (2014). "Integration of wind and solar power in Europe: Assessment of flexibility requirements." In: *Energy* 69, pp. 236–246.
- Huld, T., G. Friesen, A. Skoczek, R. P. Kenny, T. Sample, M. Field, and E. D. Dunlop (2011). "A power-rating model for crystalline silicon PV modules." In: *Solar Energy Materials and Solar Cells* 95.12, pp. 3359–3369.
- Huld, T., R. Müller, and A. Gambardella (2012). "A new solar radiation database for estimating PV performance in Europe and Africa." In: *Solar Energy* 86.6, pp. 1803–1815.
- Husein, M. and I.-Y. Chung (2019). "Day-ahead solar irradiance forecasting for microgrids using a long short-term memory recurrent neural network: A deep learning approach." In: *Energies* 12.10, p. 1856.
- IRENA (2021). *Renewable Power Generation Costs in 2020*. <https://www.irena.org/publications/2021/Jun/Renewable-Power-Costs-in-2020>, Accessed: 2023-03-21. International Renewable Energy Agency.
- International Energy Agency (2019). *Offshore Wind Outlook 2019 - World Energy Outlook special report*. version for public consultation, <https://www.iea.org/reports/offshore-wind-outlook-2019>, Accessed: 2023-03-17. International Energy Agency.
- James, P. (2007). "An objective classification method for Hess and Brezowsky Grosswetterlagen over Europe." In: *Theoretical and Applied Climatology* 88.1-2, pp. 17–42.
- Jebaraj, S. and S Iniyan (2006). "A review of energy models." In: *Renewable and sustainable energy reviews* 10.4, pp. 281–311.

- Jerez, S., I. Tobin, M. Turco, P. Jiménez-Guerrero, R. Vautard, and J. Montávez (2019). "Future changes, or lack thereof, in the temporal variability of the combined wind-plus-solar power production in Europe." In: *Renewable energy* 139, pp. 251–260.
- Jerez, S., F. Thais, I. Tobin, M. Wild, A. Colette, P. Yiou, and R. Vautard (2015a). "The CLIMIX model: a tool to create and evaluate spatially-resolved scenarios of photovoltaic and wind power development." In: *Renewable and sustainable energy reviews* 42, pp. 1–15.
- Jerez, S., I. Tobin, R. Vautard, J. P. Montávez, J. M. López-Romero, F. Thais, B. Bartok, O. B. Christensen, A. Colette, M. Déqué, et al. (2015b). "The impact of climate change on photovoltaic power generation in Europe." In: *Nature communications* 6.1, pp. 1–8.
- Jones, P., T. Osborn, C. Harpham, and K. R. Briffa (2014). "The development of Lamb weather types: from subjective analysis of weather charts to objective approaches using reanalyses." In: *Weather* 69.5, pp. 128–132.
- Kenny, D. and S. Fiedler (2022). "Which gridded irradiance data is best for modelling photovoltaic power production in Germany?" In: *Solar Energy* 232, pp. 444–458.
- Kenny, R. P., G. Friesen, D. Chianese, A. Bernasconi, and E. D. Dunlop (2003). "Energy rating of PV modules: comparison of methods and approach." In: *3rd World Conference on Photovoltaic Energy Conversion, 2003. Proceedings of*. Vol. 2. IEEE, pp. 2015–2018.
- Khatib, T., A. Mohamed, and K. Sopian (2012). "A review of solar energy modeling techniques." In: *Renewable and Sustainable Energy Reviews* 16.5, pp. 2864–2869.
- Klucher, T. M. (1979). "Evaluation of models to predict insolation on tilted surfaces." In: *Solar energy* 23.2, pp. 111–114.
- Koehl, M., M. Heck, S. Wiesmeier, and J. Wirth (2011). "Modeling of the nominal operating cell temperature based on outdoor weathering." In: *Solar Energy Materials and Solar Cells* 95.7, pp. 1638–1646.
- Kreuwel, F. P., W. H. Knap, L. R. Visser, W. G. van Sark, J. V.-G. de Arellano, and C. C. van Heerwaarden (2020). "Analysis of high frequency photovoltaic solar energy fluctuations." In: *Solar Energy* 206, pp. 381–389.
- Kumar, D. S., G. M. Yagli, M. Kashyap, and D. Srinivasan (2020). "Solar irradiance resource and forecasting: a comprehensive review." In: *IET Renewable Power Generation* 14.10, pp. 1641–1656.
- Kumary, S. S., V. A. A. M. T. Oo, G. Shafiullah, and A. Stojcevski (2014). "Modelling and power quality analysis of a grid-connected solar PV system." In: pp. 1–6.

- Laha, P. and B. Chakraborty (2017). "Energy model—A tool for preventing energy dysfunction." In: *Renewable and Sustainable Energy Reviews* 73, pp. 95–114.
- Lamb, H. H. (1972). "British Isles weather types and a register of the daily sequence of circulation patterns 1861–1971." In: *Geophysical Memoirs*.
- Li, M., Y. Yao, I. Simmonds, D. Luo, L. Zhong, and X. Chen (2020). "Collaborative impact of the NAO and atmospheric blocking on European heatwaves, with a focus on the hot summer of 2018." In: *Environmental Research Letters* 15.11, p. 114003.
- Lindsay, N, Q. Libois, J. Badosa, A. Migan-Dubois, and V. Bourdin (2020). "Errors in PV power modelling due to the lack of spectral and angular details of solar irradiance inputs." In: *Solar Energy* 197, pp. 266–278.
- Lundquist, J. and L Bariteau (2015). "Dissipation of Turbulence in the Wake of a Wind Turbine." In: *Boundary-Layer Meteorology* 154.2, pp. 229–241.
- Lundquist, J. K., K. K. DuVivier, D. Kaffine, and J. M. Tomaszewski (2019). "Costs and consequences of wind turbine wake effects arising from uncoordinated wind energy development." In: *Nature Energy* 4.1, pp. 26–34.
- Lydia, M, S. S. Kumar, A. I. Selvakumar, and G. E. P. Kumar (2014). "A comprehensive review on wind turbine power curve modeling techniques." In: *Renewable and Sustainable Energy Reviews* 30, pp. 452–460.
- Maimó-Far, A., V. Homar, A. Tantet, and P. Drobinski (2022). "The effect of spatial granularity on optimal renewable energy portfolios in an integrated climate-energy assessment model." In: *Sustainable Energy Technologies and Assessments* 54, p. 102827.
- Martin, N and J. Ruiz (2001). "Calculation of the PV modules angular losses under field conditions by means of an analytical model." In: *Solar energy materials and solar cells* 70.1, pp. 25–38.
- Matsueda, M. and T. Palmer (2018). "Estimates of flow-dependent predictability of wintertime Euro-Atlantic weather regimes in medium-range forecasts." In: *Quarterly Journal of the Royal Meteorological Society* 144.713, pp. 1012–1027.
- Michelangeli, P.-A., R. Vautard, and B. Legras (1995). "Weather regimes: Recurrence and quasi stationarity." In: *Journal of the atmospheric sciences* 52.8, pp. 1237–1256.
- Müller, R., U. Pfeifroth, C. Träger-Chatterjee, R. Cremer, J. Trentmann, and R. Hollmann (2015). "Surface Solar Radiation Data Set - Heliosat (SARAH) - Edition 1." In: *Satellite Application Facility on Climate Monitoring*.

- Navon, I. M. (2009). "Data assimilation for numerical weather prediction: a review." In: *Data assimilation for atmospheric, oceanic and hydrologic applications*, pp. 21–65.
- Neal, R., D. Fereday, R. Crocker, and R. E. Comer (2016). "A flexible approach to defining weather patterns and their application in weather forecasting over Europe." In: *Meteorological Applications* 23.3, pp. 389–400.
- Niermann, D., M. Borsche, A. K. Kaiser-Weiss, and F. Kaspar (2019). "Evaluating renewable-energy-relevant parameters of COSMO-REA6 by comparison with satellite data, station observations and other reanalyses." In: *Meteorologische Zeitschrift*, pp. 347–360.
- Oehrlein, J., G. Chiodo, and L. M. Polvani (2019). "Separating and quantifying the distinct impacts of El Niño and sudden stratospheric warmings on North Atlantic and Eurasian wintertime climate." In: *Atmospheric Science Letters* 20.7, e923.
- Ohba, M., S. Kadokura, and D. Nohara (2016). "Impacts of synoptic circulation patterns on wind power ramp events in East Japan." In: *Renewable energy* 96, pp. 591–602.
- Perveen, G., M. Rizwan, and N. Goel (2019). "Comparison of intelligent modelling techniques for forecasting solar energy and its application in solar PV based energy system." In: *IET Energy Systems Integration* 1.1, pp. 34–51.
- Pfenninger, S., A. Hawkes, and J. Keirstead (2014). "Energy systems modeling for twenty-first century energy challenges." In: *Renewable and Sustainable Energy Reviews* 33, pp. 74–86.
- Pfenninger, S. and I. Staffell (2016). "Long-term patterns of European PV output using 30 years of validated hourly reanalysis and satellite data." In: *Energy* 114, pp. 1251–1265.
- Quaschnig, V. (1998). "Regenerative Energiesysteme." In: *München: Hanser-Verlag*.
- Reindl, T., W. Walsh, Z. Yanqin, and M. Bieri (2017). "Energy meteorology for accurate forecasting of PV power output on different time horizons." In: *Energy Procedia* 130, pp. 130–138.
- Rex, D. F. (1951). "The effect of Atlantic blocking action upon European climate." In: *Tellus* 3.2, pp. 100–112.
- Rodriguez, R. A., S. Becker, G. B. Andresen, D. Heide, and M. Greiner (2014). "Transmission needs across a fully renewable European power system." In: *Renewable Energy* 63, pp. 467–476.
- Rohrer, M., O. Martius, C. Raible, and S. Brönnimann (2019). "Sensitivity of blocks and cyclones in ERA5 to spatial resolution and definition." In: *Geophysical Research Letters*, e2019GL085582.
- Rühle, S. (2016). "Tabulated values of the Shockley–Queisser limit for single junction solar cells." In: *Solar energy* 130, pp. 139–147.
- Saint-Drenan, Y.-M., L. Wald, T. Ranchin, L. Dubus, and A. Troccoli (2018). "An approach for the estimation of the aggregated photo-

- voltaic power generated in several European countries from meteorological data." In: *Advances in Science and Research* 15, pp. 51–62.
- Sasse, J.-P. and E. Trutnevyte (2019). "Distributional trade-offs between regionally equitable and cost-efficient allocation of renewable electricity generation." In: *Applied Energy* 254, p. 113724.
- Schlachtberger, D. P., T. Brown, M. Schäfer, S. Schramm, and M. Greiner (2018). "Cost optimal scenarios of a future highly renewable European electricity system: Exploring the influence of weather data, cost parameters and policy constraints." In: *Energy* 163, pp. 100–114.
- Schraff, C. H. (1997). "Mesoscale data assimilation and prediction of low stratus in the Alpine region." In: *Meteorology and Atmospheric Physics* 64.1, pp. 21–50.
- Sen, Z. (2008). *Solar energy fundamentals and modeling techniques: atmosphere, environment, climate change and renewable energy*. Springer Science & Business Media.
- Staffell, I. and S. Pfenninger (2016). "Using bias-corrected reanalysis to simulate current and future wind power output." In: *Energy* 114, pp. 1224–1239.
- Steinheuer, J. and P. Friederichs (2019). "Vertical profiles of wind gust statistics from a regional reanalysis using multivariate extreme value theory." In: *Nonlinear Processes in Geophysics Discussions*, pp. 1–29.
- The European Commission (2020). *Stepping up Europe's 2030 climate ambition - Investing in a climate-neutral future for the benefit of our people. Communication from the commission to the European Parliament, the council, the European economic and social committee and the committee of the regions*. <https://eur-lex.europa.eu/legal-content/EN/TXT/?uri=CELEX:52020DC0562>.
- Tobin, I., W. Greuell, S. Jerez, F. Ludwig, R. Vautard, M. Van Vliet, and F. Breón (2018). "Vulnerabilities and resilience of European power generation to 1.5 C, 2 C and 3 C warming." In: *Environmental Research Letters* 13.4, p. 044024.
- Tobin, I., S. Jerez, R. Vautard, F. Thais, E. Van Meijgaard, A. Prein, M. Déqué, S. Kotlarski, C. F. Maule, G. Nikulin, et al. (2016). "Climate change impacts on the power generation potential of a European mid-century wind farms scenario." In: *Environmental Research Letters* 11.3, p. 034013.
- Uppala, S. M., P. Källberg, A. J. Simmons, U. Andrae, V. D. C. Bechtold, M. Fiorino, J. Gibson, J. Haseler, A. Hernandez, G. Kelly, et al. (2005). "The ERA-40 re-analysis." In: *Quarterly Journal of the Royal Meteorological Society: A journal of the atmospheric sciences, applied meteorology and physical oceanography* 131.612, pp. 2961–3012.

- Urraca, R., T. Huld, A. Gracia-Amillo, F. J. Martinez-de Pison, F. Kaspar, and A. Sanz-Garcia (2018a). "Evaluation of global horizontal irradiance estimates from ERA5 and COSMO-REA6 reanalyses using ground and satellite-based data." In: *Solar Energy* 164, pp. 339–354.
- Urraca, R., T. Huld, F. J. Martinez-de Pison, and A. Sanz-Garcia (2018b). "Sources of uncertainty in annual global horizontal irradiance data." In: *Solar Energy* 170, pp. 873–884.
- Vargas, L. S., G. Bustos-Turu, and F. Larraín (2014). "Wind power curtailment and energy storage in transmission congestion management considering power plants ramp rates." In: *IEEE Transactions on Power Systems* 30.5, pp. 2498–2506.
- Vautard, R., J. Cattiaux, P. Yiou, J.-N. Thépaut, and P. Ciais (2010). "Northern Hemisphere atmospheric stilling partly attributed to an increase in surface roughness." In: *Nature geoscience* 3.11, pp. 756–761.
- Ventosa, M., A. Baillo, A. Ramos, and M. Rivier (2005). "Electricity market modeling trends." In: *Energy policy* 33.7, pp. 897–913.
- Vitart, F. and A. W. Robertson (2018). "The sub-seasonal to seasonal prediction project (S2S) and the prediction of extreme events." In: *Npj Climate and Atmospheric Science* 1.1, p. 3.
- Weide Luiz, E. and S. Fiedler (2022). "Spatio-temporal observations of nocturnal low-level jets and impacts on wind power production." In: *Wind Energy Science Discussions*, pp. 1–28.
- Wiel, K. van der, H. C. Bloomfield, R. W. Lee, L. P. Stoop, R. Blackport, J. A. Screen, and F. M. Selten (2019a). "The influence of weather regimes on European renewable energy production and demand." In: *Environmental Research Letters* 14.9, p. 094010.
- Wiel, K. van der, L. P. Stoop, B. Van Zuijlen, R. Blackport, M. Van den Broek, and F. Selten (2019b). "Meteorological conditions leading to extreme low variable renewable energy production and extreme high energy shortfall." In: *Renewable and Sustainable Energy Reviews* 111, pp. 261–275.
- Zschenderlein, P., G. Fragkoulidis, A. H. Fink, and V. Wirth (2018). "Large-scale Rossby wave and synoptic-scale dynamic analyses of the unusually late 2016 heatwave over Europe." In: *Weather* 73.9, pp. 275–283.